ORGANIZATION AND EXPRESSION OF MURINE INTERFERON REGULATORY FACTOR-1 (IRF-1) GENE

Thesis submitted to
Jawaharlal Nehru University
for the award of
the Degree of

DOCTOR OF PHILOSOPHY

SANJIV KUMAR

SCHOOL OF LIFE SCIENCES
JAWAHARLAL NEHRU UNIVERSITY
NEW DELHI-110067
INDIA
JULY, 2000

SCHOOL OF LIFE SCIENCES
Jawaharlal Nehru University
NEW DELHI-110067

CERTIFICATE

The research work included in this thesis entitled "**Organization and Expression of Murine Interferon Regulatory Factor-1 (IRF-1) Gene**" has been carried out by Mr. Sanjiv Kumar in the School of Life Sciences, Jawaharlal Nehru University, New Delhi. This work is original and has not been submitted so far, in part or full for any other degree or diploma of any other university.

Sanjiv Kumar
SANJIV KUMAR
(Candidate)

K C Upadhyaya
PROF. K. C. UPADHYAYA
(Dean)

P C Rath
DR. P. C. RATH
(Supervisor)

Dedicated to my parents……..

ACKNOWLEDGEMENTS

I am grateful to my supervisor Dr. P.C Rath for introducing me to this exciting field of molecular biology and providing guidance at all stages of the study. His valuable suggestions helped me to carry out the work. The kind gifts of the mouse IRF-1 cDNA (pIRFL) from Prof. Tadatsugu Taniguchi, University of Tokyo and the mouse IRF-1 genomic clone (pIRFC2) from Prof. Charles Weissmann, University of Zurich are gratefully acknowledged.

My gratitude goes to Dr. P.K Yadava for his invaluable suggestions and constant help. I sincerely thank Prof. K.C. Upadhyaya, Dean, School of Life Sciences for providing all necessary facilities for pursuing my research work. I also thank the former Deans of the School of Life Sciences, Prof. Shipra Guha Mukherjee, Prof. Najma Z. Baquer, and Prof. R. Prasad for their support and help. I sincerely thank Prof. K.C. Upadhyaya, Prof. R.N.K Bamezai, Prof. R.K. Saxena, Dr. S. K. Kar, Dr. R. Madhubala and Dr. S. Goswami for extending their laboratory facilities for my work. My thanks are due to Prof. A.R. Rao and Dr. R.K Kale for their constant encouragement.

I am thankful to my labmates Indranil, Mitali, Gagan and Meenakshi for their help and maintaining a cheerful atmosphere conducive for good research. My special thanks are due to Gagan and Meenakshi for their selfless help round the clock towards completion of the thesis.

My seniors Dhyan Chandra, Ramesh, Vincent, Neeraj, Praveen Verma, I.P, Praveen Singh, Jyothi, Venkiah, Nagendra, Sohita, Aparna, Rana, Pushpshankar, Anirban, Andrew, Asha, Agam, Arvind, Shubhra, Niranjan and Jaspreet, my friends Dhananjay, Suresh, Sameer, Jamal, Gurumurthy, Vidita, Raju, Amita, Giridhar, Anjana, Anand, Narendra, Anjali, Suchi, Suneet, Faizal, Reetakshi, Binuja, Krishna, Neel, R. Hindav, Vikas, Prasanna, Paromita, Ranjana, Avmeet, Padma, Dhana, Neeti, Purnima, Gayatri, Sushil, Sidhu, Bindu, Manisha, Gireesh, Suresh, Ravindra, Rashmi and all the juniors of 1995 to 1999 batches have made SLS one of the best places to work.

I am grateful to my M.Sc. friends Rajesh, Reena, Rohit, Hemant, Shastry, Monika, Naresh, Rajesh Saini and Nevil who have helped me directly or indirectly during my Ph.D.

My close friends Aklaque, Bhaskar, Ranjan, Vandana, Prashant and Vaishali were the unlimited source of joy and happiness. Their suggestions were always useful and infused me with fresh ideas.

Thanks are due to the staff of Bioinformatics Centre especially Dr. Subbarao, Chary, Inderjeet and Arun for their help in computational analysis. I thank Chhotelal and Bhagat Ram for their timely assistance. I thank Mr. Panwar and our CIF staff, Mr. Alexander, Mr. Khan, Mr. Mishra, Mr. Rajinder, Mr. Sharma, Mr. Balwant for extending their help when needed and to Mr Saini for excellent photography.

My parents' constant encouragement has enabled me to reach this stage. Words fail me here since I can never thank them enough. My elder brothers, sisters, bhabhis and Jijajis were a constant source of encouragement throughout. Special thanks to Randhir Jijaji for his help. The presence of my niece and nephews around me filled me with joy and magically erased out bad moods.

Financial support from the University Grants Commission (U.G.C.), the Council of Scientific and Industrial Research (C.S.I.R.) and the Department of Science and Technology (D.S.T.), Govt. of India are gratefully acknowledged.

Sanjiv Kumar

(Sanjiv Kumar)

Abbreviations used

-/-	Knock out
2'-5' OAS	2'-5' Oligo Adenylate Synthase
$A_{260/280}$	Absorbance at 260 / 280 nm wavelength
bp	base pairs
CAT	Chloramphenicol Acetyl Tranferase
cDNA	complementary Deoxyribonucleic Acid
CML	Chronic Myelogenous Leukemia
Con A	Concanavalin A
cpm	counts per minute
DNA	Deoxyribonucleic Acid
ds	double stranded
EMSA	Electrophoretic Mobility Shift Assay
FBS	Fetal Bovine Serum
G1	First growth phase
GBP	Guanylate Binding Protein
hrs	hours
IAD	Interferon Association Domain
ICE	Interleukin1-Converting Enzyme
ICSBP	IFN Consensus Sequence Binding Protein
IFN	Interferon
IL	Interleukin
iNOS	inducible Nitric Oxide Synthase
IRF	Interferon Regulatory Factor
ISGF	Interferon Stimulated Gene Factor
ISRE	Interferon Stimulated Response Element
kb	kilo base
kd	kilo dalton
LB	Luria Broth
LIF	Leukemia Inhibitory Factor
LMP-2	Low Molecular Weight Protein-2
LPS	Lipopolysaccharide
M	Molar
MHC	Major Histocompatibility Complex
min	minutes
ml	millilitres
mM	millimolar
mRNA	messenger Ribonucleic Acid
ng	nanograms
NK cell	Natural Killer cell
nm	nanometer
nt	nucleotide
^{o} C	degree celcius
PKR	Protein Kinase R
RNA	Ribonucleic Acid
rpm	rotations per minute
Sec.	Second
STAT	Signal Transducer and Activator of Transcription
TAP-1	Transporter associated with antigen processing-1
TNF-α	Tumor Necrosis Factor-α
U	Unit
UTR	Untranslated Region
UV	Ultraviolet
Vol.	Volume
V/V	volume by volume
VCAM-1	Vascular Cell Adhesion Molecule-1
W/V	Weight by Volume
μg	microgram
μl	microlitre

CONTENTS

SUMMARY

1. SUMMARY

Interferon Regulatory Factor-1 (IRF-1) is a positive transcription factor for many mammalian genes. It was originally identified on the basis of its DNA binding activity with a repeated sequence motif (AAGTGA or GAAAGT) present in the virus response element (VRE) of human interferon-β (IFN-β) gene promoter and ability to mediate transcriptional activation of the gene in mammalian cells following virus induction. DNA sequence elements recognized by IRF-1 are also inducible by both IFN-α and IFN-γ. Variants of a consensus hexanucleotide of the nature GAAANN (N = any nucleotide) frequently occur in promoter/enhancer(s) of many virus-inducible and IFN-inducible genes in both murine and human cells. The tetrameric hexamer, $(GAAAGT)_4$, when used as a promoter element in transfection studies, binds to IRF-1 and gets activated by IRF-1 to stimulate a down stream reporter gene following virus and IFN induction. Chromosomal IRF-1 gene is also virus- and IFN-inducible. IRF-1 activates IRF-2 which acts as a repressor for IRF-1-mediated gene expression. Thus IRF-1 is involved in a network of gene activity for cellular functions regulated by virus infection, IFNs, certain other cytokines and other agents. IRF-1 actively participates in cellular processes like defense against viruses and other pathogens, regulation of cell growth and differentiation, antioncogenesis, immune regulation and apoptosis. Therefore, IRF-1 is an important transcription factor for mammalian cells and tissues. However, most studies about IRF-1 have been carried out with either mammalian cells in culture or IRF-1 knock out mice by using a number of inducers. Information about expression of IRF-1 mRNA and DNA binding activity of IRF-1 in different tissues of mouse is limiting.

In the present work, organization of IRF-1 gene was studied in genomic DNA isolated from the mouse liver and human peripheral lymphocytes by Southern blot analysis using three types of murine IRF-1 DNA probes : cDNA probe (exons 1-10), C2 genomic probe (exons 3-10 + introns 2-10) and 194 5'

probe (exon 1). Important differences in the IRF-1 gene of the two species were observed in terms of several restriction enzyme fragments. They represented both exonic and intronic sequences. Certain DNA fragments including a 0.5 kb Pst I promoter DNA were common to both species indicating that the murine and human IRF-1 genes have a similar overall organisation but with certain distinct differences. Comparison of the nucleotide sequences of the mouse and human IRF-1 cDNAs showed amino acid variations in the human IRF-1. The N terminal DNA binding domain was conserved but the C terminal transactivation domain showed many amino acid changes in human IRF-1. Six clusters of five to six amino acids represented the significant amino acid changes in the transactivation domain of human IRF-1. Similar amino acid regions also occurred in other proteins indicating that they might represent functional sequence motifs specific to human IRF-1.

IRF-1 mRNA expression showed tissue-specific pattern in the mouse as studied by northern blot and dot blot hybridization analyses. The intestine showed a 5.5 x fold higher while the lungs and the spleen showed about 2.2 to 2.4 x fold higher steady state levels of the 2 kb IRF-1 mRNA compared to that of the thymus. The dot blot analysis showed that relative levels of IRF-1 mRNA expression in different tissues of the mouse in ascending order was from brain to heart, kidney, liver, spleen, thymus, lungs and intestine respectively. This reflected possible physiological significance of IRF-1 in mouse tissues under normal conditions.

DNA binding activities of IRF-1 and IRF-2 were studied by using the tetrameric hexamer, $(GAAAGT)_4$ and extracts prepared from different tissues of the mouse. IRF-1- and IRF-2-DNA complexes showed a tissue-specific pattern. Dimers and monomers of IRF-1 and IRF-2 were observed in the mouse spleen, dimmers of IRF-1 and IRF-2 in thymus, lungs, IRF-1 dimer in liver, multiple IRF-1/2 complexes in intestine and no detectable IRF-1/2 complex in brain, heart and very low level of IRF-1 dimer in kidney of the mouse. The IRF-1- and IRF-2-DNA complexes were specific for $(GAAAGT)_4$

sequence and were compared with recombinant GST-IRF-1-DNA complex and human IRF-1- and IRF-2-DNA complexes from U 937 cells after IFN-γ treatment for validating the complexes. IRF-1- and IRF-2-DNA complexes in whole cell extracts, cytoplasmic- and nuclear extracts from spleen and thymus of the mouse showed that most of the complexes were obtained from the nuclear fractions. There was a concentration-dependent accumulation of a higher IRF-1-DNA complex in nuclear extracts from spleen and thymus which indicated cooperative binding of IRF-1 to multimeric GAAAGT sequence. This may reflect binding of IRF-1 to promoter DNA of target genes activated by IRF-1 in the nucleus after its level is induced by several agents.

Thus, differences in (a) organisation and (b) amino acid sequence of mouse and human IRF-1 genes; tissue-specific patterns for steady state levels of IRF-1 mRNA expression and IRF-1- as well as IRF-2-DNA complexes in mouse tissues indicate physiological significance of IRF-1 and IRF-2 in mouse tissues under normal conditions as well as possible functional specialisation of human IRF-1.

INTRODUCTION

2.INTRODUCTION

2.1 INTERFERONS

Interferons (IFNs) are a group of multifunctional, secretory glycoproteins of about 20 kd that function as important cytokines and regulate a variety of functions in mammalian cells (reviewed in Stark et al., 1998). IFNs are mainly of two types: type I (IFN-α and IFN-β) and type II (IFN-γ). IFN-α molecules are coded by multiple (at least 18) genes but IFN-β and IFN-γ, each coded by a single gene. Broadly, IFNs have antiviral, antiproliferative and immunomodulatory properties (see Weissmann and Weber, 1986; DeMaeyer and DeMaeyer-Guignard, 1988). Type I IFNs are recognised by a common receptor, IFNAR but type II or IFN-γ binds to a distinct receptor, IFNGR (reviewed in Pestka et al., 1987). Both receptors are located on surface of most mammalian cells. IFN-α is mostly secreted by lymphoid cells and is often referred as lymphocyte IFN. IFN-β is mostly secreted by fibroblasts and is referred as fibroblast IFN. IFN-γ is known as immune interferon and is secreted by cells of the immune system and some other cell types.

Type I IFNs have profound antiproliferative activity on most normal and many transformed cells (reviewed in Lengyel 1982). Both IFN-α and IFN–β demonstrate remarkable antiviral action in a variety of mammalian cells (see Sen and Ransohoff, 1993). IFN-γ has also antiviral activity overlapping with IFN-α/β. IFN-γ is secreted by activated T cells, some other cell types and it functions as one of the major cytokines that specifies development of immune response. IFN-α/β has modulatory influence on immune response. IFN genes are tightly regulated in mammalian cells. They are transiently activated at transcriptional level by several agents under physiological and pathological conditions. IFNs in turn, activate specific genes and alter physiological state of the cells. Biological effects of IFNs are diverse and well documented (Stark et

al., 1998). Mammalian cells in culture, when treated with IFN-α/β show growth arrest at G1 phase of the cell cycle or may prolong other phases as well IFNs can influence many cell cycle regulatory proteins, for example *c-myc*, pRB, cyclin D3 and cdc25A and cell growth inhibitors like p21/WAF1, p27, $p57^{kip}$. IFN-α/β induce a variety of genes for mounting an antiviral response in mammalian cells, for example MX, 2' 5' oligoadenylate synthase and 2' 5' oligoadenylate-dependent ribonuclease L (RNase L), double stranded (ds) RNA-dependent kinase or PKR and signalling proteins involved in the apoptotic pathway as well as many others. Effect of IFN-α/β on differentiation of many cell types has also been documented. IFN-γ mainly stimulates immune response by activating genes involved in the immune regulation, for example cytokines like IL-5, IL-6, IL-12. It activates MHC I and MHC II genes, shows synergistic effect with tumor necrosis factor-α (TNF-α), a major inflammatory cytokine, causes antiviral response, upregulates genes in the cell death pathway, controls cell proliferation, and differentiation. IFNs also have great therapeutic potentials. Recently, IFN-α/β has been proposed to be used as therapeutic agents in human patients: IFN-α for Chronic Myelogenous Leukemia (CML) (Talpaz et. al., 1987) and IFN-β for multiple sclerosis as well as for hemangiomas through its inhibitory effects on growth factors (b-FGF & VEGF) needed for angiogenesis (Bielenberg et. al., 1999).

Studies involving molecular mechanism of IFN action has provided us knowledge about a unique biochemical pathway in cells. IFN-α/β and IFN-γ interact with their cognate cell surface receptors and trigger a cascade of signal transduction which was identified as the JAK-STAT pathway in mammalian cells (reviewed by Darnell, et al.,1994). This proceeds in several steps in a sequential manner that involves ligand binding, dimerisation of the receptor, tyr-phosphorylation in the intracellular or cytoplasmic domain of the receptor, activation of the receptor-associated JAKs (Janus Kinase) by their phosphorylation at specific tyr residues, subsequent phosphorylation of STATs

(Signal Transducer and Activation of Transcription) by the activated JAKs at specific tyr residues, dimerisation of the STATs by reciprocal interaction of their phospho-tyr residues with SH2 domain, association of other proteins with STATs, translocation of the multimeric STAT complex from the cytoplasm to the nucleus, binding of the STAT complex to specific IFN-inducible DNA sequences in the promoters of target genes and finally transcriptional activation of the genes. Thus IFNs activate IFN-stimulated genes (ISGs) and proteins coded by these ISGs specify the biochemical actions of IFNs. There are many ISGs that are common to both type I and type II IFNs and there are many more ISGs that are specific to IFN-α/β and IFN-γ in mammalian cells . The specificity of IFN-α/β and IFN-γ mediated signal transduction pathways is decided by multiple factors: such as, the distinct receptors, different JAKs (JAK1 and TYK2 for IFNAR but JAK1 and JAK2 for IFNGR), different STATs (STAT1 homodimer for IFN-γ but STAT1α/β + STAT2 for IFN-α/β), distinct DNA sequences in the promoters of IFN-α/β and IFN-γ responsive target genes. However, IFN-α/β and IFN-γ pathways also cross talk for antiviral activity (Takaoka et. al., 2000). The JAK-STAT pathway is now known to operate also in cases of many growth factors, cytokines and hormones.

IFN-α/β induces ISRE (interferon stimulated response element) and IFN-γ induces GAS (interferon-γ activation sequence) in the promoters of their target genes. The IFNα/β-inducible genes are activated by the phosphorylated complex, ISGF-3 (interferon-stimulated gene factor 3) consisting of several STAT proteins [Stat1α (p84) or Stat1β (p91), Stat2 (p113) and an associated DNA binding protein p48]. In contrast IFN-γ-inducible genes are activated by a phosphorylated complex, called GAF (IFN-γ-activated factor) which consists of dimerized Stat1α and other DNA binding protein (s) (reviewed in Darnell et al., 1994). These two transcription factor complexes, ISGF-3 and GAF, recognise different sequences in the promoters of IFN-α/β, and γ- inducible

genes respectively. By microarray based gene expression analysis, it has been shown that type I and type II IFNs activate distinct genes in mammalian cells (Der et. al., 1998). However promoter/enhancer regions of IFN-inducible chromosomal genes have more complex sequence elements that also possess additional binding sites for some other factors which should also be induced by IFNs. The family of Interferon Regulatory Factors (IRFs) represents one such example (Taniguchi et al., 1995).

2.2 INTERFERON REGULATORY FACTOR-1 (IRF-1)

2.2.1 IRF-1 and IRF-2 in IFN system

IRF-1 and IRF-2 were originally identified as factors that bound to sequences found in the IFN-α and –β promoters following virus induction of mammalian cells. Virus infection of cells resulted in transcriptional activation of IRF-1 gene prior to IFN-β gene. IRF-1 induced transcription of IFN-β gene (Miyamoto et al., 1988) and bound to the PRD I (-77 to –65) element (Fan and Maniatis, 1989) in the IFN-β gene promoter. It was observed that overexpression of mouse IRF-1 cDNA in monkey COS cells resulted in the induction of endogenous IFN-α and IFN-β genes (Fujita et al., 1989). IRF-1 and IRF-2 bind to the same element (IRF-E) and IRF-2 binds with higher affinity than IRF-1. The two factors are highly homologous to one another in their amino-terminal regions specific for the DNA binding activity and different in their C-terminal regions which specifies transcriptional function (Harada et al., 1989). IRF-1 and IRF-2 are structurally similar but functionally distinct transcription factors that partly regulate IFN system.

Gene transfection studies have shown that IRF-1 can function as an activator, inducing transcription from promoters of genes containing IRF-E (Harada et al., 1989). In contrast, IRF-2 antagonizes the function of IRF-1 by competing with it for binding to the same sites in the promoter and possibly by

repressing activators positioned nearby (Harada et al., 1990). Both IRF-1 and IRF-2 mRNAs are expressed at low constitutive levels in cells, but IRF-2 protein is more stable and thus accumulates to higher levels, with a half life of 8 hr as compared to 30 min for IRF-1 (Watanabe et al., 1991). IRF-2 may remain bound to IRF binding sites in the promoters of certain genes under normal conditions thereby keeping them transcriptionally "off". IRF-1 can overcome the dominance of IRF-2 when cells are stimulated by agents like virus, double stranded RNA (dsRNA) and interferons (Harada et al., 1989). These stimuli cause the transient up-regulation of the IRF-1 gene transcription and consequent induction of many IFN-inducible genes. Another consequence of IRF-1 up-regulation is the induction of IRF-2 gene (Harada et al., 1994). This gene regulatory circuit may thus serve to maintain a proper balance between IRF-1 and IRF-2 expression and thus the functions regulated by them.

IRF-1 is expressed at low levels or is undetectable in a variety of cell types; however, its expression is induced by virus infection, Concanavalin A (ConA) (Miyamoto et al., 1988), treatment with double-stranded RNA (ds RNA) or poly (I.C.), Type I and II IFNs, phorbol 12-myristate 13-acetate (PMA), calcium ionophore A23187 and other cytokines like tumour necrosis factor-a (TNF-a), interleukin-1 (IL-1) (Fujita et al., 1989b), IL-6 and activators like leukemia inhibitory factor (LIF) (Abdollahi et al., 1991) and prolactin (Yu-Lee et. al., 1990). In contrast, IRF-2 expression is constitutive in many cell types and is also inducible by type I IFN and virus infection but through IRF-1 (Harada et al., 1989). There are also genes which are activated by IRF-2 (Vaughan et al., 1995). In case mouse embryonal carcinoma (P19) cells, undifferentiated cells do not have IRF-1 and IRF-2, but differentiated cells possess IRF-1 and IRF-2 mRNAs and proteins, (Harada et al., 1990).

2.2.2 Structure and function of IRF-1 and IRF-2

Mouse IRF-1 is 329 amino acid (37.6 kd) and IRF-2 is 349 amino acid (49.5 kd). Structurally, IRF-1 and IRF-2 proteins are similar, sharing 76 % identity in their first 154 N-terminal amino acids but only 8 % identity in their C-terminal regions (Harada et al., 1989). IRF-1 has a DNA binding domain (DBD) from amino acid 1-140 and transcription activation domain (TAD) from 141-329. IRF-2 has a similar DBD from 1 to 154 amino acid and transcriptional repression domain (TRD) from 155 to 349 amino acid (Miyamoto et al., 1988; Harada et al., 1989). So IRF-1 functions as a transcriptional activator whereas IRF-2 acts as an antagonist or transcriptional repressor for IRF-1-activated genes. The N-terminal DBD of IRF-1 and IRF-2 recognize the virus-inducible IRF elements (IRF-E) present in the promoters of certain genes. Interestingly, DNA binding activity of IRF-1 and IRF-2 is enhanced by interaction with the TFIIB component of basal transcriptional machinery (Wang et al., 1996). Virus- or stimulator-induced IRF-1 activation occurs by post-translational modification of IRF-1 in addition to increased IRF-1 protein synthesis (Watanabe et al., 1991).

Transcriptional repression by IRF-2 is localized to the its C-terminal 59 amino acids. Fusion of this region to the C-terminal end of IRF-1 inhibits transactivation by IRF-1. A latent activation domain exists in the central region of IRF-2, between amino acid 160 to 220, which is considered to be silenced by the C-terminal repression domain. These results indicate that IRF-2 is a "mosaic" transcription factor possessing both activator and repressor activities (Yamamoto et al., 1994). One mechanism of repression by IRF-2 may involve inhibition of IRF-1 transactivation by occupying the IRF consensus site and subsequently preventing DNA binding by IRF-1 (Harada et al., 1990; Nguyen et al., 1995). IRF-2 is viewed generally as a transcriptional repressor. However there are at least two reports that IRF-2 acts as an transcriptional activator. First, the human H4 gene was found to be directly activated by IRF-2 through

binding to cell cycle element (CCE) present in the H4 gene promoter (Vaughan et al., 1995). This histone gene may play a role in IRF-2 mediated oncogenesis, since it is functionally coupled to DNA replication and cell cycle progression at G1 to S transition. Secondly, QP-promoter region of the Epstein Bar Virus encoded EBNA-1 gene has been shown to be activated by IRF-2 and IRF-1 (Nonkwelo et al., 1997). So, IRF-2 is a dual transcription factor containing both activator and repressor functions (Yamamoto et al., 1994).

2.2.3 Post-translational modification of IRF-1

It has been observed that staurosporin, a protein kinase inhibitor blocks IRF-1 mediated activation ie binding of IRF-1 to IRF-E (Watanabe et al., 1991) and calf intestinal phosphatase (CIP) inhibited the DNA binding activity of the IRF-1 (Pine et al., 1990). This suggested that phosphorylation of IRF-1 may be important for its function. The posttranslational events influencing IRF-1 may be due (in part) to phosphorylation by casein kinase II (CK II), a serine threonine protein kinase involved in the phosphorylation of over 50 proteins including transcription factors and cell growth regulators (Pinna et al., 1990). IRF-1 has a site in the DBD (amino acid 138-150) and another site in the transactivation domain (amino acid 219-230) for phosphorylation by CKII. It has also been found that recombinant CK II phosphorylates IRF-1, IRF-2 and IRF-3 *in vitro*. These results indicated that CK II may be involved in regulating IRF-1 function and highlighted CK II as a potential regulator for the co-ordinated regulation of interferon and other cytokines.(Lin and Hiscott, 1999)

2.2.4 Structure of IRF-1 + DNA complex

IRF-1 and IRF-2 are characterized by a unique "tryptophan cluster" in the DNA binding domain (DBD). This cluster ('W-repeat') contains five

tryptophan residues. Escalante et al. (1998) cocrystallized IRF-1 (residues 1-113) with a 13 bp DNA fragment containing the natural PRDI sequence (5'GAGAAGTGAAAGT3') of the IFN-β gene promoter. IRF-1 revealed a new helix-turn-helix motif that latched onto the DNA through three of the five conserved tryptophans in the DBD. IRF-1 DBD contacted to bases within the major groove of the DNA that localised to a GAAA core sequence within the 13 bp PRDI element. The amino acids mediating these contacts in the major groove (Arg 82, Cys 83, Asn 86, and Ser 87) projected from the last two turns of the IRF-1 recognition helix. Arginine 82 was in the position to form bidentate hydrogen bond with the guanine of the outer G:C base pair (GAAA), while establishing a salt link with the preceeding 5' phosphate group. Recognition of the 2nd and 3rd bp of the core sequence was due primarily to Cys 83, which through its sulfydryl group receiveed a single hydrogen bond from N_6 of the adenine at the 2nd position (GAAA) and donated a hydrogen bond to O_4 of the thymine at the 3rd position (GAAA). Arginine 82 is totally conserved within the IRF family whereas Cys 83 shows only a single substitution to serine in IRF-3.

2.2.5 Phenotypes of IRF-1 and IRF-2 knock out mice

IRF-1 and IRF-2 knock out mice showed interesting features that underlined the functions of these two transcription factors in mice *in vivo* and established their physiological importance. Taniguchi and coworkers (Matsuyama et al., 1993) have made IRF-1 and IRF-2 knock out mice by gene targeting. They reported that in IRF-1 deficient mouse fibroblasts, type I IFN mRNAs were inducible and peaked at 4 hr after induction with poly (I.C.), similar to that of the wild type cells. However, absolute mRNA level were dramatically reduced by 3 to 10 fold indicating that IRF-1 is essential for optimal induction of type I IFN by poly (I.C). But upon infection by NDV (Newcastle disease virus), type I IFN was induced in homozygous mutant cells

upto a level similar to that of the wild type and heterozygous cells. Thus, IRF-1 deficient (IRF-$1^{-/-}$) fibroblasts lacked the normally observed type I IFN induction by poly (I.C.), while type I IFN gene expression was unaffected following NDV infection.

In contrast, IRF-2-deficient fibroblasts showed upregulated type I IFN induction by NDV infection. It was observed that in IRF-$1^{-/-}$ mice there was reduction of TCR $\alpha\beta^{+}$ $CD4^{-}$ $CD8^{+}$ T-cells. IRF-2 deficient mice exhibited suppression of heamatopoiesis in bone marrow and B-cell lymphopoiesis and mortality following lymphocytic choriomeningitis virus infection (Matsuyama et. al., 1993)

Simultaneously by independent studies, Weissmann and coworkers (Ruffner et. al., 1993) reported that in IRF-1 deficient embryonic stem (ES) cells, NDV infection elicited expression of IFN-β and IFN-α mRNAs in both IRF-$1^{-/-}$ and $IRF^{+/+}$ cells, albeit at levels 1.3 to 7 fold lower in IRF-$1^{-/-}$ cells when compared to that of the wild type cells. Thus, IRF-1 although not essential for expression of type I IFN genes in ES cells, can enhance IFN gene expression (Ruffner et. al., 1993). Later, they generated mice devoid of functional IRF-1 by targeted gene disruption. In these mice, induction of type I IFN genes by virus and double stranded RNA was not impaired *in vivo*. There was also no impairment in the response of type I IFN-inducible genes. Therefore, IRF-1 was not considered to be an essential factor for IFN and IFN-inducible gene expression *in vivo*. However, $CD4^{+}/CD8^{+}$ T cell ratio was increased and IFN-γ induced macrophage iNOS mRNA level was strongly diminished in IRF-1 deficient mice. Subsequently, several other studies were done in IRF-$1^{-/-}$ mice to check the role of IRF-1 in cells. They are : (i) In IRF-$1^{-/-}$ macrophages the mRNA level for iNOS was very low, in response to stimulation by IFN-γ + LPS, which is required for production of NO (Nitric Oxide) (Kamijo et.al.,1994). Production of nitric oxide (NO) by macrophage is important for the killing of intracellular infectious agents, (ii) in IRF-$1^{-/-}$, embryonic fibroblasts can be transformed by expression of an activated *c-Ha-*

ras oncogene. The transformed phenotype could be suppressed by the expression of IRF-1 cDNA so, IRF-1 may be acting as an antioncogenic factor (Tanaka et. al., 1994), (iii) it has been reporrted that TAP1 and LMP2 and class I MHC levels were reduced in IRF-$1^{-/-}$ mice (White et.al., 1996), (iv) IRF-$1^{-/-}$ mice exhibited defective Th1 responses i.e. impaired production of IL-12 by macrophages, deficient $CD4^+$ T cell response to IL-12 (Taki et. al., 1997), (v) IRF-$1^{-/-}$ mice showed reduced numbers of mature $CD8^+$ cells within the thymus and peripheral lymphatic organs (Penninger and Mak, 1998), (vi) in IRF-$1^{-/-}$ mice the NK cell development was defective, but IRF-$1^{-/-}$ mice could generate functional NK cells when they were cultured with the IL-15, hence IL-15 gene was most likely transcriptionally regulated by IRF-1 (Ogasawara et. al., 1998).

2.2.6 Involvement of IRF-1 and IRF-2 in immune regulation

IRF-1 and IRF-2 are implicated in the regulation of various immune processes. Mice deficient in IRF-1 gene were 90% deficient in mature $CD4^-$ $CD8^+$ T-cells in the thymus suggesting impairment in the maturation of $CD8^+$ cells in these mice. IRF-2 deficient mice (IRF-$2^{-/-}$) suffered from bone marrow suppression of hematopoiesis and B cell lymphopoiesis and died following lymphocytic choriomeningitis virus (LCMV) infection (Matsuyama et al., 1993). TAP1 and LMP2 play role in the function of MHC I and their expression is IFN γ-inducible. Interestingly, levels of TAP1, LMP2 and surface class I MHC were greatly reduced in IRF-1 deficient mice (White et al., 1996). *In vivo* footprinting and electrophoretic mobility shift assays revealed that IFN-γ treatment induced protein-DNA contacts at an IRF-E site present in the promoters of both TAP1 and LMP2 genes indicating involvement of IRF-1 in the expression of these genes. IRF-1 plays a critical role during multiple stages of differentiation of Th1cells. Immune cells from IRF $^{-/-}$ mice exhibited defective Th1 responses i.e. an impaired production of

IL-12 by macrophages (Taki et al., 1997). IRF-1 is essential for the induction of NK cell-mediated cytotoxicity *in vivo*. Cytolytic activity of NK cells from IRF-$1^{-/-}$ mice were defective, even following induction by virus, ds RNA, IFN-β, IL-2 and IL-12 treatments (Duncan et al., 1996). IRF-1 is also required for the microenvironment supporting development of NK cells (Pleimann et al., 1994). Mice that do not express IRF-1 were shown to exhibit a severe NK cell deficiency. Lack of IRF-1 affected radiation-resistant cells that constitute the microenvironment required for the development of NK cells, but not NK cell progenitors. Bone marrow cells from IRF-$1^{-/-}$ mice could generate functional NK cells when cultured with the cytokine IL-15 (Ogasawara et al., 1998). Therefore, IL-15 gene is likely to be transcriptionally regulated by IRF-1.

IRF-1 is also involved in the expression of polymeric Ig receptor (pIg R) gene that codes for polymeric immunoglobulin receptor (pIg R). The transport of polymeric immunoglobulins, predominantly dimeric Ig A, across epithelial barriers of mucous membrane is mediated by pIg R. In IRF-$1^{-/-}$ mice there was a decrease in the mRNA for pIg R suggesting involvement of IRF -1 in mucosal immunity against antigens that are inhaled, ingested and sexually transmitted (Blanch et al., 1999). Thus IRF-1 is involved in the differentiation, maturation of certain immune cells and mounting an immune response against certain viruses and other pathogens.

2.2.7 Other functions of IRF-1

Mouse NIH 3T3 fibroblast cells can be arrested in the G1 phase of the cell cycle by serum-deprivation and addition of serum stimulate them to proceed through the cell cycle in a synchronous manner. Serum starvation of NIH 3T3 cells caused markedly elevated IRF-1 mRNA expression. However, following addition of serum its expression declined six fold followed by a gradual increase prior to and during DNA synthesis. In contrast, IRF-2 mRNA levels remained constant throughout the cell cycle (Harada et al., 1993). Thus

the ratio of IRF-1: IRF-2 expression oscillates during the cell cycle, being at its highest (i.e. high IRF-1) in growth-arrested cells and at its lowest (i.e. low IRF-1) following growth stimulation. Cell cycle protein cyclin D1 promoter also have IRF-1 binding site (Sato et al.,1998). Several experiments have demonstrated that alterations in IRF-1: IRF-2 expression levels can have significant consequences on cell growth. For example, ectopic overexpression of IRF-1 strongly inhibited cell proliferation in several cell types (Yamada et al., 1990 and Kirchoff et al., 1993). Conversely, overexpression of IRF-2 caused oncogenic transformation of NIH 3T3 cells, as manifested by the ability of these cells to grow to higher saturation densities in culture, attain anchorage-independent growth and form tumors in nude mice (Harada et al., 1993). Furthermore, concomitant constitutive expression of IRF-1 returned these cells to a non-transformed phenotype. Thus restrained cell growth depends upon a balance between the two mutually antagonistic transcription factors. These *in vitro* observations suggest that IRF-1 and IRF-2 can function as an anti-oncogene and oncogene respectively.

The anti-oncogenic, or tumor-suppressor function of IRF-1 has been further demonstrated in oncogenic transformation assays using embryonic fibroblasts from the IRF-$1^{-/-}$ mice. Transformation of these cells normally requires at least two oncogenes. For example, the *c-Ha-ras* gene containing an oncogenic mutation (activated *c-Ha-ras*) will not transform the embryonic fibroblasts unless they are introduced together with another oncogene such as *c-myc* or polyoma large-T antigen gene (Weinberg, 1989). However, when these embryonic fibroblasts (EFs) from IRF-1 deficient mice (IRF-$1^{-/-}$) were examined it was found that expression of activated *c-H-ras* gene alone was sufficient to transform these cells oncogenically (Tanaka et al., 1994). The IRF-$1^{+/-}$ EFs also showed resistance to *ras*-induced transformation. Transfection of the human IRF-1 cDNA into the IRF-$1^{-/-}$ EF cells resulted in strong suppression of colony formation. So *ras*- induced transformation can be reverted in significant population of these cells by expression of IRF-1. This

showed that IRF-1 may be a critical determinant of oncogene-induced cell transformation (Tanaka et al., 1994).

When normal embryonic fibroblasts (i.e. IRF-$1^{+/+}$) expressing activated *c-Ha-ras* gene were cultured in low serum condition or treated with anticancer drugs or ionizing radiation they were observed to lose vitality by a process characteristic of apoptosis (programmed cell death). In contrast, when IRF-$1^{-/-}$ fibroblasts expressing activated *c-H-ras* gene were subjected to the same treatment the cells survived (Tanaka et al., 1994). It was found that DNA-damage-induced apoptosis in thymocytes is dependent on IRF-1. Two different anti-oncogenic transcription factors, p53 and IRF-1, are required for apoptopic pathways in T lymphocytes (Tamura et al., 1995). Mitogenic induction of the interleukin-1β-converting enzyme (ICE) gene, a mammalian homolog of the *Caenorhabditis elegans* cell death gene ced3, is IRF-1-dependent. Ectopic overexpression of IRF-1 resulted in the activation of the endogenous ICE gene and enhances the sensitivity of the cells to radiation-induced apoptosis (Tamura et al., 1995). These results indicated that IRF-1 is not only involved in growth regulation of cells but also it is implicated in the process of apoptosis.

Inducible expression of IRF-1 results in increased expression of not only PKR and p21/WAF1, but also STAT1 as well as ISGF3 DNA binding activity, suggesting that IRF-1 tumour suppressor activity may involve a novel mechanism which activates the JAK-STAT pathway through STAT1 (Nguyen et al., 1997). Lysyl oxidase was identified as another IRF-1 target gene which may play a potential role in IRF-1 tumorigenicity (Tan et al., 1996).

2.2.8 IRF-1 and human disease

Clinical studies indicate that IRF-1 may function as an anti-oncogenic factor *in vivo*, preventing the development of some forms of human leukemia. This was initially hinted by the observation that IRF-1 gene mapped to the

chromosomal region 5q31.1 (Itoh et al., 1991) and deletion of this region is one of the most frequent cytogenetic abnormalities observed in patients suffering from leukemia and preleukemic myelodysplastic syndrome. However, in a study of 13 patients with leukemia or myelodysplastic syndrome (MDS) who exhibited cytogenetic abnormalities in 5q region, IRF-1 was the only gene found to be consistently deleted or rearranged in either or both alleles (William et al., 1993). It has been observed that splicing aberrations in IRF-1 gene also occur in high frequency in patients with leukemia and myelodysplastic syndrome (Harada et al., 1994). Thus the loss of IRF-1 function may be a critical event in the development of many human leukemias, although the involvement of other genes at 5q31 region has not been completely ruled out.

Bone marrow and peripheral mononuclear cells from patients with myelodysplastic syndrome (MDS) or leukemia secondary to MDS preferentially express an "exon-skipped" IRF-1 mRNA which lacks exons 2 and 3 and the protein product displays neither DNA binding nor tumour suppressor activities, suggesting a mechanism for inactivation of IRF-1 and subsequent development of human hematopoietic malignancies (Harada et al., 1994). Nucleophosmin (NPM)/B23/numatrin is a nuclear protein which was found to interact with IRF-1 and inhibit its DNA binding and transactivation activity (Kondo et al., 1997). NPM levels are elevated in several cases of human leukemia and human-derived leukemia cell lines. Expression of both IRF-1 and NPM is regulated during the cell cycle, with levels highest in G1 phase, while IRF-2 expression is unaffected (Harada et al., 1993 and Kondo et al., 1997). IRF-1 level is highest in early G1 phase, while NPM level peaks during late G1 phase. It has been suggested that IRF-1 may play a role in cancer development by a novel mechanism involving its association with and subsequent inactivation by NPM (Kondo et al., 1997). These studies thus implicated IRF-1 as a critical tumour suppressor, regulating oncogene-induced cell transformation or apoptosis (Tanaka et al., 1994). IRF-1-regulated genes

may be involved in the tumour suppressor activity of IRF-1 which may be mediated through PKR (Kirchoff et al., 1995; Yang et al., 1995; Kumar et al., 1997).

REVIEW OF LITERATURE

3. REVIEW OF LITERATURE

3.1. Identification of Interferon Regulatory Factor-1 (IRF-1)

Interferon regulatory factor-1 was cloned and characterised by Tadatsugu Taniguchi and coworkers from the Osaka University in 1988 which subsequently contributed a considerable scope for research in the field of interferon (IFN) and related cytokines. Human IFN-α1 and IFN-β genes were earlier reported to contain upstream promoter elements (virus response elements, VRE-α and VRE-β) that were induced by virus infection and this lead to activation of IFN gene transcription in mammalian cells in culture (Ryals et. al., 1986). Miyamoto et al. (1988) discovered mouse Interferon regulatory factor-1 (IRF-1) as a nuclear factor which specifically bound to the upstream regulatory region (-77 to -65) of the human IFN-β gene and mediated virus-induced transcription of the gene. IRF-1 was found to bind to the repeated hexanucleotide sequence $(AAGTGA)_4$ or $(GAAAGT)_4$ (Fujita et al., 1987). A λgt11 cDNA library prepared from mouse L929 cells was screened using multimerized (four times) AAGTGA sequence to isolate IRF-1 cDNA and recombinant IRF-1 protein was expressed in *E. coli.* Electrophoretic mobility shift assay (EMSA) of the recombinant IRF-1 protein produced a similar DNA-complex as virus-induced L 929 nuclear extract. Virus induction of mouse L 929 cells resulted in a time course dependent accumulation of IRF-1 mRNA which was followed by accumulation of the mRNA for IFN-β. Foot print analysis of the virus-inducible IFN-β gene promoter with the recombinant IRF-1 resulted in protection of the region, –100 to -64 corresponding well to the region protected by IRF-1 in L 929 cells following virus induction. Thus IRF-1 was proposed to be a positive regulatory transcription factor for the activation of IFN gene(s) by virus.

Murine IRF-1 was found to consist of 329 amino acids with the calculated molecular mass of 37.3 kd and the molecular mass of IRF-1 from L

929 cells was found to be 37.6 kd. The primary sequence of IRF-1 consisted of two distinct regions; a highly basic region (N-terminal amino acids 1-140) and another region (amino acids 140 to 329, the C-terminal region) that was biased for acidic amino acids and contained serine and threonine residues. The amino terminal half, was found to be rich in lysine and arginine residues. In fact, 31 out of 39 of the total lys and arg residues were located in this region. This region showed strong hydrophilicity and it was postulated that it may be primarily responsible for binding of IRF-1 to specific DNA sequence. In contrast to the amino-terminal region, the rest of the molecule (i.e., carboxy-terminal region) showed a relative abundance of aspartic acid (asp), glutamic acid (glu), serine (ser) and threonine (thr). Out of 189 amino acids (140 to 329), 33 (17%) represented acidic amino acids and 36 (19%) represented ser and thr. A cluster of five consecutive acidic amino acids was also found in 227 to 231. With regard to ser and thr, many appear to form clusters (at amino acids 153-156, 190-192, 206-208, and 220-222, referred as "S-T regions"). It was postulated that this region was most likely to form the transactivation domain. It was likely that IRF-1 played a crucial role in transcriptional induction of the IFN-β gene. The active form of IRF-1 with either increased binding affinity to the IFN-β gene or increased transcriptional activation properties, or both was proposed to be responsible for the virus-induced IFN-β gene transcription.

Watanabe et al. (1991) reported that casein kinase II (CK II) was involved in the phosophorylation of IRF-1 and in activating IRF-1 for binding to the IRF-E. It was earlier proposed that in view of its acidic nature, the carboxy-terminal region of IRF-1 could possess an intrinsic capacity for promoting transcription, similar to the yeast transcriptional activator GAL4 (Kakidani and Ptashne, 1988; Webster et al., 1988). Analysis of the cDNA corresponding to the human counterpart revealed that the human IRF-1 was shorter than the murine IRF-1 by four amino acids (325 instead of 329 amino acids). However, IRF-1 of the two species were highly conserved. In

particular, 133 out of 140 amino acids (95%) of the amino terminal DNA binding regions were identical in the two species. IRF-1 was found to be involved in the expression of genes such as IFN-α, MHC class I, and other IFN responsive genes. Fan and Miniatis, (1989) reported that IRF-1 binds to an element on the IFN-β promoter called PRDI (positive regulatory domain) which contained the -77GAGAAGTGAAAGT-65 region. Fujita et al. (1989) reported that overexpression of mouse IRF-1 cDNA in monkey COS cells resulted in the induction of endogenous IFN-α and IFN-β genes without virus induction. So IRF-1 was thus identified to be a powerful inducer of IFN-α and IFN-β genes.

A 500 bp Pst I promoter was also cloned by Miyamoto et al. (1988) by screening a λ-genomic library of L 929 cells. Two CAP sites for the IRF-1 mRNA were found in which the major site was located about 20 nucleotides downstream of the minor site. Typical TATA box sequence was not present within the upstream region of the gene. The promoter region was found to contain two GC boxes and one CAAT box. It was presumed that these sequences (GC and CAAT boxes) played a role in sustaining a basal level of gene expression. Transfection of the pIRFcat [Chloramphenicol acetyl transferase (CAT) reporter gene containing the IRF-1 promoter cloned upstream] construct into mouse L 929 cells gave rise to expression of low level CAT activity which was increased upon stimulation by New Castle Disease Virus (NDV). Deletion of 300 bp upstream sequence from this IRF-1 gene abolished both constitutive and induced expression of the CAT gene. It was concluded that the promoter of IRF-1 gene was virus-inducible thus explaining accumulation of IRF-1 mRNA following virus induction.

3.2 Identification of Interferon Regulatory Factor-2 (IRF-2)

Taniguchi and coworkers (Harada et al., 1989) subsequently isolated and cloned a cDNA which encoded a factor called Interferon regulatory factor-2 (IRF-2) on the basis of its hybridization to IRF-1 cDNA under low stringency. Interestingly, IRF-2 interacted with the same DNA sequence element as IRF-1 but unlike IRF-1, IRF-2 did not function as an activator, rather it suppressed the transcriptional function of IRF-1. IRF-2 is 62% identical with IRF-1 at its N-terminal region from 1-154 amino acids, whereas the rest of the molecule is only 25% related to IRF-1. A cluster of acidic residues observed in IRF-1 (amino acids 220 to 240) was missing in IRF-2. Overexpression of mouse IRF-2 in monkey COS cells failed to induce the expression of endogenous IFN genes. Even coexpression of both IRF-1 and IRF-2 did not induce IFN genes.

IRF-1 and IRF-2 were found to act as activator and repressor for the IFN-β gene and certain IFN-inducible genes respectively. The activation and repression functions of IRF-1 and IRF-2 were found to be present in their c-terminal i.e. transactivation/repression domains. Harada et al., (1989) used two chimeric proteins : One contained the N- terminal region of IRF-1 and C-terminal region of IRF-2 (IRF-1/2), another contained the N-terminal region of IRF-2 and C-terminal region of IRF-1 (IRF-2/1) and in COS cells, IRF-2/1 induced endogenous IFN gene expression, indicating that the N-terminal of IRF-2 was capable of binding to the promoters of the endogenous IFN genes. IRF-1/2 did not induce IFN genes rather suppressed IRF-1-mediated induction. So IRF-2 bound to the same promoter element on IFN genes as IRF-1 and IRF-2 possessed repression function in its C-terminal region.

3.3. Regulation of IRF-1 and IRF-2 in Embryonal Carcinoma cells

Expression of both IRF-1 and IRF-2 and IFN genes were reported to be developmentally regulated in mouse embryonic carcinoma (EC) cells (Harada, et al., 1989). The P19 (D^-) and F9 embroyonic carcinoma (EC) cells are undifferentiated cells. P19 cells differentiate into cells resembling fibroblasts or (D^+) P19 cells on treatment with retinoic acid, while F9 cells differentiate into cells resembling visceral extra embryonic endodermal cells or (D^+) F9 on retinoic acid treatment. It was observed (as depicted by the cartoon below) that in undifferentiated cells both IRF-1 and IRF-2 mRNAs were not detectable even when cells were infected with NDV.

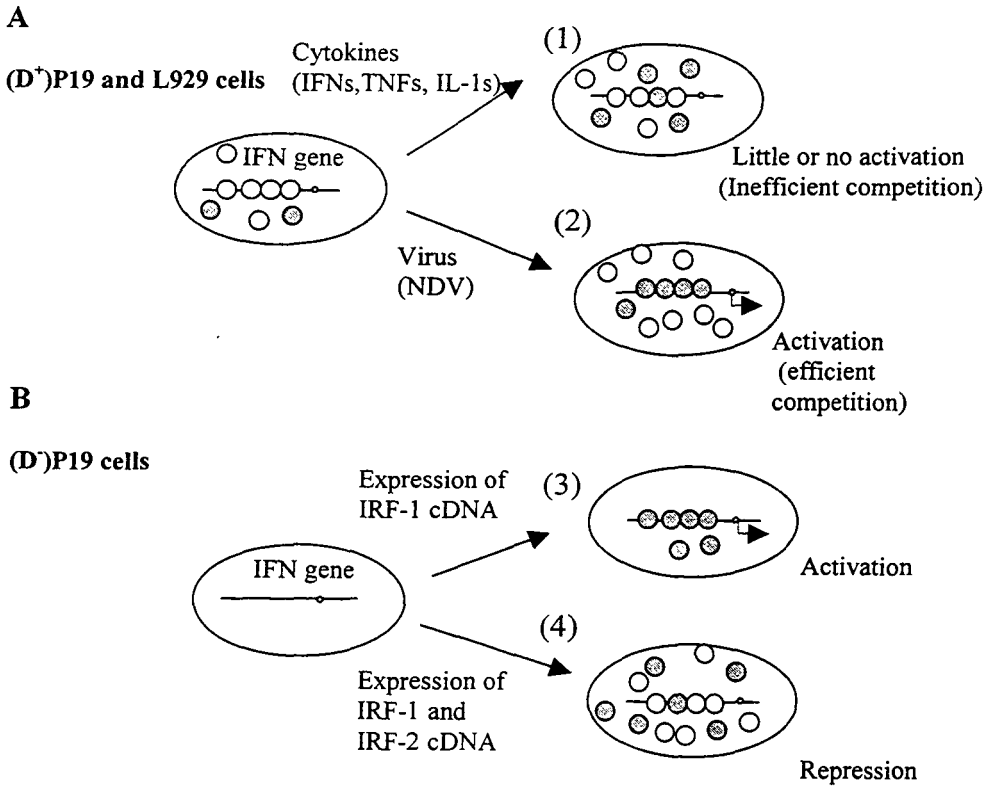

(Harada, et al., 1989)

Following differentiation of EC cells with retinoic acid, mRNAs for both IRF-1 and IRF-2 were easily detectable on induction by NDV. In (D^-) P19 cells, expression of IRF-1 cDNA induced the production of IFN-β, but when both IRF-1 and IRF-2 were transfected in the same cell, there was no IFN-β induction, proving that IRF-2 acted as a repressor (shown above). However, in (D^+) P19 differentiated cells, the IRF-2 effect predominated, as in L929 cells. The activation of endogenous IFN-α genes, upon IRF-1cDNA transfection, was inefficient in (D^+) P19 cells compared to (D^-) P19 cells. It appeared that IRF-2 might normally function as a 'safety valve" for the IFN gene in order to control IFN overproduction through the action of IRF-1, after induction with a stimulus, not like virus, such as a cytokine. In normally differentiated cells, IRF-2 might remain bound to the IFN genes, thus repressing induction. IRF-2 has a greater affinity for the DNA sequence than IRF-1 under uninduced conditions. When cells are induced by a virus, the IRF-1 level increases and it also undergoes modifications that would generate a form of IRF-1 with higher DNA binding affinity (hence it can replace IRF-2) leading to efficient activation of the IFN system. This model system of regulation of IFN genes by IRF-1 and IRF-2 subsequently increased scientific attention on these two transcription factors. However, IRF-1 knock out (IRF-$1^{-/-}$) mice revealed that IFN-α/β and some IFN-inducible genes can be activated following virus induction in the absence of IRF-1 (Matsuyama et al., 1993; Reis et. al., 1994). This led to search for other functions of IRF-1 and additional factors for IFN gene expression.

3.4.4. Other IRF family members

IRF-1 and IRF-2 are the two founder members of a growing family of IRF transcription factors. In recent past extensive reviews on IRF family have been published (see Nguyen et. al., 1997 and Mamane et. al., 1999). Other memebers of IRF family are as follows:

3.4.1. Interferon Consensus Sequence Binding Protein (ICSBP)

Diggers et al. (1990) reported that interferons (IFNs) induced transcription of major histocompatibility complex (MHC) class I gene through the conserved IFN consensus sequence (ICS) that contained an IFN response motif shared by many IFN-regulated genes. By screening mouse λZAP expression libraries with ICS probe, a cDNA clone was isolated that encoded a protein which bound to the ICS and was designated ICSBP. It was observed that ICSBP not only bound to ICS but also to IFN response motifs of many IFN-regulated genes as well as a virus-inducible element of the IFN- β gene. The ICSBP cDNA encoded 424 amino acids and a long 3' untranslated sequence, the protein size being 48.2 kd. The 3' untranslated region contained a ATTTA sequence and a number of AT streches, which was responsible for the mRNA being unstable. The N-terminal 115 amino acids of the ICSBP formed a putative DNA binding domain.

ICSBP is the third member of IRF family. IRF-1 and IRF-2 showed some similarity in their C-terminal regions, but ICSBP showed no similarity to IRF-1 or IRF-2 in this region. ICSBP mRNA was found to be expressed predominantly in lymphoid tissues and was induced by IFN-γ. The induction by IFN-γ appeared to predominate in lymphocytes and macrophages, implying that ICSBP might play a regulatory role in cells of immune system.

Sequence comparison studies revealed that ICSBP was more similar to Interferon stimulated gene factor 3 γ (ISGF3γ) than to IRF-1 or IRF-2. Unlike IRF-1, IRF-2, IRF-3 and ISGF3γ, ICSBP exhibited a tissue–restricted pattern of expression and was expressed exclusively in cells of the immune system. Expression of ICSBP was constitutive and could be dramatically enhanced by IFN-γ but not by IFN-α/β. Activation of ICSBP was rapid and independent of *de novo* protein synthesis. Unique to ICSBP was also its very weak DNA binding affinity. ICSBP DNA binding was dramatically increased following

interaction with IRF-1 and IRF-2 (Sharf et al., 1997). It was found that ICSBP not only recognized the ISRE of MHC class I gene, but also of other IFN-inducible genes such as ISG 54, 2'5'OAS and 6-16. ICSBP also bound to the promoter of IFN-β (Driggers et al., 1990). ICSBP could repress IRF-1-mediated induction of MHC class I and IFN-β promoter in the absence of IFN treatment (Nelson et al., 1993). These ICSBP-mediated inhibitory effects were alleviated by either IFN-β and IFN-γ treatment, indicating that ICSBP has a role similar to IRF-2 in selectively repressing ISRE- and PRDI-containing promoters. ICSBP also inhibited DNA binding activity of p48 (see below), although direct association between these two proteins has not been demonstrated (Bovolenta et al., 1994).

Structure of ICSBP comprised of two components, a DBD and a repressor domain (Sharf et al., 1995). DBD of ICSBP also inhibited expression of IFN-inducible genes such as ISG 54, 2'5'OAS, IRF-2, PKR and STAT1 (Thornton et al., 1996). This inhibition was not observed in cells expressing full length ICSBP. Cell lines expressing DBD of ICSBP grew slower than control cells, while the parental wild-type ICSBP clones exhibited normal growth rate. This phenotype was in contrast to the oncogenic activity of IRF-2, observed when DBD of IRF-2 was expressed in NIH3T3 cells (Naguyen et al., 1995). ICSBP interacted with IRF-1 and IRF-2 both *in vitro* and *in vivo* and this interaction greatly enhanced the otherwise very low binding affinity of ICSBP to the ISRE (Sharf et al., 1997; Bovolenta et al., 1994). The region involved in the IRF-ICSBP interaction was mapped to a 177 amino acid region (200-377) in the C-terminal repressor domain of IRF-1, IRF-2 and ICSBP. Interestingly, this region, now called the IRF association domain (IAD), was found to be conserved amongst many IRF family members, including IRF-3, IRF-4, IRF-5, and p48 (Sharf et al., 1997). Direct binding of ICSBP to DNA was prevented by tyrosine (Tyr) phosphorylation *in vitro* hence its failure to be detected by EMSA (Driggers et al., 1990). The ICSBP/IRF-2 complex was

found to be constitutively expressed, while ICSBP/IRF-1 DNA binding was induced by IFN-γ.

As with IRF-1- and IRF-2 deficient mice, ICSBP knock out ($ICSBP^{-/-}$) mice exhibited immunodeficiencies and dysregulated hematopoiesis, demonstrating a role of ICSBP in the proliferation and differentiation of hematopoietic progenitor cells (Holtschke et al., 1996). Unlike IRF-1 and IRF-2 knockout mice, homozygous $ICSBP^{-/-}$ and heterozygous $ICSBP^{+/-}$ mice displayed an obvious pathological change, a syndrome similar to human chronic myelogenous leukemia. These mice were also selectively sensitive to particular viral infections, demonstrating a critical role for ICSBP in the establishment of antiviral state. Spleen cell extracts from ICSBP knock out mice predictably did not display ICSBP or ICSBP-IRF-2 complex DNA binding activity. Wild-type ICSBP mice survived VV or LCMV infections but $ICSBP^{-/-}$ mice died within 10-20 days after infection (Holtschke et al., 1996). The antiviral activity exhibited by ICSBP extended to infection by human immunodeficiency virus-1 (HIV-1) (Thornton et al., 1996). The ICSBP DBD strongly inhibited infection by VSV and HIV when stably expressed in monocytic U937 cells. The HIV-1 genome contains an ISRE-like sequence 3' to the transcription site that binds IRF family proteins (Thornton et al., 1996).

3.4.2 ISGF3γ/p48

Interferon stimulated gene factor-3 gamma (ISGF3γ) or p48, generally exerts its transcriptional activities exclusively in association with signal transducer and activator of transcription 1 (STAT1 or p84/p91) and STAT 2 (p113) proteins. The latter two are collectively named as ISGF3γ, activated through specific phosphorylation events by type I IFNs (Levy et al., 1995; Veals et al., 1992; Bluysscn et al., 1996). This tri-molecular complex, termed ISGF3, is formed within minutes of IFN treatment and participates in the transcriptional activation of a large number of IFN-inducible genes by binding

to ISRE. In this regard, p48 functions as an immediately early protein. p48 is constitutively expressed but is also inducible by IFN-γ and viral infection (Veals et al., 1992, Kawakami et al., 1995). p48 recognizes and binds to the various ISREs and serves as an essential DBD subunit of the ISGF3. Association with ISGF3α increases p48 DNA binding activity by 25-fold, indicating that phosphorylation is essential for DNA binding affinity (Kessler et al., 1990). Like IRF-1 (Pinne et al., 1990), treatment with calf intestinal phosphatase (CIP) inhibited p48 DNA binding acivity. Removal of the N-terminal 9 amino acids of p48 dramatically decreased DNA binding affinity and specificity, demonstrating that the first 9 amino acids are essential for DNA target specificity. A 160 amino acid region responsible for ISGF3α-p48 interaction mapped to the C-terminal amino acids 217 to 377 of p48. A chimeric protein consisting of the DBD of IRF-1 fused to this interaction domain associated with ISGF3α and bound DNA in an IRF-1-specific manner (Veals et al., 1993).

3.4.3 Role of p48 and ISGF3 in type I IFN activation

The existence of IRF-1 dependent and independent pathways leading to IFN-β gene expression has been proposed. The U2 cell line, which carries mutations within both p48 alleles, exhibits defective antiviral responses to type I and type II IFN (John et al., 1991). p48 and ISGF3 associate with the IRF-Es of the IFN-β gene. The Fujita group showed that ISGF3 binds IRF-E with a higher affinity than IRF-1 and IRF-2 (Yoneyama et al., 1996). Mutations within the IFN-β promoter that affect gene expression in response to NDV also prevent p48 DNA binding (Kawakami et al., 1995). These results supported a novel role for p48 in the regulation of IFN-β gene expression in response to NDV infection. In the U2 cell line, the establishment of the antiviral state by $p48^{-/-}$ and $IRF^{-/-}$ $p48^{-/-}$ MEFs in response to type I and type II IFN responses was severely impaired following infection by at least three viruses. The most

dramatic impairment occurred with EMCV and less severe with VSV and HSV. This phenotype was similar to that seen in the type I IFN receptor (Muller et al., 1994) and STAT1 knock out mice (Meraz et al., 1996), thus reinforcing the importance of ISGF3- mediated IFN signal transduction in the activation of IFN gene expression. The ISGF3 complex was detected in wild type but not $p48^{-/-}$ MEFs following induction by NDV (Harada et al., 1996). Type I IFN induction exhibits cell-type specificity in p48 deficient mice. In $p48^{-/-}$ MEFs, NDV induction of IFN-α mRNA was reduced by 40x fold, while IFN-β mRNA levels were decreased only up to 2x fold. IFN was still detected in the MEFs' culture supernatant, suggesting the involvement of factor(s), distinct from p48, which may bind to the IFN promoters and mediate IFN gene induction by NDV. (Harada et al. 1996).

3.4.4 IRF-4 (Pip/ICSAT/LSIRF)

a. IRF-4 in B-lymphocytes

The discovery of another member of IRF family resulted from an effort to clone factor(s) binding to the murine immunoglobulin light chain enhancer E λ2- 4 (Eisenbeis et al., 1995). PU.1 interaction partner or Pip was identified as novel murine transcription factor with IRF-like N-terminal domain. Pip bound to DNA, but exclusively in association with PU.1, a member of ETS family of transcription factors that contributes to development of lymphoid and myeloid lineages (Crepieux et al., 1994). Serine phosphorylation at amino acid 148 of PU.1 was required for PU.1-IRF-4 interaction and subsequent binding of the heterodimer to ISRE-like λB site in Ig enhancer region (Eisenbeis et al., 1995; Brass et al., 1996). Recent studies by Brass et al. (1999) have shown that IRF-4/PU.1 binding is co-operative and regulated by multiple interdependent DNA-protein and protein-protein interactions.

A model of IRF-4/PU.1 complex activation has been proposed: following interaction of IRF-4 with PU.1 and DNA, IRF-4 undergoes a conformational

change that swivels the regulatory domain (amino acids 170-450) away from its own DBD (amino acids 1-150), and into direct contact with the PEST region of PU.1. Ortiz et al. (1999) also delimited the IRF-4 interaction domain to residues 245-422. Site directed mutagenesis of the conserved amino acids within two predicted α-helices confirmed the importance of these residues for IRF-4-PU.1 DNA binding and transactivation. These two α-helices are also highly conserved amongst the IRF family members and could, therefore, be involved in heterodimerization with other transcription factors (Ortiz et al. 1999). The role of IRF-4 as a transcriptionally activating partner in B cells was further reinforced by the observation that IRF-4 interacts with E47, a component of the E2A transcription factor. The ubiquitously expressed E2A is crucial for the normal B cell development and is composed of E12 and E47, which are two splice variants of the same gene. $E2A^{-/-}$ mice fail to develop B cells past the pro-B-cell stage (Nagulapalli and Atchison, 1998). IRF-4 was shown to bind together with E47 to the immunoglobulin κ 3' enhancer region and to generate a 100 fold transcriptional synergy in a reporter assay.

b. IRF-4 in T lymphocytes

Another group cloned IRF-4 as a lymphoid specific IRF (LSIRF) (Matsuyama et al., 1995), expressed at all stages of B cell development and in mature T cells. IRF-4 expression was also inducible in primary lymphocytes by antigen mimetic stimuli such as Concanavalin A, CD3 cross linking, anti-IgM and PMA treatment, whereas expression was not induced by IFNs or TNFα. IRF-4 deficient mice $IRF\text{-}4^{-/-}$ were generated and, like many other $IRF^{-/-}$ mice it developed severe immunodeficiencies (Mittrücker et al., 1997). A normal T- and B-cell distribution was observed at 4 to 5 weeks of age, but with time $IRF\text{-}4^{-/-}$ mice gradually exhibited severe lymphadenopathy. Both B- and T-cell activations were profoundly affected: serum immunoglobulin concentrations and antibody responses were decreased and cytotoxic and

antitumor responses were absent in IRF-4 knock out mice. Normal early T-cell events, such as calcium influx and expression of the T-cell activation markers CD25 and CD69 in IRF-$4^{-/-}$ T-cells, indicated that IRF-4 might function at later stages of T cell activation, possibly at the level of IL-2 production and /or IL-2 response. This hypothesis was supported by the observation that the reduced T-cell proliferation in these mice was not reserved by exogenous IL-2 treatment; thus IRF-4 appears to be essential for the function and homeostasis of both mature B and mature T lymphocytes.

c. IRF-4 in adult and T cell leukemia

The human equivalent of IRF-4 was isolated from an adult T-cell leukaemia cell line as the IFN consensus sequence-binding protein in adult T-cell leukaemia cell lines or activated T-cells (ICSAT) (Yamagata et al., 1996). Like murine IRF-4, ICSAT was structurally similar to ICSBP, and its expression was not inducible by IFN. However, ICSAT/IRF-4 possessed a very different function compared with its murine counterpart; whereas PU.1-IRF-4 functioned as a transactivator complex, ISCAT exerted an IRF-2 and ICSBP-like repressive effect on IFN- and IRF-1-induced gene activation. ICSAT/IRF-4 was expressed exclusively in a restricted subset of lymphocytes; only T-cells treated with phorbol myristate acetate (PMA) or infected with the human T-cell leukaemia virus-1 (HTLV-1) produced IRF-4. Jurkat cells transiently transfected with the HTLV-1 Tax gene also expressed IRF-4, indicating that Tax may activate the IRF-4 promoter (Yamagata et al., 1996).

3.4.5 IRF-3

I. IFN regulation by IRFs

IRF-1 was cloned and described as a positive regulator of IFN-β gene induction whereas, IRF-2 suppressed IFN-β gene expression (Miyamoto et al., 1988, Fujita et al., 1989; Harada et al., 1989, 1990). The essential role of IRF-1 in the regulation of IFN-α and IFN-β genes became controversial with the observation that mice containing homozygous deletion of IRF-1 gene (IRF-$1^{-/-}$) or cells derived from these mice were not impaired for IFN-α and IFN-β gene expression following virus infection (Matsuyama et al., 1993). In contrast, homozygous deletion of ISGF3γ/p48 or STAT1, or IFN receptors abolished the sensitivity of these mice to the antiviral effect of IFNs, and virus-infected macrophages from $p48^{-/-}$ mice showed impaired induction of IFN-α and IFN-β genes. The fact that targeted disruption of these IRF family members did not abolish induction of IFN genes in response to virus infection led to the search for other IRF family members that would be involved in IFN gene expression. Two groups had also described high molecular weight DNA binding complexes, termed VIF (virus induced factor) and DRAF (double stranded RNA activated factor), binding to ISRE-like sequences that were specifically induced by virus infection or double stranded RNA (dsRNA) treatment and which had an IFN and protein synthesis-independent activation mechanism (Daly and Reich, 1993; Génin et al., 1995). However, their precise molecular nature and their activation mechanism remained to be elucidated. IRF-3 has been recently characterised as a component of the DRAF1 complex (Weaver et al., 1998). Among the IRF family members, IRF-3 and IRF-7 have recently been identified as key regulators for the induction of IFN-β gene.

II. IRF-3 phosporylation as a signal for activation

The IRF-3 gene encodes a protein of 427 amino acid (55 kd) that is expressed constituitively in all tissues (Au et al., 1995) and is present as a single copy gene that locates to chromosome 19q13-13.4 (Bellingham et al., 1998). At the amino acid level, IRF-3 has the highest homology to ICSBP and ISGF3γ (Nguyen et al., 1997). Although it was first characterised as a potential repressor of IFN gene expression (Au et al., 1995; Schafer et al., 1998). IRF-3 demonstrates a unique response to virus infection. Latent cytoplasmic IRF-3 is post-translationally modified and activated through phosphorylation of specific serine residues located on its C-terminal end as a consequence of virus infection or treatment with dsRNA (Lin et al., 1998; Wathelet et al., 1998; Weaver et al., 1998; Yoneyama et al., 1998). This modification leads to dimerization, cytoplasm to nuclear translocation, association with the p300/CBP co-activator and stimulation of DNA binding and transcriptional activities (Hiscott et al., 1999). IRF-3 phosphorylation ultimately results in its degradation via the ubiquitin-mediated proteasome pathway (Lin et al., 1998; Ronco et al., 1998). Yoneyama et al. (1998) localized the carboxy-terminal phosporylation sites to ser 385 and ser 386. Point mutations of either of these two sites to alanine were generated and the mutant were no longer activated by virus infection (Yoneyama et al., 1998; Lin et al., 1998).

III. Structural and functional analysis of IRF-3

Using deletion mutagenesis and one hybrid analysis, a strong but atypical transactivation domain was identified between amino acids 134 and 394 of IRF-3. This transactivation domain contains a NES (nuclear export signal), the proline-rich region and the IAD. This region is flanked by two autoinhibitory domains, one region located at the carboxy-terminal end of IRF-3 (amino acids 407-427) and the second overlapping with the DNA binding and the proline-

rich region between amino acids 98 and 240. These two domains interact with each other to generate a closed conformation that masks the IAD and DBD to prevent nuclear translocation and subsequent DNA binding in uninfected cells (Lin et al., 1999). Removal of either of these two autoinhibitory domains permits DNA binding and low level of transactivation in absence of virus infection.

Following virus infection, inducible phosphorylation of IRF-3 at the carboxy-terminus relieves the intramolecular interaction between the two autoinhibitory domains, unmasking the IAD and DBD. The conformational change in IRF-3 results in the formation of homodimers through IAD. IRF-3 dimers are then able to translocate to the nucleus, associate with CBP/p300 co-activator and bind to DNA at ISRE and PRDI-PRDIII-containing promoters (Lin et al., 1999). The CBP/P300 co-activator contains several domains that interact with transcription factors. In virus-infected cells, the carboxy-terminal domain of CBP/P-300 associated with phosphorylated IRF-3 (Lin et al., 1998).

IV. IRF-3 and cellular response to viruses

IRF-3 is targeted by several different classes of viruses, although most studies has been performed with paramyxoviruses, Sendai and Newcastle Disease Virus as classical activators of IFN production (Lin et al., 1998; Wathelet et al., 1998, Weaver et al., 1998; Yoneyama et al., 1998). Navarro et al., 1998 showed that human cytomegalovirus (HCMV) induced DNA binding of an IRF-3/CBP complex that activated ISG 54 gene transcription by a protein synthesis-independent and STAT-1-independent mechanism. Juang et al. (1998) provided indirect evidence that vesicular stomatitis virus (VSV) may also activate IRF-3. The antiviral effect was dependent on the functional JAK-STAT signalling and is likely to be due to increased IFN production (Juang et al., 1998). Since dsRNA was shown to induce IRF-3 association and nuclear translocation, this intermediate of virus replication could be a signal that

triggers IRF-3 activation (Weaver et al., 1998; Yoneyama et al., 1998). Earlier studies have shown that EIA gene was able to induce formation of DRAF complex containing IRF-3 (Daly and Reich, 1993).

Another viral product, the E6 protein from human papillomavirus 16 (HPV16), was shown to interfere with IRF-3-mediated activation of IFN-β gene expression in response to Sendai virus infection (Ronco et al., 1998). New studies demonstrated that IRF-3 also plays a role in mediating virus-induced apoptosis. This constitutively active form of IRF-3, IRF-3 (5D), induced apoptosis in human embryonic kidney 293 and Jurkat T cells, whereas wild type IRF-3 alone did not induce apoptosis. Viral infection of cells, overexpressing wild type IRF-3, enhanced apoptosis by two to three fold, thus demonstrating that activation of IRF-3 can initiate apoptotic signalling.

3.4.6 IRF-7

IRF-7 was first described to bind and repress the Qp promoter region of the Epstein Barr Virus (EBV)-encoded gene EBNA-1, which contains an ISRE-like element, IRF-7 is found in multiple forms, suggesting that the IRF-7 gene encodes different splicing variants (Zhang and Pagano, 1997; Nonkwelo et al., 1997) but *in vitro* translated IRF-3 produced a protein of 67 kd (Au et al., 1998). Unlike IRF-3, IRF-7 is not expressed constitutively in cells, rather its expression is induced by IFN, LPS and virus infection. As with IRF-3, virus infection appears to induce phosphorylation of IRF-7 at its carboxy terminus, which is highly homologous to the C-terminal end of IRF-3 (Marie et al., 1998; Sato et al., 1998). IRF-7 localizes to cytoplasm in uninfected cells and translocates to nucleus after phosphorylation (Au et al., 1998; Sato et al., 1998). Potential ser residues as targets for inducible phosphorylation, by homology to IRF-3, have been identified by Marie et al, (1998) and Sato et al. (1998).

4.7 Role of IRF-3 and IRF-7 in IFN gene induction

Cummulative molecular studies with IRF-3 and IRF-7 suggested a new model for IFN gene activation. Type I IFN genes can be subdivided into two groups: (1) immediately early genes activated in response to virus infection by a protein synthesis-independent pathway (IFN-β and murine IFN-α4), (2) delayed-type genes which include other IFN-α subtypes whose expression is dependent on *de novo* protein synthesis (Marie et al., 1998). Following virus infection, IRF-3, NF-κB and ATF-2, c-Jun are post-translationally activated by inducer–mediated phosphorylation. These proteins cooperate to form a transcriptionally active enhancesome at IFN-β promoter, together with CBP/p300 transcriptional co-activator and chromatin associated HMG protein (Falvo et al., 1995; Thanos and Maniatis, 1995; Kim and Maniatis 1998; Parekh and Maniatis , 1999). IRF-3 also upregulates IFN-α4 expression in murine cells (Marie et al., 1998). Secreted IFN produced from a subset of initially infected cells acts through an autocrine and paracrine loop that requires intact IFN receptor and JAK-STAT pathways. IFN activation of ISGF3 complex results in the transcriptional upregulation of IRF-7 (Marie et al., 1998; Sato et al., 1998). Virus infection activates IRF-7 through inducible phosphorylation, and phosphorylated IRF-7 participates together with IRF-3 in transcriptional induction of immediate-early and delayed type IFN genes (Marie et al., 1998 Sato et al., 1998). In mice with a targeted disruption of either STAT-1, p48 or type I IFN receptor, IRF-7 is not upregulated, hence the amplification loop of IFN induction is not observed. Finally, the formation of distinct homo- and heterodimers between activated IRF-3 and IRF-7 may lead to differential regulation of IFN-α genes.

IRF member	Expression pattern	Inducers of expression	Transcriptional role	Known target genes	Physiological roles	Knockout phenotype	Role in resistance of
IRF-1	Most cell types Low level Constitutive Inducible	Type I IFN Type II IFN Virus infection dsRNA TNF IL-1 IL-6 LIF Con A Ca^{2+} ionophore A23187 PMA	Activator	IFN α IFN β 2'5'OAS MHC Class I GBP iNOS PKR ICE WAF-1 STAT1 Lysyl oxidase IRF-2 EBNA-1 LMP-2 TAP-1	Tumor supressor Antiviral defense Immune regulation	Impaired $CD8^+$ cell maturation	EMCV (picornaviradae)
IRF-2	Most cell types Constitutive Inducible	Type I IFN IRF-1 Virus infection	Repressor	IFN β Histone H4 EBNA-1	Oncogene Antiviral defenses Immune regulation	Bone marrow supression of hematopoiesis and B lymphopoeisis	LCMV (arenavirus)
IRF-3	Most cell types Constitutive Inducible	PHA TPA	Activator	ISG-15 IFN α IFN β	Immune response	N/A	Paramyxo virus

IRF member	Expression pattern	Inducers of expression	Transcriptional role	Known target genes	Physiological roles	Knockout phenotype	Role in resistance of
ISGF3γ/ p48	Most cell types Constitutive	Type II IFN Virus infection	Activator	Many ISRE containing IFN- inducible genes IFN α IFN β	Antiviral defense	Impaired antiviral response	NDV (Paramyxoviradae) EMCV (picornaviradae) VSV (Rhabdoviridae) HSV (Herpesviridae)
ICSBP	Cells of macrophage and lymphoid lineages Low level Constitutive Inducible	Type II IFN	Repressor	MHC I ISG-54 2'5'OAS 6-16 IFN β	Antiviral defense Immune regulation	Deregulated hematopoeisis Human CML - like syndrome	VV (poxviridae) LCMV (arenavirus) HIV (retroviridae) VSV (Rhabdoviridae)
IRF-4	Activated T-cells ATL cells	PMA HTLV-1 Tax	Repressor	Unknown	Immune regulation	Severe lymph adenopathy Impared T and B cell activation	N/A

Summary of the properties and functions of IRFs

3.4.7 vIRFs

Human Herpes Virus 8 (HHV-8) is the etiologic agent of Kaposi's sarcoma, which is frequently observed as a complication of late stage HIV infection. HHV-8 encodes four IRF homologs, termed vIRFs, that inhibit responses to type I and II interferons and block IRF-1-mediated transcription, vIRF-1, a protein of 442 amino acids does not compete with IRF-1, but seems to inhibit IFNs and IRF-1 through an yet undefined mechanism (Li et al., 1998; Zimring et al., 1998). By inhibiting IFNs and IRF-1, HHV-8 may interfere with the antiviral immune response and growth suppression. vIRF-1 also confers resistance of Daudi human B lymphocytes to anti-proliferative effects of IFN-α. By inhibiting IRF-1 transactivation of IFN-inducible genes, vIRF abolishes IFN-mediated growth control in these cells. vIRF-2, a protein of 147 amino acids, has been characterised from HHV-8 (Burysek et al., 1999). vIRF-2 has distinct expression pattern and characteristics compared with the cellular IRFs or vIRF-1 and low levels of vIRF-2 mRNA are detected in HHV-8 positive BCBL-1 tumor cell line. Recombinant vIRF-2 forms homodimers *in vitro* and interacts with several IRFs *in vitro* (Burysek et al., 1999).

3.4.8 Cross-regulation among IRF family members

In addition to participating in the regulation of many IFN-inducible genes, the IRFs also regulate expression of each other. For example, IRF-2 promoter contains an IRF consensus site which is activated by IRF-1 (Cha, et al 1994). IRF-2 expression is inducible by transient or stable IRF-1 expression (Harada et al 1994), suggesting that IRF-1 may play a role in the regulation of its partner IRF-2 gene. An IFN-γ activated sequence was identified in the IRF-1 and murine ICSBP promoter and was shown to be bound by STAT1 (p91)

subunit of ISGF3 (Pine et al., 1994). Activation via Tyr-phosphorylation of STAT 1 correlates with transcription of IRF-1 in response to IFN-γ treatment, thus establishing a direct link between the IFN JAK-STAT signal transduction pathway and IRF expression. (Pine et al., 1994)

Furthermore, IRF-1 upregulates STAT1 expression as well (Nguyen et al., 1997), implying feedback regulation of STAT1 expression by IRF-1. Both IRF-1 and IRF-2 gene promoters contain the consensus binding site for the NF-κB family of transcription factors which in their own right play a role in the expression of IFN-β as well as many other immunoregulatory genes (Cha and Deisseroth 1994; Harada et al 1994, Sims et al., 1993). Cross-regulation of expression among the IRFs and interactions among IRF family members suggest a complex gene network in the regulation of IFN system. IRF-1 is one of these important genes.

3.5 Target genes of IRF-1

IRF-1 is involved in a network of gene expression to regulate different cellular functions. IRF-1 is induced by virus, Con A (Miyamoto et al., 1988), type I and type II IFNs, poly (rI.rC), TNF-α, IL-1, PMA (Fujita et al., 1989), IL-6, Leukemia inhibitor factor (LIF) (Abdollahi et al., 1991), prolactin (Yu-Lee et al., 1990). IRF-1 functions by regulating a number of cellular processes directly or indirectly such as anti-viral response, antiproliferation, development of NK cells, immune response against intracellular parasites, antioncogensis, cell grwth regulation, apoptosis and others.

IRF-1 binds to promoters of a number of genes. For example, IRF-1 binding to IFN-β–promoter upregulates the production IFN-β, which acts as an antiviral agent during viral infection (Miyamoto et al., 1988). IRF-1 knock out mice (IRF-$1^{-/-}$) have been shown to exhibit a severe NK cell deficiency, but when bone marrow cells from these mice were cultured with IL-15 they could generate functional NK-cells. So it meant that IL-15 gene is transcriptionally

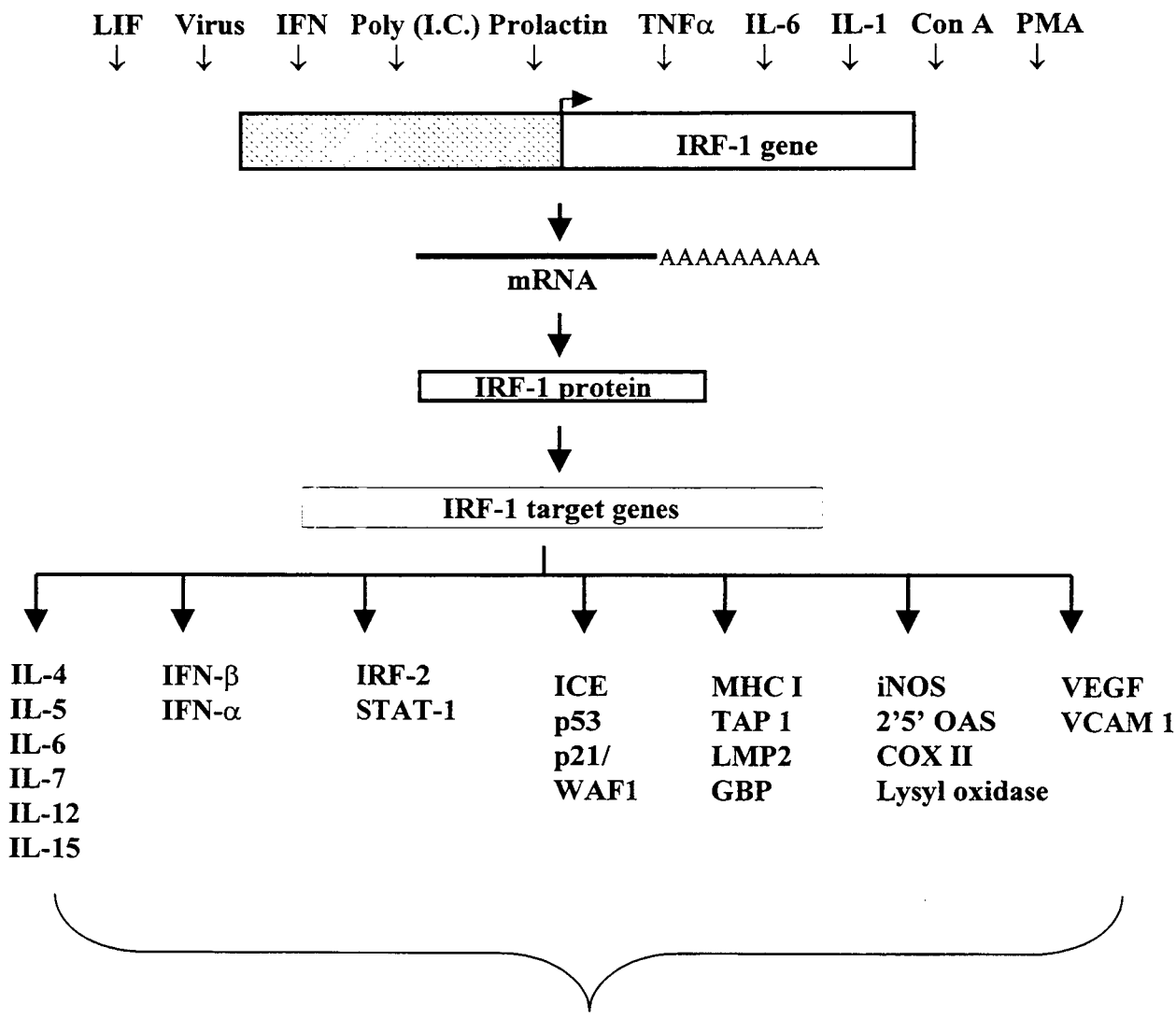

Induction of IRF-1, IRF-1-regulated genes and cellular response

regulated by IRF-1 (Ogasawara et al., 1998). Macrophages from IRF-$1^{-/-}$ mice synthesized barely detectable iNOS mRNA in response to stimulation by IFN-γ + LPS (Reis et al., 1994 and Kamijo et al., 1994). IRF-1 was found to regulate the production of inducible nitric oxide synthase (iNOS), which in turn forms nitric oxide and that is responsible for killing intracellular infectious agents (Kamijo et al., 1994). Within the iNOS promoter sequence two adjacent potential IRF-1 binding motifs have been reported (Tanaka et al., 1993) . In T lymphocytes, Interleukin-β Converting Enzyme (ICE) gene which participates in DNA-damage induced apoptosis, is also regulated by IRF-1 (Tamura et al., 1995).

IRF-1 is also involved in regulating the function of several other genes such as MHC class I (Miyamato et al., 1988) Guanylate Binding Protein (GBP) (Kimura et al.,1994; McKinsey et al., 1996), p21/WAF1, a member of the family of cylin-dependent kinase inhibitors which plays a primary role in cell cycle regulation (Ozawa et al., 1996), STAT1, the IFN-γ-mediated signalling molecule (Nguyen et al., 1997), lysyl oxidase which play a role in tumorigenicity (Tan et al., 1996), IRF-2, repressor of IRF-1 also having oncogenic effect (Harada et al.,1994), LMP-2, TAP-1, involved in the function of MHC class I (White et al., 1996), 2' 5' OAS which is responsible for the synthesis of 2'5' oligoadenylate cofactors for RNase L that degrades RNA in cells infected with viruses (Reis et. al., 1992), etc. The schematic representation below shows a number of inducers for the activation of IRF-1 gene and subsequently a number of target genes that are induced by IRF-1 leading to many cellular functions. The inducers are viruses, double stranded RNA (ds RNA) or poly (rI.rC.), IFNs etc. The IRF-1-activated genes are IFN-β, iNOS, VCAM-1, 2'5' OAS and others. Thus IRF-1 is involved in a network of gene activity in mammalian cells.

3.6 Physiological significance of IRF-1 and future prospects

Under normal conditions IRF-1 in most mammalian cells occur at a low level. Several physiological substances like cytokines (IFNs, TNF etc.) and pathological agents (viruses, bacteria and other pathogens) and conditions (ischemia, infection etc.) are known to induce IRF-1 gene expression. IRF-1, in turn, activate many IRF-1-dependent genes (mentioned above) and influence the gene expression pattern and therefore cellular environment. Primarily, there are four types of effects of IRF-1: (1) direct effects due to expression of IRF-1-dependent genes, e.g. antiviral effects of IFN, 2'5'OAS etc., (2) indirect effects due to activation of further gene expression due to other transcription factors, e.g. IRF-2, STAT1, p53 etc. and (3) effects due to activation of cytokines and growth regulatory molecules e.g. interleukins 4, 5, 6, 7, 15; VCAM-1, VEGF etc. as well as (4) cell growth arrest and apoptotic effects due to activation of p21/WAF1 CDK-inhibitor, ICE protease etc. There are many more aspects of IRF-1 which need to be studied more carefully in future. They include how IRF-1 protein is regulated at post-translational level? Is there any other ser-thr kinase which phosphorylate IRF-1 other than CK II ? What are the differences between phosphorylated and unphosphorylated IRF-1 in terms of molecular properties ? Is any of these properties linked to any specific function of IRF-1 such as transcription ? Are there differences in the functional specialisation of IRF-1 between mouse and man, especially with reference to the transcriptional activation domain ? If cellular concentrations of IRF-1 and IRF-2 are regulated in coordination, how IRF-2 is also accordingly regulated ? Is IRF-1 involved in any of the death pathway function other than activating ICE gene ? Answers to these questions will define over all function of IRF-1 on a more broad base to address and evaluate its physiological significance.

STATEMENT OF THE PROBLEM

4. STATEMENT OF THE PROBLEM

Interferon regulatory factor-1 (IRF-1) belongs to the IRF-family of transcription factors involved in the regulation of many genes, the expression of which are induced by pathogens like viruses, physiological inducers like cytokines, growth factor(s) and hormone(s) as well as certain other agents. IRF-1 occupies an important position in regulation of the cytokine network. Most studies highlighting function of IRF-1 have been carried out in murine and human cell lines as well as in IRF-1 knock out mice using various inducers. However, information on expression of IRF-1 gene in different tissues of mouse under normal physiological conditions is limiting.

Murine and human IRF-1 genes are highly similar, still certain properties of the human IRF-1 gene have been shown to be different from that of the mouse. So it is important to study the organization of mouse and human IRF-1 genes and find out their differences.

Comparison of the amino acid sequence of IRF-1 in mouse and human may provide interesting information. The N-terminal DNA binding domains of murine and human IRF-1 interact with similar *cis*-acting DNA elements and their C-terminal regions activate transcription of IRF-1-dependent genes. Differences in the transactivation domain of IRF-1 of mouse and man may provide information about their functional specialisation.

A variety of agents like viruses, IFNs, IL-1, TNF-α, LPS, Con A and double stranded RNA or poly (I.C.) activate expression of IRF-1 gene and stimulate its mRNA level in many mammalian cell types. IRF-1 can bind to promoters of many important genes such as IFN-β, MHC I (H-2D, H 2K), ISG 54, 2' 5' oligo A synthetase, ICE, iNOS, GBP, IL-6, IL-15, VCAM-1 etc. IRF-1 actively participates in processes like cellular defense against viruses and other pathogens, regulation of cell growth, antioncogenic effect, immune regulation and apoptosis. Therefore, IRF-1is an important transcription factor. Expression of IRF-1 mRNA and the DNA binding activity of IRF-1 in

different tissues of the mouse will provide information about its tissue-specific expression pattern and function under normal conditions in mouse.

With this background the following questions were asked :

1. What are the gross differences in the structural organization of the mouse and human IRF-1 gene ?
2. What are the differences in the nucleotide sequences in the mouse and human IRF-1 cDNA and how these differences are reflected in their amino acid sequences ?
3. What is the expression pattern of IRF-1 mRNA in various tissues of the mouse ?
4. What is the expression pattern of the DNA binding activities of IRF-1 (the activator) and IRF-2 (the suppressor) in various tissues of the mouse ?

In order to address these questions the following experiments were performed :

1.Organization of IRF-1 gene was studied in genomic DNA isolated from the mouse liver and human peripheral lymphocytes by Southern blot hybridization using three types of murine IRF-1 DNA probes: exons 1-10, exons 3-10 + introns 2-10 and exon 1.

2.Differences in the nucleotide sequences and restriction enzyme sites in mouse and human IRF-1 cDNAs as well as variations in their amino acid sequences were found out by sequence comparison and analysis.

3.IRF-1 mRNA expression in different tissues of the mouse was studied by dot and northern blot analyses using murine IRF-1 cDNA as the probe. IRF-1 mRNA levels were quantitated.

4.Expression of DNA binding activities of IRF-1 and IRF-2 was studied by electrophoretic mobility shift assay (EMSA) using a 24 bp synthetic DNA sequence frequently occurring in the promoter/enhancer(s) of many genes induced by viruses and interferons (IFNs). IRF-1- and IRF-2 – DNA complexes were quantitated.

MATERIALS AND METHODS

5. MATERIALS AND METHODS

5.1 Materials

5.1.1 Reagents

1. Acetic acid: -Acetic acid glacial (Merck-GR, Qualigens-AR) concentration 99.7%. Stored at RT.

2. Acrylamide 30%: - (Sigma A-9909). 29 gm Acrylamide + 1 gm Bis N-N' Methylene acrylamide (Sigma - M 7256) dissolved in water to final volume 100 ml, filtered through Whatman 1 MM filter paper, stored at 4°C in a dark bottle.

3. Agar plates: - LB agar: (Hi media RM-301). 15 gm agar (1.5%) in 1 litre medium, autoclaved, cooled down to 45 ^{0}C. The antibiotics were added from sterile stocks (Ampicillin 50-100 µg/ml or Tetracycline 10 µg/ml to final conc.) and were poured into 90 mm plates.

4. Agarose gel: - Agarose, Type V high melt, (Sigma-A-3768) or Type VII low melt, (Sigma A-4018) or ultra pure grade (Gibco BRL 15510-027). Typically 0.6-2% agarose gels in 1 x TAE buffer were used with a final conc. of 0.5 µg/ml ethidium bromide (EtBr).

5. Antibiotics: - (a) Ampicillin: Ampicillin sodium injection solution (Biocilin, India) 500mg of ampicillin salt was dissolved in 5ml of sterile water, final conc. was 100mg/ml., kept frozen as 500 µl aliquots at –20°C. (b)Nalidixic acid: Nalidixic acid sodium salt, (Sigma N-3143) was dissolved (5 mg/ml) in water and stored as 100 µl aliquots at –20°C.conc. (C) Tetracycline: Tetracycline hydrochloride (Sigma T-7508). Stock conc. was 10 mg/ml in 50% ethanol and was stored as 100-500 µl aliquots at –20°C. (d) Kanamycine : Kanamycine monosulfate(Sigma K-4000) stock conc. was 10 mg/ml in water and stored as 100-500 µl aliquot at -20°C.

6. Aprotinin :- (Sigma, A-6279), a protease inhibitor, (conc. 1 µg /µl), stored at 4°C or -20°C.

7. APS 10%: - (Sigma, A-9164), 0.10 gm ammonium per sulfate dissolved in 1 ml water (10%). Freshly prepared before use.

8. Benzamidine:- (Sigma, B-6506), a protease inhibitor, stored at -20°C.

9. β. M. E: - β-Mercaptoethanol, (Merck-GR), 13.7 M, stored at 4°C.

10. BSA:- Bovine serum albumin (Sigma, fraction V, A-9647) 1mg/ml solution in sterile water, stored at –20°C.

11. Buffer A (10x): - 150 mM Tris-Cl, 150 mM NaCl, 250 mM KCl, 2.5 mM EDTA, 0.5 m EGTA and 0.34 M Sucrose in water. pH was adjusted to 7.4 with HCl, autoclaved and stored at 4°C. 25 mM β-Mercaptoethanol, 1.5 mM Spermine, 5 mM Spermidine and 2 mM PMSF were added to final concentration just before use.

12. Carrier DNA: - Salmon sperm DNA (sodium salt, Sigma D-1626) or calf thymus DNA (sodium salt, Sigma D-1501). 1 mg/ml in 10 mM Tris-Cl pH-8.0, 10 mM NaCl (NT-buffer), sonicated, once phenol : chloroform extracted, ethanol precipitated, redissolved and was stored as 250 µl aliquots at –20 ^{0}C.

13. Chloroform: E. Merck (GR), Cat. No. 2445 , stored at room temperature.

14. CIAP: - Calf intestinal alkaline phosphatase, (New England Biolabs, 290S), conc. was 10 U/µl, stored at –20 ^{0}C in supplier's buffer.

15. CIAP buffer (10x): - 1 M NaCl, 500 mM Tris-Cl (pH-8.2), 100 mM $MgCl_2$ and 10 mM DTT (pH 7.9). Stored at –20 ^{0}C as aliquots.

16. DEPC: - Diethyl pyrocarbonate, (Sigma D 5758), stored at 4°C in a dark bottle.

17. Developer: - (Kodak, MAH-1, 9006974), 1.02 kg of developer was dissolved in 9 litre water final volume, filtered through Whatman 1 MM filter paper and stored at RT in brown bottle in dark.

18. Denhardts' : - reagent (50x) 1 gm Ficoll, (Sigma F-2637), 1 gm polyvinyl pyrolidone (Sigma P-5288) and 1 gm Bovine serum albumin (fraction V, Sigma A-9647) were dissolved in 100ml H_2O and stored as aliquots at –20 ^{0}C.

19. DTT: - DL- Dithiothreitol, (Sigma D-9779) was dissolved upto 100 mM in deionised water, filter sterilized through 0.22 µM membrane and was stored frozen as 100 µl aliquots at –20 ^{0}C.

20. EDTA: - Ethylene diamine tetra acetic acid, disodium salt, (Qualigens-AR) was gradually dissolved upto 0.5 M in water as the pH adjusted to 7.5 or 8.0 with NaoH pellets and 5 M NaOH soln., autoclaved and stored at RT.

21. EGTA: - Ethylene glycol-bis- [B-amino ethyl ether]-N,N,N',N', tetra acetic acid (Sigma, E-3889) was gradually dissolved upto 0.5 M in water as the pH was adjusted by NaoH pellets and soln., filtered sterilized through 0.22 μM membrane, stored as 500 μl aliquots at –20 ^{0}C.

22. EMSA buffer (5x):- 0.25 M Tris , 2.0 M Glycine , 0.01 M EDTA, pH 8.5, stored at RT.

23. EtBr: - Ethidium bromide (Sigma,E-8751) was dissolved at 10 mg/ml in sterile water, stored as 100 μl aliquots at 4 ^{0}C in dark.

24. FA dye (6x): - 0.25% Bromophenol blue (Sigma, B-7021), 0.25% Xylene cyanol (Sigma, X-4126) and 15% Ficoll (Sigma, F-2637) in sterile water. Stored as 100 μl aliquots at –20 ^{0}C.

25. FBS:- Fetal Bovine Serum (Life Technology,USA), cat # 16000-036. The serum was heat-inactivated at 56°C for 20min.,stored at –20^{0}C in 50 ml aliquots, used at a final concentration of 10% in RPMI-1640 medium.

26. FCS:- Fetal Calf Serum, (Biological Industries, Israel), cat #04-001-1B. The serum was heat-inactivated at 56°C for 20 min., stored at –20^{0}C, used at a final concentration of 10% in RPMI-1640 medium.

27. Fixer: - Fixer (Kodak, F-9000720). 2.38 Kg was dissolved in 9-litre water final vol., filtered through Whatman 1 MM paper and stored at RT in brown bottle in dark.

28. Formaldehyde: - Formaldehyde solution (37%), (Qualigens-AR). Stored at RT.

29. Formamide: - (Sigma, F-7508). Deionised by DOWEX MR-3 mixed bed resin (Sigma 1-9005), stored as 1 ml aliquots at –20 ^{0}C.

30. Heparin: - Commercially available Heparin sodium injection (25,000 I.U in 5 ml) obtained from Biological E. limited. India, stored at –20 ^{0}C.

31. HEPES :- (Sigma, H-3375) for 1 M. 23.83 gm was dissolved in 70-80 ml of distilled water , adjusted pH 7.9 with NaOH, vol. made upto 100ml, autoclaved and stored at room temperature.

32. Isopropanol: - Isopropanol (HPLC grade), (Spectrochem, India). Stored at RT.

33. KCl :- Pottassium Chloride (Qualigens-AR grade , MW= 74.55)

34. Leupeptin:- (Sigma, L-0649), a protease inhibitor, (conc. 1 μg/ μl) stored at -20°C.

35. LiCl: - Lithium chloride anhydrous, (Sigma, L-0505), stored at RT.

36. Loading Buffer: - 0.25% Bromophenol blue (Sigma, B-7021), 0.25% Xylene (6x) cyanol (Sigma, X-4126) in 30% glycerol, stored at –20 ^{0}C as 500 μl aliquots.

37. Lysis buffer : - 50 mM Glucose (Qualigens-AR grade), 25 mM Tris-Cl (pH 8.0), 10 mM EDTA, 4 mg/ml Lysozyme, freshly prepared before use.

38. Lysozyme: - (SRL, 1240123), 10 mg/ml Lysozyme in 50 mM Tris-Cl (pH-8.0), stored at –20 ^{0}C as 100 μl aliquots.

39. Media: - (a) LB medium: 10 gm Bacto-tryptone (Hi-media, RM-014), 5 gm Bacto yeast extract (Hi-media RM-027), 10 gm NaCl (Qualigens-AR) in 1 litre water. pH was adjusted to 7.0 with 5 M NaOH, autoclaved and stored at 4 ^{0}C.

40. (b) YT medium: 16 gm Bacto-tryptone (Hi-media, RM-014), 10 gm Bacto yeast extract (Hi-media RM-027), 5 gm NaCl (Qualigens-AR) was dissolved in 1 litre water. pH was adjusted to 7.0 with 5 M NaOH, autoclaved and stored at 4 ^{0}C.

41. Membranes: - (a) Millipore: (GS, WP-02400), pore size 0.22 μM filters for filter-sterilization from Millipore Corporation, USA.(b) Nytran nylon membrane: (Sigma, N-0894), charge- modified nylon membrane, approximately 50% positive and 50% negative charges from Schleischer and Shcull.(c) Hybond N plus membrane: (Amersham, RPN303B), highly positively charged nylon membrane.

42. Methanol: - Qualigens-AR grade.

43. $MgSO_4$ (1M): - (Qualigens-AR grade), 246.5 gm $MgSO_4.7H_2O$ was dissolved in 1 litre water, autoclaved and stored at RT.

44. $MgCl_2$ (1M): - (Qualigens-AR grade), 203.31 gm $MgCl_2.6H_2O$ was dissolved in 1 litre water, autoclaved and stored at RT.

45. MOPS (1M): - MOPS-free acid (Sigma, M 8899), 209.3 gm was dissolved in 100 ml water, pH adjusted to 7.0 with NaOH, filter-sterilized and stored at 4 ^{0}C.

46. NP-40:- Nonidet P-40 (Sigma, N-0896)

47. Nucleotide triphosphates: - (a) Deoxynucleotides: (dATP, dGTP, dCTP, dTTP), 100 mM stocks were from Promega Corporation,USA

and NEB,USA and diluted stocks were 25 mM, both were stored at –20 ^{0}C. (b) Radio active nucleotide triphosphates: (i) [α ^{32}P] dATP: BRIT, India, (LCP-103, 3000 Ci/mmole, 10 μCi/μl) or Amersham, cat no. AA0074 (6000 Ci/mmole, 10 μCi/μl), stored at –20 ^{0}C. (ii) [γ ^{32}P] ATP: Amersham, cat no. AA0018 (6000 Ci/mmole, 10 μCi/μl, stored at –20 ^{0}C.

48. 1x PBS:- 130 mM NaCl, 2 mM KCl, 7.8 mM $Na_2PHO_4.2H_2O$, 1.4 mM $KH_2PO_4.2H_2O$ made in water, pH 7.4 with HCl, autoclaved and stored at RT.

49. PEG: - Polyethylene glycol 8000 (Sigma, P-5413), 30% solution made in water, autoclaved and stored at RT.

50. Phenol: - Ranbaxy (AR grade), glass distilled and equilibrated to saturation with water or 1xTNE or 0.5 M NaCl as per the need, stored with some saturating medium in 50-100 ml aliquots at – 20 ^{0}C.

51. Phosphate buffer: - 0.5 M Na_2HPO_4 (Qualigens-AR grade) in water, pH was adjusted to 7.2 with phosphoric acid, autoclaved and was stored at RT.

52. Poly (dI.dC):- Poly deoxy inosinic acid -deoxy cytidylic acid (Sigma, P-4929) used as carrier DNA, stock concentration is 1μg/μl, store at -20°C

53. PMSF: - Phenyl methyl sulfonyl fluoride (Sigma P-7626), 100 mM in isopropyl alcohol, kept in dark brown bottle as 25 ml or 50 ml aliquot at 4 ^{0}C.

54. Polymerases: - Klenow fragment: From *E.coli* DNA polymerase I, (New England Biolabs, 21OL), 5 U/μl, stored at –20 ^{0}C and 10x Klenow buffer: 0.1 M Tris-Cl (pH-7.5), 50 mM $MgCl_2$, 75 mM DTT, stored at –20 ^{0}C.

55. Potassium acetate: - 30 ml 5 M potassium acetate (Qualigens-AR grade) and (3/5 M soln.) 5.75 ml glacial acetic acid were mixed to final 50 ml vol., autoclaved and was stored at RT.

56. Pronase: - (Sigma, P-5147), 20 mg/ml dissolved in 0.15 M EDTA, self digested at 37°C for 2 hr, stored frozen at –20°C in 200 μl aliquots.

57. Proteinase K:- (Sigma, P-6556) stock conc. 20mg/ml in sterile water, stored as 100 μl aliquots at –20° C.

58. NEBlot Kit :- (NEB, 1550-50) Random primer Klenow based labeling kit

59. Restriction enzymes: - (a) From New England Biolabs, U.S.A. stored at –20 ^{0}C. Bam HI: (20 U/µl), 101L, Sac I: (20 U/µl), 156L, Xho I:(20U/:l), 146 S, Xba I :(20U/:l), 145 S, Bst XI: (10U/:l), 113L, Bam HI buffer (10x): 150 mM NaCl, 10 mM Tris-Cl, 10 mM $MgCl_2$,1mM DTT and 1 mg/ml acetylated BSA, stored at –20 ^{0}C, Sac I buffer (10x): 100 mM bis Tris Propane-HCl, 100 mM $MgCl_2$, 10 mM DTT (pH 7.0) and 1 mg/ml acetylated BSA. Stored at –20 ^{0}C, Xho I buffer: (10x) 50 mM NaCl, 10 mM Tris-Cl, 10 mM $MgCl_2$,1 mM DTT and 1 mg/ml acetylated BSA. Stored at -20°, Xba I buffer : (10x) 50 mM NaCl, 10 mM Tris-Cl, 10 mM $MgCl_2$,1mM DTT and 1 mg/ml acetylated BSA. Stored at -20°, Bst XI buffer (10x): 100 mM NaCl , 50 mM Tris-HCl, 10 mM $MgCl_2$, 1 mM DTT . Stored at -20°C.

(b) From Life Technology, U.S.A., stored at -20°CEco RI: 10U/:l, 15202-021, Hind III: 10U/:l, 15207-020, Pst I : 10U/:l, 15215-049, Hind III and Pst I buffer (REACT 2, 10X) : 500 mM Tris-HCl (pH 8.0) , 100 mM $MgCl_2$, 500 mM NaCl, stored at -20°C, Eco RI Buffer (REACT 3, 10X) 500 mM Tris-HCl (pH 8.0) , 100 mM $MgCl_2$,1000 mM NaCl, stored at -20° C .

60. RNA lysis buffer:- 6 M urea, 3 M LiCl, 50 mM NaOAc, 0.1% SDS and 200 µg/ml heparin (last two components added freshly just before use).

61. RNase A: - Pancreatic RNase A (Sigma, R-9009), 10 mg/ml dissolved in 1x TNE and was incubated at 85°C for 10 min to inactivate contaminating DNase, stored as 100 µl aliquots at –20 ^{0}C.

62. SDS: - Sodium dodecyl sulfate (Sigma, L 4390), 20% (W/V) SDS dissolved in 50 mM Tris-Cl, pH 8.0, heat-treated at 65 ^{0}C for 2 hr and stored at RT.

63. RPMI-1640:- Sigma, cat # R8005, made to a final of 1x conc. as per manufacturer's instructions.

64. Sephadex: - G-100, (Sigma,G100-120) and G-50 (Sigma, G50-80). 10 gm was soaked and washed properly with excess water, re-suspended in 100 ml 1x TNE, autoclaved and was stored at 4 °C.

65. Sodium chloride: - Sodium chloride (NaCl) (Qualigens-AR grade), stored at RT.

66. Sodium acetate: - (Qualigens-AR grade), stored at RT.

67. Spermidine: - (Sigma, S-0266), 1 M Spermidine in 10 mM Tris-Cl (pH 9.5), 0.1 mM EDTA, stored as 500 µl aliquots at –20 ^{0}C.

68. Spermine: - (Sigma, S-1141), 1 M Spermine in 10 mM Tris-Cl (pH 9.5), 0.1 mM EDTA. Stored as 500 µl aliquots at –20 ^{0}C.

69. SSC (20x): - 3 M NaCl and 0.3 M sodium citrate, 175.3 gm NaCl + 88.2 gm Sodium citrate (Qualigens-AR grade) dissolved in 1 litre water, adjusted pH to 7.0 with Citric acid, autoclaved, stored at RT.

70. Sucrose: - (SRL-1944115) or (BDH-AR grade), stored at RT, soln kept at 4°C for limited period.

71. TAE (50x): - 242 gm Tris base, 57.1 ml glacial acetic acid, 100 ml 0.5 M EDTA (pH 8.0) and volume was adjusted to 1 litre with water, autoclaved and stored at RT.

72. TBE 10x: - 0.9 M Tris, 0.9 M Boric acid and 0.025 M $Na_2EDTA.2H_2O$, 108 gm Tris-base, 55 gm boric acid and 9.3 gm $Na_2EDTA.2H_2O$ were dissolved to 1 litre with water, pH was ~8.3 (not adjusted), autoclaved and stored at RT.

73. TCM buffer: - 0.3 M $CaCl_2$, 0.3 M $MgCl_2$ and 0.1 M Tris-Cl (pH-7.5), autoclaved and stored at RT.

74. TE buffer: - 10 mM Tris-Cl (pH-7.5 or 8.0) and 1 mM EDTA, autoclaved and stored at RT.

75. TELT buffer: - 50 mM Tris-Cl (pH 7.5), 62.5 mM EDTA, 0.4% Triton X-100 and 2.5 M LiCl, autoclaved and stored at RT.

76. TEMED: - N,N,N',N', Tetra methyl ethylene diamine. (Sigma, T-7024), stored at 4 ^{0}C.

77. Tfb I :- 30 mM Pot. acetate, 50 mM $MnCl_2$, 100 mM KCl, 10 mM $CaCl_2$, 150 gm/l glycerol (pH 7.0), stored at 4°C.

78. Tfb II:- 10 mM Na-MOPS, 75 mM $CaCl_2$, 10 mM KCl, 150 gm/l glycerol, stored at 4°C.

79. TNE (10x): - 0.5 M Tris-Cl (pH-7.5), 1 M NaCl and 0.05 M EDTA. pH was 7.4-7.5 in a 1/10 dilution, autoclaved and stored at RT.

80. Tris-HCl: - (Qualigens-AR grade). Tris base 1 M in water, pH was adjusted to 7.5 or 8.0 with HCl, autoclaved and stored at RT.

81. Triton X-100: - (Sigma, T-8787), diluted to 25% in water and stored at RT.

82. Water: - Milli Q Water (Millipore deionizer) or double Quartz distilled autoclaved water.

83. Trypsin:- (Sigma, cat # T2271), working solution of 0.25% in 1x PBS, 1 mM EDTA solution was used.

84. Whatman: - Whatman 3 MM Paper (3030917) from Whatman, England.

85. X-ray films: - Kodak (XAR-5) or Sigma (F-5388) or Amersham (Hyperfilm^{TM} MP), stored at 4°C.

5.1.2 Cells, plasmids, oligonucleotides and recombinant protein used

#	Name	Features	Reference
1	*E. coli* cells:- DH5α	*E.coli* DH5α, (genotype: F'/endA1 hsdR17 (rk-Mk+) sup E44, thi-1, λ, rec. A1 gyr A (Nal r) relA1 Δ (lac lZYA-argF)U169 deoR (φ80dlc (lacZ ΔM15)).	Stratagene, U.S.A.
	XL-1 Blue	*E. coli* XL-1 Blue:- genotype: endA1, hsdR17 (rk-, mk+) sup E44, thi-1, λ, rec. A1 gyr A 96, rel A1, (lac) [F', pro AB, lac^qZ Δ M15, Tn10 (tet^R)]	Stratagene, U.S.A.
	MC1061/P3	*E. coli* MC1061/P3:- genotype: F⁻, *ara*D139 Δ(*ara*ABC-*leu*) 7679 *gal* U *gal* K Δ *lac*X74 *hsd*R ($r^-_k m^+_k$) *rps*L(str^R) *thi*-1 *mcr*B{P3: kan^R Amp^R (amber), Tet^R(amber)}	Invitrogen, U.S.A.
2	Plasmids:- PIRFL	Containing 2082 bp murine IRF-1 cDNA in pCDM8 vector.	Prof. T. Taniguchi (Tokyo)
	pIRF2.5	Containing 2435 bp murine IRF-2 cDNA in pCDM8 vector.	Prof. T. Taniguchi (Tokyo)
	pCDM8	4.4 kb mammalian expression vector.	Invitrogen,U.S.A
	pIRFC2	5.3 kb Bam HI IRF-1 genomic DNA fragment (exons 3-10 + introns 2-10) in pBluescript KS vector	Prof. Charles Weissmann, (Zurich)
	pBluescript	2961 bp plasmid with fi origin, col E1 origin with T3 and T7 promoter.	Stratagene
3	EMSA oligonucleotides $(GAAAGT)_4$ or $(GT)_4$	5' GAA AGT GAA AGT GAA AGT GAA AGT 3' reverse complement : 5' ACT TTC ACT TTC ACT TTC ACT TTC 3'	Macromolecular resources, U.S.A.
	$(GAAA)_6$ or $(GA)_6$	5' GAA AGA AAG AAA GAA AGA AAG AAA 3' Reverse complement : 5' TTT CTT TCT TTC TTT CTT TCT TTC 3'	
4	Mammalian Cell lines		
	L 929	Mouse fibroblast cell line	ATCC, U.S.A.
	U 937	Human macrophage/monocyte cell line	ATCC, U.S.A.
5	GST-IRF-1	GST-IRF-1 fusion protein expressed in *E. coli* XL-1 blue cells, ~67 kd.	Meenakshi Upreti J.N.U. N.Delhi

5.2 METHODS

5.2.1 Animals

Healthy female swiss albino mice of 33 and 63 days of age were obtained from the animal house facility of the School of Life Sciences; J.N.U. Mice were sacrificed by cervical dislocation and desired tissues were collected immediately and washed with cold normal saline (0.9 % NaCl) and briefly kept on ice. All experiments were conducted with fresh tissues.

5.2.2 General methods

5.2.2.1 Preparation of competent *E. coli* cells

E. coli XL-1 blue cells were made competent for transformation as per the method Hanahan et al., (1985). Cells were streaked on LB +1.5% agar + tetracycline (tet) 10 μg/ml plate and allowed to grow at 37° C overnight to select for pure antibiotic resistant strain . 5ml LB + tet (10 μg/ml) was then inoculated with a single colony from the plate and allowed to grow overnight at 37° C, 200 rpm. Next day 100 ml LB + tet (10 μg/ml) medium was inoculated with 1ml of overnight grown culture and allowed to grow at 37° C, 200 rpm for 2 to 3 hours until O.D. at 550 nm of the culture reached 0.4 to 0.6, which corresponded to approximately 5- 6 X 10^7 cells/ml. Cells were pelleted down in 250 ml GSA bottles at 3500 rpm for 5 min. at 4° C in a Sorvall RC5B centrifuge using GSA rotor. The pellet was then gently resuspended in 40 ml of ice cold TfbI buffer (30 mM Pot. Acetate, 50 mM $MnCl_2$, 100 mM KCl, 10 mM $CaCl_2$, 150 g/L glycerol, pH 5.8) on ice. After being left undisturbed on ice for 15 min, the cells were pelleted down at 3500 rpm at 4° C for 5 min. The pellet was then gently resuspended in 4ml of Tfb II (10 mM Na-MOPS, 75 mM $CaCl_2$, 10 mM KCl, 150g/L glycerol, pH 7.0) on ice. Aliquots of 100 to

200 µl cells were saved in prechilled 0.5 ml Eppendorf tubes and stored at -80° C. *E. coli* DH 5 α cells were selected on LB + 1.5%agar + nalidixic acid (15 µg/ml). *E. coli* MC1061/P3 cells were selected on LB + 1.5 % agar + amp. (100 µg/ml) and tet. (10 µg/ml) antibiotic plates, the rest of the procedure for the preparation of competent cells were same as above .

5.2.2.2 Transformation of *E. coli* with plasmid DNA

Transformation of the competent *E. coli* cells with plasmid DNA was carried out according to Sambrook et. al., (1989). An aliquot of competent cells was thawed on ice for 15 to 30 min. 0.1, 0.2, 0.5 and 1ng of plasmid DNA were mixed with 2 µl TCM buffer (0.3 M $CaCl_2$, 0.3 M $MgCl_2$, 0.1 M Tris-HCL pH 7.5) and kept on ice for 5 min. 50 µl of competent cells were mixed with the DNA+TCM buffer mixture and left undisturbed on ice for 30 min. The cells were then given a heat shock at 42° C for 90 sec. The cells were then immediately transferred to ice and left for 5min. 1ml LB medium was added to each tube and the cells were incubated at 37° C for 1hr with shaking at 200 rpm. 200 µl of the transformation mixture was spread on LB + 1.5% agar + amp. (100 µg/ml) plates. Plates were incubated at 37° C overnight. The number of colonies was counted and the transformation efficiency was checked with 0.1 to 1 ng of plasmid DNA and expressed as number of colonies /µg plasmid DNA. Transformation efficiency of the cells was in the order of 10^7 to 10^9 cfu/µg DNA.

5.2.2.3 Purification of plasmid DNA

(A) LiCl boiling method for mini - preparation of plamid DNA

Mini preparation of the plasmid DNA was carried out by a LiCl boiling method of Holmes and Quigley (1981). 5ml LB+amp (100 μg/ml) medium was inoculated with a single transformed bacterial colony and allowed to grow at 37° C, 200 rpm overnight. 1.5 ml of the overnight grown culture was pelleted down by spinning at 12000 rpm for 30 sec. at room temperature. The supernatant was aspirated without disturbing the pellet. The bacterial pellet was then resuspended in 100 μl TELT Buffer (50 mM Tris-HCL pH 7.5, 62.5 mM EDTA, 0.4% Triton X-100, 2.5 M LiCl) by vortexing, to which 10 μl of freshly prepared aqueous solution of lysozyme (10 mg/ml) was added. The tubes were immediately transferred to boiling water bath for 1min, then incubated on ice for 5 min. The tubes were centrifuged at 12000 rpm for 8 min. at room temperature to pellet down cell debris, which was removed with a sterile toothpick. The supernatant was treated once with equal volume of phenol : chloroform (1:1) mixture. The aqueous layer was collected in a fresh Eppendorf tube and precipitated with equal volume of isopropanol in presence of 0.3 M sodium acetate, kept at -20° C for 30 min. DNA was pelleted at 15000 rpm for 20 min. at 4°C and washed once with 80% ethanol to remove excess of salt. The pellet was air dried 30 min. and dissolved in 20 μl TE. This purified plasmid DNA was used to check for recombinant DNA clones by restriction digestion and agarose gel electrophoresis.

(B) Alkaline lysis method for midi-preparation of plasmid DNA

Midipreparation of plasmid DNA was carried out according to Sambrook et. al., (1989). 15 ml of LB + antibiotic was inoculated with a single

transformed colony, allowed to grow overnight at 37° C, 200 rpm. Cells were pelleted down by spinning at 6000 rpm for 5 min. at 4° C in a Sorvall RC 5B centrifuge. Cell pellet was washed in 1ml TNE buffer (0.05 M Tris-HCL, pH 7.5, 0.1 M NaCl, 0.005 M EDTA, pH 7.5) and then transferred to 2 ml Eppendorf tube. The cell pellet was resuspended by vortexing in 300 µl lysis buffer (50 mM glucose, 25 mM Tris-HCl and 10 mM EDTA, pH 8.0) containing 4 mg/ml freshly prepared Lysozyme. The lysed cell suspension was denatured by adding 600 µl of freshly prepared 0.2 N NaOH + 1% SDS and mixed by inverting the tube. After 5 min., 450 µl of 3/5 M pottasium acetate was added, mixed by inverting and left on ice for 5 min. The tubes were then centrifuged at 12000 rpm for 15 min at room temp and to the supernatant in fresh Eppendorf tube 5 µl of DNase free RNase (10 mg/ml), incubated for one hour at 37°C. The plasmid DNA solution was extracted twice with equal volume of phenol : chloroform (1:1) and once with chloroform. The plasmid DNA was precipitated by adding 0.7 volume of isopropanol in presence of 0.3 M sod. acetate and kept at -20°C for 1hour. DNA was pelleted by spinning at 15000 rpm for 20 min. at 4°C and the pellet was washed with 80% ethanol to remove excess salt. The pellet was then air dried for 30 min. at RT and dissolved in 100 µl TE (10 mM Tris-HCl, 1 mM EDTA, pH 8.0). 1µl DNA was loaded on 1% agarose-TAE gel to check the quality and quantity of plasmid DNA. The DNA was pure enough to carry out restriction digestion, kinasing and probe preparation.

(C) Large scale purification of plasmid DNA

Large scale plasmid purification was carried out by modified method of Sambrook et. al., (1989). 5ml of LB medium with appropriate antibiotic was inoculated with a single transformed colony and allowed to grow at 37° C, 200 rpm for overnight. 1 ml of overnight grown culture was used to inoculate a 250

ml LB + antibiotic medium and allowed to grow at 37° C, 200 rpm for 14-16 hours. Cells were pelleted down at 6000 rpm for 20 min at 4° C in a Sorvall RC 5B centrifuge with a GSA rotor. The cell pellet was resuspended in 12 ml of 50 mM Tris-HCl, pH 8.0. The cell suspension was transferred from GSA bottle to 35 ml tube and 3 ml lysozyme (10 mg/ml) was added while vortexing and kept on ice for 10min. Then 1.8 ml 0.5 M EDTA (pH 8.0) was added and mixed by vortexing. To the mixture 750 µl of 2% Triton X-100 was added and vortexed. The extract was left on ice for 60 min. and then centrifuged at 15,000 rpm for 30 min. at 4^0 C in a SS34 rotor in a Sorvall RC5 B centrifuge. The supernatant was transferred to a fresh 35 ml tube, allowed to reach room temperature. 1.8 ml freshly prepared 1 M NaOH was then added with stirring for denaturing the genomic DNA and left for 10 min. at room temperature. The pH was checked with pH paper and it was around 12.5. The mixture was then neutralized by adding 8 ml 1 M Tris (pH 7.5) and kept for 3 min, the pH of the mixture came down to 8.3 - 8.5. To the crude mixture, 3 ml 5 M NaCl was added. The mixture was extracted with equal volume of 0.5 M NaCl saturated phenol, centrifuged at 10,000 rpm for 15 min at 4^0 C. The aqueous layer was extracted twice with equal volume of chloroform. The aqueous phase was collected. The RNA in the aqueous phase was digested with 50 µl DNase free RNase A (10 mg/ml), kept at 37^0 C for 1 hr. DNA was precipitated by adding 3 ml of 5 M NaCl and 5 ml of 30% PEG 6000. The mixture was mixed by vortexing and kept on ice overnight. The precipitated DNA was pelleted down by centrifuging at 10,000 rpm for 30 min. at 4^0 C in a HB4 rotor of Sorvall RC5B centrifuge. The DNA pellet was washed with 80% ethanol, air dried for 30 min. and to the dried pellet 400 µl TNE buffer was added and kept at 37^0 C for 1 hr to dissolve the DNA. To the DNA solution 10 µl 20 % SDS (1/40 volume) and 8 µl (1/50 volume) pronase (20 mg/ml) were added and incubated at 37^0C for 30 min. The reaction mixture was extracted twice with equal volume of phenol: chloroform (1:1) and once with equal volume of

chloroform. DNA was precipitated by 0.7 volume of isopropanol in the presence of 0.3 M Sodium acetate (pH 5.2), kept at -20^0 C for 1 - 2 hr. or - 80^0 C for 30 min. DNA precipitate was pelleted down by centrifuging at 15,000 rpm for 20 min. at 4^0 C. The pellet was washed with 70 % ethanol; air dried for 30 min. and dissolved in 200 µl 10 mM Tris-HCl (pH 8.0). 1 µl DNA solution was checked on 1 % TAE agarose gel. DNA quantity was measured at $A_{260/280\ nm}$ and the quality by wavelength scan from A 200nm-300nm in a UV-160A Shimadzu spectrophotometer. The yield of the pBluescript plasmid was 1.6 - 1.8 mg from a 250 ml culture. Plasmid DNA isolated by this method was pure enough to be used for restriction digestion, preparation of probe by random priming, kinasing and all other purposes.

5.2.2.4 Purification of plasmid DNA through Sephadex G-100 column

Plasmid DNA was purified through Sephadex G-100 as per the method of Sambrook et. al., (1989).Sephadex G-100 was soaked overnight in water and washed 2-3 times, autoclaved and resuspended in TNE buffer. Column was prepared by packing Sephadex G-100 in a 3 ml glass pasture pipette (h = 11 cm, d = 0.6 cm) with glass wool at the outlet. Approximately, 50 µg plasmid DNA in 100µl TE was loaded and 200 µl fractions were collected. 4 µl was checked on a 1% agarose/TAE gel. Fractions with plasmid DNA were pooled from 4-5 fractions and precipitated at –80 ^{0}C for 15 min by adding 2.5 volume ethanol in presence of 0.3 M Na-acetate. DNA was collected by centrifugation at 12,000 rpm, 15 min at 4 ^{0}C, washed once with 80% ethanol and was finally dissolved in 100 µl 10 mM Tris-HCl (pH 8.0). This plasmid DNA is pure enough to be used for all purposes and remained good even after prolonged storage at –20 ^{0}C.

5.2.2.5 Purification of linear DNA through low melting agarose gel

DNA was purified from agarose gels by the method of Ausubel et. al., (1995). Plasmid DNA, digested with appropriate restriction enzymes was loaded to 1 % high melting agarose gel, and electrophoresed till the DNA had resolved into distinct bands. A cavity was made ahead of the desired band into which 1% low melting agarose was poured and allowed to set at 4^0C for 15-30 min. The gel was electrophoresed till the desired band entered into the low melting agarose block. The desired band was cut out with a sterile blade and melted at 65^0 C for 10 min. Then equal volume of 50 mM Tris-HCl (pH 7.5) was added. The mixture was vortexed and heated at 65^0 C for 5 min. and immediately transferred to 37^0 C for 5 min. An equal volume of TNE saturated phenol (prewarmed to 37^0 C) was added and mixed properly by vortexing to extract the DNA. The aqueous layer, obtained after centrifugation at 10,000 rpm at room temperature, was taken in a fresh tube. The DNA in the aqueous phase was precipitated by adding 0.7 volume of isopropanol in presence of 0.3 M sodium acetate (pH 5.2) and was precipitated at -20^0 C for 1 - 2 hr. The DNA was collected by centrifuging at 15,000 rpm for 10 minutes at 4^0 C. The DNA pellet was washed with 80 % ethanol, air dried for 15-20 minutes and dissolved in 20-50µl 10 mM Tris-HCl (pH 8.0). 1 µl of the DNA solution was loaded on 1% agarose gel to check the approximate concentration by comparing with DNA of known concentration.

5.2.2.6 Purification of linear DNA through high melting agarose gel

Plasmid DNA, digested with appropriate restriction enzyme was loaded to a 1 % high melting agarose gel, and electrophoresed till the DNA resolved into distinct bands. A sterile blade was used to cut out the desired band. The cut out agarose block was trimmed off excess agarose and taken in a fresh Eppendorf tube, 1 ml of TNE-saturated phenol was added to it and stored at -

70° C overnight. The Eppendorf tube was centrifuged at 12000 rpm for 30 minutes at 4° C to extract the nucleic acids from the pieces of agarose suspended in phenol. The aqueous layer was then extracted with chloroform. DNA was ethanol precipitated in presence of 0.3 M sod. acetate at -70° C for 30 minutes and centrifuged at 15000 rpm for 20 minutes at 4°C. The supernatant was discarded and the pellet was washed with 80% ethanol, air dried and dissolved in 20 µl of TE buffer (pH 8.0). The quantity and quality of the purified DNA was checked in a 1% agarose gel in TAE buffer. The purified DNA fragment was stored at -20°C.

5.2.3. Southern blot analysis

5.2.3.1 Purification of nuclei and isolation of genomic DNA from mouse liver

Nuclei and genomic DNA were purified from the mouse liver as per the methods of Hewish and Burgoyne (1973) as modified by and Chaturvedi and Kanungo (1985) respectively. Mouse liver was dissected out, washed in cold normal saline (0.9% NaCl in water), blotted to dry on filter paper and weighed.The liver was minced into small pieces on ice, then a 10% (w/v) homogenate of the minced liver was prepared in solution I (0.34 M Sucrose, 15 mM Tris-HCl (pH-7.4), 15 mM NaCl, 60 mM KCl, 15 mM β–Mercaptoethanol, 0.5 mM Spermidine, 0.15 mM Spermine, 0.2 mM PMSF, 2 mM EDTA, 0.5 mM EGTA, 0.5% Triton X-100) by 10 to 15 ups and down in a tight teflon pestle and glass homogenizer at 3000 rpm motor speed on ice at 4^0 C. The homogenate was filtered through double layered autoclaved cheese cloth, centrifuged in 35 ml tubes, at 3500 rpm at 4° C for 15min. The crude nuclear pellet was washed three times with equal volume of Solution I and the pellet was resuspended in 2 ml ice cold Solution III (0.34 M Sucrose, 15 mM Tris-Cl, pH-7.4, 15 mM NaCl, 60 mM KCl, 15 mM β–Mercaptoethanol, 0.5 mM Spermidine, 0.15 mM Spermine, 0.2 mM PMSF)

for 1 hour on ice, so that the nuclei were swollen properly. A drop of nuclear suspension was observed under a phase contrast microscope for checking the purity of nuclei. A rough calculation of the amount of genomic DNA in the nuclear suspension was made by disrupting 10 µl of nuclear suspension in 1 ml of 5 M Urea + 2 M NaCl solution and taking its OD at 260 nm and 280 nm and wavelength scan from 200 to 300 nm. The yield and quality of the nuclear preparation was judged from A260 nm units and 200 to 300 nm scan respectively. The nuclear suspension was adjusted to 500 µg DNA/ml conc.

Vigorous shaking or vortexing was strictly avoided during further purification steps to prevent shearing of the genomic DNA. The nuclei in Solution III were lysed with 1 M NaCl and 1% SDS at a final DNA concentration of 500 µg/ml by gentle mixing at room temperature for 20 to 30 min . DNA solution was extracted with equal volume of TNE-saturated phenol overnight at room temperature by very gentle rolling. On the subsequent morning the tubes were centrifuged at 10,000 rpm for 15 min at 4° C, the viscous aqueous phase was extracted once more with equal volume of TNE-saturated phenol and twice with equal volume of phenol : chloroform (1:1) and once with equal volume of chloroform respectively. The genomic DNA was precipitated from the final aqueous phase with 0.7 volume of isopropanol in presence of 0.3 M sodium acetate (pH 5.2). The genomic DNA was spooled out in fresh Eppendorf tubes with the help of a thin glass rod with helical grooves. It was washed three times with 80% ethanol to remove excess of salt, briefly dried at room temperature for 10 min, then dissolved in 500 µl NT buffer (10 mM NaCl, 10 mM Tris-HCl, pH 7.5) and kept at room temperature to completely dissolve the pellet. RNA was digested by adding 20 µl of DNase-free RNase A (10 mg/ml) and digesting at 37° C for 1 hour, followed by digestion of protein by adding 5 µl of 20% SDS and 10 µl of Pronase (20 mg/ml) and keeping at 37° C for 1 hour. The genomic DNA was extracted twice as an aqueous layer at 10000 rpm for 10 min at 4° C with equal volume

of phenol : chloroform (1:1). It was then precipitated with 0.7 volume of isopropanol in the presence of 0.3 M sod. acetate (pH 5.2) by keeping on ice for one hour. Genomic DNA was carefully spooled out into a fresh Eppendorf tube, washed three times with 80 % ethenol, briefly dried at room temperature and finally the pellet was dissolved in 500 µl of NT buffer at room temperature. The yield and purity of the genomic DNA was estimated at A 260 and 280 nm and wavelength scan at 200 to 300 nm in a UV-vis spectrophotometer. To check the integrity, the DNA was loaded on to a 0.6 % agarose-TAE gel. DNA was stored for further use in the form of ethanol precipitated aliquots at -20° C.

5.2.3.2 Isolation of genomic DNA from human lymphocytes

Genomic DNA was isolated from peripheral blood drawn from healthy adult human subjects as per the method of Kunkel et. al., (1985). Six to seven ml of blood was resuspended in 50 ml of lysis buffer (5 mM $MgCl_2$, 10 mM Tris-HCl, pH 8.0, 1% Trition X-100, 320 mM sucrose) and mixed gently on ice for 15 minutes. The mixture was centrifuged at 4000 rpm for 15 minutes at 4° C and the supernatant was discarded. The transparent white pellet obtained was resuspended in 4.5 ml of nuclear buffer (100 mM NaCl, 24 mM EDTA). The nuclei were lysed by adding 250 µl of 10% SDS and 5 µl of Proteinase K (20 mg/ml) and the tubes were incubated at 37°C overnight. The solution was cooled to room temperature, equal volume of TNE-saturated phenol was added and the two phases were gently mixed by slowly turning the tube end to end for 15 minutes until the two phases formed an emulsion. The tubes were centrifuged at 4000 rpm for 15 minutes at 4° C. The aqueous phase was transferred to a clean 35 ml tube using a thick bore Pasteur pipette. The extraction was repeated once with phenol and twice with chloroform : isoamylalcohol (24: 1) mixture. To the aqueous phase 0.1 volume 3M sodium acetate (pH 5.2) and 0.7 volume isopropanol were added. The DNA was

allowed to precipitate at room temperature and transferred to an Eppendorf tube using a wide mouth tip. The DNA pellet was washed thrice with 80% ethanol at room temperature for 10 minutes each. The DNA was allowed to briefly dry at 37° C and the pellet was resuspended in 250 µl of TE buffer (pH 8.0). It was allowed to dissolve at room temperature and stored at 4° C .

5.2.3.3 Preparation and purification of ^{32}P labeled random primed DNA probes

^{32}P labeled DNA probes were prepared by random primed DNA synthesis *in vitro* as per manufacturer's instructions. Typically, 25 ng of gel-purified DNA fragment in water was boiled for 3 min in a boiling water bath and immediately chilled on ice for 5 min. It was ^{32}P labeled using NEBlot™ Kit (NEB, USA, cat. No. 1550-50) as recommended by the manufacturer and mentioned below.

Stock	*volume*	*final concentration*
Labeling buffer (10 X) (containing random primers)	2.5 µl	1 X
dGTP (100 mM)	1.0 µl	4 mM
dCTP (100 mM)	1.0 µl	4 mM
dTTP (100 mM)	1.0 µl	4 mM
α ^{32}P dATP (10 µCi /µl) (Sp. Activity = 6000 Ci/mmole)	2.0 µl	20 µCi
E. coli DNA polymerase I (Klenow fragment, 5U/µl)	0.5 µl	2.5 U

The total reaction volume was 25 µl and it was incubated at 37°C for 1 hour. The reaction was terminated by 2µl of 0.5 M EDTA. and processed for purification or stored at -20°C .

The probe purification was done by a Sephadex G-50 spin columns. The nozzle of a sterile 1 ml syringe was plugged with autoclaved siliconized glass wool. Sephadex G-50 was swollen in H_2O, fines were removed, the resin was resuspended in TNE buffer and was autoclaved. The column was filled by adding sephadex G-50 suspension slowly and allowed to pack uniformly by gravity and then by centrifugation at 3000 rpm for 1 minute in a clinical centrifuge with swinging bucket rotor. The column was washed twice with 100 µl TE buffer (pH 8.0) by centrifugation at 3000 rpm for 1 minute each. 75 µl of TE (pH 8.0) buffer was added to the 25 µl of labeled probe and this 100 µl mixture was loaded on to the column which was lodged inside an improvised stand made out of a Falcon tube (15 ml) with a hole in the cap and containing an Eppendorf tube on a paper cushion inside to collect the elute. This was done in such a manner that the nozzle of the column was into the collection tube and there was no chance of leakage of ^{32}P material out side the small tube. Centrifugation at 3000 rpm for 3 minutes brought the purified ^{32}P probe into the Eppendorf tube, which was then taken out with a fine forceps, closed with the cap, stored at -20° C. 1 µl from it was aliquoted to check for the specific activity of the in a LKB β–counter by Cerenkov counting. The specific activity of the probe was found to be about 5-9 X 10^8 cpm/ µg.

5.2.3.4 Gel electrophoresis and Southern hybridization

Agarose gel electrophoresis of DNA and Southern blot hybridization were carried out as per the modified method of Sambrook et. al., (1989) and Church and Gilbert. 20 µg of mouse or human genomic DNA was digested by Bam HI, Eco RI, Hind III and Pst I restriction enzymes and checked in small gels for the digestion and finally electrophoresed in 1% agarose gels in TAE buffer (large gels : 20 x 25 x 0.4 cm^3) or (small gels : 13 x 13 x 0.3 cm^3) containing 0.5 µg/ml ethidium bromide at 20-30 Volts for overnight (14 -16 hr) for large gels or 3 - 4 hr for small gels at 100 - 120 Volts. ^{32}P labeled λ DNA digested

by Eco RI + Hind III or unlabeled λ DNA digested by Eco RI + Hind III size marker was used for Southern blot analyses. The gel was observed under transilluminated UV light (300 nm) in a IBI-Kodak transilluminator and photographed by a polaroid camera. The gel was depurinated in 0.25 N HCl by slow shaking at room temperature for 15 min., washed with autoclaved distilled water to remove excess acid. The gel was denatured by keeping in denaturation solution (1.5 M NaCl + 0.5 M NaOH) twice for 30 min. with gentle shaking at room temperature. (After this step the gel could be transferred by vacuum blotting sysytem.) Then the gel was neutralized by keeping in neutralization solution (1.5 M NaCl and 1 M Tris – HCl, pH 7.5) twice for 30 min with gentle shaking. DNA was transferred on to nylon membrane (neutral Nytran membrane, Sigma or Hybond N+ membrane, Amersham) either by a improvised vacuum blotting system in the alkaline buffer itself for 1-2 hr or by the conventional capillary blotting method in 10 x SSC for 16-20 hours on bench. The moist blot was UV crosslinked for 1 min at 1200 μJoules in a UV cross linker (Amersham). The blot was washed in 6 x SSC, dried at room temp. and sealed in polypropylene bag and stored at 4 ° C until used.

For Southern hybridization, DNA blot was put inside hybridization bottle and first rinsed with 5 x SSC at room temperature, 10 ml of prehybridization solution (0.3 M phosphate buffer, pH = 7.2, 7% SDS (w/v), and 1mM EDTA) was added into the hybridization bottle and prehybridization was carried out at 65 °C for 30 min to 1 hour with constant rolling of the bottle in a hybridization incubator (Robbins Scientific, USA). ^{32}P labeled probe (>10^5 cpm/ml) and Salmon sperm carrier DNA (100 μg/ml) was mixed well, denatured by heating in a boiling water bath for 5 min, immediately chilled on ice for 5 min and then added to the hybridization bottle (containing the prehybridization solution). Hybridization was carried out at 65° C for 16-20 hours with constant rolling of the bottle in the hybridization incubator.

Then the hybridized membrane was taken out, first washed in 2 x SSC and 1% SDS for 20 min at room temp, followed by washing at 65°C by following the sequence of low to high stringency as follows : 1x SSC + 0.5% SDS, 0.6 x SSC + 0.1% SDS, 0.4 x SSC + 0.1% SDS, 0.2 x SSC + 0.1% SDS, for 20 min each. The radioactivity on the blot was monitored by a hand held radioactive monitor (Rad-Monitor™, USA) to check the signal : background ratio as well as the positive and negative controls. If required, washing was continued further. The blot was checked for reference and was warpped in saran wrap and exposed to X-ray film (Kodak Xomat, XAR.5 or Amersham Hyper film) with intensifying screens in the dark room. The cassette was kept at -70 °C for 3 to 5 days. The X-ray film was developed manually in developer (Sigma GBX developer) for 1-2 min (in dark room), rinsed sufficiently in water for 5 min and fixed in fixer solution (Kodak, cat. No. 900 0720) for 3-4 min., then the film was again washed in running tap water for 15-30 min. to remove fixer and air dried, visualized and stored at room temperature.

For calculating the size of the DNA fragments obtained from the Southern blot a standard curve was plotted between log of bp and migration in cm of λ DNA marker fragments from the same gel as shown below. The sizes of fragments from the Southern blots were calculated by extrapolating the migration (cm) of the fragments from this curve. DNA fragments from the mouse and human genomes detected for specific probes were documented in the form of tables and tentative restriction maps were constructed on the basis of these fragments.

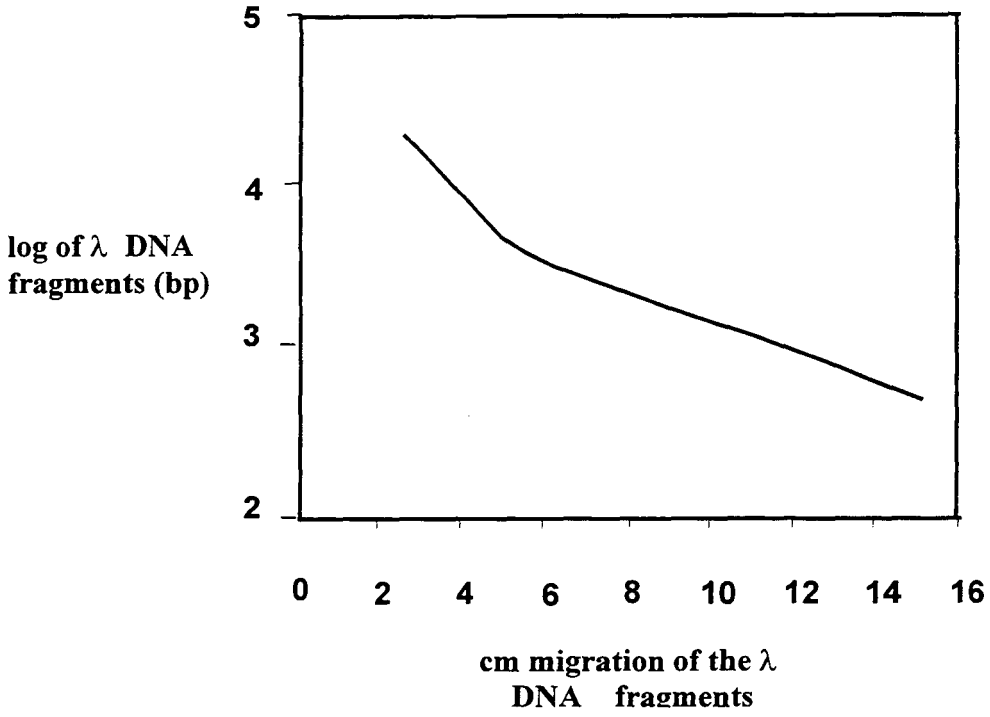

A representative graph plotted between log of λ DNA fragments (bp) and their migration (cm) resolved in a 1% agarose-TAE gel

5.2.4 Electrophoretic Mobility Shift Assay (EMSA)

Electrophoretic mobility shift assay (EMSA) of extracts from mouse and human cells and mouse tissues as well as cytoplasmic and nuclear fractions of certain mouse tissues were carried out using ^{32}P labeled specific oligonucleotide sequence.

5.2.4.1 Cell culture and cytokine treatment

Mouse fibroblast (L 929) cells were grown in RPMI + 5% fetal calf serum (FCS) in T-25 flask upto 75-85% confluency at 37° C with 95% air and 5% CO_2 . Human macrophage/monocyte (U 937) cells were grown in RPMI 1640 + 10% fetal bovine serum (FBS) between 0.3 to 0.8 x10^6/ml density in T-25 flasks at 37° C with 5% CO_2 as suspension culture . U 937 cells at 2 x 10^6/ml density in 1ml volume were treated with recombinant human interferon-γ (hIFN- γ) (a gift from Genentech, USA) at 1 nM for 0, 30 and 60 min at 37° C. Cells were chilled by addition of 0.5 ml ice cold PBS and immediately collected into 1.5 ml Eppendorf tubes and kept on ice. Cells were immediately processed for preparation of extracts. L 929 cells were treated with 0.25% Trypsin (Sigma) in PBS at 37°C for 2-3 min, then thoroughly washed with excess PBS and collected by low speed centrifugation. Cell pellet was resuspended in PBS for washing. Whole cell extracts of L 929 cells and nuclear and cytoplasmic extracts of U 937 cells were prepared as mentioned below.

5.2.4.2 Preparation of whole cell extract from mouse cells and tissues

Swiss albino mice were sacrificed by cervical dislocation, the tissues were dissected out, cleaned by washing in 0.9% saline, put immediately on ice and blotted dry and weighed. The whole cell extract from cells and tissues was prepared according to the mini-extract preparation method of Sakatsume and Finbleoom (1996) with certain modifications. For every 0.1gm of tissue 500 µl of buffer was added. The tissue was transferred to a glass hand homogenizer kept on ice using an autoclaved forceps and homogenized for 5-10 min. after addition of the required amount of homogenizing whole cell extraction buffer (0.1% Triton X-100, 10 mM HEPES pH 7.9, 400 mM KCl, 10% Glycerol, 2 mM EDTA, 1 mM EGTA, 1 mM DTT, 500 µM PMSF, 5 µg/ml leupeptin, 5

μg/ml aprotinin, 1.25 μg/ml benzamidine) . The homogenate was taken in a fresh Eppendorf tube and sonicated on ice at 12 amp for 15 seconds giving an interval of 45 sec between every two sonications. The number of sonications varied from 5-7 times for brain, thymus, liver, spleen and intestine and to 7-10 times for lung, kidney and heart. Heating of the Eppendorf tube was avoided by performing the sonications on ice and keeping the extract on ice between two consecutive sonications. Following this, the extracts were centrifuged at 15,000 rpm at 4^0 C for 5 minutes. The supernatants (WE) were stored at -80^0 C for subsequent use. L 929 whole cell extract was prepared by taking $1X10^6$ cells per 500 μl homogenizing buffer and sonicating on ice 5 times at 12 Amp for 15sec. with a break of 45 sec between two consecutive pulses.

5.2.4.3 Preparation of cytoplasmic and nuclear extracts from mouse tissues and human cell lines

This is a modified method of Schreiber et. al., (1989). The tissues of interest were dissected out from mouse, washed with 0.9% NaCl, weighed and kept on ice. To every 0.1 gm of tissue 500 μl of ice cold cytoplasmic lysis buffer (10 mM HEPES, pH 7.9, 10 mM KCl, 0.1 mM EDTA, pH 8.0, 0.1 mM EGTA, pH 7.0, 1.0 mM DTT, 1.0 mM PMSF, 2 μg/ml leupeptin, 2 μg/ml aprotinin, 0.5 mg/ml benzamidine) was added. It was homogenized manually in a glass hand homogenizer for 10 min on ice and then kept for another 15 min on ice for the cells to swell up. 15 μl of 10% NP-40 was added and the cells were thoroughly vortexed twice for 10 sec. to lyse the cells. Following which they were given a spin at 12000 rpm at 4^0 C for 5 min. The supernatant (cytoplasmic extract or CE) was saved into a fresh Eppendorf tube and stored at -80^0 C. To the nuclear pellet, which was transparently white (reddish for some tissues), 250 μl of nuclear extraction buffer (20 mM HEPES, pH 7.9, 400 mM NaCl, 1.0 mM DTT, 0.5 mM PMSF, 2 μg /ml leupeptin , 2 μg /ml

aprotinin and 0.5 mg/ml benzamidine) was added and kept on ice for 30 min with intermittent vigorous vortexing at every 5min to extract the nuclei. This was followed by centrifugation at 15000 rpm for 5 min at 4^0 C. the supernatant (nuclear extract or NE) was stored at -80^0 C.

L 929 (after trypsinisation as per standard procedure) or U 937 cells were collected by low speed centrifugation at 3,500 RPM at room temp and resuspended in PBS at 2 x 10^6 cells/ml and 1 ml was taken in 1.5 ml Eppendorf tubes kept on ice. The cells were pelleted, washed once with 1 ml ice cold PBS. The cell pellet was resuspended in 400 µl of ice cold cytoplasmic lysis buffer (as above) using a P-200 pipette. The cell suspension was incubated on ice for 15 min allowing the cells to swell. This was followed by addition of 12.5 µl of 10% NP-40 and vigorous vortexing for 10 secs twice to lyse the cells. After centrifugation for 5 min at 15000 rpm at 4^0 C, the supernatant was collected and stored at -80^0 C. 25 µl of ice cold nuclear extraction buffer (as above) was added to the transparently white nuclear pellet and kept on ice for 30 min with intermittent vortexing every 5 min to extract the nuclei. The extract was centrifuged at 15000 rpm for 5 min at 4^0 C to obtain the nuclear extract as the supernatant which was transferred to a fresh Eppendorf tube and stored at -80^0 C. However, these whole cell extracts, cytoplasmic and nuclear extracts were used for experiments as soon as possible (within one week of their preparation) and were thawed only 1 to 2 times on ice before use.

5.2.4.4 Estimation of protein in various extracts

Protein concentration in cell and tissue extracts were measured by Bradford assay (Bradford, 1976). A serially diluted stock of 10 µg/ml, 20 µg/ml, 40 µg/ml, 60 µg/ml, 80 µg/ml and 100 µg/ml of BSA was prepared from a stock of 1000 µg/ml in water. 50 µl of BSA for each dilution was taken

in duplicates and added to a row of wells in a 96 well plate. In the subsequent rows, 2 µl of whole cell, cytoplasmic or nuclear extracts of cells or tissues were added to 50 µl of double distilled autoclaved water in deplicates along with the blank (ie 50 µl of water alone). 150 µl of Bradford's solution (0.01 % Coomassie brilliant blue G-250, 4.75% ethanol, 8.5% o-phosphoric acid) was added to each well. Estimation of O. D. was carried out by a ELISA plate reader at 590 nm wave length against water blank. A standard curve was drawn for BSA conc. (10-100 µg/ml) and protein conc. (µg/ml) of the extract was calculated from this standard curve.

5.2.4.5 ^{32}P Labeling and annealing of oligonucleotides

Synthetic single stranded oligonucleotides with 5'-OH group were ^{32}P labeled by kinasing of the oligos (Sambrook et. al., 1989) : $(GAAAGT)_4$ and $(GAAA)_6$ in the following manner:

Stock	*volume*	*Final conc.*
Oligo [$(GAAAGT)_4$ or $(GAAA)_6$] (3 pmole/µl)	1 µl	3 pmole
Reaction Buffer (NEB) 10X (700 mM Tris-HCl, pH 7.6, 100 mM $MgCl_2$, 50 mM DTT)	2 µl	1X
γ^{32}P ATP (10µCi/µl) (Sp. Activity = 5000 Ci/mmole)	1.5 µl	15 µCi
DTT (20 mM)	1 µl	1 mM
T_4 Polynucleotide Kinase (NEB) (10U/µl)	1 µl	10 U
Water	13.5µl	
Vol.	20µl	

The final reaction was made to 20 µl with deionised double distilled water, mixed, given a pulse spin and incubated at 37^0 C for 30 min. The reaction was stopped by quickly putting it on ice. Annealing of the ^{32}P labeled oligo with the reverse complementary oligo was done in the following way:

Stock	*Volume*	*Final conc.*
Reaction Mix	20 µl	3 pmole
Reverse Complementary oligo (10 pmole/µl)	1 µ l	10 pmole
NaCl (1M)	1.0 µl	50 mM
	22.0 µl	

The annealing reaction mixture was mixed and given a pulse spin and kept in a 85^0 C water bath for 10 min. The water bath was then switched off allowing the reaction mixture to cool gradually overnight. Purification of ^{32}P oligo was done by G50-TNE spin column. 1 µl of the elute was counted for ^{32}P Cerenkov counting in a scintillation counter (LKB). Usually 1 µl ^{32}P double stranded oligo gave about 20,000 to 40, 000 cpm. Specific activity of the double stranded oligo was about $2\text{-}5x10^6$ cpm/pmole. Both single stranded (annealed) and double stranded (annealed) oligonucleotides were checked by native polyacrylamide gel to check the proportion of ^{32}P labeled double stranded oligo which was found to be very close to 100%.

5.2.4.6 Mobility Shift Assay

Electrophoretic mobility shift assay (EMSA) was carried out as described in Ausubel et al. (1995) with certain modifications. The extracts were thawed on ice. The entire reaction was set on ice unless otherwise mentioned. The components of the binding reaction were added in the following sequence: water, 10 x binding buffer (200 mM HEPES, pH 7.9, 4 mM EDTA, pH 8.0, 4

mM DTT, 50% glycerol) to a final 1x conc., 2 μg Poly (dI:dC) or sonicated and purified calf thymus DNA as nonspecific DNA, 50 fmole ^{32}P labeled double stranded oligo $(GAAAGT)_4$, 10% NP-40 (final conc. 1%) and lastly the appropriate amount (μg protein) of the extract. Usually 5-20 μg extract was used. The reaction was mixed and given a pulse spin. Incubated for 30 min. at 37^0 C. The tubes were then quickly transferred to ice and one-sixth of 6 x loading dye was added, to make 1 x final conc. The mixture was quickly spin at room temperature. The binding reactions were then loaded to a 7% native polyacrylamide gel (18x20x1.5 cm) in TBE buffer, which was polymerized at least 1-2 hr before and prerun at 150V (~ 40 mA) for 30 min and wells were cleaned before loading the samples. The gel was usually run at 150V (~ 40 mA) for 3-4 hrs in cold room or below 20^0C. After the run was over, the gel was transferred onto a Whatmann 3MM filter paper, covered with saran wrap and dried in a gel dryer for 60 to 90 min at 80^0 C under vacuum. The dried gel was then exposed to imaging plate for 18-24 hr. at room temperature and the image was visualised in a Fuji Film Phosophoimager, BAS 1800. DNA-Protein complexes were quantitated with the help of Image Gauge V2.54 software. The pixel values for DNA-protein complex was considered for all calculations and graphic representations. Gels were also exposed to X-ray films (Kodak X-omat, XAR.5 or Amersham Hyper film) for autoradiographic picture which was scanned and imported to the electronic form in the computer using standard PC based methods.

5.2.5 Northern blot and RNA dot blot assay

5.2.5.1 RNA isolation from different mouse tissues

Total RNA from mouse tissues was isolated by the method of Auffray and Rougeon (1980). Fresh tissues (brain, thymus, lungs, heart, liver, spleen, kidney and intestine) from the mice were collected, washed in normal saline twice at 4^0 C to remove blood, blotted, weighed and then minced into small pieces on ice. All following steps were carried out under RNase-free conditions (as per standard protocol) and on ice at 0-4 ^{0}C unless otherwise mentioned. Lysis buffer (6 M urea, 3 M LiCl, 50 mM NaOAc, 0.1% SDS and 200 μg/ml heparin, last two components added freshly just before use) was added to the minced tissue to make a 10% homogenate and was throughly homogenized in a glass homogenizer with a teflon pestle. Homogenates were then sonicated on ice in a ultrasonicator for 30 sec each for 6 times with 1 min gap in between and were kept on ice at 4^0 C for 16-18 hr for precipitation. The extracts were centrifuged in a Sorvall, SS-34 rotor, at 10,000 rpm for 15 min at 4 ^{0}C. Precipitates were pelleted and resuspended/washed in 4 ml (8 M urea + 4 M LiCl) and centrifuged as before. Final precipitates were dissolved in 3-5ml (200 mM NaOAc pH 5.0, 0.2% SDS and 1 mM EDTA) by vigorous vortexing until it was soluble. The RNA solutions were extracted twice: once with equal volume of TNE-phenol and then with equal volume of phenol: chloroform (1:1). Care was taken to ensure that there was no residual interphase material. Aqueous phases were collected by centrifugation at 12,000 rpm for 8 min, at 4^0 C. RNA was then precipitated by adding 2.5 volume chilled ethanol in presence of 0.3 M sodium acetate (pH 5.0), kept at -20^0 C for overnight. RNA was precipitated by centrifugation at 12000 rpm for 15 min, at 4 ^{0}C. It was throughly washed with 80% ethanol, air-dried and finally dissolved in 100 μl sterile distilled water. A260/A280 nm ratio of the RNA and A200-300 nm scan were also measured spectrophotometrically. Both the yield and quality of the

RNA were determined from the A260 nm value and the ratio of A260nm/280nm values as well as the A200-300 nm spectrum as per standard recommendations. RNA solutions were also routinely checked in 1% agarose-TAE gels, stained with ethidium bromide to visualise the intactness of the 28S and 18S ribosomal RNAs. For short storage RNA solutions were stored at –80^{0}C and for long storage they were stored at –20^{0}C as 70% ethanol precipitates.

5.2.5.2 RNA dot blot assay

RNA was quantitated by measuring OD at 260 nm. 5, 10 and 20 µg of the RNA was taken in Eppendorf tubes and dried in the Speedvac. The RNA was then dissolved in 4 µl sterile distilled water. RNA was denatured by 2min in boiling water bath then chilled on ice spin and used. 2 µl of the RNA solution was applied to the dry membrane (‚Hybond N^+ membrane, Amersham), allowed to dry and then the remaining 2µl was applied to the same spot to prevent spreading of the RNA.. The membrane was then exposed to 1200 µjoules/cm^2 UV for 1 min to cross link the RNA onto the membrane. The membrane was washed with 5 x SSC then dried at 37^0 C, then stored at 4^{0}C after sealing it in polypropylene bag.

5.2.5.3 Northern blot and dot blot hybridizations

Northern blot and dot blot hybridizations were carried out as per the method of Sambrook et al. (1989). 30 µg of RNA from each tissue was aliquoted and pelleted after ethanol precipitation. It was dissolved in 4.5 µl deionised water and then mixed with 2 µl 5 x formaldehyde buffer (0.1 M

MOPS, pH 7.0, 40 mM sod. acetate, 5 mM EDTA, pH 8.0), 3.5 µl 37% formaldehyde and 10 µl deionised formamide (98%) and was denatured at 65^0 C for 15 min followed by qui k chilling on ice for 5 min. The denatured RNA sample was mixed with 4 µl 6 x FA dye and was electrophoresed along with 1kb cDNA as the positive control for hybridization. For a 13 x 13 x 0.3 cm^3 denaturing 1.0% agarose-formaldehyde gel, 1.0 gm agarose was resuspended in 62 ml DEPC treated water, boiled for 5-10 min till it completely dissolved, cooled down to ~60 ^{0}C. Then 20 ml 5 x formaldehyde buffer (0.1 M MOPS, pH 7.0, 40 mM sodium acetate pH 5.0, 5 mM EDTA, pH 8.0) and 17.8 ml 37% formaldehyde were added, 5 µl of ethidium bromide (10 mg/ml) was added, mixed and poured. The gel was allowed to set at least for 1-2 hr. Electrophoresis was carried out in 1x MOPS-formaldehyde buffer at 100 mA constant current for 3-4 hrs. After electrophoresis, the gel was washed with sterile distilled water for 3-4 times for 15 min each time to remove formaldehyde. The gel was transferred onto a nylon membrane by conventional capillary blotting, for 16-18 hr using 10 x SSC as the transfer buffer. RNA on the moist membrane was UV-cross-linked in a UV-cross linker at 1200 µjoules for 1 min. The membrane was washed in 2 x SSC, dried and stored in a sealed polypropylene bag at 4 ^{0}C until further use.

For Northern blot and dot blot hybridization, RNA-nylon membrane was prehybridized at 42^0 C in a hybridization bottle with 10 ml prehybridization solution [50% deionised formamide, 5 x Denhardt's solution, 5 x SSC, 0.5% SDS, 1 mM EDTA, 0.05 M Na_2HPO_4, pH 7.2, and denatured Salmon sperm DNA (100 µg/ml)]. After 2-3 hr, prehybridization solution was added with purified heat-denatured probe (>10^5 cpm/ml) and hybridization was carried out at 42^0 C for 16 to 18 hr. Membranes was successively washed thrice in 2 x SSC + 0.1% SDS at RT for 15 min each, twice in 0.2 x SSC + 0.1% SDS at 42^0 C, radioactivity was counted by a hand-held radioactive monitor and if required washed with 1 x SSC + 0.1% SDS at 50^0 C and 0.2 x SSC + 0.1%

SDS at 50^0 C to remove background. Signal to noise ratio was checked during washing. Membrane was wrapped with saran wrap and was exposed to phosphor screens of a phospl ›imager (fujifilm,BAS 1800) and the image was developed and quantitated with Image Gauge V2.54 software.The blot was also exposed to X-ray film with intensifying screen at -80 ^{0}C for desired time period to develop an autoradiogram.

5.2.5 Comparison of mouse, rat and human IRF-1 cDNA and amino acid sequences

Mouse, rat and human IRF-1cDNAs were retrieved from GeneBank database available online at www.ncbi.nlm.nih.gov. web site. The IRF-1 accession numbers were M 21065 (Mouse), M 34253 (Rat) and X 14454 (Human) respectively [ref : Mouse IRF-1- Miyamoto, M., et. al., (1988) Cell 54: 903-913, Rat - Yu-lee et. al., (1990) Mol. Cell. Biol. 10: 3087-3094, Human- Maruyama, M., et. al., (1989) Nucleic Acid Res. 17(8): 3292]. IRF-1 cDNA sequences from these three species were compared to find out first restriction enzyme sites that may vary between the mouse and the human IRF-1. Then nucleotide sequences were compared around these regions to find out if a restriction site can coincide with any amino acid change. A few such were detected. The cDNA sequences were converted into amino acid sequences with the help of PC gene software and this matched with the published data. The amino acid sequences of IRF-1 was compared between mouse and rat as well as between mouse and human using the computer program Clustal W. The changes were represented as bar diagram in fig. 13. and table 3.6. Both substitutions and absence of amino acids were considered as changes. The bar representing IRF-1 with the DNA binding- and transcription activation domains contained horizontal lines inside the bars at respective amino acid positions. Mouse IRF-1 was taken as the reference for comparison and a detailed analysis was carried out.

RESULTS

6. RESULTS

Results constitute of four sections: (1) Organization of IRF-1 gene, (2) Amino acid changes in IRF-1, (3) Expression of IRF-1 mRNA and (4) DNA binding activity of IRF-1.

6.1 Organization of IRF-1 gene:

6.1.1 Purification of nuclei, genomic DNA and plasmid DNA

Purified nuclei (nuclear suspension equivalent to 500 μg DNA/ml) from the mouse liver were observed under phase contrast microscope at 1250 X magnification. Nuclei were round, intact, present in good density and largely free from cytoplasmic contamination. In some nuclei, nucleolus was also visible. Spectrophotometric scan ($\lambda_{200\text{-}300}$ nm) of disrupted nuclei in 2 M NaCl + 5 M Urea at 200 to 300 nm showed the characteristic pattern (peak at A_{220} and A_{260} nm along with a shoulder at A_{240} nm) as expected for nucleoprotein complex of the mammalian chromatin (Bonner et al. (1968). Yield and $A_{260/280}$ nm ratio of the purified nuclei were 1.67 mg/gm wet-weight and 1.78 for the liver respectively. These parameters were regularly measured to check purity of the nuclear preparation before using it for further experiments.

Genomic DNA purified from the liver was checked by 0.6 % agarose gel by electrophoresis. It was devoid of degradation by mechanical damage or nuclease activity and the molecular mass of the DNA was more than 21 kb. Spectrophotometric scan of the genomic DNA at 200 to 300 nm showed the characteristic pattern for DNA with a clear peak at 260 nm and the ratio of $A_{260/280}$ nm was 1.72. The yield of genomic DNA was 450-550 μg/gm wet-weight. Even after prolonged storage at 4 ^{0}C (with one drop of chloroform) or

storage at –20 ^{0}C in 80 % ethanol (in precipitated form) quality of the DNA was good. This genomic DNA was used for Southern blot analysis.

Plasmid DNA purified by all three methods (LiCl-boiling mini-preparation, alkaline-lysis midi-preparation and large-scale preparation) were regularly checked for their yield and quality by agarose gel electrophoresis and absorption at 260, 280 nm by spectrophotometer. Two topological forms, covalently closed circular (CCC) and open circular (OC) were routinely observed, with a little bit of denatured form due to the alkali treatment. Presence of genomic DNA contamination was seen rather rarely. The covalently closed circular (CCC) form of plasmid DNA moved fastest in the gel due to its compactness followed by open circular (OC) form. Wavelength scan ($\lambda_{200\text{-}300}$ nm) of plasmid DNA at 200 to 300 nm showed the characteristic pattern of pure DNA with a peak at 260 nm and $A_{260/280}$ ratio was around 1.6 - 1.8. The yield of the plasmid DNA (pBluescript) was ~10 μg/5 ml, ~100 μg/15 ml and ~1.6 mg/250 ml culture. Plasmid DNA purified by the large-scale method was further purified through Sephadex-G50/TNE column to remove small size contaminating DNA/RNA. These plasmid DNAs were good enough for further experimental purposes even after long storage in aqueous form at – 20 ^{0}C.

6.1.2 IRF-1 gene probes, nucleotide and amino acid sequences

For studying IRF-1 gene organization by Southern blot analysis, we have used three probes. The pIRFL plasmid was digested by Xho I and the two 1 kb IRF-1 cDNA fragment(s) (**1 kb cDNA probe**) was released. The 5' IRF-1 proximal exon probe was obtained by digesting the pIRFL plasmid first by Hind III and then by Pst I to release the 194 bp 5' 1st exon probe with a few

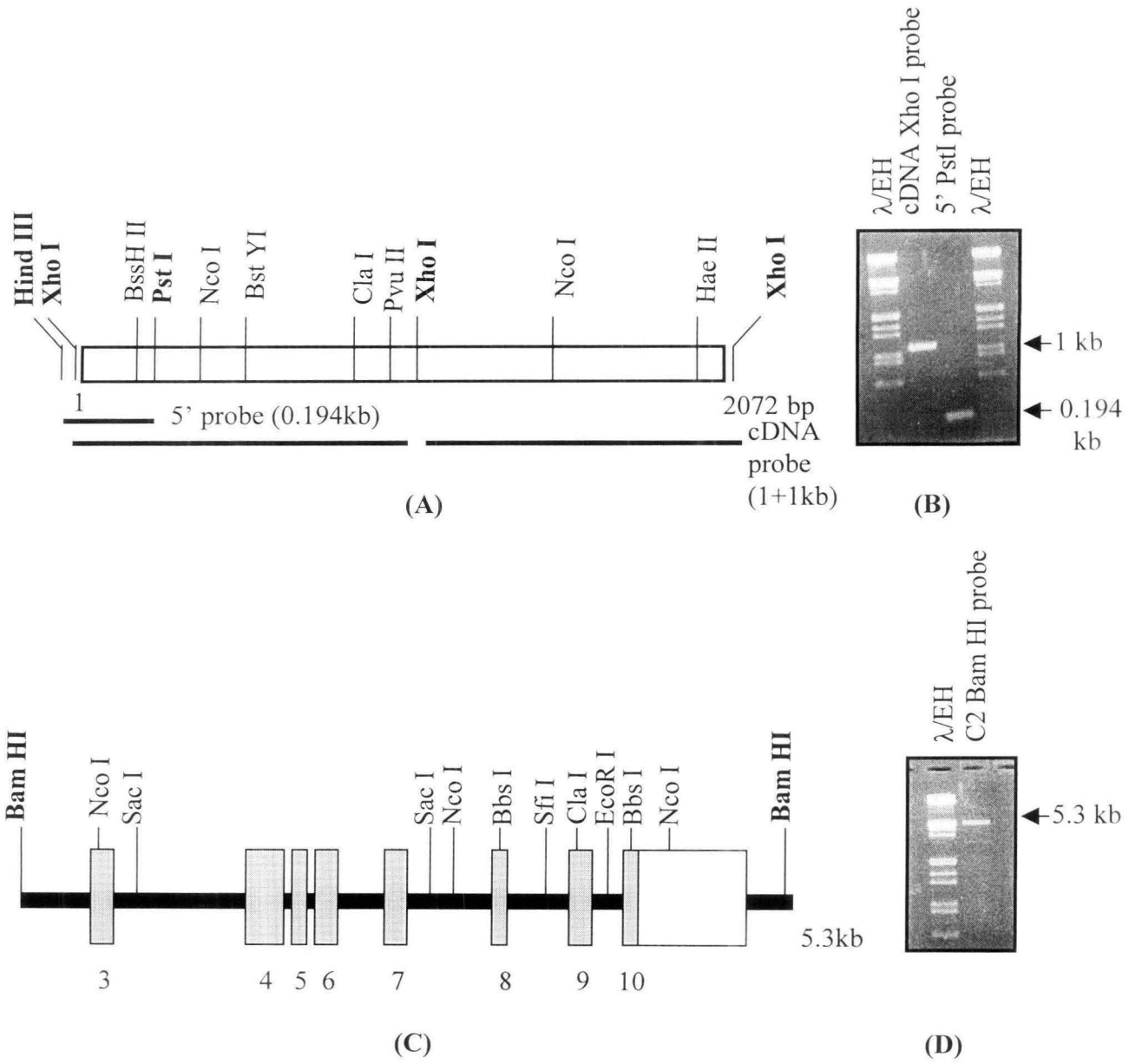

Fig. 1 Restriction maps of murine (A) IRF-1 cDNA (pIRFL) (Miyamoto, M. et al.*Cell*, 54: 903-913,1988) and (C) IRF-1 genomic DNA (pIRFC2) clones (Reis, L.F.L. et al. *The EMBO J.*13: 4798-4806,1994). Ethidium bromide stained gels for purified cDNA probe, 5' 1st exon probe (B) and C2 genomic DNA probe (D) are shown. Numbers in (C) refer to exons. λ/EH is λDNA digested by EcoR I and Hind III and used as a molecular size marker.

Fig. 2 Murine IRF-1 (A) cDNA, (B) amino acid sequences (Miyamoto, M. et al. 1988 *Cell* 54: (903-913), and (C) different domains in IRF-1 protein. DBD –DNA binding domain with tryptophan (W) repeats, TAD - Transcriptional activation domain with IRF-association domain (IAD).

Fig. 3 Murine IRF-2 (A) cDNA, (B) amino acid sequences (Harada, H., et al. 1989 *Cell* 58: 729-739) and (C) different domains in IRF-2 protein. DBD- DNA binding domain with tryptophan (W) repeats and TRD-Transcriptional repression domain containing IRF association domain (IAD).

1GGACGTGCTT TCACAGTCTA AGCCGAACCG AACCGAACCG AACCGAACCG AACCGGGCCG
AGTTGCGCCG AGGTCAGCCG AGGTGGCCAG AGGACCCCAG CATCTCGGGC ATCTTTCGCT
TCGTGCGCGC ATCGCGTACC TACACCGCAA CTCCGTGCCT CGCTCTCCGG CACCCTCTGC
GAATCGCTCC TGCAGCAAAG CCACC**ATG**CC AATCACTCGA ATGCGGATGA GACCCTGGCT
AGAGATGCAG ATTAATTCCA ACCAAATCCC AGGGCTGATC TGGATCAATA AAGAAGAGAT
GATCTTCCAG ATTCCATGGA AGCACGCTGC TAAGCACGGC TGGGACATCA ACAAGGATGC
CTGTCTGTTC CGGAGCTGGG CCATTCACAC AGGCCGATAC AAAGCAGGAG AAAAAGAGCC
AGATCCCAAG ACATGGAAGG CAAACTTCCG TTGTGCCATG AACTCCCTGC CAGACATCGA
GGAAGTGAAG GATCAGAGTA GGAACAAGGG CAGCTCTGCT GTGCGGGTGT ACCGGATGCT
GCCACCCCTC ACCAGGAACC AGAGGAAAGA GAGAAAGTCC AAGTCCAGCC GAGACACTAA
GAGCAAAACC AAGAGGAAGC TGTGTGGAGA TGTTAGCCCG GACACTTTCT CTGATGGACT
CAGCAGCTCT ACCCTACCTG ATGACCACAG CAGTTACACC ACTCAGGGCT ACCTGGGTCA
GGACTTGGAT ATGGAAAGGG ACATAACTCC AGCACTGTCA CCGTGTGTCG TCAGCAGCAG
TCTCTCTGAG TGGCATATGC AGATGGACAT TATACCAGAT AGCACCACTG ATCTGTATAA
CCTACAGGTG TCACCCATGC CTTCCACCTC CGAAGCCGCA ACAGACGAGG ATGAGGAAGG
GAAGATAGCC GAAGACCTTA TGAAGCTCTT TGAACAGTCT GAGTGGCAGC CGACACACAT
CGATGGCAAG GGATACTTGC TCAATGAGCC AGGGACCCAG CTCTCTTCTG TCTATGGAGA
CTTCAGCTGC AAAGAGGAAC CAGAGATTGA CAGCCCTCGA GGGGACATTG GGATAGGCAT
ACAACATGTC TTCACGGAGA TGAAGAATAT GGACTCCATC ATGTGGATGG ACAGCCTGCT
GGGCAACTCT GTGAGGCTGC CGCCCTCTAT TCAGGCCATT CCTTGTGCAC CA**TAG**TTTGG
GTCTCTGACC CGTTCTTGCC CTCCTGAGTG AGTTAGGCCT TGGCATCATG GTGGCTGTGA
TACAAAAAAA GCTAGACTCC TGTGGGCCCC TTGACACATG GCAAAGCATA GTCCCACTGC
AAACAGGGGA CCATCCTCCT TGGGTCAGTG GGCTCTCAGG GCTTAGGAGG CAGAGTCTGA
GTTTTCTTGT GAGGTGAAGC TGGCCCTGAC TCCTAGGAAG ATGGATTGGG GGGTCTGAGG
TGTAAGGCAG AGGCCATGGA CAGGAGTCAT CTTCTAGCTT TTTAAAAGCC TTGTTGCATA
GAGAGGGTCT TATCGCTGGG CTGGCCCTGA GGGGAATAGA CCAGCGCCCA CAGAAGAGCA
TAGCACTGGC CCTAGAGCTG GCTCTGTACT AGGAGACAAT TGCACTAAAT GAGTCCTATT
CCCAAAGAAC TGCTGCCCTT CCCAACCGAG CCCTGGGATG GTTCCCAAGC CAGTGAAATG
TGAAGGGAAA AAAAATGGGG TCCTGTGAAG GTTGGCTCCC TTAGCCTCAG AGGGAATCTG
CCTCACTACC TGCTCCAGCT GTGGGGCTCA GGAAAAAAAA ATGGCACTTT CTCTGTGGAC
TTTGCCACAT TTCTGATCAG AGGTGTACAC TAACATTTCT CCCCAGTCTA GGCCTTTGCA
TTTATTTATA TAGTGCCTTG CCTGGTGCCT GCTGTCTCCT CAGGCCTTGG CAGTCCTCAG
CAGGCCCAGG GAAAAGGGGG GTTGTGAGCG CCTTGGCGTG ACTCTTGACT ATCTATTAGA
AACGCCACCT AACTGCTAAA TGGTGTTTGG TCATGTGGTG GACCTGTGTA AATATGTATA
TTTGTCTTTT TATAAAAATT TAAGTTGTTT AC 2072

(A)

1MPITRMRMRPWLEMQINSNQIPGLIWINKEEMIFQIPWKHAAKHGWDINKDACLFRSWAIHTGRYKAGEKEPDP
KTWKANFRCAMNSLPDIEEVKDQSRNKGSSAVRVYRMLPPLTRNQRKERKSKSSRDTKSKTKRKLCGDVSPDTFS
DGLSSSTLPDDHSSYTTQGYLGQDLDMERDITPALSPCVVSSSLSEWHMQMDIIPDSTTDLYNLQVSPMPSTSEA
ATDEDEEGKIAEDLMKLFEQSEWQPTHIDGKGYLLNEPGTQLSSVYGDFSCKEEPEIDSPRGDIGIGIQHVFTEM
KNMDSIMWMDSLLGNSVRLPPSIQAIPCAP 329

(B)

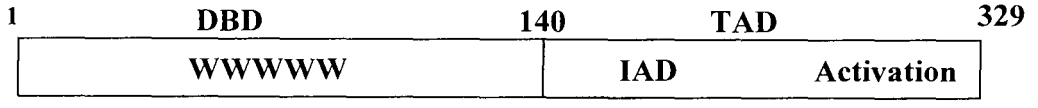

(C)

Fig. 2

```
1  TCTCAGGCAA GCCGGGGACT AACTTTTAGT TTTGCTCCTG CGATTATTCA ACTGACGGGC
   TTTCATTTCC ATTTTACACA CCCTAACAAC ACTCACACCT TGCGGGATTG TATTGGTAGC
   GTGGAAAAAA AAAAAGCACA TTGAGAGGGT ACCATGCCGG TGGAACGGAT GCGAATGCGC
   CCGTGGCTGG AGGAGCAGAT AAATTCCAAT ACGATACCAG GGCTAAAGTG GCTGAACAAG
   GAGAAGAAGA TTTTCCAGAT CCCCTGGATG CATGCGGCTC GGCACGGATG GGACGTGGAA
   AAGGATGCTC CGCTCTTCAG AAACTGGGCG ATCCATACAG GAAAGCATCA ACCAGGAATA
   GATAAACCAG ATCCAAAAAC ATGGAAAGCA AATTTTCGAT GTGCCATGAA TTCCCTGCCC
   GACATTGAGG AAGTGAAGGA CAGAAGCATA AAGAAAGGAA ACAACGCCTT CAGAGTCTAC
   CGGATGCTGC CCTTATCCGA ACGACCTTCC AAGAAAGGAA AGAAACCAAA GACAGAAAAA
   GAAGAGAGAG TTAAGCACAT CAAGCAAGAA CCAGTTGAGT CATCTTTGGG GCTTAGTAAT
   GGAGTAAGTG GCTTTTCTCC TGAGTATGCG GTCCTGACTT CAGCTATAAA AAATGAAGTG
   GATAGTACGG TGAACATCAT AGTTGTAGGA CAGTCCCATC TGGACAGCAA CATTGAAGAT
   CAAGAGATCG TCACTAACCC GCCAGACATC TGCCAGGTTG TAGAAGTGAC CACTGAGAGT
   GATGACCAGC CAGTCAGCAT GAGTGAGCTC TACCCTCTAC AGATTTCTCC TGTGTCTTCC
   TACGCAGAAA GCGAAACTAC CGACAGTGTG GCCAGTGATG AAGAGAACGC AGAGGGGAGA
   CCACACTGGA GGAAGAGGAG CATCGAAGGC AAGCAGTACC TCAGCAACAT GGGGACACGG
   AACACCTATC TGCTGCCCAG CATGGCGACC TTTGTCACCT CCAACAAGCC AGATCTGCAG
   GTCACCATCA AAGAGGATAG CTGTCCGATG CCTTACAACA GCTCCTGGCC CCCATTTACA
   GACCTTCCCC TTCCTGCCCC AGTGACCCCC ACGCCCAGCA GCAGTCGGCC AGACCGGGAG
   ACCCGGGCCA GTGTCATCAA GAAGACATCT GATATCACCC AGGCCCGTGT CAAGAGCTGT
   TAAGCCTTTG ACTCTCCCTG GTGGTTGTTG GGATTTCTTA GCTTTGTGTT GTTCTTTGTT
   TGTATTATAT TATTTTTTTT CTCTATGATA CCTATCTTAG ACACATCTAA GGGAGAAAGC
   CTTGACGATA GATTATTGAT TGCTGTGTCC AACTCCAGAG CTGGAGCTTC TTCTTAACTC
   AGGACTCCAG CCCCCCCCCC CCCTCGGTAG ATGCGTATCT CTAGAACCTG CTGGATCTGC
   CAGGGCTACT CCCTCAAGTT CAAGGACCAA CAGCCACACG GGCAGTGGAG GTGCTGCGTT
   GCCTACGGTC AAGGCCAGCA TGGTGGAGTG GATGCCTCAG AACGGAGGAG AAAATGTGAA
   CTAGCTGGAA TTTTTTTATT CTTGTGAATA TGTACATAGG CAGTACGAGC AATGTCGCGG
   GCTGCTTCTG CACCTTATCT TGAAGCACTT ACAATAGGCC TTCTTGTAAT CTTGCTCTCC
   TTCACAGCAC ACTCGGCGAC CCCTTCTGTG TCCACTACCC CACTACCCAC CCCTCCCTCC
   TCAACCCCTC CATCCCGGTC CTCTATGCGC CCCTTCCCCC CAACCAATCC CATCACAACC
   TCTTACCTAT CCTTTCCCTC CCAACCCCTT CTATCCCAGC CCACCACCTA CCCCACTCCT
   CCCCAACTCC TCCATTCTAG CCCATTACCC ACGCCTCTCT CCTCAGCCCA GCCTACCCCA
   TCCCACCCTG TTCCTTTCCT CCAGTTTCCT CTCCTCAAAG GCAAGGCTCT ACATCTTGGA
   GGAGGAGGAG GAGAAGAAAA TGAGTTTCTT CACCGCTGTC CCATTTTAAG ACTGCTTGAA
   TAATAAAAAA AAATCTTTCT AATCTGCTAT GCTTGAATGG CACGCGGTAC AAAGGAAAAC
   TGTCATGGAA ATATTATGCA AATTCCCAGA TCTGAAGACG GAAAATACTC TAATTCTAAC
   CAGAGCAAGC TTTTTTATTT TTTTATACAA GGGGAATATT TTATTCAAGG TAAAAAAATT
   CTAAATAAAA TATAATTGTT TTTTATCTTT TCTACAGCAA ATTTATAATT TTAAGATTCC
   TTTTCCTGTT CATCAGCAGT TGTTATTACA TCCCTTGTGG CACATTTTTT TTTTAATTTT
   GTAAAGGTGA AAAAAAAACT TTTATGAGCT CATGTAGCAA TCAAATTATC CTGTGGATTG
   ATAATAAATG AATATGGTAT ATAGTTAAAG ATTTT 2436
```

(A)

```
1MPVERMRMRPWLEEQINSNTIPGLKWLNKEKKIFQIPWMHAARHGWDVEKDAPLFRNWAIHTGKHQPGIDKPDPKTWK
ANFRCAMNSLPDIEEVKDRSIKKGNNAFRVYRMLPLSERPSKKGKKPKTEKEERVKHIKQEPVESSLGLSNGVSGFSPE
YAVLTSAIKNEVDSTVNIIVGQSHLDSNIEDQEIVTNPPDICQVVEVTTESDDQPVSMSELYPLQISPVSSYAESETTD
SVASDEENAEGRPHWRKRSIEGKQYLSNMGTRNTYLLPSMATFVTSNKPDLQVTIKEDSCPMPYNSSWPPFTDLPLPAP
VTPTPSSSRPDRETRASVIKKTSDITQARVKSC 349
```

(B)

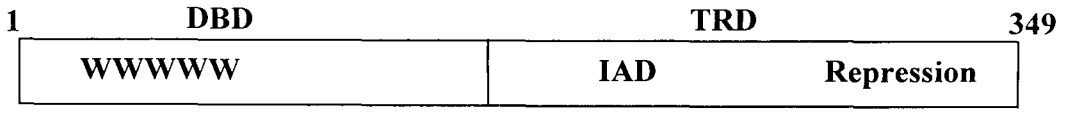

(C)

Fig. 3

base pairs from the vector DNA. This probe was referred to as **194 5' probe.** The IRF-1 genomic DNA probe was obtained by digesting the pIRF C2 plasmid by Bam HI and re'easing the 5.3 kb IRF-1 gene fragment which contained exon 3 to 10 and intron 2 to 10. This was referred to as **C2 genomic probe.** These three probes were purified as DNA fragments from 1% low melt agarose gels through phenol extraction and ethanol precipitation. Usually the purified DNAs were again checked in agarose gel, maintained and used as 20 ng/μl stock solutions.at –20 ^{0}C for preparing ^{32}P labeled DNA probes by random priming reactions for the hybridization studies. Fig.1 shows the map of IRF-1 cDNA (A) and genomic DNA (C). 1 kb cDNA, 194 5' and C2 genomic probe DNA fragments are shown in (B) and (D) respectively.

The nucleotide sequence, cDNA-predicted amino acid sequence and the basic organization of the DNA binding domain (DBD) as well as the transcriptional activation domain (TAD) containing IRF-association domain (IAD) of the mouse IRF-1 (M21065) cDNA are shown in fig.2 (A), (B) and (C) respectively. Similarly, mouse IRF-2 cDNA (J03168) nucleotide-, amino acid sequences and the DNA binding domain (DBD) as well as transcriptional repression domain (TRD) containing IRF-association domain (IAD) are shown in fig.3 (A), (B) and (C) respectively. It is evident from literature that the DNA binding domains of both IRF-1 and IRF-2 contain tryptophan (W) residues which are important for their DNA binding activity. IRF-1 and IRF-2 have very similar DNA binding activity in terms of the DNA sequence-specificity rather IRF-2 has an higher affinity towards the same sequence motif(s) to which IRF-1 binds in promoter(s) of certain mammalian gene(s). The DNA binding domain of IRF-1 and IRF-2 can be exchanged between them without affecting the function of either IRF-1's transactivation domain or IRF-2's repression domain in terms of transcription. The IRF-association domain functions for protein-protein association between different IRF-family members.

6.1.3 Optimization of Southern blot hybridization

Southern blot hybridization for the mouse IRF-1 gene was optimized by using 50, 25, 10 and 5 pg of the 5.3 kb Bam HI fragment of the murine IRF-1 genomic clone (pIRF C2 DNA digested by Bam HI) and ^{32}P labeled 5.3 kb DNA as the probe. ^{32}P labeled λ DNA digested by Eco RI +Hind III was used as the size marker. Fig. 4 shows that at least 5 pg DNA/band was detected for the 5.3 kb IRF-1 gene fragment. 5-50 pg of the IRF-1 gene fragment was detected with increasing signal density as per the loading. The efficiency of detection was considered to be optimum for detecting single copy gene(s) from the genomic DNA digests by Southern blot hybridization.

6.1.4 Southern blot analysis

(A) Mouse IRF-1 gene

For studying organization of the mouse IRF-1 gene, 20 μg genomic DNA from the mouse liver was digested with Bam HI, Eco RI, Hind III and Pst I. The digested DNA was run in 1% agarose gel along with 2 and 20 pg of IRF-1 cDNA as positive control and Eco RI and Hind III digested λ DNA used as molecular size marker. The Ethidium bromide stained agarose gel is shown in fig. 5 (B). The gel was transferred on to a nylon membrane and hybridized with ^{32}P labeled 1kb cDNA probe as shown in fig. 5 (A). A schematic representation of the 1 kb IRF-1 cDNA probe used is shown in fig. 5 (C). Many IRF-1 genomic DNA fragments were detected in fig. 5 (A). The 2 and 20 pg positive controls were strongly detected. To calculate the size of the DNA fragments hybridized with the probes, a graph was plotted between log bp of fragments against migration of λ/ Eco RI + Hind III bands in cm . The

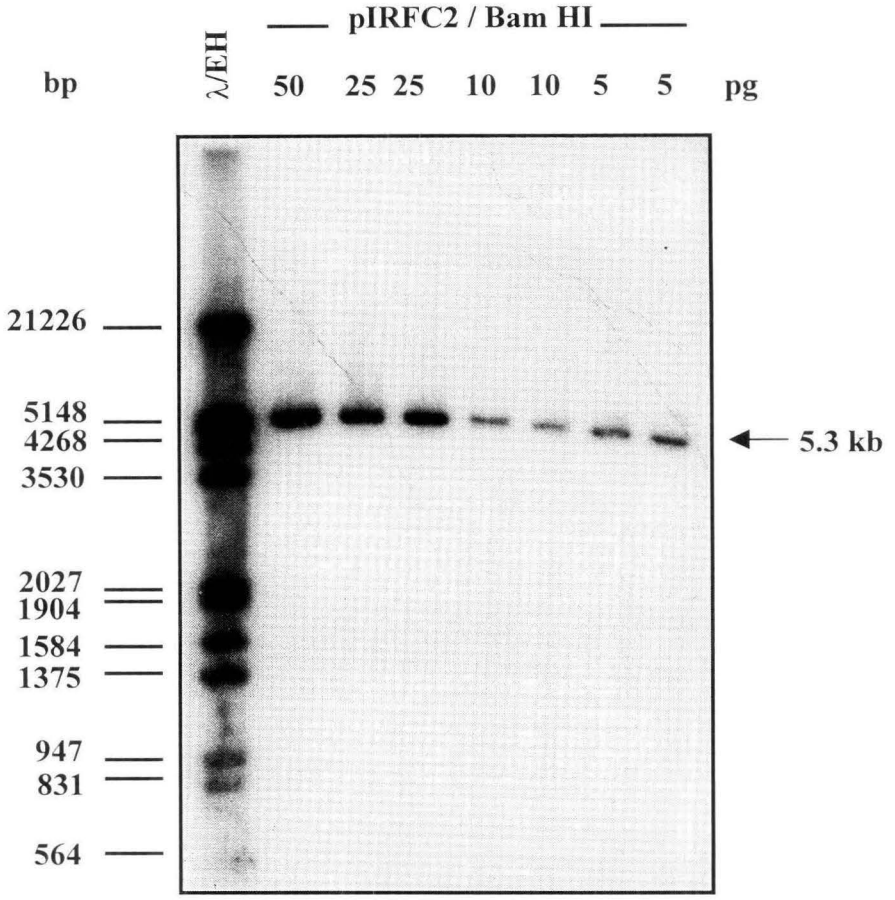

Fig. 4 Optimization of Southern blot hybridization. 50, 25, 10 and 5 pg of genomic clone i.e. pIRFC2/ Bam HI digested DNA was hybridized with ^{32}P labeled 5.3 kb gel purified C2 genomic DNA probe of mouse IRF-1. λ/EH is λ DNA digested by EcoRI and Hind III, ^{32}P labeled and used as molecular size marker.

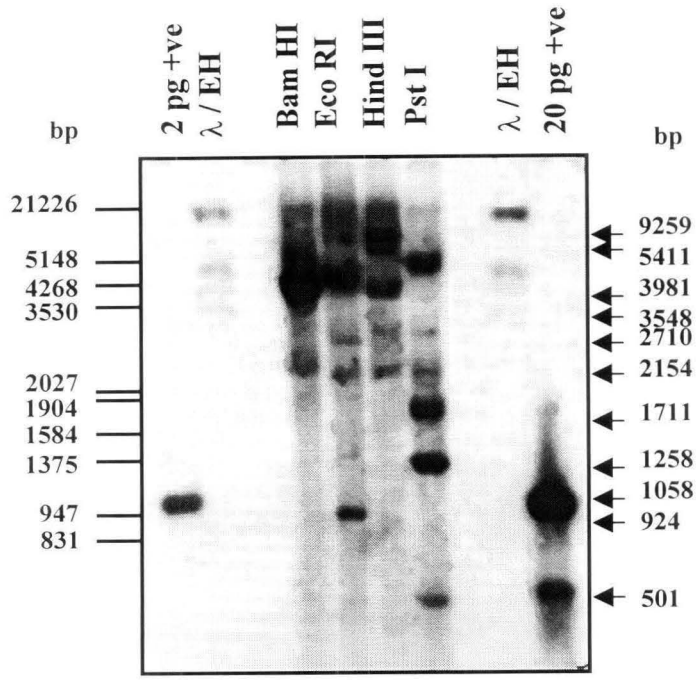

(A) Mouse IRF-1 gene

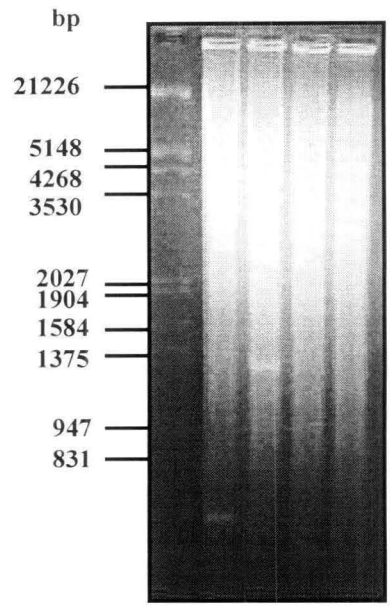

(B) EtBr stained gel

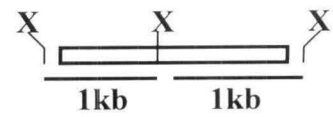

(C) 1 kb cDNA probe

Fig. 5 Southern blot analysis of mouse IRF-1 gene. (A) 20 μg mouse genomic DNA was digested by Bam HI, Eco RI, Hind III and Pst I and hybridized with ^{32}P labeled IRF-1 cDNA probe. (B) Ethidium bromide stained agarose gel and (C) 1kb cDNA probe of IRF-1. (A) and (B) are aligned lanewise. 2 and 20 pg 1kb XhoI cDNA was used as +ve control for hybridization. λ DNA digested by Eco RI and Hind III (λ/EH) was used as molecular size marker.

sizes of the fragments that hybridized to the probes were then calculated by extrapolating their migration in cm. to the migration of the standards. Since we already know that there exis' ; a IRF-gene family in mouse and man, only the strong bands after stringent hybridization and washing conditions were considered although there were also some weak bands still detected. The weak bands may represent IRF-1-like sequences from related genes. The size of the IRF-1 gene fragments detected after hybridization are mentioned in table 1. Bam HI digest of the mouse genomic DNA produced four fragments (9260, 5411, 3548, and 2322 bp). Eco RI digest produced seven fragments (19952, 9259, 4136, 2710, 2154, 1412 and 924 bp) and five fragments (25118, 14125, 8912, 3981 and 2238 bp) were detected by Hind III digestion while four fragments (5248, 1711, 1258 and 501 bp) were observed with PstI-digested genomic DNA. The 1kb Xho I DNA of the mouse IRF-1 cDNA was used as the probe.

Fig. 6 shows that 20 μg genomic DNA was digested with Bam HI, Eco RI, Hind III and Pst I. The digested DNA was run in 1% agarose gel along with 5 and 10 pg of IRF-1 cDNA as positive control and Eco RI and Hind III digested λ DNA used as molecular size marker and hybridized with the ^{32}P labeled 5.3 kb IRF-1 C2 genomic probe. The ethidium bromide stained agarose gel is shown in Fig. 6 (B). The 5 and 10 pg positive controls were detected strongly. The size of the bands obtained after hybridization have been mentioned in table 1. Bam HI produced 5411bp but Eco RI produced two bands, 5843 and 1412 bp. Hind III digested DNA showed 2 fragments of 14125 and 4640 bp and Pst I produced five fragments, 10796, 6309, 2154, 1711 and 1258 bp.

Fig. 7 shows that 20 μg mouse genomic DNA was digested with Bam HI, Eco RI, Hind III and Pst I. The digested DNA was run in 1% agrose gel along with 2 and 20 pg of IRF-1 cDNA as positive control . λ DNA digested with Eco RI + Hind III was used as molecular size marker. The Ethidium bromide stained agarose gel is shown in Fig. 7 (B). This gel was transferred on

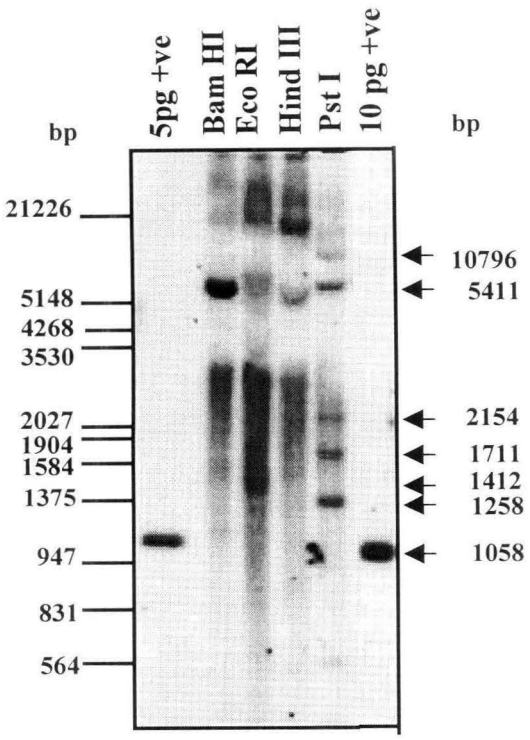

(A) Mouse IRF-1 gene

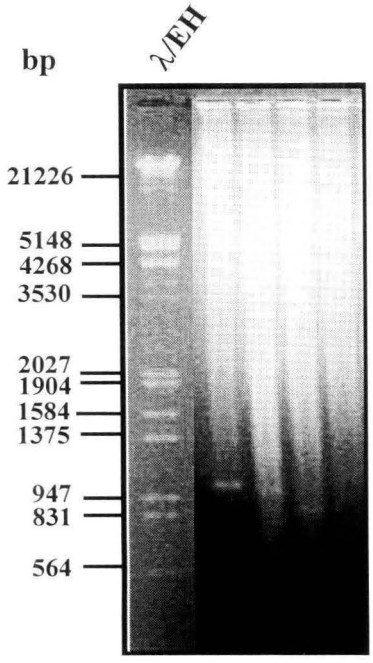

(B) EtBr Stained gel

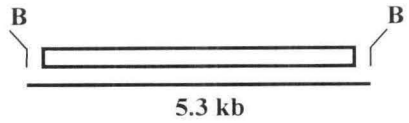

(C) C2 genomic probe (5.3 kb)

Fig. 6 Southern blot analysis of mouse IRF-1 gene. (A) 20 μg of mouse genomic DNA was digested by Bam HI, Eco RI, Hind III, Pst I, and hybridized with ^{32}P labeled 5.3 kb IRF-1 genomic DNA probe. (B) Ethidium Bromide stained agarose gel and (C) C2 genomic probe of IRF-1. (A) and (B) are aligned lanewise . 5 and 10 pg 1kb Xho I cDNA was used as +ve control for hybridization. λ DNA digested by EcoRI and Hind III (λ/EH) was used as molecular size marker.

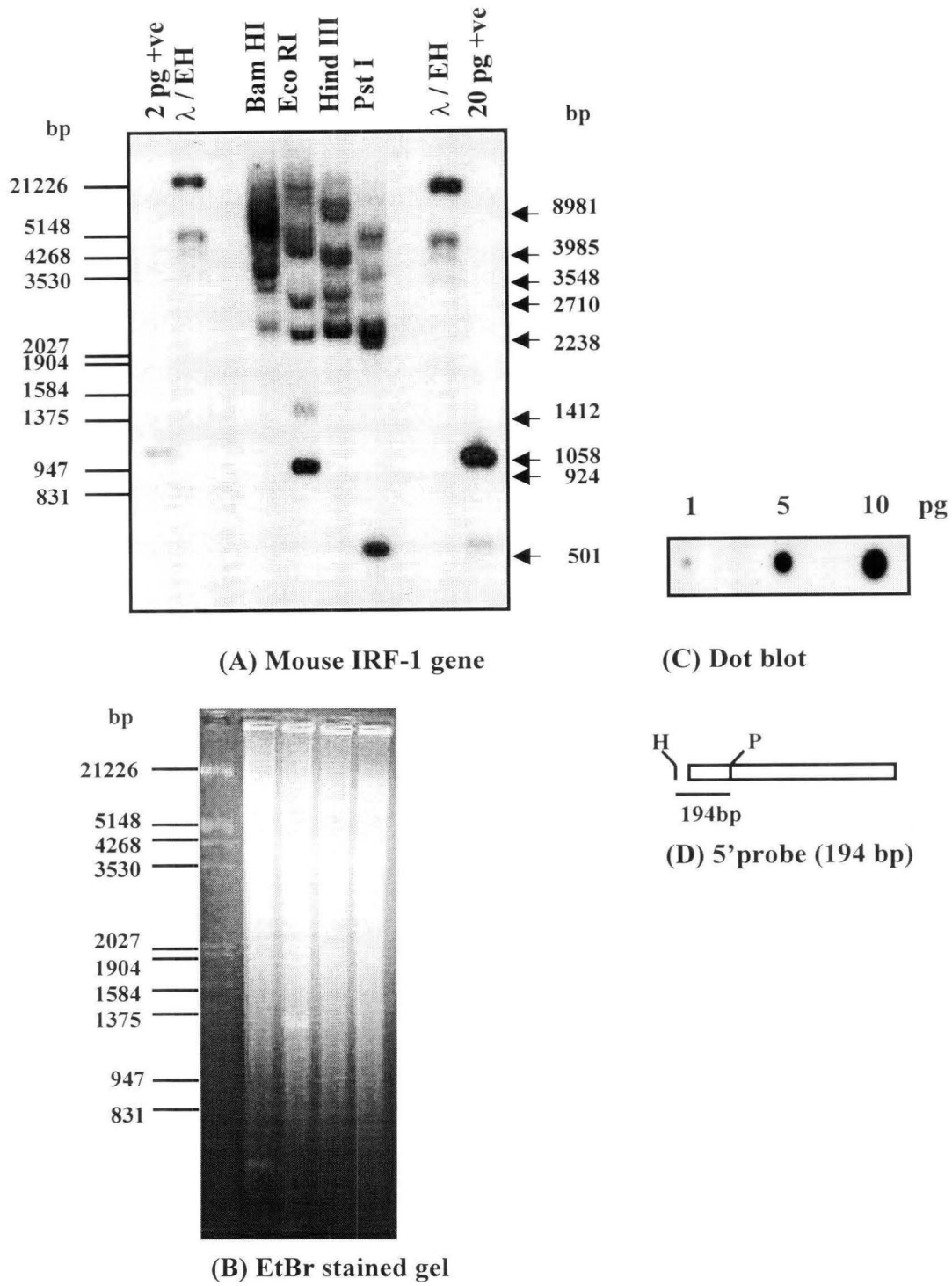

Fig. 7 Southern blot analysis of mouse IRF-1 gene. (A) 20 μg mouse genomic DNA was digested by Bam HI, Eco RI, Hind III, Pst I and hybridized with ^{32}P labeled 194 bp 5' proximal exon probe of IRF-1. (B) Ethidium bromide stained agarose gel. (C) dot blot hybridization of 1, 5 and 10 pg IRF-1 cDNA with 5' proximal exon probe used as a positive control. (D) 194 5' Pst I probe of IRF-1. (A) and (B) are aligned lanewise. 2 and 20 pg 1 kb Xho I cDNA was used as +ve control for hybridization. λ DNA digested by Eco RI and Hind III (λ/EH) was used as molecular size marker.

to a nylon membrane and hybridized with ^{32}P 194 5' probe and shown in fig. 7 (A). The 20 pg positive control DNA hybridized strongly. Several strong bands were detected from the mouse genome. The size of the bands obtained have been mentioned in table 1. Bam HI digested mouse genomic DNA revealed 4 fragments (9260, 4634, 3548 and 2322 bp), while five fragments were detected with Eco RI digested genomic DNA (4136, 2710, 2154, 1412 and 924 bp). Hind III digest revealed 5 fragments (14125, 8981, 3981, 3012 and 2238 bp). With Pst I digested DNA, 4 fragments were observed (5248, 3985, 2325 and 501 bp). In (C) 1, 5 and 10 pg of IRF-1 DNA is shown as dot blot hybridization with the 194 5' probe. In (D) a schematic representation of the 194 5' probe is shown.

(B) Human IRF-1 gene

For studying organization of the human IRF-1 gene, 20 μg genomic DNA isolated from human peripheral blood lymphocytes was digested with Bam HI, Eco RI, Hind III and Pst I. The digested DNA was run in 1% agarose gel along with Eco RI and Hind III digested λ DNA as a molecular size marker. The Ethidium bromide stained agarose gel is shown in Fig. 8 (B). The gel was transferred on to a nylon membrane and hybridized with ^{32}P labeled 1kb IRF-1 cDNA probe as shown in fig. 8 (A). Fig. 8 (C) shows a schematic representation of the 1 kb IRF-1 cDNA probe. Many distinct IRF-1 gene fragments were detected. The size of the bands are mentioned in table 2. Bam HI digest of the human genomic DNA produced two fragments, 3602 and 1079 bp, Eco RI produced three fragments (20730, 13592 and 3981 bp). Four fragments (15848, 6812, 3414 and 3336 bp) with Hind III and four fragments (4136, 1412, 860, and 541 bp) with Pst I digested genomic DNA were observed. In addition to this many weakly hybridizing bands were also detected. They could be IRF-1-related sequences from the human genome.

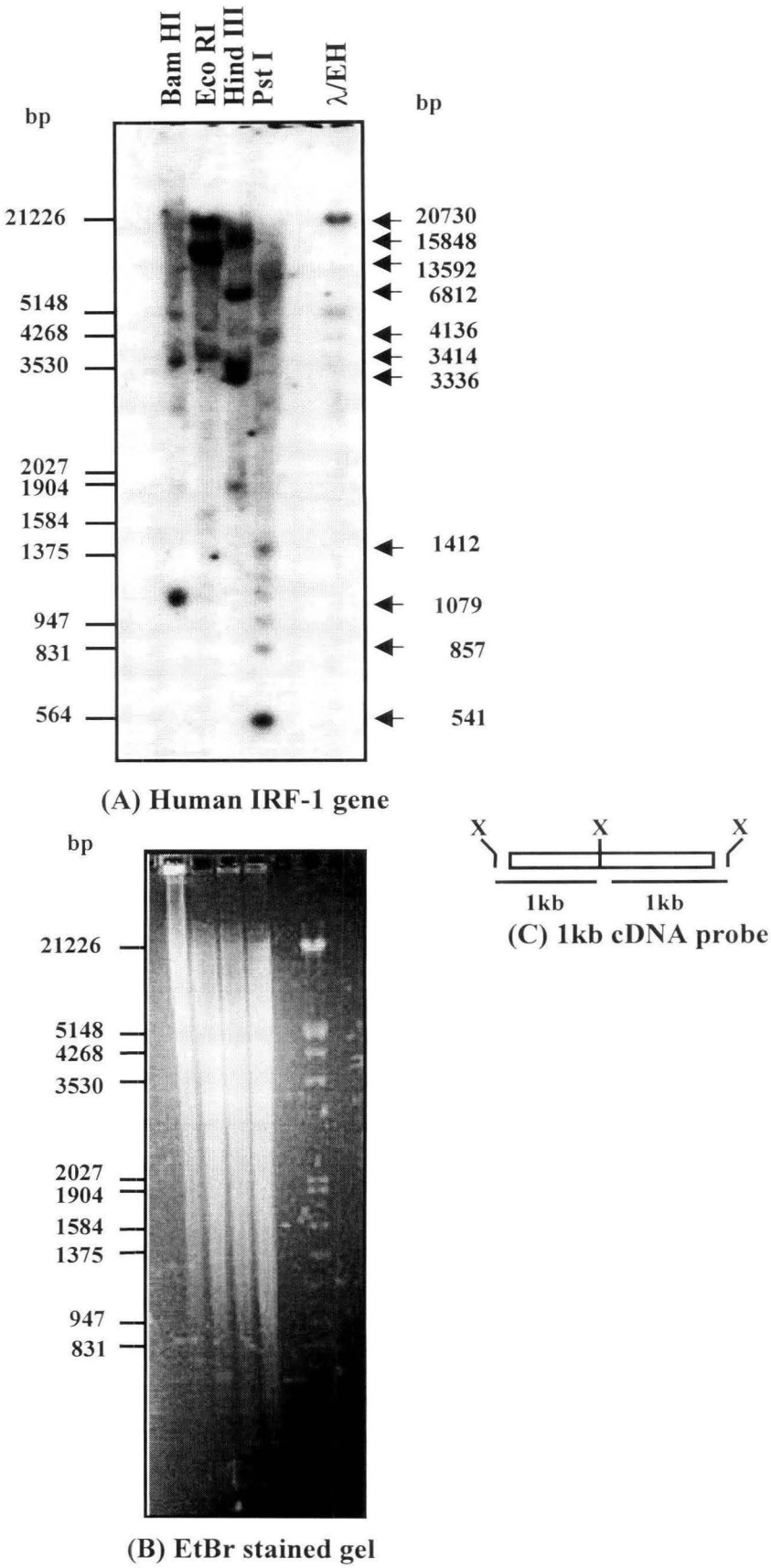

Fig. 8 Southern blot analysis of human IRF-1 gene. (A) 20 μg of genomic DNA from human lymphocytes was digested by Bam HI, Eco RI, Hind III, Pst I and hybridized with ^{32}P labeled IRF-1 cDNA probe. (B) Ethidium bromide stained agarose gel. (C) 1 kb cDNA probe of IRF-1. (A) and (B) are aligned lanewise. λ DNA digested by Eco RI and Hind III (λ/EH) was used as molecular size marker.

Fig. 9 shows human IRF-1 genomic fragments detected by the C2 genomic probe. 20 μg human peripheral lymphocyte genomic DNA was digested with Bam HI, Eco ℜI, Hind III and Pst I. The digested DNA was resolved in 1% agarose gel along with 15 and 30 pg of IRF-1 cDNA as the positive control. λ DNA digested with Eco RI + Hind III was used as molecular size marker. The Ethidium bromide stained agarose gel is shown in Fig. 9 (B). The gel was transferred on to a nylon membrane and hybridized with ^{32}P labeled 5.3 kb C2 genomic DNA probe and shown in fig. 9 (A). A schematic representation of the probe is shown in (C). The size of the IRF-1 genomic DNA fragments obtained after hybridization are mentioned in table 2. When C_2 genomic probe was hybridized with Bam HI digested human genomic DNA a 3630 bp DNA was detected. Another 1995 bp weak band was also detected. Similarly, Eco RI, Hind III, Pst I and Sac I digests detected single fragments of 2660, 2712, 3467, 3285 bp were observed respectively. The 15 and 30 pg IRF-1 cDNA were strongly detected as positive control.

Fig. 10 shows that 20 μg human lymphocyte genomic DNA was digested with Bam HI, Eco RI, Hind III and Pst I. The digested DNA was run in 1% agarose gel along with Eco RI and Hind III digested λ DNA as molecular size marker. 1, 5 and 10 pg of IRF-1 cDNA dot blot was used as positive control for hybridization. The Ethidium bromide stained agarose gel is shown in Fig. 10 (B). The gel was transferred on to a nylon membrane and hybridized with ^{32}P labeled 194 5' probe and shown in fig. 10 (A). Fig. 10 (D) shows a schematic representation of the 194 5' probe. Two strong human IRF-1 genomic DNA bands of different sizes were detected in each lane. A few weak IRF-1-related DNA sequences were also detected. The size of the bands obtained after hybridization are mentioned in table 2. Bam HI digested human genomic DNA showed 2 fragments of 3206 and 1079 bp. Two fragments of 13529 and 3981 bp were also detected with Eco RI digested genomic DNA. Hind III digest revealed 2 fragments of 6812 and 3414 bp. Pst I digested DNA detected 2 fragments of 4136 and 541 bp.

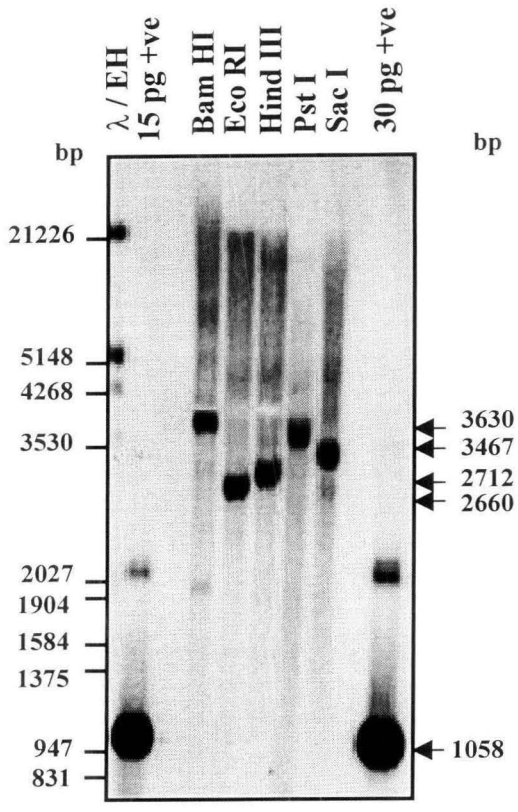

(A) Human IRF-1 gene

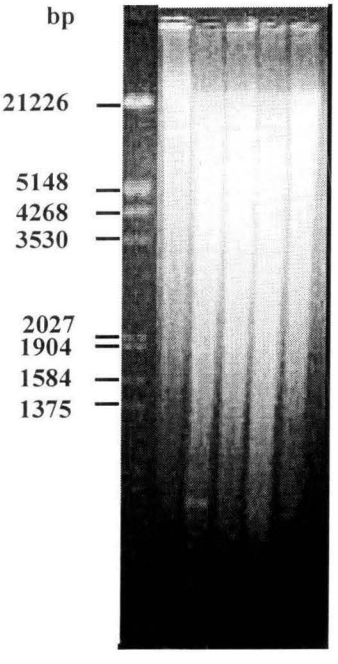

(B) EtBr stained gel

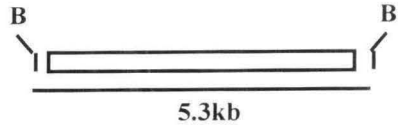

(C) C2 genomic probe (5.3 kb)

Fig. 9 Southern blot analysis of human IRF-1 gene. (A) 20 μg of genomic DNA from human lymphocytes was digested by Bam HI, Eco RI, Hind III, Pst I, Sac I and hybridized with ^{32}P labeled 5.3 kb IRF-1 genomic probe. (B) Ethidium bromide stained agarose gel and (C) 5.3 kb C2 genomic probe of IRF-1. (A) and (B) are aligned lanewise. 15 and 30 pg IRF-1 cDNA was used as +ve control for hybridization. λ DNA digested by Eco RI and Hind III (λ/EH) was used as molecular size marker.

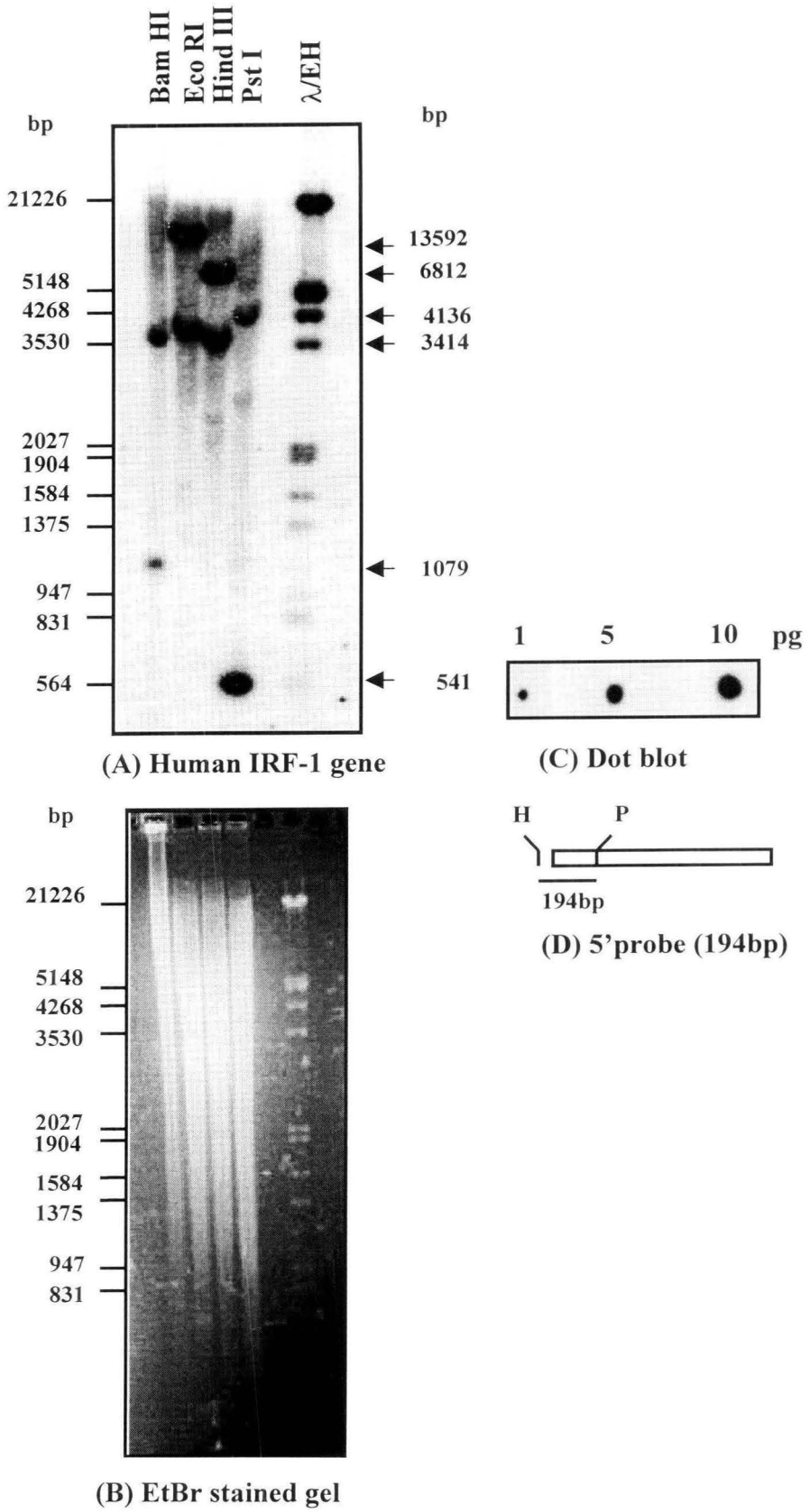

Fig. 10 Southern blot analysis of human IRF-1 gene. (A) 20 μg of genomic DNA from human lymphocytes was digested by Bam HI, Eco RI, Hind III, Pst I and hybridized with ^{32}P labeled 5' proximal exon probe of IRF-1. (B) Ethidium bromide stained gel. (C) dot blot hybridization of 1, 5 and 10 pg IRF-1 cDNA with 5' proximal exon probe used as a positive control. (D) 194 5' probe of IRF-1. (A) and (B) are aligned lanewise. λ DNA digested by EcoRI and HindIII (λ/EH) was used as molecular size marker.

There were some mouse DNA fragments which only hybridized with 5' probe, like the 4634 bp DNA in Bam HI digest, 3012 bp in Hind III and 3985, 2325 bp in Pst I digest. These have been showed as bold in table 1. These IRF-1 DNA fragments should contain IRF-1 promoter since they did not hybridize with IRF-1 genomic DNA probe beyond 2nd exon.

In table 1 there are some fragments from the mouse genome which only hybridized with the 1kb IRF-1 cDNA probe for example, the 5411 bp in Bam HI digest, the 19952 and 9259 bp in Eco RI digest and the 25118 bp in Hind III digest and in Pst I digest the 1711, 1258 bp DNA. Similarly, the 5843 bp Eco RI DNA, the 4640 bp Hind III DNA and the 10796, 6309, 2154 bp Pst I DNA were only detected by the IRF-1 C2 genomic probe. The DNA fragments specifically detected by the C2 genomic probe but not by the cDNA probe could be intronic fragments of the mouse IRF-1 gene. In table 2 from the human genomic DNA, the 20730 bp DNA in Eco RI digest, 3336 bp Hind III DNA and the 1412, 860 bp Pst I DNA were specifically detected by the IRF-1 cDNA probe. Similarly, the 2660 bp Eco RI DNA, 2712 bp Hind III DNA, 3467 bp Pst I DNA and 3285 bp Sac I DNA were specifically detected by the IRF-1 C2 genomic probe. These fragments should represent intronic fragments from the human IRF-1 gene.

In fig. 11 and fig. 12 linear restriction maps of the mouse and human IRF-1 genes are shown respectively. The maps were made based on the results obtained from the Southern blot analyses. The maps are tentative and not drawn to the scale. From the maps, it is possible to make out which genomic DNA fragment hybridizes to which IRF-1probe. The restriction fragments are colour coded. DNA fragments hybridizing to the same probe are overlapping even though they are generated by different restriction enzymes. DNA fragments generated by a single restriction enzyme and not hybridizing to the same probe are likely to come from different regions of the gene. DNA fragments strongly hybridizing to the 194 5' probe but not to the C2 genomic probe should be the 5' flanking DNA containing the IRF-1 gene promoter.

Restriction enzyme	Fragment size (bp)		
	5' probe	cDNA probe	Genomic probe
Bam HI	9260 **4634** 3548 2322	9260 **5411** 3548 2322	**5411**
Eco RI	 4136 2710 2154 1412 924	**19952** **9259** 4136 2710 2154 1412 924	**5843** 1412
Hind III	14125 8981 3981 **3012** 2238	**25118** 14125 8912 3981 2238	14125 **4640**
Pst I	 5248 **3985** **2325** 501	 5248 **1711** **1258** 501	**10796** **6309** **2154** **1711** **1258**

Table 1 Restriction fragments of mouse IRF-1 gene. Bam HI, Eco RI, Hind III and Pst I DNA fragments from the mouse genomic DNA hybridizing with IRF-1 probes (194 bp 5' probe, 1kb cDNA probe: 2x1kb XhoI DNA and genomic probe: 5.3 kb Bam HI C2 DNA) by Southern blot analysis (Fig. 5-7) were considered for size calculation based on λ/Eco RI+ Hind III molecular size marker. Size in bold indicates different gene fragments detected by different IRF-1 probes.

Restriction enzyme	Fragment size (bp)		
	5'probe	cDNA probe	Genomic probe
Bam HI	3206 1079	3602 1079	3630
Eco RI	13529 3981	**20730** 13592 3981	**2660**
Hind III	6812 3414	15848 6812 3414 **3336**	**2712**
Pst I	4136 541	4136 **1412** **860** 541	**3467**
Sac I	N.U.	N.U.	**3285**

Table 2 Restriction fragments of human IRF-1 gene . Bam HI, Eco RI, Hind III and Pst I DNA fragments from the mouse genomic DNA hybridizing with IRF-1 probes (194 bp 5' probe, 1kb cDNA probe: 2X1kb Xho I DNA and genomic probe: 5.3 kb Bam HI C2 DNA) by Southern blot analysis (Fig. 8-10) were considered for size calculation based on λ/Eco RI+ Hind III molecular size marker. Size in bold indicates different gene fragments detected by different IRF-1 probes. N.U.- not used.

Fig. 11 Linear restriction map of mouse IRF-1 gene based on Southern blot hybridization. Thick black line is genomic DNA. B-BamH I, E-EcoR I, H-Hind III, P-Pst I. Thin black line is intronic sequence. Green boxes represent exons. Small red box indicates the 194 bp 5'probe. Coloured arrow head lines represent restriction fragments detected by Southern hybridization and are colour coded as per restriction enzymes used. Break in the lines represents discontinuity in the gene. The map is tentative and not drawn to scale. Overlaps of coloured arrow head lines represent hybridization of different restriction fragments to same probe.

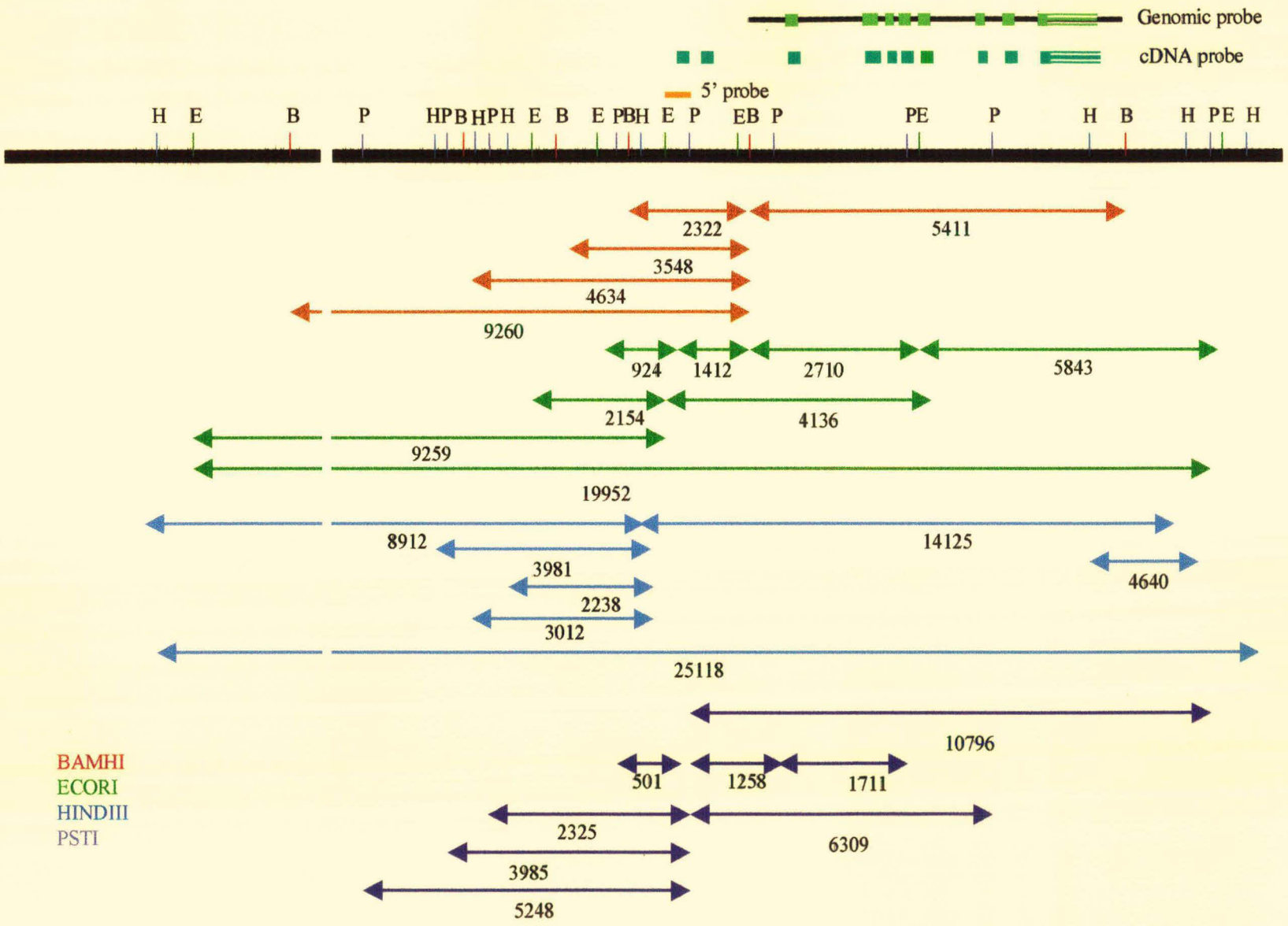
Genomic probe
cDNA probe
5' probe
H E B P HPBHPH E B E PBH E P EB P PE P H B H PE H
2322
5411
3548
4634
9260
924
1412
2710
5843
2154
4136
9259
19952
8912
14125
3981
4640
2238
3012
25118
10796
501
1258
1711
2325
6309
3985
5248
BAMHI
ECORI
HINDIII
PSTI

Fig. 12 Linear restriction map of human IRF-1 gene based on Southern blot hybridization. Thick black line is genomic DNA. B-Bam HI, E-Eco RI, H-Hind III, P-Pst I. Thin black line is intronic sequence. Green boxes represent exons. Small red box indicates the 5'probe. Coloured arrow head line represent restriction fragments detected by Southern hybridization and are colour coded as per restriction enzymes used. Break in the lines represents discontinuity in the gene. The map is tentative and not drawn to scale. Overlaps of coloured arrow head lines represent hybridization of different restriction fragments to same probe.

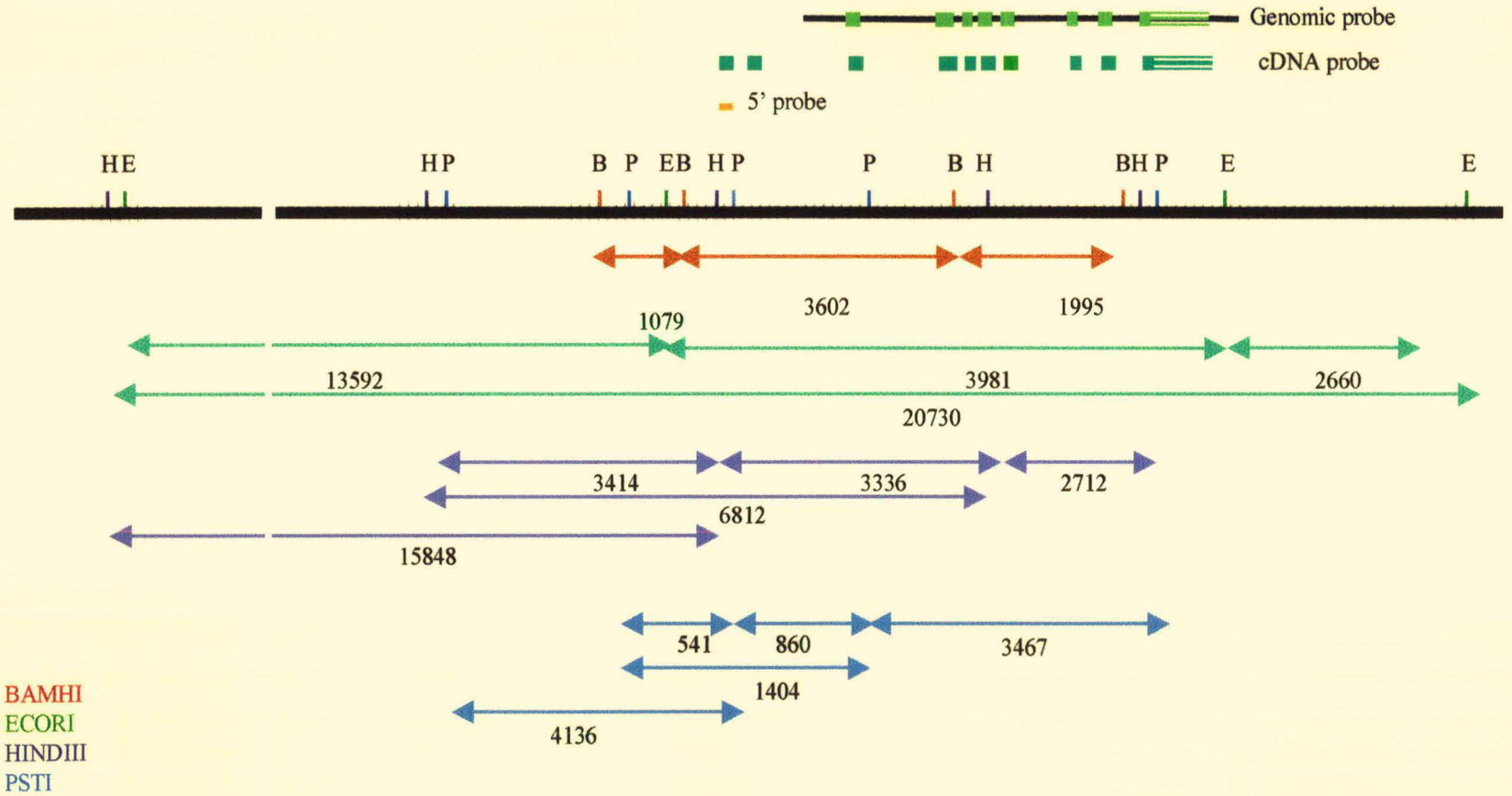
Genomic probe
cDNA probe
5' probe
HE
HP
B P EB H P
P
B H
BH P
E
E
3602
1995
1079
13592
3981
2660
20730
3414
3336
2712
6812
15848
541
860
3467
1404
4136
BAMHI
ECORI
HINDIII
PSTI

DNA fragments specifically detected by the C2 probe but not by 1kb cDNA probe should contain intronic sequences of the IRF-1 gene. Since exonic sequences (except the 1st and nd exon) are common to the cDNA probe and the C2 probe, they detected some common restriction fragments. There were also certain differences between the mouse and the human IRF-1 genes. For example, the 1079 and 3414 bp Bam HI DNA were detected by the 194 5' probe from human IRF-1 gene but the same probe detected 2322, 3548 and 9260 bp Bam HI DNA from murine IRF-1 gene. This indicates that the structure of 5' flanking DNA containing IRF-1 gene promoter is different between mouse and human. Fig. 11 and 12 as well as table 1 and 2 show these differences.

6.2 Amino acid changes in IRF-1

IRF-1 has a DNA binding domain and a transcription activation domain. The DNA binding domain interacts with specific DNA sequence(s) in the promoter/enhancer regions of certain mammalian genes while the transcription activation domain is responsible for establishing protein-protein interactions with RNA polymerase II, other transcription factors and coactivators during transcription of the gene(s). Since the DNA binding domains of IRF-1 and IRF-2 are very similar but their transcription activation/repression domains are different both in structure and function, an attempt was made to compare the amino acid sequences of the mouse and human IRF-1 molecules in order to find out their similarity and divergence in amino acid sequence in these two domains.

6.2.1 Comparison of mouse, rat and human IRF-1

Mouse (M21065), rat (M34253) and human (X 14454) IRF-1 cDNA sequences were retrieved from GenBank and converted to amino acid

S.No.	Position of amino acid	Mouse	Rat	Human
1	5	R	R	**W**
2	25	I	**S**	I
3	34	F	F	**L**
4	35	Q	Q	**E**
5	43	K	**L**	K
6	117	**R**	K	K
7	131	T	T	**A**
8	135	T	T	**A**
9	139	L	L	**S**
10	143	**V**	S	S
11	166	**T**	**A**	**V**
12	167	Q	Q	**P**
13	170	L	L	**M**
14	171	G	G	*
15	175	D	D	**E**
16	176	M	M	**V**
17	177	E	D	E
18	178	R	R	**Q**
19	179	D	D	**A**
20	180	I	I	**L**
21	188	V	V	**A**
22	192	S	S	**T**
23	194	S	S	**P**
24	195	E	E	**D**
25	198	M	M	**I**
26	199	Q	Q	**P**
27	200	M	M	**V**
28	201	D	D	**E**
29	202	I	I	**V**
30	203	**I**	**M**	**V**
31	208	T	T	**S**
32	213	L	L	**F**
33	221	T	T	**I**
34	225	A	A	**T**
35	234	**I**	L	L
36	235	**A**	P	P
37	238	**L**	I	I
38	242	F	F	**L**
39	251	H	H	**N**
40	252	**I**	V	V
41	264	**T**	**A**	**V**
42	266	L	L	P
43	267	S	S	T

S.No.	Position of amino acid	Mouse	Rat	Human
44	268	S	**T**	S
45	285	**R**	G	G
46	289	G	**E**	G
47	290	I	I	**L**
48	291	G	G	**S**
49	292	I	I	**L**
50	294	**H**	R	R
51	298	E	E	**D**
52	299	M	M	**L**
53	304	**S**	**P**	**A**
54	305	**I**	**V**	**T**
55	306	M	M	*
56	308	M	M	**L**
57	310	S	**T**	S
58	313	G	G	**T**
59	314	N	N	**P**
60	315	S	S	*
61	316	V	T	**V**
62	318	L	*	L
63	320	P	P	*

Table 3 A serial list of amino acid changes in IRF-1 of mouse, rat and human at various positions. Single letter codes for amino acids are used. Significant changes are in bold. * indicates absence of an amino acid at that position.(Ref. : mouse - M 21065, rat - M 34253 and human - X 14454).

	No. of changes	%age changes	Changes in DNA binding domain	Changes in Transactivation domain
Total	68	100	9	59
Mouse	13/329	19.11	1	12
Rat	12/328	17.64	2	10
Human	43/325	63.23	6	37

Table 4 Percentage of amino acid changes in IRF-1 of mouse, rat and human. Total changes at 68 positions are considered as 100 per cent. (Ref.: mouse - M 21065, rat - M 34253 and human - X 14454).

I. ^{175} **Glu Val** Glu **Gln Ala Leu** ^{180}
II. ^{198} **Ile Pro Val Glu Val Val** ^{203}
III. ^{264} **Val** Gln **Pro Thr** Ser Val ^{269}
IV. ^{289} Gly **Leu Ser Leu** Gln **Arg** ^{294}
V. ^{304} **Ala Thr** * Trp **Leu** Gln Arg ^{310}
VI. ^{313} **Thr Pro** * Val Arg Leu Pro ^{318}

1. ^{175} **EVEQAL** ^{180}
2. ^{198} **IPVEVV** ^{203}
3. ^{264} **VQPTSV** ^{269}
4. ^{289} **GLSLQR** ^{294}
5. ^{304} **AT*WLDS** ^{310}
6. ^{313} **TP*VRLP** ^{318}

Table 5 Amino acid changes in the transactivation domain of human IRF-1with reference to murine IRF-1. Six regions (I – VI) containing clusters of six amino acids were identified in the transactivation domain of human IRF-1. Bold letters indicate change in amino acid.(Ref. : mouse - M 21065, rat - M 34253 and human - X 14454).

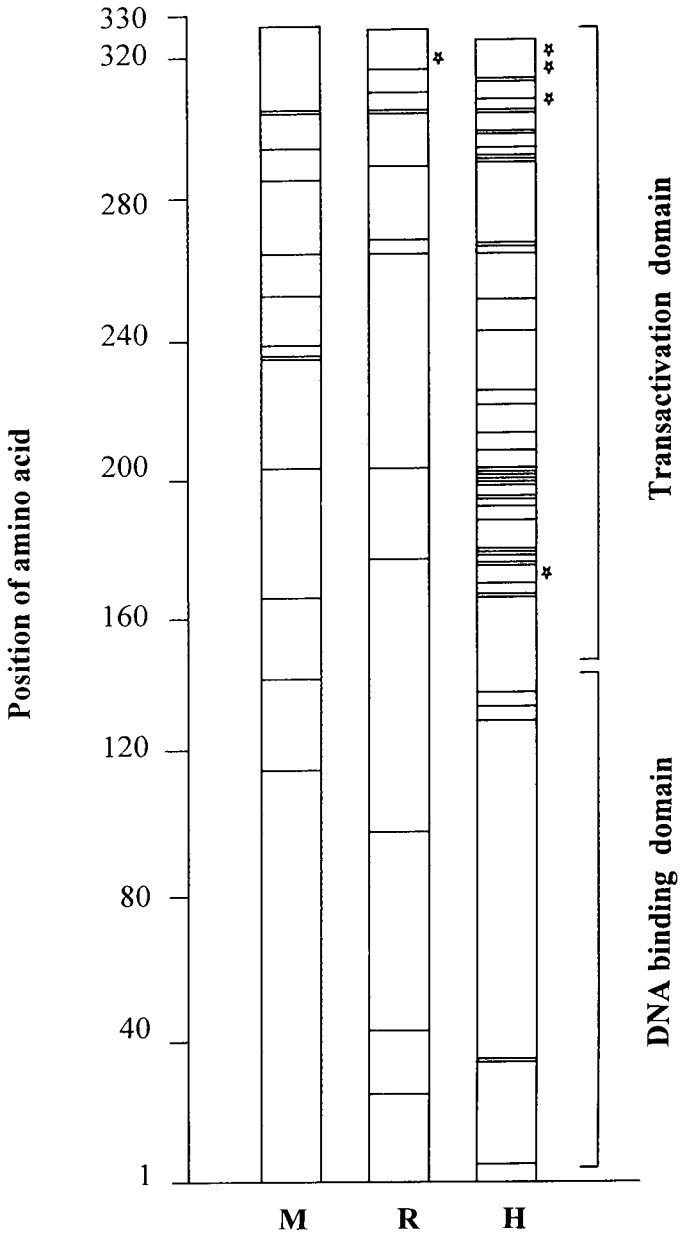

Fig. 13 Amino acid changes in IRF-1 of mouse (M), rat (R) and human (H). Bars represent IRF-1 protein, horizontal lines inside the bar represent amino acid changes at positions on y-axis and * represents an amino acid missing at that position. Mouse IRF-1 is taken as the reference for comparison of the rat and human IRF-1. Changes in murine IRF-1 with reference to the rat or human are also mentioned . Maximum changes are in the transactivation domain of human IRF-1. (Ref. : mouse - M 21065, rat- M 34253 and human- X 14454).

sequence with the help of PC gene software which matched the published data. Mouse IRF-1 has 329 amino acid, rat IRF-1 has 328 amino acid and human IRF-1 has 325 amino acid. The amino acid sequence of IRF-1 was compared between mouse and rat as well as between mouse and human using the computer program Clustal W and is represented as bar diagram in fig. 13. Both substitution and absence of an amino acid were considered as change. The bar represents IRF-1 with the DNA binding- and transcription activation domains. A change in amino acid is shown as a horizontal line inside the bar at respective positions. Mouse IRF-1 was taken as the reference for comparison. In table 4, it is shown that a total of 68 amino acid changes were observed in IRF-1 protein on comparison between mouse, rat and human. Of the 68 changes 13 were in mouse, 12 in rat and 43 in human IRF-1 protein. If 68 changes are considered as 100% then percentage change in mouse is 19.11%, in rat 17.64%, and in human 63.23%. Between mouse and rat IRF-1, 12 – 13 amino acids out of 328 –329 were different but between mouse and human IRF-1, 43 amino acids differed out of 325 – 329. Out of a total of 68 amino acid changes among all three, 9 were in the DNA binding domain but 59 in the transcription activation domain indicating that the DNA binding domain is conserved while the transcription activation domain is variable. In the three species these changes are as follows: mouse has a single change in DNA binding domain and 12 changes in transactivation domain, rat has 2 changes in DNA binding domain and 10 changes in transactivation domain when mouse and rat IRF-1 are compared to each other. In human, there are 6 changes in DNA binding domain and 37 changes in transactivation domain, when mouse and human IRF-1 are compared to each other. Thus out of a maximum of 63% amino acid changes observed in the human IRF-1 alone most are located in the transcription activation domain. Fig. 13 clearly shows that maximum amino acid changes have accumulated in the transcription activation domain of human IRF-1.

6.2.2 Identification of six clustered amino acid changes in the transactivation domain of human IRF-1

The amino acid substitutions in IRF-1 of mouse, rat and human are shown in table 4. Upon visualization, it was found out that four amino acids at positions 171, 306, 315, 320 of mouse IRF-1 – all in the transactivation domain, are absent in the human IRF-1. Moreover, some amino acid changes in human IRF-1 are significant, like arg (5) to trp (5), arg (178) to gln (178), glu (195) to asp (195) etc. but some changes like Ile (180) to leu (180), Ile (202) to val (202) etc. are not so significant. Finally, table 5 shows that six regions (I-VI) in the transactivation domain of human IRF-1 were identified which contained five to six amino acids and accounted for maximum amino acid change in continuous stretch. Out of six amino acids, six changed in region II, five changed in region I, four changed in region IV, three changed in regions III and V and two changed in region VI. These regions are : I = 175-Glu-Val-Glu-Gln-Ala-Leu-180, region II = 198-Ile-Pro-Val-Glu-Val-Val-203, region III = 264-Val-Gln-Pro-Thr-Ser-Val-269, region IV = 289-Gly-Leu-Ser-Leu-Gln-Arg-294, region V = 304-Ala-Thr-*-Trp-Leu-Gln-Arg-310, region VI = 313-Thr-Pro-*-Val-Arg-Leu-Pro-318. The bold amino acids indicate substitutions and * indicates absence of an existing amino acid at that position. Thus it is clear that the transactivation domain of human IRF-1 has accumulated such clusters of amino acid changes when compared to that of mouse and rat. In order to find out whether these amino acid regions constitute any motif and/or they are also present in other proteins the sequences were searched in the protein database. Table 6 shows that EVEQAL, IPVEVV, GLSLQR, ATWLDS, VQPTSV and TPVRLP amino acid sequences are present in many proteins in the database. Homology search out put by blastp were as follows : EVEQAL has 100% homology with Capsid protein precursor [Thosea asigna virus], Mitogen-activated protein kinase [*Homo sapiens*], Extracellular signal-regulated kinase (ERK2) [*Bos taurus*], Cyclosporine

s. no.	amino acid	output	region	%age homology
1	EVEQAL	Interferon regulatory factor 1 – human (B31595)	175-180	100 (6/6)
		Capsid protein precursor [Thosea asigna virus] (AF062037)	74 -79	100 (6/6)
		Rat Map Kinase Erk2 with an arginine mutation at position 52	307-312	100 (6/6)
		Mitogen-activated protein kinase [*Homo sapiens*] (Z11695)	291-296	100 (6/6)
		Extracellular signal regulated kinase (ERK2) [*Bos taurus*] (Z14089)	303-308	100 (6/6)
		Cyclosporine synthetase [*Tolypocladium inflatum*] (S41309)	13080-13085	100 (6/6)
2	IPVEVV	Human interferon regulatory factor – 1 (IRF-1) (B31595)	198-203	100 (6/6)
		Conserved hypothetical protein [*Thermotoga maritima*] (F72315)	204-209	100 (6/6)
		Eukaryotic translation initiation factor 3 beta subunit of fission yeast (*Schizosaccharomyces pombe*) (T38379)	448-453	100 (6/6)
		Human GMP synthase [glutamine hydrolyzing] (glutamine amidotransferase) (P49915)	657-662	100 (6/6)
		Putative receptor-like protein kinase [*Arabidopsis thaliana*] (AC005967)	433-438	100 (6/6)
		BcDNA : GH02712 gene product [*Drosophila melanogaster*] (AE003840)	1985-1990	100 (6/6)
		Hypothetical zinc metalloproteinase [*Caenorhabditis elegans*] (P55113)	59-64	100 (6/6)

s. no.	amino acid	output	region	%age homology
3	GLSLQR	Human interferon regulatory factor-1 (IRF-1) (B31595)	289-294	100 (6/6)
		NADH dehydrogenase subunit 4L [*Lampetra fluviatilis*] (Y18683)	16-21	100 (6/6)
		Rat gastric inhibitory polypeptide receptor precursor (GIP-R) (glucose-dependent insulinotropic polypeptide receptor) [*Rattus norvegicus*] (P43219)	14-19	100 (6/6)
		DNA gyrase B subunit [*Photobacterium damselae*] (AJ249849)	635-640	100 (6/6)
		NADH dehydrogenase subunit 4L [*Petromyzon marinus*] (U11880)	16-21	100 (6/6)
		Ribonucleotide reductase large subunit [Equine herpesvirus 4] (X75354)	255-260	100 (6/6)
4	ATWLDS	Human interferon regulatory factor 1 (IRF-1) (B31595)	304-309	100 (6/6)
		Replication protein [Human papillomavirus type 83] (AF151983)	101-106	83 (5/6)
		Envelope glycoprotein [Human immunodeficiency virus type 1] (AF138315)	131-136	83 (5/6)
		Hypothetical protein L5213.06 [*Leishmania major*] (AL352992)	457-462	83 (5/6)
		Xylanase [*Bacillus stearothermophilus*] (D28122)	564-568	100 (5/5)
		Erythroid protein 4.1 isoform B [*Homo sapiens]* (J03796)	19-23	100 (5/5)

s. no.	amino acid	output	region	%age homology
		Spalt-like zinc finger protein [*Homo sapiens*] (AJ007421)	483-487	100 (5/5)
		Zinc finger protein [*Xenopus laevis*] (L46583)	544-548	100 (5/5)
5	**VQPTSV**	Human interferon regulatory factor 1 (IRF-1) (B31595)	264-269	100 (6/6)
		Ubiquitin-protein ligase 1 [*Arabidopsis thaliana*] (AF127564)	1183-1188	100 (6/6)
		F-box and leucine-rich repeat protein 8 [*Mus musculus*] (AF176523)	178-183	100 (6/6)
		Polyprotein [Equine Rhinovirus type 2] (X96871)	875-880	100 (6/6)
		Receptor adenylate cyclase [*Leishmania donovani*] (T18309)	733-738	100 (6/6)
		Calcium ATPase [*Caenorhabditis elegans*] (AJ010708)	1039-1044	83 (5/6)
		Putative acyl-CoA synthase [*Pseudomonas stutzeri*] (AF196567)	88-93	83 (5/6)
6	**TPVRLP**	Human interferon regulatory factor 1 (IRF-1) (B31595)	313-318	100 (6/6)
		Zinc finger protein [*Mus musculus*] (AF159455)	559-564	83 (5/6)
		Alkaline exonuclease [murine herpesvirus 68] (U97553)	440-445	83 (5/6)
		GTP-binding protein S10 (human) homolog [*Caenorhabditis elegans*] (Z35640)	58-63	83 (5/6)

s. no.	amino acid	output	region	%age homology
		Origin recognition complex protein 1 [*Xenopus laevis*] (U67190)	332-337	83 (5/6)
		Glycosyl hydrolase family protein [*Chlamydia muridarum*] (AE002298)	135-140	83 (5/6)

Table 6 Homology of the six amino acid clusters from the transactivation domain of human IRF-1 with identical or similar regions in other proteins present in the data base. BLASTp homology search was performed. Number in parenthesis indicates identical amino acids.

synthetase [*Tolypocladium inflatum*]. IPVEVV shows 100% homology with eukaryotic translation initiation factor 3 beta subunit of fission yeast (*Schizosaccharomyces p mbe*), human GMP synthase [glutamine-hydrolyzing] (glutamine amidotransferase), putative receptor-like protein kinase [*Arabidopsis thaliana*], BcDNA : GH02712 gene product [*Drosophila melanogaster*], hypothetical zinc metalloproteinase [*Caenorhabditis elegans*]. GLSLQR shows 100% homology with NADH dehydrogenase subunit 4L [*Lampetra fluviatilis*], rat gastric inhibitory polypeptide receptor precursor (GIP-R) (glucose-dependent insulinotropic polypeptide receptor) [*Rattus norvegicus*], DNA gyrase B subunit [*Photobacterium damselae*], NADH dehydrogenase subunit 4L [*Petromyzon marinus*], ribonucleotide reductase large subunit [equine herpesvirus 4]. ATWLDS shows 83% homology with replication protein [human papillomavirus type 83], envelope glycoprotein [human immunodeficiency virus type 1], hypothetical protein L5213.06 [*Leishmania major*] and 100% homology in a stretch of five amino acids with Xylanase [*Bacillus stearothermophilus*], erythroid protein 4.1 isoform B [*Homo sapiens*], spalt-like zinc finger protein [*Homo sapiens*], zinc finger protein [*Xenopus laevis*]. VQPTSV shows 100% homology with ubiquitin-protein ligase 1 [*Arabidopsis thaliana*], F-box and leucine-rich repeat protein 8 [*Mus musculus*], polyprotein [equine rhinovirus type 2], receptor- adenylate cyclase [*Leishmania donovani*], while calcium ATPase [*Caenorhabditis elegans*] and putative acyl-Co A synthase [*Pseudomonas stutzeri*] showed homology of 83% . TPVRLP shows 83% homology with zinc finger protein [*Mus musculus*], alkaline exonuclease [murine herpesvirus 68], GTP-binding protein S10 (human) homolog [*Caenorhabditis elegans*], origin recognition complex protein 1 [*Xenopus laevis*] and glycosyl hydrolase family protein [*Chlamydia muridarum*]. It will be interesting to find out if these amino acid clusters would represent any functional sequence motif(s).

6.2.3 Change in restriction site coinciding with change in amino acid

cDNA sequences of IR. -1of mouse, rat and human were also analysed for their restriction enzyme site profile. Any difference in restriction sites that coincided with the change in amino acid was noted. Table 7 shows that in human IRF-1 cDNA, Nae I site is present at nucleotide position 48 in IRF-1 cDNA which falls in the 5' UTR sequence but is absent in the mouse cDNA. A Sma I site is present at nucleotide position 262 in the human IRF-1cDNA but is not present in the mouse cDNA. This change corresponds to amino acid position 25 in the IRF-1 protein. In addition, two Bst X I sites are present at nucleotide positions 1112 and 1479 of IRF-1 cDNA which corresponds to amino acid 308 and 3'UTR of human cDNA, while the mouse cDNA lacks these. At nucleotide position 1344 of IRF-1 cDNA, a Sfi I site is present in human IRF-1 which corresponds to 3' UTR of IRF-1 mRNA but this site is absent in mouse IRF-1. In the mouse IRF-1 cDNA, a Cla I site is present at nucleotide position 960 and this site corresponds to 252 amino acid position in the IRF-1 protein but this site is absent in the human cDNA. A Xho I site is present at nucleotide position 1056 of mouse IRF-1 cDNA and it corresponds to 285 amino acid position in IRF-1 protein but this site is absent in human IRF-1 cDNA. Fig. 14 shows diagrammatic representation of changes in restriction enzyme sites in IRF-1 cDNA coinciding with changes in amino acids in the coding regions or nucleotides in the untranslated regions (UTR) of murine and human IRF-1 cDNAs. This indicates that there are structural differences between mouse and human IRF-1.

6.3. Expression of IRF-1 mRNA

Most of the studies involving IRF-1 mRNA expression have been reported from mammalian cells in culture. Normally virus, double stranded RNA or poly (I.C.) or cytokines like interferon-α (IFN-α) or IFN-γ have been

S. No.	Restriction Enzyme site	IRF-1 cDNA (nt)	Mouse	Human	Feature/ amino acid
1	Nae I	48	-	+	5' UTR
2	Sma I	262	-	+	25
3	Cla I	960	+	-	252
4	Xho I	1056	+	-	285
5	Bst XI	1112 1479	-	+	308 3'UTR
6	Sfi I	1344	-	+	3' UTR

Table 7 Distribution of characteristic restriction enzyme sites in murine and human IRF-1 cDNAs which coincide with changes in amino acids in coding or nucleotides in untranslated regions (UTR).

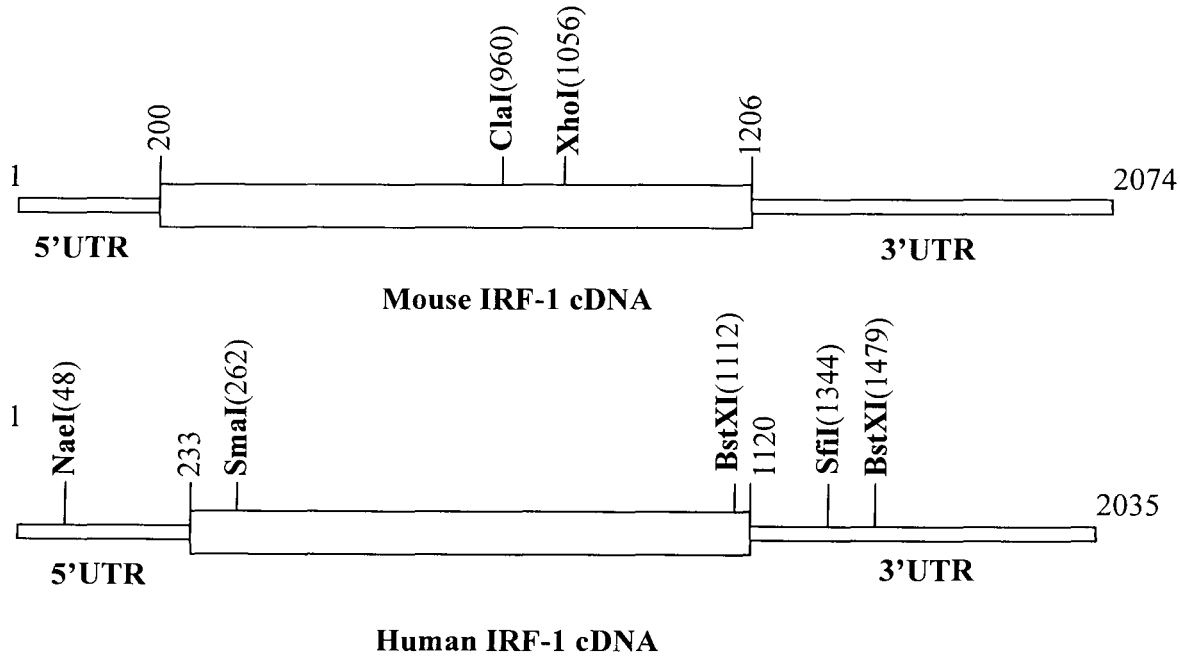

Fig 14 Diagrammatic representation of changes in restriction enzyme sites coinciding with changes in amino acids or nucleotides in untranslated regions (UTR) of murine and human IRF-1 cDNAs .

used as inducers to activate IRF-1 gene expression at mRNA level. Fibroblast cells, lymphocytes, macrophage/monocytic cells and other myeloid cells as well as embryonal carcinoma cells have been used for IRF-1 mRNA expression studies. Tissues of IRF-1 knock out mice also have been analysed for IRF-1 mRNA expression. The present study was designed to find out IRF-1 mRNA expression in the tissues from normal swiss albino mice.

6.3.1 Northern blot analysis of IRF-1 mRNA

Northern blot hybridization was carried out to check the expression and size of IRF-1 mRNA in thymus, intestine, spleen and lung tissues of 33 day old mice. 30 μg of total RNA was loaded in each lane of the gel along with 10 pg of 1 kb Xho I IRF-1 cDNA as a positive control. 5, 10 and 20 pg of IRF-1 cDNA was dot blotted and used as positive control for hybridization. ^{32}P labeled 1 kb IRF-1 cDNA was used as probe. Fig. 15 shows that ~ 2 kb IRF-1 mRNA in three tissues, intestine, spleen and lungs, was observed. A weak band was also observed in the thymus. The position of 28S and 18S rRNAs are marked.

The image was developed with the help of a phosphoimager (Fujifilm, BAS 1800) and the expression of IRF-1 mRNA was checked by quantitating the band intensities with the help of Image Gauge V2.54 software. The pixel values for the intensity of IRF-1 mRNA band was 194 for thymus, 1066 for intestine, 433 for spleen and 475 for lungs of the mice. The positive control dot blot of 5, 10 and 20 pg IRF-1 cDNA showed 4642, 12710 and 44400 pixel values respectively indicating that the hybridization was linear at least upto this value. Pixel values of the IRF-1 mRNA band and 5, 10, 20 pg IRF-1 cDNA dot blots have been plotted as histograms in fig. 15(C) and (D). From the Quantitations, it was observed that the intestine was found to have maximum expression of IRF-1 mRNA followed by the lungs, the spleen and the thymus. IRF-1 mRNA level in the spleen and lungs was about 2.2 to 2.4 x

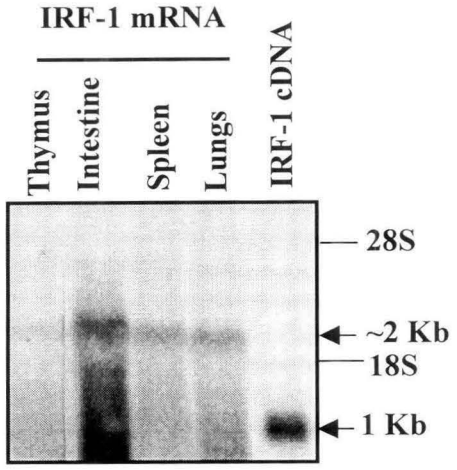

(A) Northern blot

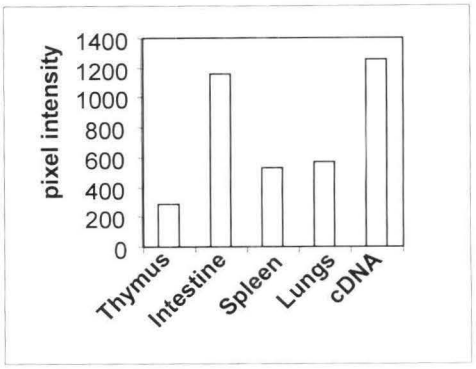

(B) Quantitation of Northern blot

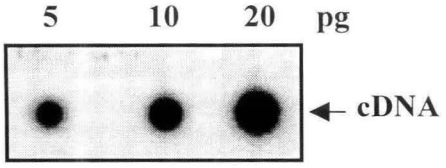

(C) Dot blot

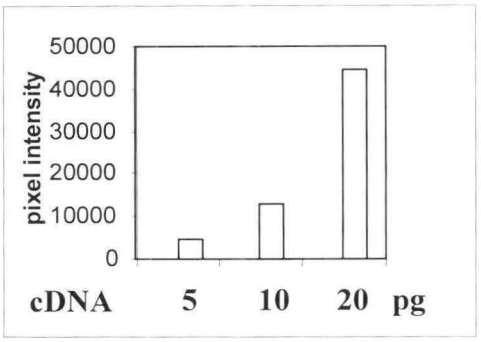

(D) Quantitation of dot blot

Fig. 15 Expression of IRF-1 mRNA in thymus, intestine, spleen and lungs of 33 day old mice. (A) Northern blot and (C) dot blot hybridization using ^{32}P labeled IRF-1 cDNA (pIRFL/Xho I) probe. 30 μg total RNA was loaded per lane and 10pg of IRF-1 cDNA was used as a positive control. 5,10, 20 pg IRF-1 cDNA was spotted for dot blot. The image was developed with the help of a phosphoimager (Fujifilm, BAS 1800) and quantitated by Image Gauge V2.54 software shown in histograms. (B) quantitation of Northern blot and (D) quantitation of dot blot.

fold more and that of the intestine was 5.5 x fold more than the level in thymus indicating a tissue-specific pattern of expression. IRF-1 mRNA was not detected in the brain. Other . ssues were not examined in this assay.

6.3.2 RNA dot blot hybridization

Dot blot hybridization was carried out to estimate the expression of IRF-1 mRNA in brain, thymus, lungs, heart, liver, spleen and kidney tissues of the 63 day old mouse. 5, 10 and 20 μg of total RNA of each tissue of 63 day old mice was used and as a positive control 5, 10, 20 and 40 pg of IRF-1 cDNA was used. ^{32}P labeled 1kb IRF-1 cDNA was used as the probe. Image was developed with the help of a phosphoimager (Fujifilm, BAS 1800) and shown in fig. 16. To check the expression of IRF-1 mRNA in each tissue the dot blot was quantitated using Image Gauge V2.54 software. The positive control: 5, 10, 20, 40 pg of IRF-1 cDNA showed strong signals with 377, 1113, 2300 and 3749 pixel respectively indicating that the assay was linear atleast upto this level. The pixel values of IRF-1 mRNA in 5, 10 and 20 μg of brain RNA was 220, 344 562, thymus showed 700, 993 and 1526 pixel and Lungs showed 803, 1245, 1830 pixel for the same range of RNA. Similarly, heart showed 292, 444 and 695 pixel and liver showed 414, 621, 1070 pixel for 5, 10, 20μg of RNA respectively. The spleen showed 495, 811 and 1299 pixel and kidney showed 452, 689, 942 pixel and intestine showed 2066, 3598 and 4993 pixel for 5, 10, 20μg of RNA respectively. In table 8 the pixel values shows that maximum amount of IRF-1 mRNA was expressed in intestine followed by lungs, thymus, spleen and then liver. Kidney, heart and brain had lowest amount of IRF-1 mRNA expression. Pixel intensity of IRF-1 mRNA present in 5, 10 and 20μg of total RNA of different tissues was plotted as linear graph and histogram as shown in Fig. 17 (A) and (B). The level of IRF-1 mRNA in the ascending order was from brain, heart, kidney, liver, spleen, thymus, lungs and intestine

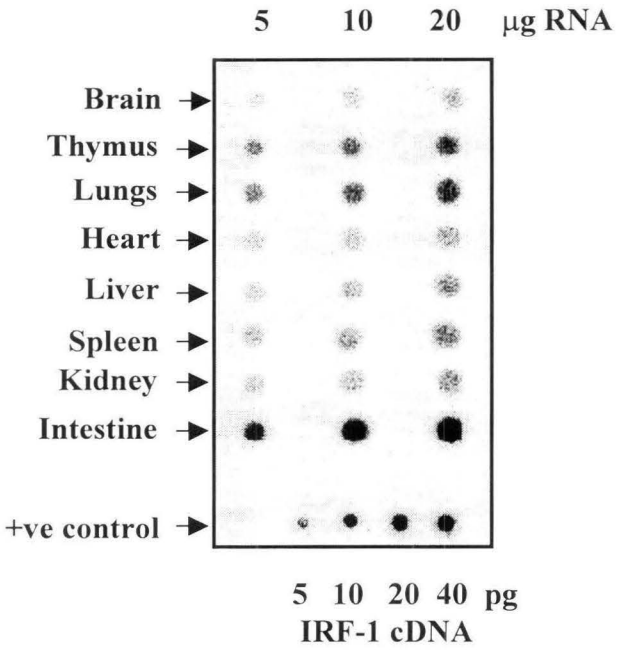

Fig. 16 RNA dot blot analysis for expression of IRF-1 mRNA in brain, thymus, lungs, heart, liver, spleen, kidney and intestine of 63 day old mice. 5, 10, 20 μg of total RNA was used for each tissue. 5, 10, 20, 40 pg of IRF-1 cDNA was used as a +ve control. ^{32}P labeled IRF-1 cDNA probe was used for hybridization. The image was developed with the help of a Phosphoimager (Fujifilm BAS 1800).

Tissue	Amount	Signal intensity (pixel/dot)
Brain	5μg	220
	10μg	344
	20μg	562
Thymus	5μg	700
	10μg	993
	20μg	1526
Lungs	5μg	803
	10μg	1245
	20μg	1830
Heart	5μg	292
	10μg	444
	20μg	695
Liver	5μg	414
	10μg	621
	20μg	1070
Spleen	5μg	495
	10μg	811
	20μg	1299
Kidney	5μg	452
	10μg	689
	20μg	942
Intestine	5μg	2066
	10μg	3598
	20μg	4993
+ve control (IRF-1 cDNA)	5pg	377
	10 pg	1113
	20 pg	2300
	40 pg	3749

Table 8 Pixel intensity values of RNA dot blot for IRF-1 mRNA expression in 5, 10, 20 μg total RNA from brain, thymus, lungs, heart, liver, kidney and intestine of 63 day old mice. 5, 10, 20, 40 pg of IRF-1 cDNA was used as +ve control (Fig.16). Pixel intensity was quantitated by a phosphoimager (Fujifilm, BAS 1800) using Image gauge V2.54 software.

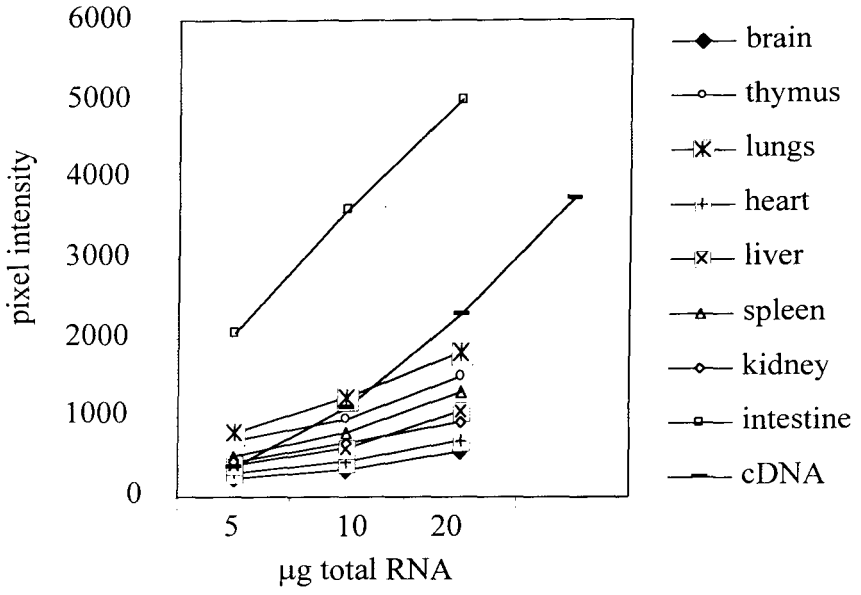

(A)

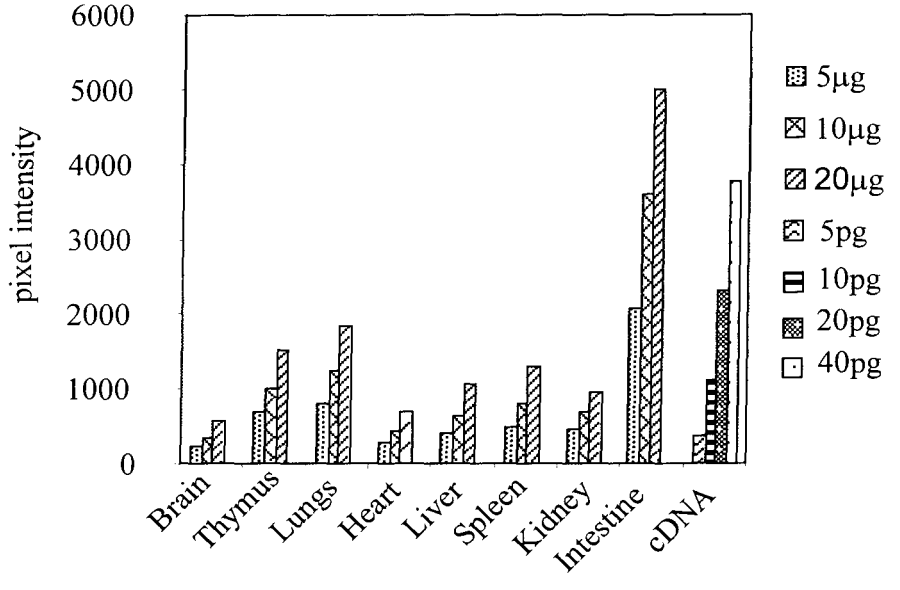

(B)

Fig. 17 Expression of IRF-1 mRNA in mouse tissues. Graphical represention of pixel intensity of IRF-1 mRNA in 5, 10, 20 µg total RNA isolated from brain, thymus, lungs, heart, liver, spleen, kidney, intestine of 63 day old mice is shown as (A) line drawing and (B) histogram. 5, 10, 20, 40 pg of IRF-1 cDNA was used as positive control (Table 8).

respectively. This clearly showed a tissue-specific expression pattern for IRF-1 mRNA in the mouse.

6.4 DNA binding activity of IRF-1

IRF-1 is a transcription factor. It recognizes GAAANN sequences. GAAANN sequences are present in the promoter/enhancers of many mammalian genes that are inducible by virus, interferon and double stranded RNA or poly (I.C.). The GAAANN sequence may vary at the NN positions, for example NN could be GT, GG, CC, GC, CG and TG etc., thus it provides specificity to the sequence element. IRF-1 interacts with GAAANN sequence(s) depending on the nucleotide specificity at NN positions, for example GAAAGT is a IRF-1 binding sequence. So far no other factor has been shown to bind directly to $(GAAAGT)_4$ in the absence of IRF-1 or IRF-2. At least, two copies of this hexamer is needed for IRF-1 binding and transcription. Examples of genes containing IRF-1 binding sites in their promoter/enhancers are IFN-β (human), IFN–α1 (human), Mx (mouse), H-2D, H-2K (mouse), ISG 54 (human), 2' 5' oligo A synthase (mouse), IP-10 (human), complement factor B (human), β_2–microglobulin (human), guanylate-binding protein or GBP (human), IL-4 (human), IL-5 (human), IL-7 receptor (human), p53 (human), E-cadherin (human) and IRF-2 (mouse and human) as shown in table 9. IRF-1 binding site in the human IFN-β gene promoter is AAGTGA. A multimer of AAGTGA and GAAAGT will produce the same sequence motif. All the DNA binding activity experiments for IRF-1 in this work was performed with a 24 bp synthetic oligonucleotide sequence containing $(GAAAGT)_4$ and a negative control for this was $(GAAA)_6$, also a 24 bp sequence. In short they are referred to as $(GT)_4$ and $(GA)_6$.

The DNA binding domain of IRF-1 and IRF-2 transcription factors binds to the specific sequence $(GAAAGT)_4$ i.e. GAAAGTGAAAGTGAAAGTGAAGT. The oligonucleotide was first end

Gene	Sequence	Position	Reference
IFN-β (human)	AAATGT	-109 to-104	Fujita et al. (1985)
	AAATGA	-103 to-98	
	ATAGGA	-96 to-91	
	AACTGA	-89 to-84	
	AAGGGA	-83 to -78	
	AAGTGA	-76 to -71	
	AAGTGG	-70 to -65	
IFN- α1 (human)	AAATGG	-81 to -76	Ryals et al. (1985)
	AAGTGG	-74 to -69	
	AAGTGG	-54 to -49	
MX (mouse)	AACTCA[1]	-128 to -133	Hug et al. (1988)
	AAACGA[1]	-122 to -127	
	AATTGA[1]	-55 to -60	
H-2D, H-2K (mouse)	AAGTGA[1]	-148 to -153	Korber et al. (1988)
	AACTGA[1]	-142 to -147	Levy et al. (1988)
ISG54 (human)	AAGTGA[1]	-104 to -109	Levy et al. (1988)
	AACTAG[1]	-97 to -102	
	AAGTGA[1]	-91 to -96	
	AAGGGA[1]	-85 to -90	
ISG15 (human)	GAAACCGAAACT	-106 to –95	Reich et al. (1987)
2' 5' oligo A Synthase (mouse)	AAATGG	-69 to -64	Cohen et al. (1988)
IP-10 (human)	GAAAGTGAAACC	-220 to –208	Luster et al. (1987)
Complement factor B (human)	GAAAGTGAAACT	-470 to –481	Wa et al. (1987)
Guanylate-binding protein (human)	GAAACTGAAAGT	-118 to –129	Lew et al. (1991)
β_2- microglobulin (human)	GAAACTGAAA A TC	-139 to –127	Israel et al. (1987)
IL-4 (human)	GAAATGAAACC	-193 to –124	Eder et al. (1988)
IL-5 (human)	GAAATGGAAATG	-447 to –458	Tanabe et al. (1987)
IL-7 receptor (human)	GAAATGGAAGAGT	-261 to –249	Pleiman et al. (1991)
P^{53} (human)	CAAACGCAAAGC	-337 to –324	Tuck, S. P., and L. Crawford (1989)
E –cadherin (human)	CAAAACGGAAACC	-273 to –261	Behrens et al. (1991)
IRF-2 (mouse and human)	GAAAATGAAATT	-258 to –247	Harada et al. (1994)
VCAM-1 (human)	GAAATAGAAAGT[1]	-2 to –13	Andrew et al. (1995)
iNOS (human)	GAAAGTGAAATC[1]	-913 to –924	Xie et al. (1993)
IL-6	GAAAAAAAGAAAGT	-267 to –254	Laura et al. (1997)

[1] antisense stand

Table 9 Occurrence of GAAANN oligonucleotides as cis-acting sequence motifs in promoters of virus-inducible and Interferon (IFN)- inducible genes in mammalian cells.

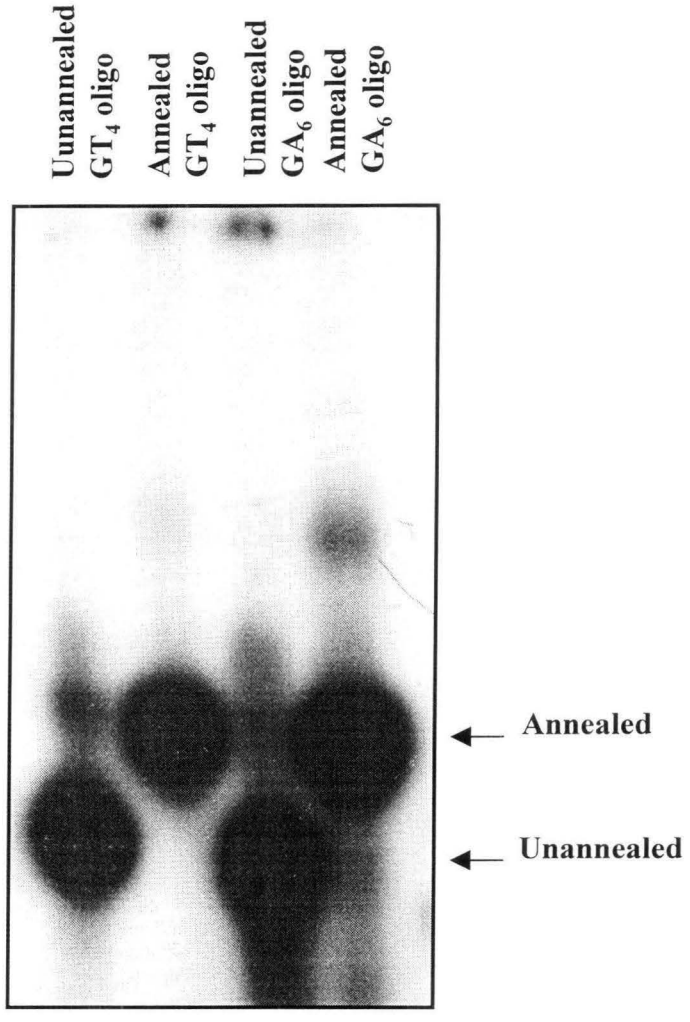

Fig. 18 ^{32}P Labeling and annealing of GT_4 and GA_6 oligonucleotides. 3 pmole of GT_4 $(GAAAGT)_4$ or GA_6 $(GAAA)_6$ oligo was ^{32}P labeled by γ (^{32}P) ATP and T_4 polynucleotide kinase upto a specific activity of 3-5 $x10^6$ cpm/pmole end and annealed to 9 pmole of reverse complementary oligo. About 30,000 cpm and 50 fmole annealed and unannealed oligo were analyzed in a 12% native polyacrylamide gel in TBE buffer.

labeled by γ ^{32}P ATP, followed by annealing with excess of the reverse complimentary oligonucleotide. Fig.18 shows that unannealed and annealed $(GT)_4$ and $(GA)_6$ oligonucleotides are resolved in a native polyacrylamide (12%) gel and almost all ^{32}P $(GT)_4$ and $(GA)_6$ oligonucleotides are in the double stranded (ds) form. The ds $(GT)_4$ and $(GA)_6$ were used for IRF-1 binding. Similarly, for competition assay cold or unlabeled ds $(GT)_4$ and ds $(GA)_6$ were used. Fig. 19 shows that for optimization of IRF-1 binding, 8 μg whole cell extract of a murine fibroblast cell line, L 929 and 10 μg of whole cell extract from spleen of adult mouse was used to check the binding activity of IRF-1 and IRF-2 with 50 fmole of ^{32}P labeled 24 bp $(GAAAGT)_4$ oligonucleotide. IRF-1 and IRF-2 complexes were observed using the L 929 cell extract pattern as the standard according to published literature. The amount of IRF-2 was more than IRF-1in the L929 extract. The mouse spleen extract showed strong IRF-1 (and IRF-1-like) DNA binding activity. The $(GAAA)_6$ oligo also showed some DNA binding activity in the L929 extract but not in the spleen extract. The $(GAAA)_6$-spleen extract complex should be considered as some non-specific. The $(GAAA)_6$-L929 extract complex should be considered as some factor probably recognizing the (GAAA)n as a simple repeat motif of DNA. The (GAAA)n complex binding pattern was different in L929 cell and spleen extracts. $(GAAAGT)_4$ + IRF-1 (and IRF-1 -like) DNA-protein complexes (six complexes were observed in low exposure) were much more prominently and abundantly detected than that of $(GAAA)_6$ + protein in the spleen extract. This clearly showed the specificity of $(GAAAGT)_4$ sequence.

6.4.1 DNA binding activity of IRF-1 and IRF-2 in mouse tissues

Fig. 20 shows that whole cell extract of different mouse tissues (brain, thymus, lungs, heart, liver, spleen, kidney and intestine) were used to screen for the presence of IRF-1 and IRF-2. For DNA binding activity of IRF-1 and

Fig. 19 Electrophoretic Mobility Shift Assay (EMSA) for DNA binding activity of IRF-1 in whole cell extracts (WE) from mouse fibroblast L 929 cells (8 μg) and mouse spleen tissue (10 μg). 50 fmole of ^{32}P labeled GT_4= $(GAAAGT)_4$ or GA_6 = $(GAAA)_6$ 24 bp synthetic double stranded oligonucleotides were used for binding. A 4% native polyacrylamide gel in TBE buffer was used to resolve the DNA- protein complexes by electrophoresis at 200 Volts (35 mA) for 2 hrs at 4° C. IRF-1 or IRF-1-like complex(es) were observed in the mouse spleen. L 929 extract was used as a reference.

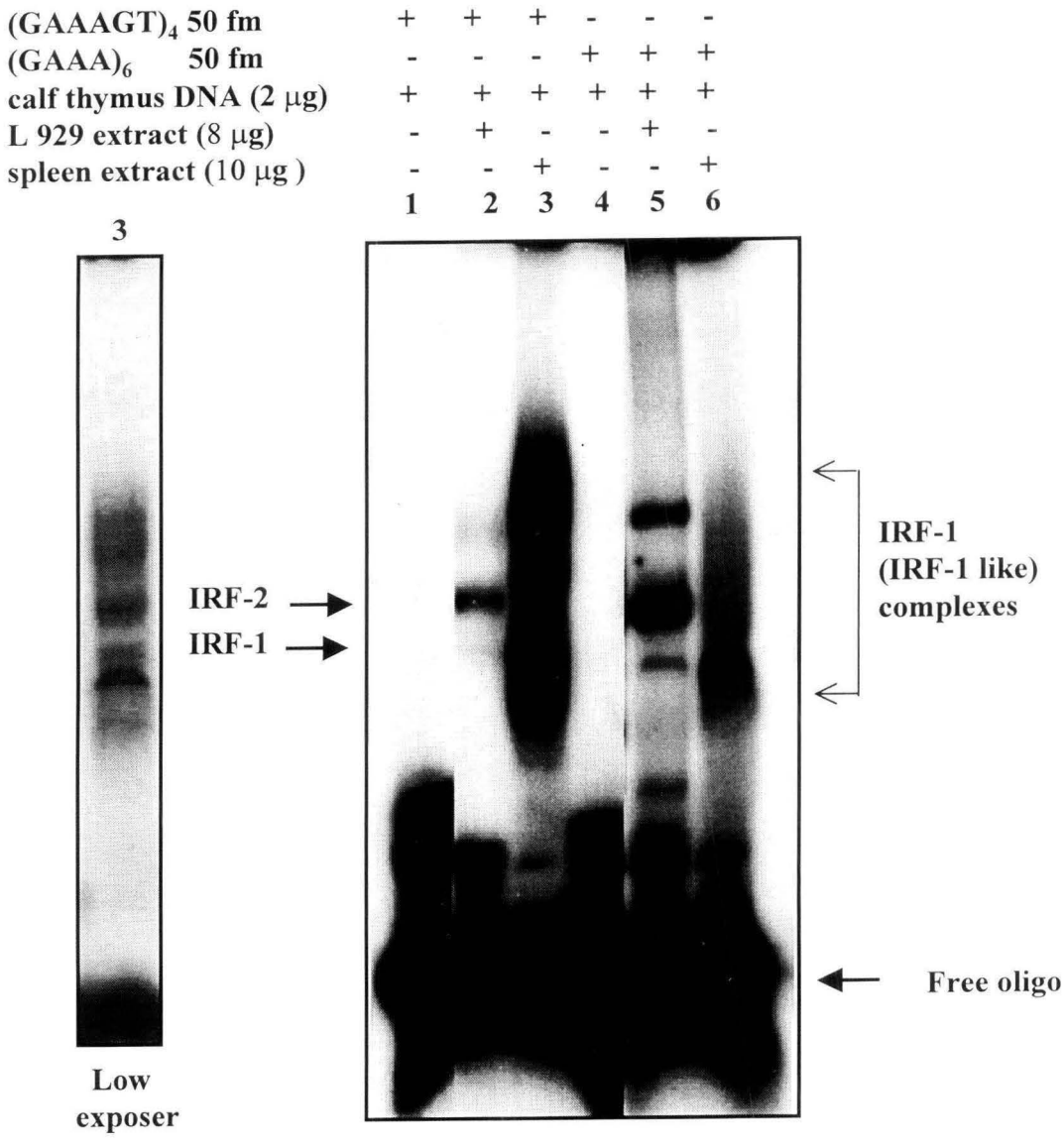
(GAAAGT)4 50 fm + + + - - -
(GAAA)6 50 fm - - - + + +
calf thymus DNA (2 μg) + + + + + +
L 929 extract (8 μg) - + - - + -
spleen extract (10 μg) - - + - - +
1 2 3 4 5 6
3
IRF-2
IRF-1
IRF-1
(IRF-1 like)
complexes
Free oligo
Low
exposer

Fig. 19

Fig. 20 Electrophoretic mobility shift assay (EMSA) for DNA binding activity of IRF-1 and IRF-2 in 20 μg whole cell extracts (WE) from spleen (S), brain (B), thymus (T), lungs (Lu), heart (H), liver (Li), kidney (K), intestine (I) of 63 day old mice. a1 and d1 are additional IRF-1 complexes detected. Recombinant GST-IRF-1 protein (a gift from Meenakshi Upreti) was used as a reference. 50 fmole ^{32}P labeled GT_4 oligo was used for binding and 100 x fold molar excess of GT_4 or GA_6 oligo was used for competition. A 7.5% native polyacrylamide gel in TBE buffer was used. IRF-1 and IRF-2-DNA complex(es) in various mouse tissues are shown.

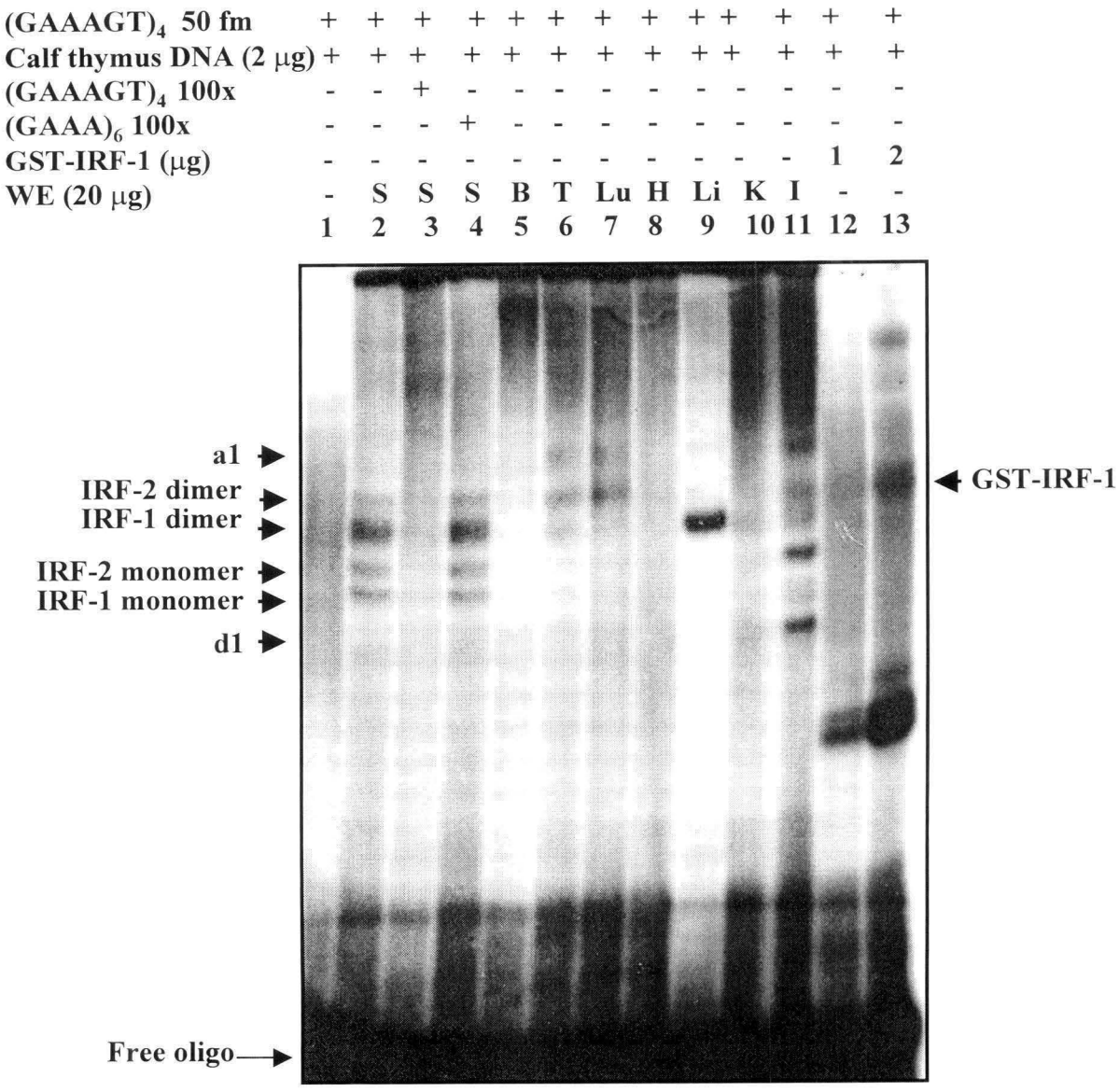
(GAAAGT)4 50 fm + + + + + + + + + + + + +
Calf thymus DNA (2 μg) + + + + + + + + + + + + +
(GAAAGT)4 100x - - + - - - - - - - - - -
(GAAA)6 100x - - - + - - - - - - - - -
GST-IRF-1 (μg) - - - - - - - - - - - 1 2
WE (20 μg) - S S S B T Lu H Li K I - -
1 2 3 4 5 6 7 8 9 10 11 12 13
a1
IRF-2 dimer
IRF-1 dimer
IRF-2 monomer
IRF-1 monomer
d1
Free oligo
GST-IRF-1

Fig. 20

Tissue extract	IRF complex	Signal intensity (Pixel/complex)
Spleen	a ••	8208.00
	b oo	20270.00
	c •	10210.00
	d o	9776.00
Spleen $(GAAAGT)_4$ competition	-	no Complex
Spleen $(GAAA)_6$ competition	a ••	8047.00
	b oo	19280.00
	c •	9233.00
	d o	8633.00
Brain	-	no complex
Thymus	a1	8930.00
	a ••	9783.00
	b oo	5626.00
Lungs	a1	10210.00
	a ••	11970.00
Heart	-	no complex
Liver	a1	1736.00
	a ••	1591.00
	b oo	23800.00
Kidney	-	no complex
Intestine	a1	12790.00
	a ••	8193.00
	b oo	5834.00
	c •	12380.00
	d1	11980.00
GST-IRF-I (2 µg *E. coli* extract)	i	16680.00
	ii	13600.00
	iii	**39010.00**
	iv	21460.00
	v	124300.00

Table 10 Pixel intensity values for IRF-1 and IRF-2 complexes present in 20 µg whole cell extract (WE) of spleen, brain, thymus, lungs, heart, liver, kidney and intestine tissues from 63 day old mice (Fig.20). 2 µg of *E. coli* extract containing recombinant GST-IRF-1 (iii) was used as a reference. a, b, c, d represent IRF-2 dimer (••), IRF-1 dimer (oo), IRF-2 monomer (•) and IRF-1 monomer (o) DNA complexes respectively. a1 and d1 are additional IRF-1 complexes detected. Pixel intensity was calculated with the help of a Phosphoimager (Fujifilm BAS 1800) using Image Gauge V2.54 software.

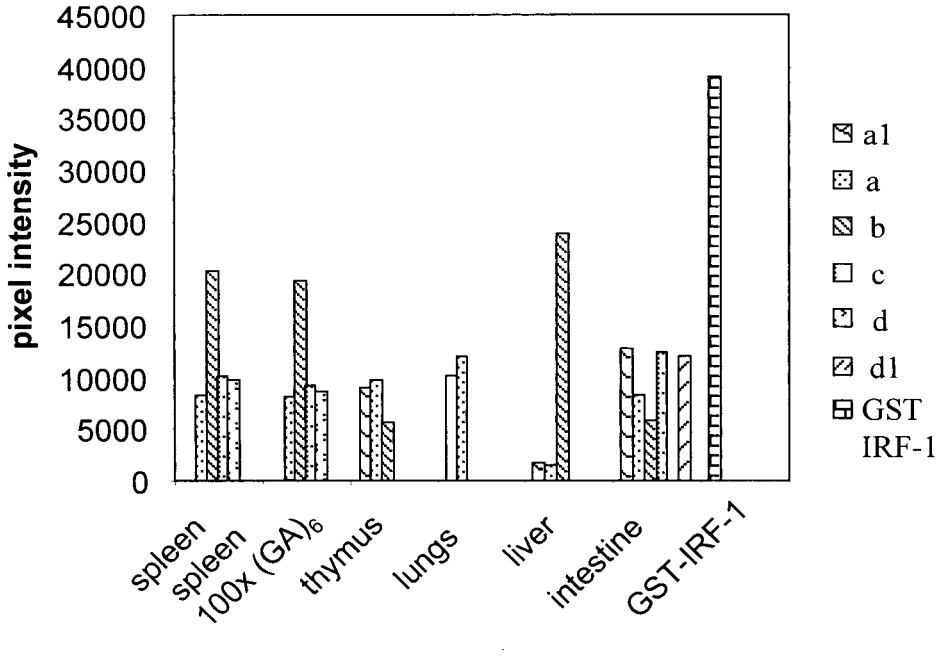

Fig. 21 Expression of IRF-1 and IRF-2 in mouse tissues. Pixel intensity of IRF-1 and IRF-2 complexes in 20 μg whole cell extracts of spleen, spleen + competition with GA_6 oligo, thymus, lungs, liver, intestine of 63 day old mice. 2 μg of *E. coli* extract containing recombinant GST-IRF-1 protein was used as a reference. ^{32}P $(GAAAGT)_4$ was used for the binding assay and 100 x molar excess of $(GAAA)_6$ was used for competition in spleen extract. a, b, c and d are IRF-2 dimer, IRF-1 dimer, IRF-2 monomer and IRF-1 monomer respectively. a1 and d1 are additional IRF- complexes (Fig. 20).

IRF-2, 20 μg whole cell extracts of spleen (S), brain (B), thymus (T), lungs (Lu), heart (H), liver (Li), kidney (K), intestine (I) and 1, 2 μg of recombinant GST-IRF-1 protein (a kind gift from Meenakshi Upreti) were used. For each binding assay, 50 fmole of ^{32}P labeled 24 bp $(GAAAGT)_4$ ds oligonucleotide and for competition 100x molar excess of specific competitor ds $(GAAAGT)_4$ and nonspecific competitor ds $(GAAA)_6$ were used. 2 μg calf thymus DNA was used as a carrier DNA in all binding reactions. In spleen, IRF1 and IRF-2 were observed as four complexes, from top to bottom were IRF-2 dimer (a), IRF-1 dimer (b), IRF-2 monomer (c) and IRF-1 monomer (d) as shown in Fig. 20. Mouse IRF-1 is 329 and IRF-2 is 349 amino acids long. The molecular mass of murine IRF-1 is 37.6 kd and that of IRF-2 is 49.5 kd. GST-IRF-1 used for this study is about 66-67 kd since in SDS-PAGE of IPTG-induced *E. coli* extracts it always appeared as a protein band at little higher than the 66 kd band of BSA and its calculated size is about 66 kd. (Upreti, M. and Rath, P.C., unpublished). The four complexes observed in the spleen were compared with the size of GST-IRF-1 and the band pattern was compared with the four IFN-γ-inducible bands obtained with the nuclear extract from a human macrophage/monocyte (U 937) cell line (fig. 27 showing four IRF-1/IRF-2 DNA complexes). Based on these two comparisons it was understood that complexes (a), (b), (c) and (d) were IRF-2 dimer, IRF-1 dimer, IRF-2 monomer and IRF-1 monomer respectively.

These four complexes were competed out with 50 x molar excess of ds cold $(GAAAGT)_4$ but were not competed out with ds cold $(GAAA)_6$ oligonucleotide. This proved that the complexes were specific for $(GAAAGT)_4$ sequence which binds to IRF-1 and IRF-2. Brain, heart, and kidney tissues did not show detectable levels of IRF-1/IRF-2 complexes in the assay. Thymus showed three complexes, one each similar to the size of IRF-2 dimer (a), IRF-1 dimer (b) and an additional complex (a1) that was more than the size of the IRF-2 dimer. Lungs also had additional IRF-complexes (a_1) and (a), IRF-2 dimer. Liver, interestingly, showed a higher amount of IRF-1 complex in

dimer form (a_1) and two more weak complexes, one same as IRF-2 dimer and another at a higher position identical to (a1). Five complexes were observed in the intestine : IRF-2 dimer (a), IRF-1 dimer (b), IRF-2 monomer (c) and two additional IRF-complexes (a_1) and (d_1). The IRF-2 monomer and complex (d1) were strongly detected in the intestine. The size of (a_1) is more than (a) and (d_1) is smaller than IRF-1 monomer (d). The *E. coli* extract containing recombinant GST-IRF-1 produced one complex above the dimer of IRF-1 and this approximately matched with the expected size of GST-IRF-1 protein, when compared to BSA standard (data not shown). The smaller GST-IRF-1 DNA complex may contain a part of GST-IRF-1 after it was probably cleaved from the GST-IRF-1 at the protease (enterokinase) site at the N-terminus assuming that such a protease activity may exist in *E. coli*. Otherwise, another degradation product without retaining the DNA binding domain of IRF-1 should not show complex formation. Thus a tissue-specific pattern of IRF-1 and IRF-2 DNA binding activity was observed in the mouse.

The complexes were quantitated by Image Gauge $V_{2.54}$ software in a phosphoimager (Fujifilm, BAS 1800) and the signal intensities are shown in table 10. Four complexes in the spleen whole cell extract produced pixel intensities as follows : IRF-2 dimer (a) = 8208, IRF-1 dimer (b) = 20270, IRF-2 monomer (c) = 10210 and IRF-1 monomer (d) = 9776. Pixel intensities of three complexes of thymus were : IRF-2 dimer (a) = 9783, IRF-1 dimer (b) = 5626. Lungs showed two complexes, one additional IRF complex (a_1) = 10210 and IRF-2 dimer (a) = 11970 pixel values. In liver, the complexes showed pixel intensities as follows : IRF-1 dimer (b) was 23800. Intestine showed five complexes with pixel intensities of IRF-2 dimer (a) = 8193, IRF-1 dimer (b) = 5834, IRF-2 monomer (c) = 12380. Additional IRF-1 complexes with 12790 pixel intensity for a1 and 11980 pixel intensity for d1 were also detected. GST-IRF-1 showed 39010 pixel value. The pixel values of IRF-1/IRF-2 complexes mentioned in table 10 have been plotted as histogram and

shown in fig. 21. The spleen and liver showed higher IRF-1 dimer complexes indicating their possible transcriptional activity.

6.4.2 DNA binding activity of IRF-1 and IRF-2 in whole cell-, cytoplasmic- and nuclear extracts of mouse spleen

Since mouse spleen tissue showed constitutively expressed IRF-1 and IRF-2 DNA binding activities in fig. 20, subcellular fractions like the whole cell extract, cytoplasmic extract and nuclear extract of the spleen of adult mouse were subsequently checked for IRF-1 and IRF-2. 50 fmole of ^{32}P labeled 24 bp $(GAAAGT)_4$ oligonucleotide was used for binding reactions using 20 μg of whole cell extract (WE), 20 μg of cytoplasmic extract (CE), and 5, 10 and 20 μg of nuclear extract (NE) prepared from spleen tissue of the mouse (Fig. 22). This time 2 μg of poly (dI.dC) was used as the carrier DNA in each reaction to ensure that poly (dI.dC.) produced similar results as the calf thymus DNA. In 20 μg spleen whole cell extract, six complexes were observed; IRF-2-, IRF-1 dimers and monomers (a, b, c, d complexes, respectively) were consistently reproduced. Two additional complexes : (c1) and (a1) were also detected. In 20 μg of cytoplasmic extract five weak complexes were detected indicating that small quantities of IRF-1 and IRF-2 were present in the cytoplasm of the spleen cells. They corresponded to dimers and monomers of IRF-2 and IRF-1 (complexes a,b, c, d, respectively) and an additional IRF complex (c_1). The (c1) complex was observed in the whole cell extract and cytoplasmic extract but not in nuclear extract (not even in 20 μg) indicating that this complex was in the cytoplasm. Cold competition with 100x $(GAAAGT)_4$ completely competed out binding of ^{32}P $(GAAAGT)_4$ with 20 μg of whole cell extract proving again that the complex formation was sequence-specific for $(GAAAGT)_4$.

Fig. 22 Electrophoretic mobility shift assay (EMSA) for DNA binding activity of IRF-1 and IRF-2 in 20 μg whole cell extract (WE), cytoplasmic extract (CE) and 5, 10, 20 μg nuclear extract (NE) from adult mouse spleen (S). 0.5 and 1 μg of *E. coli* extract containing recombinant GST-IRF-1 protein (a gift from Meenakshi Upreti) was used as a reference. 50 fmole ^{32}P labeled GT_4 oligo was used for binding and 100 x fold molar excess of cold GT_4 or GA_6 was used for competition. A 7.5% native polyacrylamide gel in TBE buffer was used to resolve IRF-1 and IRF-2 DNA complexes. C1 and C2 are additional IRF-1 complexes detected.

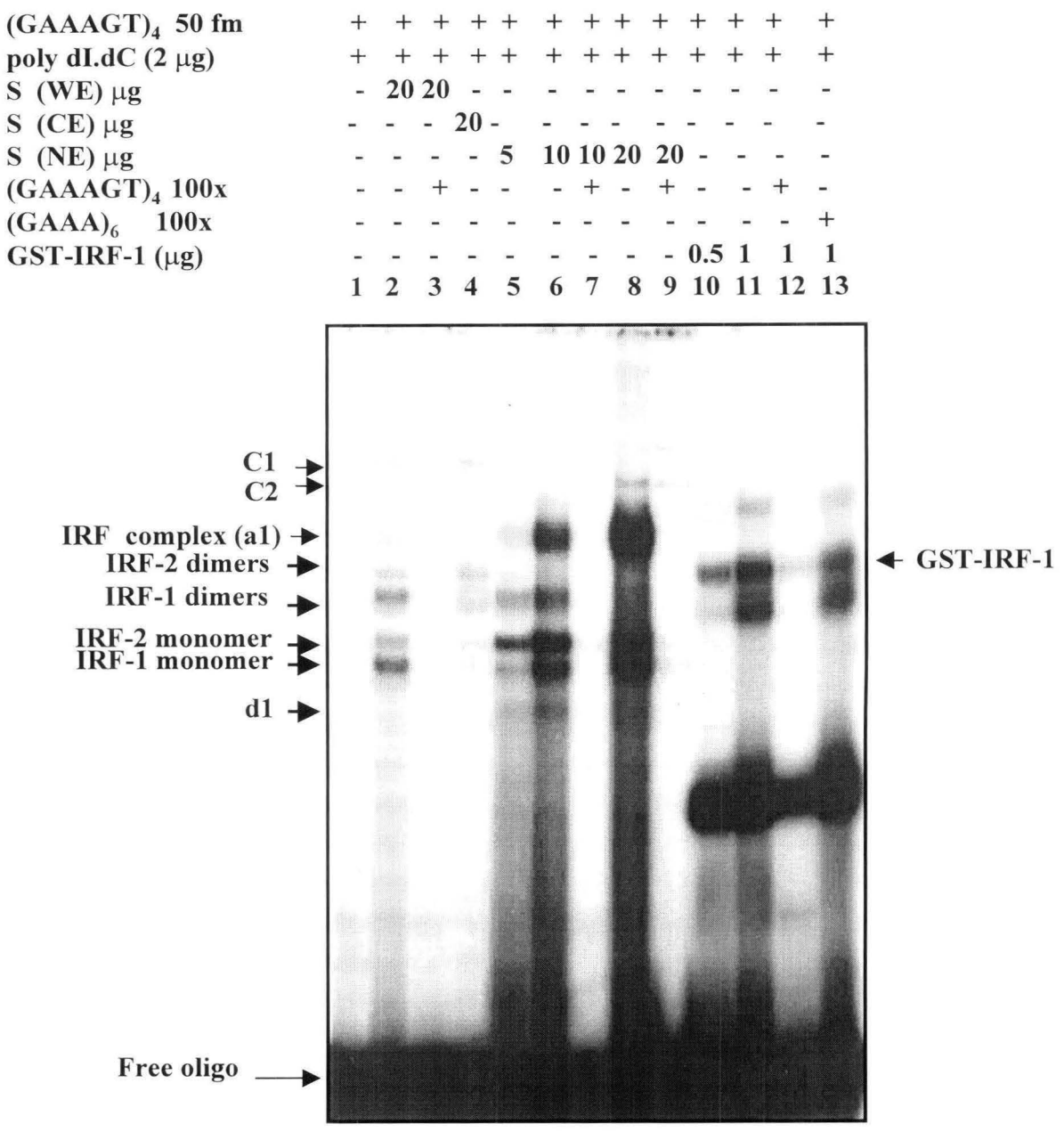
(GAAAGT)4 50 fm + + + + + + + + + + + + +
poly dI.dC (2 μg) + + + + + + + + + + + + +
S (WE) μg - 20 20 - - - - - - - - - -
S (CE) μg - - - 20 - - - - - - - - -
S (NE) μg - - - - 5 10 10 20 20 - - - -
(GAAAGT)4 100x - - + - - - + - + - - + -
(GAAA)6 100x - - - - - - - - - - - - +
GST-IRF-1 (μg) - - - - - - - - - 0.5 1 1 1
1 2 3 4 5 6 7 8 9 10 11 12 13
C1
C2
IRF complex (a1)
IRF-2 dimers
IRF-1 dimers
IRF-2 monomer
IRF-1 monomer
d1
Free oligo
GST-IRF-1

Fig. 22

Spleen extract	IRF complex	Signal intensity (Pixel/complex)
Whole Cell Extract (WE) (20 μg)	C1	57503
	a1	49523
	a ••	46308
	b oo	67660
	c •	58807
	d o	130581
Cytoplasmic Extract (CE) (20 μg)	C1	79069
	a ••	54494
	b oo	26567
	c •	19402
	d o	10465
Nuclear Extract (NE) (5 μg)	a1	17334
	b oo	40593
	c •	25678
	d o	14833
	d1	11639
Nuclear Extract (NE) (10 μg)	a1	83381
	b oo	30338
	c •	22819
	d o	21988
	d1	22576
Nuclear Extract (NE) (20 μg)	C2	52986
	a1	345283
	c •	19283
	d o	23608
GST-IRF-I (1 μg *E. coli* extract)	i	67037
	ii	65529
	iii	**89732**
	iv	217847

Table 11 Pixel intensity values for IRF-1 and IRF-2 complexes present in spleen extract. 20 μg of whole cell extract (WE), cytoplasmic extract (CE) and 5, 10, 20 μg of nuclear extract (NE) of spleen from 63 day old mice were used. 1μg of *E. coli* extract containing recombinant GST-IRF-1 was used as a reference. a, b, c, d represent IRF-2 dimer (••), IRF-1 dimer (oo), IRF-2 monomer (•) and IRF-1 monomer (o) DNA complexes respectively. C1, C2, a1, and d1 are additional IRF complexes detected. Complex (iii) is GST-IRF-1. Pixel intensity was calculated with the help of a Phosphoimager (Fujifilm, BAS-1800) using Image Gauge V2.54 software.

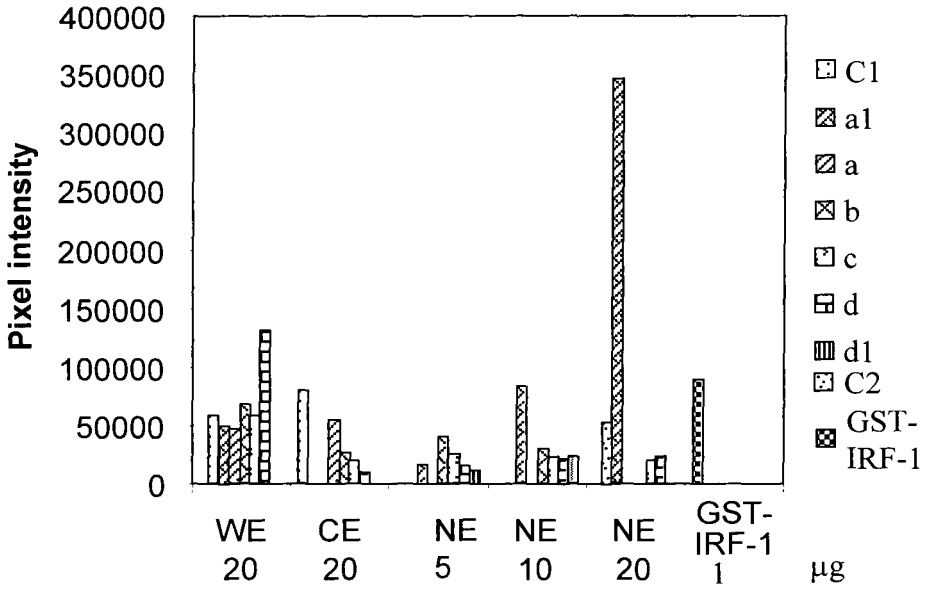

Fig. 23 Expression of IRF-1 and IRF-2 in nuclear and cytoplasmic fraction of mouse spleen. Pixel intensity of IRF-1and IRF-2 complexes in 20 μg whole cell extract (WE), cytoplasmic extract (CE) and 5, 10 and 20 μg of nuclear extract (NE) of spleen of 63 day old mice. 1 μg of *E.coli* extract containing recombinant GST-IRF-1 protein was used as a reference (Fig. 22).

5 and 10 μg of the spleen nuclear extract was found to contain IRF-1 dimer (b), IRF-2 monomer (c) less of IRF-1 monomer (d) and no IRF-2 dimer (a). Complexes (a1) and a_1 were additional IRF complexes. Complex (a1) should be a higher form of IRF-1 (IRF-1 tetramer ?) since GST-IRF-1 alone could also form higher complexes by itself, therefore, ruling out the need for another factor. 20 μg of spleen nuclear extract was found to contain IRF-2 monomer (c), IRF-1 monomer (d), and (c2), (a1) as additional IRF complexes. It was observed that 20 μg of the spleen NE had maximum amount of (a1) complex which contained IRF-1. Its amount increased with increasing amount of the nuclear extract from 5 to 10 and 20 μg . Cold competition with 100 x $(GAAAGT)_4$ completely competed out all IRF-1 and IRF-2 complexes formed by ^{32}P $(GAAAGT)_4$ in presence of 10 μg of nuclear extract. The 0.5 and 1μg of *E. coli* extract containing recombinant GST-IRF-1 protein was loaded as IRF-1 reference. The 67 kd GST-IRF-1 and the lower IRF-1 complexes were detected as before. These complexes were competed out with 100x molar excess of $(GAAAGT)_4$ and could not be competed out with non specific 100x molar excess of $(GAAA)_6$. These complexes were quantitated by Image Gauge V2.54 software in a phosphoimager (Fujifilm, BAS 1800) (Table11). In 20 μg of whole cell extract of spleen pixel values of the seven complexes is as follows : IRF-2 dimer (a) has 46308, IRF-1 dimer (b) has 67660, IRF-2 monomer (c) has 58807, IRF-1 monomer (d) has 130581. Additional IRF complexes (c1) and (a1) have pixel values of 57503 and 49523 respectively. In 20 μg cytoplasmic extract the pixel values of five complexes is as follows: IRF-2 dimer (a) has 54494, IRF-1 dimer (b) has 26567, IRF-2 monomer (c) has 19402, IRF-1 monomer (d) has 10465 and additional IRF complex (c1) has pixel value 79069. In 5 μg nuclear extract the pixel values of five complexes are : IRF-1 dimer (b) has 40593, IRF-2 monomer (c) has 25678, IRF-1 monomer (d) has 14833. Additional IRF complexes (a1) and (d1) have pixel values 17334 and 11639 respectively. The pixel values of the complexes in 10

μg extract are: IRF-1 dimer (b) has 30338, IRF-2 monomer (c) has 22819, IRF-1 monomer (d) has 21988. Additional IRF complexes (a1) and (d1) have pixel values of 83381 and 22576 respectively. In 20 μg nuclear extract the pixel values of the four complexes : IRF-2 monomer (c) has 19283, IRF-1 monomer (d) has 23608. Additional IRF complexes (c2) and (a1) have pixel values 52986 and 345283 respectively. Recombinant IRF-1 (GST-IRF-1) has a pixel value of 89732. The pixel values of complexes have been plotted in histogram and shown in fig. 23. It is clear that the (a1) IRF-1 complex is specific for the nuclear extract and it appeared with increase in the concentration of nuclear proteins in the binding reaction. With 2 x and 4 x fold increase in the nuclear protein concentration in the binding reaction there was a 4.8 x and 20 x fold increase in the (a1) complex formation respectively. It is possible that (a1) IRF-1 complex may be tetrameric IRF-1 and is formed by IRF-IRF association and the same amount (20 μg) of total cell extract did not produce this complex because in presence of the cytoplasmic proteins the nuclear IRF-1 concentration was not achieved. This may be due to cooperative binding of IRF-1 with multimeric $(GAAAGT)_4$ sequence.

6.4.3 Comparison of poly (dI. dC) and calf thymus DNA as carrier for IRF-1 and IRF-2 binding

Poly (dI.dC) or calf thymus DNA was used as carrier DNA in the IRF-1 and IRF-2 binding reactions with $(GAAAGT)_4$, to check which of these two was better. 20 μg of the whole cell extract (WE) and 5 and 10 μg of nuclear extract from adult mouse spleen were used. 0.5μg of *E. coli* extract containing GST-IRF-1 was used as a positive control. These binding reactions were set in two sets, one contained 2 μg of poly (dI.dC) and the other set contained 2 μg of calf thymus DNA as the carrier DNA. Results (Fig. 24) suggested that IRF-

Fig. 24 Electrophoretic mobility shift assay (EMSA) for DNA binding activity of IRF-1 and IRF-2 in 20 μg whole cell extract (WE) and 5, 10 μg nuclear extract (NE) from 63 day old mouse spleen (S). 0.5 μg of *E. coli* extract containing recombinant GST-IRF-1 protein (a gift from Meenakshi Upreti) was used as a reference. 2 μg poly (dI.dC) or calf thymus DNA was used as nonspecific carrier DNA to compare IRF complex(es). 50 fmole ^{32}P labeled GT_4 oligo was used for binding and 100 x fold molar excess of cold GT_4 was used for competition. A 7.5 % native polyacrylamide gel in TBE buffer was used to resolve IRF-1 and IRF-2 DNA comlexes. C1 and C2 are additional IRF complexes detected.

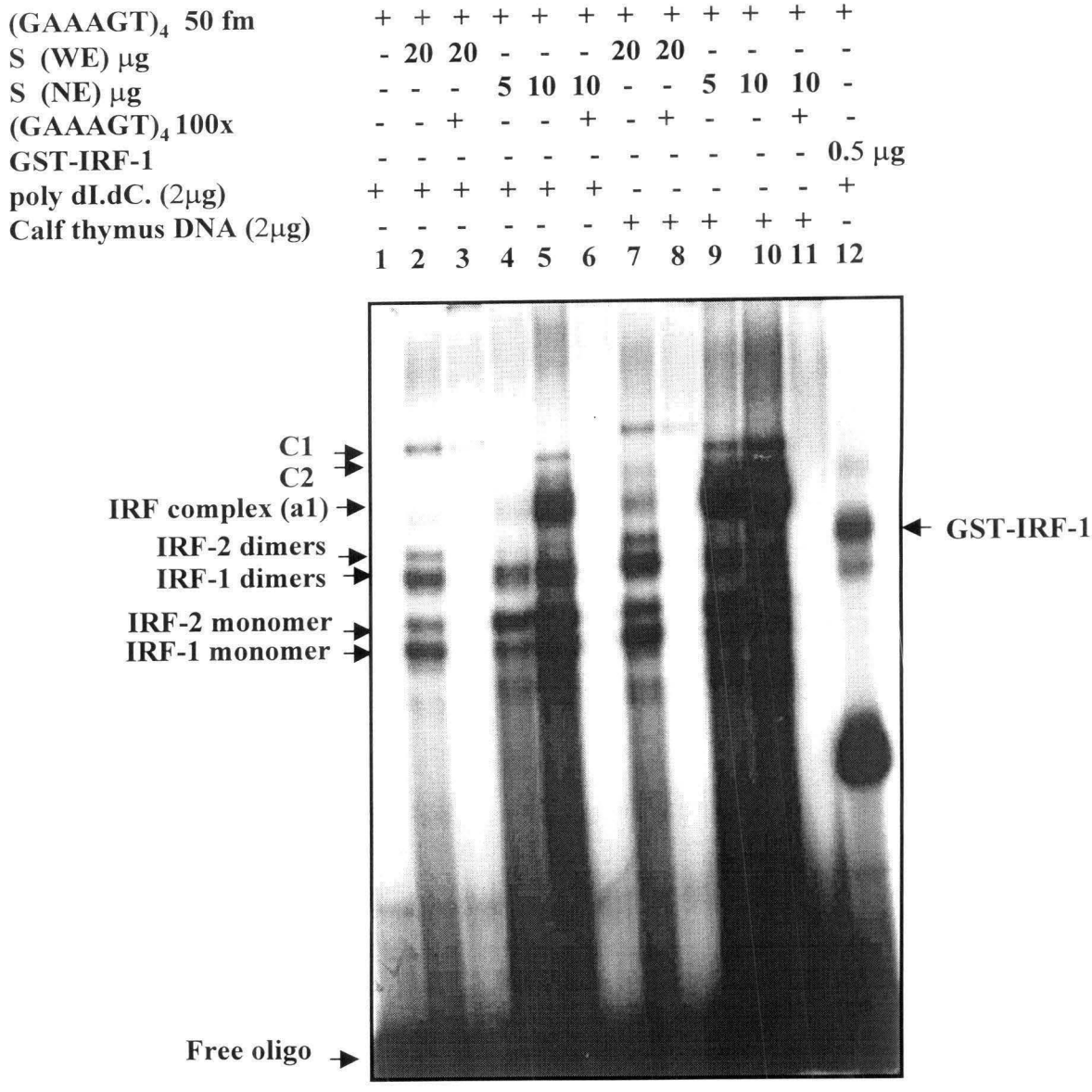
(GAAAGT)4 50 fm + + + + + + + + + + + +
S (WE) µg - 20 20 - - - 20 20 - - - -
S (NE) µg - - - 5 10 10 - - 5 10 10 -
(GAAAGT)4 100x - - + - - + - + - - + -
GST-IRF-1 - - - - - - - - - - - 0.5 µg
poly dI.dC. (2µg) + + + + + + - - - - - +
Calf thymus DNA (2µg) - - - - - - + + + + + -
1 2 3 4 5 6 7 8 9 10 11 12
C1
C2
IRF complex (a1)
IRF-2 dimers
IRF-1 dimers
IRF-2 monomer
IRF-1 monomer
Free oligo
GST-IRF-1

Fig. 24

1 and IRF-2–DNA complexes were formed better in the presence of calf thymus DNA than in poly (dI.dC) as the carrier DNA. However, the band pattern was identical except for an increase in the intensity of the bands.

6.4.4 DNA binding activity of IRF-1 and IRF-2 in cytoplasmic and nuclear extracts of mouse thymus

Presence of IRF-1 and IRF-2-DNA complexes were also checked in the cytoplasmic and nuclear extracts of thymus of the 63 day old mice. 50 f mole of ^{32}P labeled $(GAAAGT)_4$ oligo and 2 μg poly (dI.dC) were used. Fig. 25 shows that in the thymus, no IRF-complex was strongly detected in 20 μg of cytoplasmic extract but weak bands were observed after quantitation. In 5, 10 and 20 μg of nuclear extract (NE) IRF-2 dimer (a), IRF-1 dimer (b) and very little of IRF-2 monomer (c) and IRF-1 monomer (d) were observed. The (a1) complex, similar to that in the spleen extract, was strongly detected as a complex higher than IRF-2 dimer in 5, 10 and 20 μg nuclear extract. The amount of this complex in 5 μg of nuclear extract was detected and it also increased with increasing amount of nuclear protein, similar to the pattern observed for the spleen extract. This complex may be considered as IRF-1 tetramer. 1μg of *E. coli* extract of the clone expressing GST-IRF-1 recombinant protein was used as a positive control.

The complexes were quantitated by Image Gauge V2.54 software in a phosphoimager (Fujifilm, BAS 1800) and shown in table12. Pixel intensity of three complexes in 20 μg of cytoplasmic extract were : IRF-2 dimer (a) has 1232, IRF-1 dimer (b) has 4836, additional IRF complex (a1) has 1568 and C1 has 8836. In 5 μg nuclear extract, pixel intensity of the five complexes : IRF-2 dimer (a) has 7706, IRF-1 dimer (b) has 10406, IRF-2 monomer (c) has 4550, IRF-1 monomer (d) has 3552 and additional IRF complex (a1) has pixel value of 16693. In 10 μg nuclear extract, pixel intensity of the five complexes

Fig. 25 Electrophoretic mobility shift assay (EMSA) for DNA binding activity of IRF-1 and IRF-2 in 20 μg cytoplasmic extract (CE) and 5, 10, 20 μg nuclear extract (NE) from thymus (T) of 63 day old mice. 1 μg of *E. coli* extract containing recombinant GST-IRF-1 protein (a gift from Meenakshi Upreti) was used as a reference. 50 fmole ^{32}P labeled GT_4 oligo was used for binding and 100 x fold molar excess of GT_4 or GA_6 oligo was used for competition. A 7.5 % native polyacrylamide gel in TBE buffer was used to resolve IRF-1 and IRF-2 DNA complexes . C1 and a1 is additional complex detected.

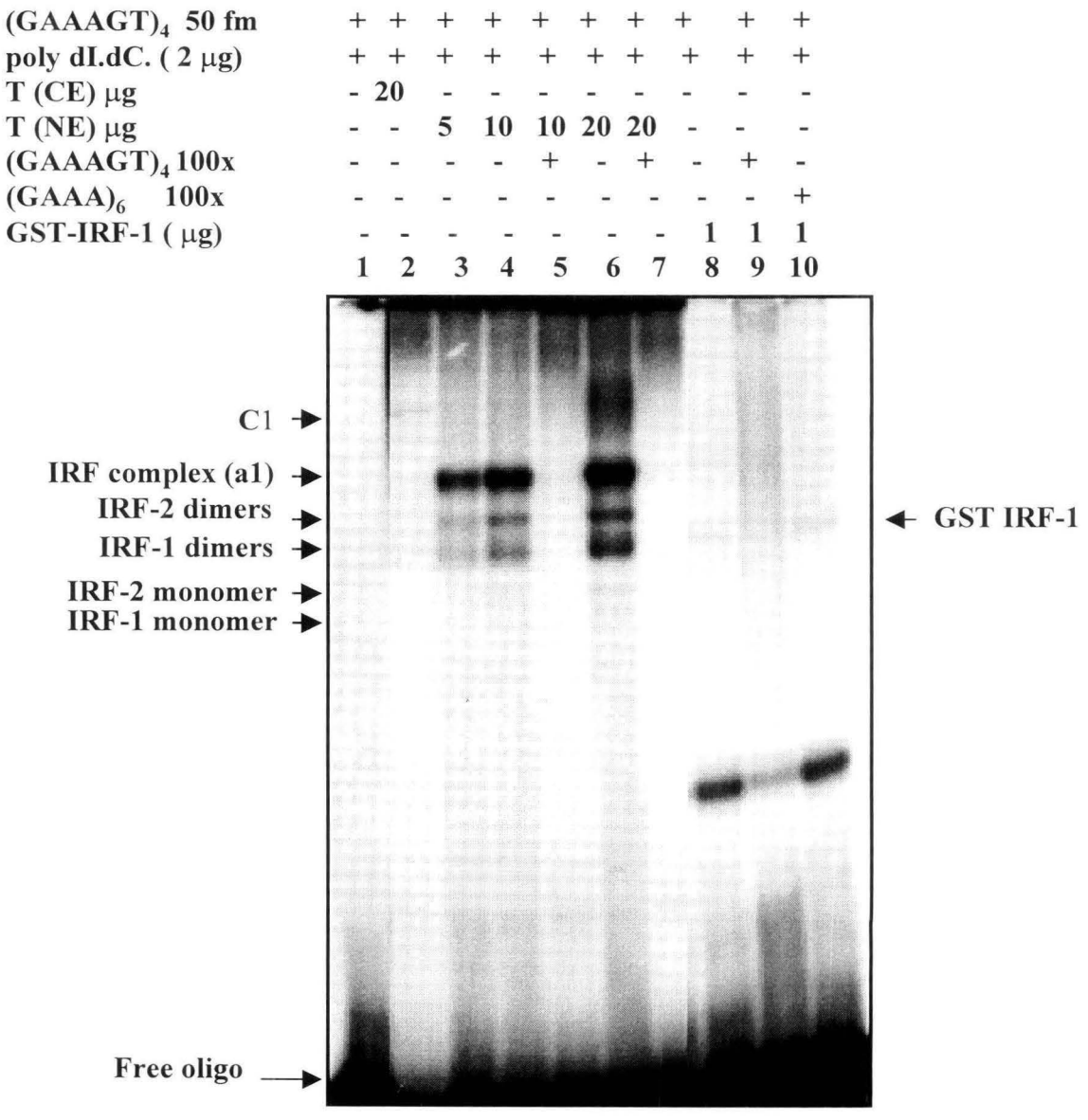
(GAAAGT)4 50 fm + + + + + + + + + +
poly dI.dC. (2 μg) + + + + + + + + + +
T (CE) μg - 20 - - - - - - - -
T (NE) μg - - 5 10 10 20 20 - - -
(GAAAGT)4 100x - - - - + - + - + -
(GAAA)6 100x - - - - - - - - - +
GST-IRF-1 (μg) - - - - - - - 1 1 1
1 2 3 4 5 6 7 8 9 10
C1
IRF complex (a1)
IRF-2 dimers
IRF-1 dimers
IRF-2 monomer
IRF-1 monomer
GST IRF-1
Free oligo

Fig. 25

Thymus extract	IRF complex	Signal intensity (pixel/complex)
Cytoplasmic extract CE (20 μg)	a1	1568
	a ••	1232
	b oo	4836
Nuclear extract NE (5 μg)	a1	16693
	a ••	7706
	b oo	10406
	c •	4550
	d o	3552
Nuclear extract NE (10 μg)	a1	25662
	a ••	11196
	b oo	17964
	c •	7402
	d o	3522
Nuclear extract NE (20 μg)	C1	19248
	a1	29748
	a ••	20868
	b oo	25507
	c •	8784
	d o	6610
GST-IRF-1 (1μg *E. coli* extract)	i	5540
	ii	6540
	iii	**6038**
	iv	26546

Table 12 Pixel intensity values for IRF-1 and IRF-2 complexes present in thymus extracts. 20 μg of cytoplasmic extract (CE) and 5, 10, 20 μg of nuclear extract (NE) of thymus from 63 day old mice were used. 1μg of *E. coli* extract containing recombinant GST-IRF-1 was used as a reference. a, b, c, d represent IRF-2 dimer (••), IRF-1 dimer (oo), IRF-2 monomer (•) and IRF-1 monomer (o) DNA complexes respectively. C1 and a1 are additional complexes detected. Complex (iii) is GST-IRF-1. Pixel intensity was calculated with the help of a Phosphoimager (Fujifilm BAS-1800) using Image Gauge V2.54 software.

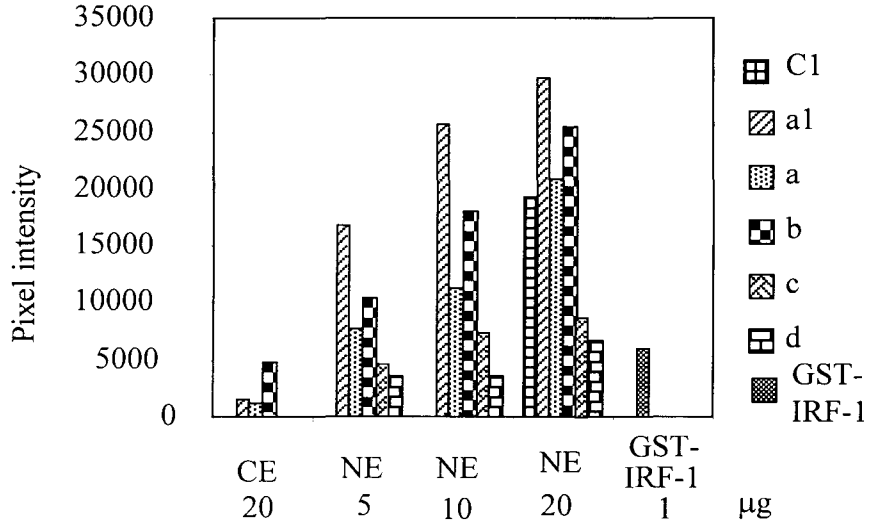

Fig. 26 Expression of IRF-1 and IRF-2 in nuclear and cytoplasmic fractions of mouse thymus. Pixel intensity of IRF-1 and IRF-2 complexes in 20 μg cytoplasmic extract (CE) and 5, 10 and 20 μg nuclear extract (NE) of thymus of 63 day old mice. 1 μg of *E. coli* extract containing recombinant GST-IRF-1 protein was used as a reference. (Fig. 25)

are IRF-2 dimer (a) has 11196, IRF-1 dimer (b) has 17964, IRF-2 monomer (c) has 7402, IRF-1 monomer (d) has 3522 and additional IRF complex (a1) has 25662. In 20 μg nuclear extract, pixel intensity of the six complexes are IRF-2 dimer (a) has 20868, IRF-1 dimer (b) has 25507, IRF-2 monomer (c) has 8784, IRF-1 monomer (d) has 6610 and additional IRF complexes (C1) and (a1) have pixel values of 19248 and 29748 respectively. These pixel values for IRF-1 and IRF-2 complexes have been plotted as histogram and shown in fig. 26. The most important observation from this is that the IRF-1 complexes, (a1) and (b) increased with increasing amount of nuclear protein from 5, 10 to 20 μg.

6.4.5 DNA binding activity of IRF-1 and IRF-2 in U 937 cells after interferon-γ (IFN-γ) treatment

For comparison of mouse and human IRF-1 and IRF-2 DNA binding activity pattern nuclear extracts from a human macrophage/monocyte (U 937) cell line was checked for IRF-1 and IRF-2 binding with ^{32}P $(GAAAGT)_4$ oligonucleotide under normal and after human IFN-γ treatment. IFN-γ is a known inducer of IRF-1 activity in many mammalian cells. U 937 cells were cultured in RPMI 1640 medium + 10% fetal calf serum in presence of standard antibiotics and antimycotics. Cells were grown from 0.2 x 10^6 to 0.6 x 10^6 cells/ml density in CO_2 incubator at 37^0C and were routinely observed. Cells were harvested, counted in a Haemocytometer and replated in a 24 well plate as 1ml/well at 2 x10^6/ml density incubated at 37^0C for 30 min. Cells were treated with 1 nM recombinant human interferon-γ (hIFN- γ) for 0, 30 and 60 min. At the end of the treatment 0.5 ml chilled PBS was added per well and cells were harvested and collected in 1.5 ml tubes on ice. Nuclear extracts were prepared and IRF-1 and IRF-2 binding activity was measured by EMSA. IRF-1 and IRF-2 binding was carried out with 30 fmole ^{32}P labeled $(GAAAGT)_4$ oligonucleotide and 6 μg of nuclear extract. Fig. 27 shows that

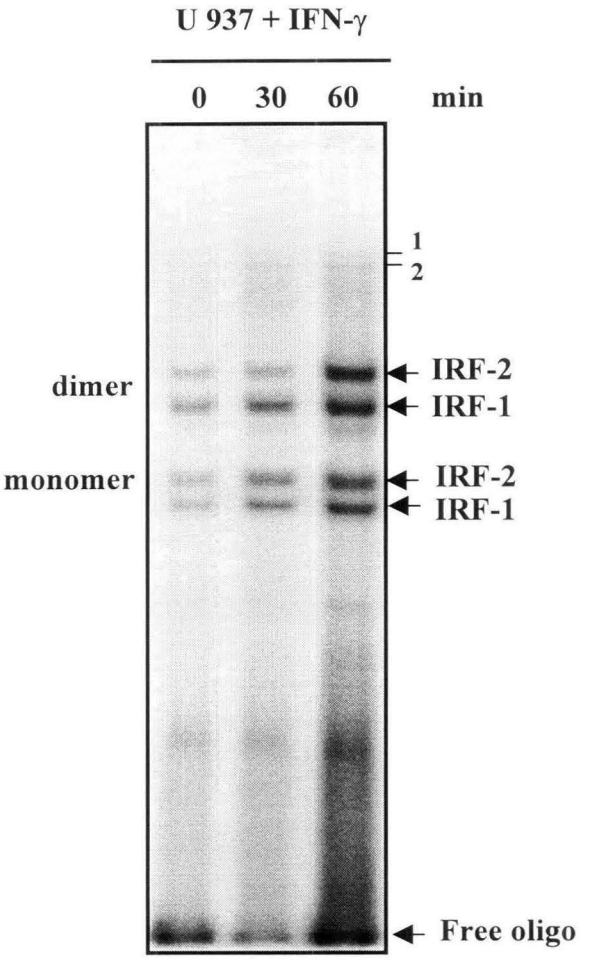

Fig. 27 Electrophoretic mobility shift assay (EMSA) for DNA binding activity of human. IRF-1 and IRF-2 in nuclear extracts (8μg) from U 937 cells treated with 1 nm Interferon γ (IFN γ) for 0, 30, 60 min. 30 fmole ^{32}P labeled GT_4 oligo was used for binding. A 7.5 % native polyacrylamide gel in TBE buffer was used to resolve IRF-1 and IRF-2 DNA complexes. 1 and 2 are additional higher complexes detected.

dimers and monomers of IRF-1 and IRF-2 were observed resembling the pattern obtained for the mouse spleen extract shown in fig. 20 and 22. IFN-γ (1 nM) treatment induced dimmers and monomers of both IRF-1 and IRF-2 after 30 and 60 min. The induction also increased from 30 to 60 min indicating the time course of IFN treatment. It is possible that the induction of both IRF-1 and IRF-2 is mediated through protein synthesis resulting in the increase in IRF-1 and IRF-2 levels. Complex 1 and 2 are additional IRF-1/IRF-2 complex(es) with higher molecular mass possibly resulting due to IRF-association. The U 937 cell pattern of IRF-1 and IRF-2 and their induction by IFN-γ treatment were used as a reference for the mouse IRF-1 and IRF-2 pattern and to confirm that the band shift pattern was due to IRF-1 and IRF-2.

DISCUSSION

7. DISCUSSION

IRF-1 was originally identified and cloned on the basis of its binding specificity with a DNA sequence (AAGTGA) from the virus response element (VRE) of human interferon-β (IFN-β) gene promoter and its ability to mediate transcriptional activation of the IFN-β gene following virus infection (Miyamoto et al., 1988). IRF-1 binds to the positive regulatory domain (PRDI) element of the IFN-β gene promoter which has the following sequence: 5'GAGAAGTGAAAGT3' (Fan and Maniatis, 1989). Subsequently, IRF-2 was identified as a homologue of IRF-1 that could bind to the same DNA sequence as IRF-1 but suppressed IRF-1-mediated gene transcription (Harada, et al. 1989, 90). These two factors (IRF-1 and IRF-2) are highly homologous to each other in their amino-terminal DNA binding regions but different in their carboxy-terminal regions. IRF-1 and IRF-2 are structurally similar but functionally distinct. The DNA sequence that confers DNA binding specificity to IRF-1 and IRF-2 is designated as IRF-element or IRF-E (Harada et al., 1989, Tanaka et al., 1993). IRF-1 functions as an activator for many genes, the promoters of which have IRF-E (Harada et al., 1989). In contrast, IRF-2 antagonizes the function of IRF-1 by competing with the same binding site in the promoter, even with a higher affinity, hence IRF-2 functions as a repressor for such genes (Harada et al., 1990, Yamamoto et al., 1994). Both IRF-1 and IRF-2 are normally expressed at low constitutive levels in mammalian cells. IRF-2 protein is more stable and thus may accumulate to higher levels (Watanabe et al., 1991, Harada et al., 1993). Under normal conditions, in mouse fibroblast (L 929) cells IRF-2 is bound to the IRF-E in IFN-β gene promoter. Following virus infection, IRF-1 gene is activated and its mRNA and protein levels are induced and most likely IRF-1 protein is also modified. Now IRF-1 can replace IRF-2 from the promoter and carry out transcription of IFN-β gene in cooperation with other factors. Once IFN is produced from cells it can also activate IRF-1 gene. But subsequently, IRF-2

gene is also activated by IRF-1 since IRF-2 promoter has IRF-1 binding site and therefore IRF-1 is again replaced by IRF-2 (Harada et al., 1990). IRF-1 mRNA has sequence element in its 3'untranslated region (3'UTR) which contributes to its short half life. Thus cellular concentrations of IRF-1 and IRF-2 mRNA and their protein products are regulated and they are key regulatory factors deciding their function(s) in cells. In addition to this, both IRF-1 and IRF-2 are post translationally modified resulting in alterations in their functional ability. IRF-association domains in IRF-1 and IRF-2 are also sites for interaction(s) of IRFs. This allows them to form multimeric complexes and perform a variety of functions. Now many (at least seven) other IRF-family members have been reported. They have distinct physiological significance.

When cells are stimulated by virus, double stranded RNA (dsRNA) or poly (I.C.) and interferons IRF-1 gene is activated at transcriptional level (Harada et al., 1989, Fujita et al., 1989, Harada et al., 1994). Functionally, IRF-1 is involved in immune response against viruses, bacteria and other pathogens, cell growth regulation, gene expression in cytokine network, maturation of CD8+ T cells in thymus, NK cell differentiation, apoptosis and negative regulation of carcinogenesis. IRF-2 is involved in B lymphocyte differentiation and negative regulation of IRF-1 function in cells and it has oncogenic potential. Most studies with IRF-1 have been carried out with mammalian cells in culture using various inducers to activate IRF-1 gene expression as model systems. However information on IRF-1 gene expression in tissues of normal mouse is limiting.

Therefore, the present study describes an account of the comparison of murine and human IRF-1 gene structure and organization as studied by Southern blot analysis. It also describes studies on IRF-1 mRNA expression by Northern and RNA dot blot analyses in the normal tissues of mouse. Expression of IRF-1 and IRF-2 proteins in the mouse tissues has been studied by their DNA binding activity with a specific IRF-E sequence $(GAAAGT)_4$ which is prevalent in many promoter/enhancer regions of mammalian genes

that are induced by viruses and interferons. Cytoplasmic and nuclear fractions of the mouse spleen and thymus, the two major sites for eliciting immune response, are shown to possess differential patterns of IRF-1 and IRF-2 DNA binding activity. The cytoplasmic and nuclear fractions from the mouse spleen and thymus also showed nuclear-specific IRF-1 complex. The study reports significant information about structural differences in the murine and human IRF-1 gene(s) and *in vivo* occurrence of IRF-1 and IRF-2 DNA binding activities and their variation in mouse tissues under normal conditions. This should be physiologically significant.

7.1. Organization of IRF-1 gene :

7.1.1 Probe used for IRF-1 southern blot hybridization

Organization of the IRF-1 gene was studied by using three types of probes (fig. 1): (a) 194 5' probe, (b) 1kb IRF-1 cDNA probe and (c) C2 genomic probe. The 194bp 5' probe essentially contained the 1st exon, the 1kb cDNA probe contained all (1-10) exons and the 5.3 kb C2 genomic probe contained exons 3-10 and introns 2-10 of the murine IRF-1 gene. 194 bp 5' probe fragment was obtained by digesting plasmid pIRFL (Miyamoto et al., 1988) with Hind III and Pst I. The 194 5' probe was used to identify the 5' flanking promoter DNA fragments of mouse and human IRF-1 gene. The 1 kb cDNA was obtained by digesting pIRFL plasmid with Xho I. The IRF-1 cDNA was cleaved at Xho I site in the middle and at the two Xho I sites in cloning junctions. The cDNA was obtained as two 1kb fragments containing all the exons. This fragment was used to detect full length gene fragments. The 5.3 kb C2 genomic probe was used to identify full length IRF-1 gene fragments as well as its intronic fragments. IRF-1 gene consists of 10 exons in which the translation start site (ATG) is present in the 2nd exon. The 5' and cDNA probes as well as the cDNA and C2 genomic probes have separate

overlapping regions containing sequences from exons 1 and 3-10 respectively. The restriction maps and the probe fragments of the mouse IRF-1 gene are shown in fig.1. Fig. 2 and fig. 3 show IRF-1 and IRF-2 DNA sequences and their diagramatic representations.

7.1.2 Optimization of Southern blot hybridization

Southern blot hybridization assay for the mouse IRF-1 gene was optimized by using decreasing amount (50, 25, 10 and 5 pg) of the 5.3 kb Bam HI fragment from the murine IRF-1 genomic clone (pIRF C2 DNA digested by Bam HI) and ^{32}P labeled 5.3 kb DNA as the probe (fig. 4). At least 5 pg DNA/band was detected for the 5.3 kb IRF-1 gene fragment. 5-50 pg of the IRF-1 gene fragment was clearly detected as per the loading. This efficiency of detection was considered to be optimum for detecting single copy gene(s) from the genomic DNA digests by Southern blot hybridization. In 12 pg of genomic DNA (diploid set of chromosomes per mammalian cell) usually there are two copies for a single copy gene. For each lane in the Southern blot 20 μg of the genomic DNA digest was loaded which was equivalent to 1.6 $x10^6$ copies of a single copy gene. For the IRF-1 gene fragment, 5 pg of the 5.3 kb C2 DNA was equivalent to 8.85 $x10^5$ molecules.

7.1.3 Southern blot analysis

(A) Mouse IRF-1 gene

For studying the organization of mouse IRF-1 gene, 1kb murine IRF-1 cDNA probe was hybridized with Bam HI digested genomic DNA. It detected four DNA fragments : 9.26, 5.41, 3.55 and 2.32 kb DNA. Eco RI digested genomic DNA hybridized to 6 fragments of 19.95, 9.26, 4.14, 2.71, 2.15, 1.41

and 0.92 kb DNA. Hind III digested DNA hybridized to 5 fragments of 25.12, 14.13, 8.91, 3.98, and 2.24 kb. While with Pst I digested mouse genomic DNA 4 fragments of 5.25, 1.71, 1.26 and 0.5 kb were detected. The 1 kb cDNA probe contained all the exons for the mouse IRF-1 gene. Out of the above mentioned fragments, 5.41 kb Bam HI, 19.95 kb and 9.26 kb Eco RI, 25.12 kb Hind III and 1.71 and 1.26 kb Pst I DNA hybridized only to the 1 kb cDNA probe. These fragments have been shown in bold digits in table1. This indicates that these DNA fragments are produced from the mouse IRF-1 gene and they have more sequence homology with IRF-1 exons but less homology with IRF-1 introns.

Hybridization of the 5.3 kb IRF-1 genomic probe with Bam HI digested mouse genomic DNA detected a single fragment of 5.41 kb, with Eco RI digest two fragments of 5.84, and 1.41 kb were observed. With Hind III digested genomic DNA two fragments of 14.13 and 4.64 kb were detected, while with Pst I digest five fragments of 10.8, 6.31, 2.15, 1.71 and 1.26 kb were detected. Use of the three overlapping probes resulted in the detection of some fragments common to either two probes or to all the three probes. Of all the fragments hybridizing with the 5.3 kb genomic probe, the 5.41 kb Bam HI DNA, 5.84 kb Eco RI DNA, 4.64 kb Hind III DNA and 10.8, 6.31 and 2.15 kb Pst I DNA hybridized only to this probe. These fragments are shown in bold digits in table1. Therefore, these fragments have more homology with the introns than the exons.

Hybridization of 194bp 5' probe with the Bam HI digested mouse genomic DNA detected four fragments of 2.32, 3.55, 4.63 and 9.26 kb, with Eco RI five fragments of 4.14, 2.71, 2.15,1.41 and 9.24 kb were observed, with Hind III digest five fragments of 14.13, 8.98, 3.98, 3.01, 2.24 kb while with Pst I digested mouse genomic DNA four fragments of 5.25, 3.99, 2.33 and 0.5 kb were detected. As some fragments hybridized only with the 194 5' 1st exon probe they should contain the 5' flanking promoter DNA regions of the mouse IRF-1 gene. Out of all the fragments 4.63 kb Bam HI DNA, 3.01 kb Hind III

DNA, 3.79, 2.33, 0.5 kb Pst I DNA hybridized only with the 194 5' probe and these fragments are shown in bold digits in table1.

Miyamoto et al. (1988) screened a mouse genomic library and reported a 500 bp Pst I fragment as a promoter DNA fragment from the IRF-1 gene. This 500 bp IRF-1 promoter DNA contained part of the first exon and –299 bp promoter which was transcriptionally activated by virus infection in a transfection assay. A similar size DNA fragment of 501 bp was observed in the Pst I digest of the mouse genomic DNA in this study by using 194 5' and 1 kb cDNA probe. Therefore, this 501 bp Pst I DNA of the mouse liver IRF-1 gene should contain the proximal promoter. Reis et al. (1994) have reported a 5.3 kb Bam HI DNA fragment with the C2 genomic probe . A similar fragment of 5.41 kb was observed with Bam HI digest of the mouse liver genomic DNA by using the genomic DNA probe that contained 3^{rd} to 10^{th} exons and 2^{nd} to 10^{th} introns. This 5.4 kb fragment should, therefore, contain exons 3-10 and introns 2-10 region of the gene.

(B) Human IRF-1 gene

Human IRF-1 gene is located at 5q31.1 chromosomal region (Harada et al.,1994). Organization of the human IRF-1 gene was studied in the genomic DNA isolated from the peripheral lymphocytes. The 1kb cDNA probe hybridized to two Bam HI fragments of 3.6 and 1.08 kb, three Eco RI DNA fragments of 20.73, 13.59 and 3.98 kb, four Hind III fragments of 15.85, 6.81, 3.41, and 3.34 kb as well as four Pst I fragments of 4.14, 1.41, 0.86 and 0.54 kb. Out of the above mentioned fragments, 20.73 kb Eco RI, 3.34 kb Hind III, 1.41 and 0.86 kb Pst I DNA hybridized only to the 1 kb cDNA probe indicating that they contain exonic sequences. These fragments have been shown as bold digits in table2.

Hybridization of the 5.3 kb C2 genomic probe with the Bam HI digested human genomic DNA detected .wo fragments of 3.63 and 1.99 kb, with Eco RI digest one fragment of 2.66 kb was observed, with Hind III digested genomic DNA one fragment of 2.71 kb was detected, while with Pst I digest one fragment of 3.47 kb and with Sac I digest a fragment of 3.29 kb was detected. Of the fragments hybridizing with the 5.3 kb genomic probe, the 1.99 kb Bam HI, 2.66 kb Eco RI, 2.71 kb Hind III and 3.47 kb Pst I DNA hybridized only to the C2 IRF-1 genomic probe indicating that they should contain intronic fragments from the human IRF-1 gene. These fragments have been shown in bold digits in table2.

Hybridization of the 194 bp 5' probe with the Bam HI digested human genomic DNA detected two fragments of 3.2 and 1.08 kb, with Eco RI two fragments of 13.53 and 3.98 kb, with Hind III three fragments of 15.85, 6.81 and 3.41 kb, while with Pst I digested human genomic DNA two fragments of 4.14 and 0.54 kb were detected. Some fragments hybridized with both the 5' 194 probe and the 1kb cDNA probe (as it also contained the 5' probe). They may contain human IRF-1 promoter DNA region(s). These fragments are the 1.08 kb Bam HI DNA, 13.53, 3.98 kb Eco RI, 6.81 and 3.41 kb Hind III DNA. The 0.54 kb Pst I fragment hybridized strongly with the 194 5' probe and with 1 kb cDNA probe. These fragments should contain human IRF-1 gene promoter.

On comparing the Southern hybridization pattern of mouse and human genomic DNA for the same restriction enzyme and IRF-1 DNA probe, certain genomic fragments showed almost similar size in both species. The 1 kb cDNA probe upon hybridization with the Eco RI digest of mouse genomic DNA detected a 19.55 kb DNA fragment which was similar in size to 20.73 kb Eco RI DNA from human genomic DNA. The 14.13 kb Hind III DNA of mouse IRF-1 was similar to the 15.85 kb Hind III DNA from human genome. Pst I digested mouse genomic DNA upon hybridization with the 194 5' and 1 kb cDNA probe revealed a fragment of 0.5 kb. A similar fragment of 0. 54 kb

was observed when human genomic DNA was digested with Pst I and hybridized to the same probe. This 500 bp fragment of mouse genomic DNA has been reported to contain the IRF-1 proximal promoter region upto –299 bp (Miyamoto et al., 1988). It is most likely that the 541 bp fragment from the human genomic DNA may also contain the promoter region of IRF-1 gene indicating that this region is most likely conserved in mouse and man. After comparison of DNA fragments from mouse and human, there are some fragments, which are different in the two species. In mouse, the largest fragment obtained was 25.118 kb in Hind III digest and in human, the largest fragment obtained was 20.730 kb in Eco RI digest. These fragments may contain 5' and 3' terminal regions, hence the complete IRF-1 gene. They may contain mouse and human IRF-1 gene promoters also. Table 1 and table 2 have summarized the Southern blot hybridization patterns for the mouse and human IRF-1 gene as detected by the three probes : the 1 kb cDNA, the C2 genomic and the 194 5' probe. Fig. 11 and 12 diagrammatically represent IRF-1 gene fragments from the mouse and human genomes. DNA fragments specifically detected by a probe are highlighted. Comparison of table 1 and 2 indicates similarities and differences between the mouse and human IRF-1 gene structure and organization. During southern hybridization, some weak bands were also observed. These weak bands may contain DNA fragments from IRF gene family that contain gene fragments other than IRF-1 and possess homology to IRF-1 gene. These DNA fragments may be interesting genomic regions for cloning novel genes belonging to the growing IRF-family.

7.2 Amino acid changes in IRF-1

Mouse IRF-1 cDNA is 2072 bp and IRF-2 cDNA is 2436 bp. Protein-wise mouse IRF-1 protein has 329 amino acids (37.6 kd) and IRF-2 protein has 349 amino acids (49.5 kd). Both the IRFs have five Tryptophan repeats in their N-terminal regions, out of the five three have been shown to be used in

binding to GAAA of IRF-E (Escalante et al., 1998). Towards the C-terminal region both IRF-1 and IRF-2 have IRF-association domain (IAD) and IRF-1 has transcription activation domain but IRF-2 has transcription repression domain (Fig. 2 and 3). In IRF-1, from 1 to 140 amino acid is the DNA binding domain (DBD) and from 141 to 329 amino acid is the Transcription activation domain (TAD). The DNA binding domain is rich in lysine and arginine residues, but the transactivation domain is rich in aspartic acid, glutamic acid, serine and threonine residues (Miyamoto et al., 1988).

For comparison of IRF-1 from mouse, rat and human, cDNA sequences of mouse (M21065), rat (M 34243) and human (X 14454) were retrieved from the Gene Bank and converted into amino acid sequence using PC gene software. The amino acid sequences of IRF-1 from the three species were compared using mouse IRF-1 as the reference. Changes in amino acid sequence of IRF-1 among mouse, rat and human were found out and represented as a bar diagram in fig. 13. It is clear that in mouse and rat the number of changes are rather small i.e. 13/329 in mouse and 12/328 in rat when they were compared between themselves. In human, 43/325 amino acid changes were observed which represented ~ 63% of the total changes (68) among the three species. There were six changes in the DNA binding domain but 37 changes in the transactivation domain (Table 4) indicating that the DNA binding domain of IRF-1 has been conserved but the transcription activation domain has accumulated alterations during evolution of this gene from rodents to humans.

It was observed that in human IRF-1, majority of these changes were in the transactivation domain. From the evolutionary point of view the two rodent species are closer to each other than human. Therefore, these changes represent an evolutionary trend. DBD of the transcription factor is used for binding with IRF-E element , but transactivation domain has to interact with other protein factors to bring about transcription. So, the transactivation domain of human IRF-1 may interact with different proteins in comparison to

that of mouse or rat. This indicates functional diversification or flexibility which is a key factor for the adaptive value of any protein. Less number of amino acid changes in the DNA binding domain of IRF-1 from the rodents to humans indicates the fact that this transcription factor interacts with similar DNA elements in promoters of genes across the species, so the DNA binding domain is conserved so as the DNA sequence it interacts with. This also indicates that similar genes in humans may be activated by IRF-1 but its regulation of transcription through the transcription activation domain may be more complex than that of the mouse.

Amino acid changes in the transactivation domain of human IRF-1 gene can be divided into six regions (I-VI, as shown in Table 5) containing clusters of six amino acids for each. In ^{175}EVEQAL ^{180} variations at five positions out of six was observed. In ^{198}IPVEVV ^{203} all the six amino acids in this cluster were changed. In ^{264}VQPTSV ^{269} three out of six amino acids changed. In ^{289}GLSLQR ^{294} variations at 4 positions were observed. In ^{304}AT*WLDS ^{309} 3 changes were detected. In ^{313}TP*VRLP^{318} variations at two positions were observed (Table 5). It is possible that through these regions the human IRF-1 may interact with other proteins and thereby bring about functional specialization for the human IRF-1.

When these amino acid regions were searched in the database interesting features were noted. EVEQAL picked homology with rat MAP kinase ERK 2, human MAP kinase, ERK 2 from bull, cyclosporine synthetase and capsid protein of a virus. IPVEVV picked homology with eIF3 β subunit of fission yeast, GMP synthase (glutamine amidotransferase), a putative receptor-like protein kinase from Arabidopsis, a hypothetical zinc metalloproteinase. GLSLQR picked homology with NADH dehydrogenase subunit 4L, rat gastric inhibitory receptor, DNA gyrase B, ribonucleotide reductase. ATWLDS picked homology with HIV-1 envelope glycoprotein, replication protein from human papilloma virus, xylanase, erythroid protein isoform, human zinc finger protein and a hypothetical protein from Leishmania. VQPTSV picked

homology with ubiquitin protein ligase 1, F-box and leucine-rich repeat protein, receptor adenylate cyclase, calcium ATPase, putative acyl-coA synthase. TPVRLP picked homology with zinc finger protein, alkaline exonuclease, GTP binding protein, origin recognition complex protein 1, glycosyl hydrolase. From these homologies it may be speculated that functions like protein-protein interactions may be specified by such amino acid sequence motifs of IRF-1 which also occur in a variety of other proteins. A detailed analysis of function(s) of these amino acid sequence motifs in the transcription activation domain of human IRF-1 will provide more information regarding the functional specialization of the human IRF-1 over mouse IRF-1.

Changes in the restriction sites were also observed in the coding as well as untranslated regions of the IRF-1 cDNA of mouse and human. The changes in the coding regions were close enough to the changes in the amino acid sequence. A site for Nae I was present in the human IRF-1 at position 48 bp of the cDNA but was absent in the mouse. This coincided with the 5' UTR. A Sma I site was present at 262 bp in the human IRF-1 cDNA but was absent in the mouse. This coincided with the amino acid at 25th position from the N-terminus of IRF-1. A Cla I site was present at 960 bp in the mouse IRF-1 cDNA but absent in the human. This coincided with the amino acid at 252 position. A Xho I site was present at 1056 bp in the mouse IRF-1 cDNA but absent in the human. This coincided with the amino acid at 285 position. A Bst XI site was present in two positions, at 1112 bp and 1479 bp in the human IRF-1 cDNA but absent in the mouse. The 1112 Bst XI site coincided with amino acid at 308 position but the 1479 Bst XI site coincided with the 3' UTR. A Sfi I site is present at 1344 bp in the human IRF-1 cDNA but absent in the mouse. This coincided with the 3' UTR. These are some differences in the restriction enzyme sites in IRF-1 cDNA that accounts for some of the changes in the nucleotide sequences in the 5' or 3' UTR regions and in the coding sequences resulting in some amino acid changes. Out of the above restriction site changes coinciding with the amino acid changes in the human IRF-1

compared to the mouse IRF-1, two changes are significant, for example, at 285 an arg is changed to a gly (alteration of 1056 Xho I site of mouse) and at 308 a met is changed to a leu (creation of 1112 Bst XI site in human). Whereas at two other positions either there was no change or the change was insignificant. At 25 (creation of 262 Sma I in human) Ileu was not changed and at 252 (alteration of 960 Cla I of mouse) a val was changed for an Ileu. The 285 arg to gly and the 308 met to leu (in region V) amino acid changes again are located in the transactivation domain of human IRF-1. In addition to this, there are more changes in the transactivation domain of human IRF-1 as shown in table 3, for example at 166, 167 threonine, glutamine are changed to a valine, proline, respectively. In the DNA binding domain from mouse to human IRF-1, at amino acid 5 an arginine is changed to trptophan, at 35 a glutamine is changed to glutamic acid, at 131 and 135 two threonines are changed to two alanines, at 139 a leucine is changed to a serine. Lin and Hiscott, (1999) have reported that the amino acid 138-150 cluster of IRF-1's DNA binding domain and the amino acid 219-230 cluster in the transactivation domain are sites for phosphorylation by Casein Kinase II to post-translationally regulate IRF-1 protein. The phosphorylated IRF-1 is proposed to be the active form after induction by virus and other inducers. However, specific effect of phosphorylated IRF-1 in the process of transcription is not clearly understood. It would be interesting to find out the effect of *in vitro* phosphorylated recombinant IRF-1 on transcription.

7.3 Expression of IRF-1 mRNA

7.3.1 Northern blot analysis of IRF-1 mRNA

Northern blot analysis was carried out to check the size and steady state level of IRF-1 mRNA in thymus, intestine, spleen and lungs. IRF-1 mRNA was detected as a ~2 kb band in the 33 day old mice. This agreed to the earlier report by Miyamoto et al. (1988) that the size of IRF-1 mRNA was around 2

kb. As judged from the pixel values of the IRF-1 mRNA band the expression of IRF-1 mRNA was found to be maximum in the intestine followed by lungs, spleen and thymus of the mouse. The steady state level of IRF-1 mRNA was 2.2 to 2.4 x and 5.5 x fold more in spleen, lungs and intestine than in thymus respectively. The 1 kb IRF-1 cDNA band served as the positive control. The dot blot of 5, 10 and 20 pg of IRF-1 cDNA served as positive control and showed signals with increasing pixel values indicating the linear range of hybridization. Taniguchi and coworkers (Miyamoto, et al. 1988) had reported IRF-1 mRNA expression in different mouse tissues by northern blot analysis. In 5 μg whole cell RNA from the mouse brain, heart, liver, lungs, spleen, thymus, kidney, muscle, intestine and Con A stimulated spleen cells an approximately 2.0 kb mRNA was observed in the heart, lungs, thymus, kidney and intestine. Con A greatly induced IRF-1 mRNA level in the spleen cells. Con A activated human Jurkat T cell line was also reported to show IRF-1 mRNA induction. This tissue specific expression pattern of IRF-1 mRNA suggests that IRF-1 may regulate different sets of genes in different tissues or organs of the mouse under normal conditions.

7.3.2 RNA dot blot hybridization

RNA dot blot was carried out to quantitate expression of IRF-1 mRNA in various tissues of the 63 day old mice. Total RNA was isolated from the brain, thymus, lungs, heart, liver, spleen, kidney and intestine of the adult mice, quantitated, denatured and dot blotted (5, 10, 20 μg) onto the nylon membrane. The blot was hybridized to ^{32}P labeled 1 kb cDNA probe (table 8, fig. 16). The dot blot containing 5, 10, 20, 40 pg of the 1 kb IRF-1 cDNA served as the positive control. Expression of IRF-1 mRNA was quantitated with the help of V 2.54 Image gauge software in a phosphoimager. Pixel intensities for each tissue were plotted (table 8, fig. 17). It was observed that maximum amount of IRF-1 mRNA was present in the intestine, followed by lungs, thymus, spleen,

liver and kidney. IRF-1 mRNA level was very low in the heart and brain. The intensity of IRF-1 mRNA ir the intestine was 1.3 times more than 40 pg of IRF-1 cDNA in the positive control, 2.7 times more than that of lungs and 3.2 times more than that of thymus, when 20 μg of total RNA was used for the assay.

The role of IRF-1 is important in the intestine. IRF-1 controls the expression of polymeric IgR (pIgR), the receptor for IgA, which mediates transcytosis of IgA molecules across the epithelial barrier of mucous membrane of intestine (Blanch et al. 1999). Therefore, IRF-1 participates in mucosal immunity by indirectly regulating the transport of IgA. Blanch et al., (1999) used a HT-29 human colon carcinoma cell line to perform this study which agrees to our observation that the steady state IRF-1 mRNA level is maximum in intestine of the mouse.

7.4 DNA binding activity of IRF-1

IRF-1 was originally shown to possess binding activity with the DNA sequence from the virus response element (VRE) of interferon-β (IFN-β) gene promoter and ability to mediate transcriptional stimulation of IFN-β gene by Taniguchi and coworkers (Miyamoto et al., 1988). Fujita, et al. (1987) reported that the sequence: AAGTGA is the most efficient sequence for virus-induced activation of IFN-β gene transcription and it manifested properties of an inducible enhancer. Following that, Kuhl et al. (1987) reported that the tetrameric hexamer (GAAAGT or AAGTGA) conferred inducibility by virus, on a reporter gene, when it was placed upstream of a complete or truncated promoter indicating that such sequence motifs can act as enhancer elements. Miyamoto et al. (1988) found that in mouse fibroblast (L 929) cells, IRF-1 specifically bound to the IFN-β regulatory sequence as well as to the functional repeat hexanucleotide $(AAAGTG)_4$ sequence.

Variants of the consensus hexanucleotide of the nature of GAAANN (N = any nucleotide) frequently occurs in the promoter/enhancer(s) of virus-inducible and IFN-inducible genes in mammalian cells. They have been proposed to mediate virus-inducibility of human IFN-β and IFN-α1 gene(s) through different pathways (MacDonald, et al., 1990). Multimerization of GAAANN generates sequences frequent in virus-inducible promoters. Weissmann and coworkers (MacDonald et al, 1990) proposed that there existed three types of GAAANN sequence motifs. Type I (NN = GT, GC, CT or CC) responds to IFNs and to IRF-1 and causes silencing of an enhancer. Type II (NN = TG) and type III (NN = CG) neither silence nor respond to IRF-1 or IFN. Type III mediates constitutive transcription and binds the constitutive IEFga factor, whereas type II was proposed to bind a novel "TG protein".

The human IFN-β and IFN-α1 gene promoters contain different response elements. IFN-β promoter has a type I-like sequence (PRD I) and an Nuclear Transcription Factor kappa B (NF-κB) binding sequence (PRD II) while IFN-α1 promoter has a type II-like "TG sequence" and possibly additional elements but does not bind NF-κB. Type I, type II and NF-kB elements represent three distinct terminal pathways mediating virus induction. In the IFN-β gene promoter, following virus induction IRF-1 binds to PRDI and NF-kB binds to PRDII. Both IRF-1 and NF-kB are inducible by virus infection of cells. IRF-1 and NF-κB positively interact with each other (in association with other factors) to stimulate IFN-β gene transcription. IRF-1 is IFN-inducible but NF-κB has not been clearly shown to be regulated by IFN.

Table 9 shows an example of a variety of hexameric sequences occurring in the promoters of many important genes involved in a multitude of functions in mammalian cells. Mostly, they are cytokines (IFNs, IL-4, IL-5, IL-6, IL-7) or cytokine-inducible genes (MX, H-2D, H-2K, ISG 54, ISG 15, 2'5' oligo A synthase, IP-10, complement factor B, GBP, β2-microglobulin, VCAM-1,

iNOS). Many of these sequences are type I-like and some have GAAAGT. This indicates that IRF-1 is involved in regulating the expression of many such genes.

Most investigators have used mouse and human cell lines for studies involving both induction as well as activation of IRF-1 for its DNA binding activity and also transcription of target genes by IRF-1 hence, information on the DNA binding activity of IRF-1 and IRF-2 in normal mouse tissues is limiting. In this study, we have used a tetrameric repeat (24 bp) of the hexamer $(GAAAGT)_4$ (5'GAAAGTGAAAGTGAAAGTGAAAGT3'), a type I GAAANN element, as the specific oligonucleotide and a similar 24 bp hexameric repeat of the tetramer : $(GAAA)_6$ or (5'GAAAGAAAGAAAGAAAGAAAGAAA3') as the nonspecific oligonucleotide to study expression of the DNA binding activity of IRF-1 and IRF-2 in different tissues of the mouse. 5' ^{32}P labeling of the $(GAAAGT)_4$ or $(GAAA)_6$ oligos and annealing of them to their reverse complementary oligos are shown in fig. 18. Results in fig. 19 showed that IRF-1 (or IRF-1-like)-DNA complexes existed in the mouse spleen extract and they were specific for $(GAAAGT)_4$ and not for $(GAAA)_6$ proving that the GT in the GAAAGT hexameric sequence are essential for this binding specificity. The L 929 extract showed IRF-2-DNA complex and much less of IRF-1-DNA complex as has been reported by Taniguchi and coworkers (see Miyamoto, et al. 1988, and Harada, et al. 1990). IRF-2 was shown to be present in L 929 cells under normal conditions and IRF-1 was shown to be induced after New Castle Disease virus (NDV) induction. In fig.19, the $(GAAA)_6$ oligo also formed some complex in the L 929 extract which was considered possibly due to some simple repeat binding protein. This aspect (though could be interesting) was not studied further as the L 929 extract was used just as a reference extract here. The binding reactions were performed in presence of calf thymus DNA as the carrier DNA and showed good complex formation.

7.4.1 DNA binding activity of IRF-1 and IRF-2 in mouse tissues

Expression of IRF-1 was studied in whole cell extracts of various tissues (spleen, brain, thymus, lungs, heart, liver, kidney and intestine) of the adult mouse by EMSA. Fig. 20 shows that spleen showed monomers and dimers of both IRF-1 as well as IRF-2. IRF-1 dimer is the major form. Liver also showed IRF-1 dimer as the major form. Thymus and lungs showed IRF-1 dimer, IRF-2 dimer and a larger complex (a1). Intestine showed IRF-2 monomer and a smaller complex (d1) as well as a larger complex (a1) along with lesser amounts of IRF-1 and IRF-2 dimers. In the kidney, heart and brain IRF-1/IRF-2 complex was not detected. The monomers and dimers of IRF-1 and IRF-2 were identified on the basis of (i) relative pattern of the four complexes to match the molecular mass of murine IRF-1 (37.6 kd) and IRF-2 (49.5 kd), (ii) comparison with the recombinant GST-IRF-1 protein (66 kd)-DNA complex and (iii) comparison of the murine IRF-1/IRF-2 pattern with that of human cells (U 937 cell nuclear extract as well as its induction by IFN-γ, see fig. 27). Table 10 and fig. 21 show pixel values for IRF-1 and IRF-2 complexes in various tissues of the mouse. Spleen and liver showed maximum amount of IRF-1 dimer indicating IRF-1-dependent gene expression in these tissues under normal conditions.

The DNA binding activity of IRF-1 and IRF-2 was further analysed in the mouse spleen. Fig. 22 shows IRF-1 and IRF-2 in 20 μg whole cell extract (WE), 20 μg cytoplasmic extract (CE) and 5, 10 and 20 μg of nuclear extract. GST-IRF-1 showed IRF-1 specific DNA complex(es). Table 11 and fig. 22, 23 show the pixel values of various IRF-1 and IRF-2 complexes. In the whole cell extract of spleen, there were 4 complexes of IRF-1 and IRF-2 monomers and dimers respectively. IRF-1 was more than IRF-2. Four complexes were also present in 10 and 20 μg of the nuclear extract. As the amount of nuclear extract was increased, the (a1) complex (IRF-1 tetramer ?) increased more in intensity in comparison to the IRF-1 and IRF-2 monomers and dimers. For 2 x

and 4 x fold increase in the nuclear protein concentration in the binding reactions there was 4.88 x and 20 x fold increase in IRF-1 (a1) complex formation indicating that formation of this higher IRF-1 complex was cooperative. Higher mass of IRF-1 (IRF-1 tetramer) (a1) complex was the most important aspect of the spleen nuclear extract. It appears that with increase in concentration of IRF-1, this complex is formed. Recombinant GST-IRF-1 also showed the property of forming multiple IRF-1-DNA complex indicating that additional protein was not needed for this. This may be due to cooperative binding of IRF-1 to the $(GAAAGT)_4$ DNA. 20 μg of the cytoplasmic or whole cell extract did not form this higher IRF-1 complex. The (c1) complex was specifically formed in the whole cell extract and cytoplasmic extract but not in the nuclear extract. One interesting feature of IRF-1 is that an IRF association domain (IAD) is present in the C-terminal region of IRF-1. IAD is conserved in many IRF family members and it is essential for interaction with other IRF proteins. For example, Meraro et al. (1999) showed that the IAD is an independent module used by the Interferon Consensus Sequence Binding Protein (ICSBP) and IRF-4 for protein-protein interactions and an IAD of IRF-2 (IAD2) is necessary for interaction with ICSBP and this was also found to be conserved in IRF-1. So it may be possible that the additional complexes observed may be IRF-1 or IRF-2 associated with some other protein(s) of IRF family. It would be interesting to find out if the nuclear-specific (a1) IRF complex is transcriptionally competent and may be preferable.

Mammalian spleen is the largest of the secondary lymphoid organs. It is highly active in trapping and concentrating foreign substances carried in the blood. It is the major organ in the body in which antibodies are synthesized and from which they are released into the circulation. The transcription factor IRF-1 has been also implicated in the regulation of MHC gene expression by IFNs as well as in the regulation of production of many cytokines. Furthermore, Hobart et al. (1996) investigated the role of IRF-1 *in vivo* in the

systemic regulation of MHC expression in hosts undergoing rejection of allogeneic tumors by comparing MHC induction in mice with normal IRF-1 genes (wild type or WT mice) with mice with disrupted IRF-1 gene (IRF-1 knockout or IRF-1 KO mice). Impaired MHC class I and II induction was seen in the spleen of IRF-1 KO mice. It has been reported by Ogasawara et. al. (1998) that IRF-1 is required for the development of the natural killer cells in the spleen while Senaldi et al. (1999) have reported that IRF-1 KO mouse (IRF-1 $^{-/-}$) have smaller spleens than the control WT mice which contained similar percentage but lower absolute count of macrophages and lower percentage and absolute count of NK cells. To investigate the role of type I interferon (IFN) and its regulatory trans-acting proteins, interferon regulatory factors (IRF-1 and IRF-2), in early protection against infection with virulent Venezuelan equine encephalitis virus (VEE), Grieder and Vogel (1999) utilized mice with targeted mutations in the IFN-α/β receptor, IRF-1, or IRF-2 genes. In IRF-1 and IRF-2 knockout mice (IRF-1$^{-/-}$ and IRF-2$^{-/-}$, the 100% protection against virulent VEE, that is conferred by attenuated VEE within 24 h in control C57BL/6 mice, was completely absent in IRF-2$^{-/-}$ mice, whereas 50% of IRF-1$^{-/-}$ mice were protected. IRF-2$^{-/-}$ mice were deficient in clearing VEE virus from the spleen and the brain compared to the heterozygous IRF-2$^{+/-}$ knockout or C57BL/6 (+/+) mice. These findings implied that the altered immune response in IRF-1 and IRF-2 knock out mice results in altered virus dissemination, altered virus clearance, and altered virus-induced pathology. IRF-1$^{-/-}$ mice also showed differential antiviral immune response towards encephalomyocarditis virus (EMCV) and vesiculostomatitis virus (VSV), IFN maintains an antiviral response against EMCV through IRF-1, but in VSV it is independent of IRF-1.(Kimura et al., 1994). IRF-1$^{-/-}$ mouse macrophages were also shown to be incapable of inducing inducible Nitric Oxide Synthase (iNOS) mRNA when induced by IFN-γ (Reis et al., 1994). Results of the present study showed that IRF-1 is highly active in the mouse spleen. It would

be interesting to find out IRF-1/IRF-2 activities in different cell types of the spleen.

Fig. 20 showed that no IRF-1 or IRF-2 complex was observed by EMSA in the mouse brain. IRF-1 is involved in the molecular mechanisms of inflammation and apoptosis, processes that contribute to ischemic brain injury. IRF-1 gene expression increases in barin after brain injury. Recently, Iadecole et al. (1999) reported the induction of IRF-1 in response to cerebral ishemia and found that IRF-1 gene expression was markedly upregulated within 12 hrs of occlusion of the middle cerebral artery. They concluded that IRF-1 is the first nuclear trans-acting factor demonstrated to contribute directly to cerebral ischemic damage. Paschen et al. (1998) evaluated the role of IRF-1 in brain under severe form of metabolic stress. They found that transient cerebral ischemia induces activation of the interferon system. The results of RNA hybridization and EMSA show that there was no expression of IRF-1 or IRF-2 in the mouse brain.

Fig. 24 shows a comparative EMSA of IRF-1/IRF-2 in the whole cell (WE), cytoplasmic (CE) and nuclear (NE) extracts of mouse spleen carried out in presence of poly (dI.dC) or calf thymus DNA as carrier DNA. The pattern was reproduced as observed in fig. 22. IRF-1 and IRF-2 complexes were formed more in presence of calf thymus DNA than in poly (dI.dC.). The higher IRF-1 (a1) complex was again formed only in 10 μg nuclear extract (5 μg showed a very weak complex comparable to that of 20 μg of whole cell extract) in presence of poly (dI.dC.) but in 5 and 10 μg nuclear extract in presence of calf thymus DNA.

In nuclear extract of thymus of the adult mice, 3 main complexes were observed (Fig. 25). Two were the dimers of IRF-1 and IRF-2 respectively, one was of higher size, equivalent to the higher IRF-1 (a1) complex of the spleen nuclear extract. On comparison between 20 μg cytoplasmic extract and 5, 10 and 20 μg of nuclear extract, six complexes were observed in 20μg of nuclear extract, monomers of IRF-1 and IRF-2, dimers of IRF-1 and IRF-2. Additional

complexes (a1) and (c1) both higher than the size of the IRF-2 dimer. These complexes (a1 and c1) cc .ld be formed due to binding of IRF-1 to other IRFs/proteins probably through its IAD binding domain. Table 12 and fig. 26 shows the quantitation of pixel intensity of IRF-1 and IRF-2 in thymus. Except for complex (d), all others increased with increasing concentration of the extract, Overall the thymus pattern differed from that of the spleen.

Thymus is a vital part of the immune system. Thymus is absolutely required for the differentiation of immature precursor T cells into the T cells with the characteristics of functional T cells. Penninger et al. (1997) reported that mice lacking the interferon regulatory factor-1 (IRF-1) had reduced numbers of mature $CD8^+$ cells within the thymus and peripheral lymphatic organs. They showed that positive and negative T cell selection of two MHC class I-restricted TCR alpha beta transgenes, H-Y and P14, are impaired in IRF-1 ($^{-/-}$) mice. Absence of IRF-1 resulted in a decreased expression of LMP2, TAP1 and MHC class I on thymic stromal cells, the cells which nurse and educate T cells in the thymus. Moreover, IRF-$1^{-/-}$ thymocytes displayed impaired TCR mediated signal transduction. Their results suggested that IRF-1 regulates gene expression in developing thymocytes required for lineage commitment and selection of $CD8^+$ thymocytes. On the contrary, Simon et al. (1997) reported that though IRF-1 and IRF-2 DNA binding activities resulting from antigen stimulation are developmentally regulated, there was no evidence for a selective role of IRF-1 in the development of $CD8^+$ lineage. However the decrease in CD8+ T cells in the IRF-1 (-/-) mice clearly demonstrated that there exists an important role for IRF-1 in the maturation and survival of cytotoxic T cells in thymus.

It has been observed that IRF-1 is required for mucosal immunity against inhaled antigens as IRF-1 activates the gene for the polymeric immunoglobulin receptor (pIgR). pIgR helps in the transport of dimeric IgA across epithelial barriers of mucosal membranes (Blanch et al., 1999). IRF-1 may also play a role in the Lungs.

EMSA of heart extract also revealed no IRF-1 and IRF-2 complexes. Heart has a very low or undetectable level of IRF-1. Production of NO by inducible NO synthase (iNOS) has been implicated in the pathology of spontaneous and antigen-induced autoimmune diseases and iNOS is activated in the myocardium of patients with heart failure (Bachmaier et al. (1997). The authors also provided the *in vivo* evidence that iNOS expression and NO synthesis in macrophages and distinct cardiomyocytes are elicited in experimental murine inflammatory disease and showed that IRF-1 controls iNOS expression and NO synthesis during the disease.

In liver three complexes were seen (Fig. 20). one intense major band of IRF-1 dimer and two weak complexes : one is dimer of IRF-2 and the other may be IRF-1 interacting with other IRF family member(s) through the IAD. IRF-1 dimer may be involved in IRF-1-dependent gene expression in the liver. Gellere al. (1993) identified IRF-1 expression during sepsis in hepatocytes. Cytokines induce IRF-1 in hepatocytes: IFNγ can induce its expression by 17 fold, TNFα can induce it upto 3 fold while IL-1β can induce IRF-1 mRNA level by 2 fold. Prost et al. (1998) observed that IRF-1-deficient hepatocytes showed reduced DNA repair activity when compared with the wild-type. IRF-1 deficiency produced dysregulation of p53. Selandi et al. (1999) observed that IRF-1($^{-/-}$) mice showed lower TNF and IFNγ mRNA levels in liver as compared to that of the wild type mice. Lack of IRF-1 appeared to result in impaired production of TNF and IFNγ, reflecting a down regulation of gene expression in the liver. Growth hormone (GH) has been found to stimulate IRF-1 gene expression in the liver (Le Stunff et al. 1998). They showed that GH also causes a pronounced induction of the hepatic nuclear protein binding to IRF-1 promoter element.

In kidney the expression of IRF-1 was low or almost undetectable. Kidney is a nonlymphoidal organ. Sims et al. (1997) studied injured kidneys (by ischemia or by gentamycin toxicity) for gene expression of IFNγ and IRF-1. Hobart et al. (1997) observed that in the kidney of IRF-1 knock out mice,

basal class I MHC expression was decreased particularly on arterial endothelial cells but basal class II MHC expression was uncahanged.

Intestine have five complexes (Fig. 20), two are IRF-2 and IRF-1 dimers, one is IRF-2 monomer, one complex = (a1), higher than IRF-2 dimer. In intestine IRF-1 is expressed. Blanch et al., 1999 have reported that IRF-1 is needed for controlling the expression of polymeric immunoglobulin receptor for transcytosis of IgA across epithelial barrier of mucous membranes. So IRF-1 is involved in mucosal immunity by regulating the IgA transport.

From the above results it is clear that spleen, liver and intestine have reasonable amounts of IRF-1 and IRF-2, thymus and lungs have moderate levels of IRF-1 and IRF-2. Brain, heart and kidney have non-detectable amount of IRF-1 and IRF-2 in the mouse under normal conditions.

7.4.2 DNA binding activity of human IRF-1 and IRF-2 in U 937 cells

U 937 cells are human macrophage/monocyte cell line. DNA binding activity of IRF-1 and IRF-2 in U 937 cells showed four complex IRF-2 dimer, IRF-1 dimer, IRF-2 monomer, IRF-1 monomer and two additional weak complex(es) as shown in Fig. 27. These four IRF-1 and IRF-2 band pattern matched with that of the mouse spleen. The U 937 cells were treated with 1 nM recombinant human interferon-γ (IFN–γ) for 0, 30 and 60 min. The amount of IRF-1 and IRF-2-DNA complexes increased after interferon-γ. This confirmed that these complex(es) were monomers and dimmers of IRF-1 and IRF-2. IFN-γ induces IRF-1 at transcriptional level through activation of the JAK-STAT pathway recruiting STAT-1 to IRF-1 promoter. IRF-1 induces IRF-2. Thus for IFN it is a positive feed back loop but for IRF-1 it finally regulates negatively. The IRF-1 and IRF-2 pattern and its induction by IFN-γ was to confirm the mouse spleen pattern.

CONCLUSIONS

8. CONCLUSIONS

8.1 MOUSE IRF-1 GENE

Organization of murine and human IRF-1 genes were studied by Southern blot analyses using three IRF-1 DNA probes: cDNA (exons 1-10), genomic DNA (exons 3-10 and introns 2-10) and 5' proximal exon. In the mouse genomic DNA, the 5.41 kb Bam HI, 19.95 kb and 9.26 kb Eco RI, 25.12 kb Hind III and 1.71 and 1.26 kb Pst I DNA hybridized only to the 1 kb cDNA probe indicating more sequence homology with IRF-1 exons but less homology with the introns. The 5.3 kb IRF-1 genomic DNA probe specifically detected the 5.41 kb Bam HI DNA, 5.84 kb Eco RI DNA, 4.64 kb Hind III DNA and 10.8, 6.31 and 2.15 kb Pst I DNA indicating more homology with the introns than the exons. The 4.63 kb Bam HI DNA, 3.01 kb Hind III DNA, 3.79, 2.33, 0.5 kb Pst I DNA hybridized only with the 5' probe implying that they should contain the 5' upstream promoter DNA regions of the mouse IRF-1 gene.

8.2 HUMAN IRF-1 GENE

Similarly, in the human genomic DNA , 20.73 kb Eco RI, 3.34 kb Hind III, 1.41 and 0.86 kb Pst I DNA hybridized only to the 1 kb cDNA probe indicating that they contain exonic sequences. The 1.99 kb Bam HI, 2.66 kb Eco RI, 2.71 kb Hind III and 3.47 kb Pst I DNA hybridized only to the C2 IRF-1 genomic probe indicating that they should contain intronic fragments from the human IRF-1 gene. The 0.54 kb human Pst I fragment hybridized strongly with the 194 5' probe and with 1 kb cDNA probe. These fragments should contain human IRF-1 gene promoter. A similar 0.5 kb Pst I fragment was obtained from the mouse genomic DNA. The 0.5 kb Pst I DNA should contain the proximal promoter and 5.4 kb Bam HI DNA should contain exons 3-10 and introns 2-10 regions of the human IRF-1 gene. On comparing mouse

and human Southern blot patterns there were also certain differences between the mouse and the human IRF -1 genes. For example, the 1.08 and 3.41 kb Bam HI DNA were detected by the 5' probe from the human IRF-1 gene but the same probe detected 2.32, 3.55 and 9.26 kb Bam HI DNA from the murine IRF-1 gene. This indicated that the structure of 5' flanking DNA containing the promoter is different between mouse and human IRF-1 gene.

8.3 AMINO ACID CHANGES IN IRF-1

Amino acid sequences of mouse, rat and human IRF-1 genes were compared among themselves and a total of 68 changes were found. Human IRF-1 showed 63.23 % changes, rat IRF-1 showed 17.64 % changes and mouse IRF-1 showed 19.11 % changes. Out of 68 changes, 9 were in the DNA binding domain (DBD) and 59 in the transactivation domain (TAD). In mouse, out of 13 changes only 1 occurred in DBD and 12 in TAD. In rat, out of 12 changes only 2 occurred in DBD and 10 in TAD. Interestingly, in human, out of 43 changes only 6 occurred in DBD and 37 in TAD. Thus, DNA binding domain of IRF-1 is conserved in the three species, as it interacts with very similar DNA elements. But the transactivation domain of IRF-1 has accumulated amino acid changes during evolution. The human IRF-1 has maximally changed its transactivation domain compared to that of the mouse and the rat. Six regions (I-VI) in the transactivation domain of human IRF-1 contained five to six amino acids and accounted for maximum amino acid change in continuous stretch. Changes in the restriction sites were also observed in the coding as well as untranslated regions of the IRF-1 cDNA of mouse and human. These changes in the coding regions were close enough to the changes in the amino acid sequence. For example, the restriction site for Nae I, Sma I, Sfi I and two Bst XI sites were present in human IRF-1 cDNA but absent in the mouse. These sites coincided with changes in 5' UTR, amino acid 25, 3' UTR, amino acid 308 and 3' UTR respectively. The restriction sites Cla I and

Xho I were present in the mouse cDNA but absent in the human. These sites coincided with amino acid positions 252 and 285 respectively.

8.4 IRF-1 mRNA EXPRESSION

IRF-1 mRNA expression in different tissues of the mouse was studied by dot and northern blot analyses using murine IRF-1 cDNA as the probe. By northern blot analysis the ~ 2 kb IRF-1 mRNA was observed in intestine, spleen and lungs and thymus of the mouse. The steady state level of IRF-1 mRNA expression in spleen and lungs was about 2.2 to 2.4 x fold more and 5.5 x fold more in intestine than in thymus indicating a tissue-specific pattern of expression. Comparative dot blot hybridization analysis showed that maximum amount of IRF-1 mRNA was expressed in the mouse intestine followed by lungs, thymus, spleen and liver whereas kidney, heart and brain showed lowest amount of IRF-1 mRNA expression. IRF-1 mRNA expression level in the intestine was 1.3 x fold more than the signal intensity obtained with 40 pg of IRF-1 cDNA in the positive control, 2.7 x fold more than that of the lungs and 3.2 x fold more than that of the thymus.

8.5 IRF-1 AND IRF-2 DNA BINDING ACTIVITY

Expression of DNA binding activities of IRF-1 and IRF-2 was studied by electrophoretic mobility shift assay (EMSA) using a 24 bp synthetic DNA sequence, $(GAAAGT)_4$, frequently occurring in the promoter/enhancer(s) of many murine and human genes induced by viruses and interferons (IFNs). EMSA of the whole cell extracts of brain, thymus, lungs, heart, liver, spleen, kidney and intestine of adult mouse was performed to measure expression of IRF-1 and IRF-2. Recombinant GST-IRF-1-DNA as well as human IRF-1 and IRF-2-DNA complexes from U 937 cells after IFN-γ treatment were used for comparison. Mouse spleen showed monomers and dimers of both IRF-1 and

IRF-2, IRF-1 dimer being the major form. Liver also showed IRF-1 dimer as the major form. Thymus and lungs showed IRF-1 dimer, IRF-2 dimer and a larger IRF-complex (a1). Intestine showed IRF-2 monomer and a smaller complex (d1) as well as the larger (a1) complex along with lesser amounts of IRF-1 and IRF-2 dimers. In the kidney, heart and brain IRF-1/IRF-2 complex was undetectable. The spleen and liver showed IRF-1 dimers indicating their possible transcriptional activity. In whole cell extract and nuclear extract of the spleen monomers and dimers of IRF-2 and IRF-1 and the higher IRF-complex (a1). As the amount of nuclear extract was increased, the (a1) complex increased more in intensity in comparison to the IRF-1 and IRF-2 monomers and dimers. For 2 x and 4 x fold increase in the nuclear protein concentration in the binding reactions there was 4.88 x and 20 x fold increase in IRF-(a1) complex formation indicating that formation of this higher IRF-complex (IRF-1 tetramer ?) was cooperative. This may reflect IRF-1-DNA complex formation in the nucleus of mammalian cells under conditions when IRF-1 gene is transcriptionally induced by various agents like viruses and cytokines and IRF-1 protein accumulates. Mouse spleen, liver and intestine have reasonable amounts of IRF-1 and IRF-2 whereas thymus and lungs have moderate levels of IRF-1 and IRF-2. Brain, heart and kidney have non-detectable amount of IRF-1 and IRF-2. Thus DNA binding activity of IRF-1 and IRF-2 also showed tissue-specific pattern in the mouse under normal conditions. However, the steady state mRNA levels of IRF-1 did not necessarily match the DNA binding activity of IRF-1 in different mouse tissues indicating possible post-transcriptional and/or post-translational regulation(s) of IRF-1.

Thus, differences in (a) organisation and (b) amino acid sequence of mouse and human IRF-1 genes; tissue-specific patterns for steady state level of IRF-1 mRNA expression and IRF-1- as well as IRF-2-DNA complexes indicate physiological significance of IRF-1 and IRF-2 in mouse tissues under normal conditions as well as possible functional specialisation of human IRF-1.

REFERENCES

9. REFERENCES

1. Abdollahi, A., Lord, K.A., Hoffman-Liebermann, B. and Liebermann, D.A. (1991) Interferon regulatory factor I is a myeloid differentiation primary response gene induced by interleukin-6 and leukemia inhibitory factor role in growth inhibition. *Cell Growth Differ.* 2: 401-407.

2. Ausubel, F., Brent, R., Kingston, R. E., Moore D. D., Seidman, J. G., Smith, J. A. and Struhl, K. (1995)In: *Short protocols in molecular biology.* Wiley. New York.

3. Au, W.C., Moore, P.A., Lowther, W., Juang, Y.T., and Pitha, P.M. (1995) Identification of member of the interferon regulatory family that binds to the interferon-stimulated response element and activates expression of interferon induced genes. *Proc. Natl. Acad. Sci. USA* 92: 11657-11661.

4. Auffray C., Rougeon F. (1980) Purification of mouse immunoglobulin heavy-chain messenger RNAs from total myeloma tumor RNA. *Eur J Biochem* 107(2):303-14.

5. Bachmaier, K., Neu, N., Pummerer, C., Duncan, G.S., Mak, T.W., Matsuyama, T., and Penninger, J..M. (1997) iNOS expression and nitrotyrosine formation in myocardium in response to inflamation is controlled by the interferon regulatory transcription factor 1. *Circulation* 96: 585-591.

6. Bellingham, J., Gregory-Evans, K., and Gregory-Evans, C.Y. (1998) Mapping of human interferon regulatory factor-3 (IRF-3) to chromosome 19q13.3-13.4 by intragenic polymorphic markers. Ann. Hum. Genet. 62: 231-234

7. Bielenberg, D. R., Bucana, C.D., Sanchez, R., Mulliken, J. B., Folkman, J., and Fidler, I. J. (1999) Progressive growth of infantile cutaneous hemangiomas is directly correlated with hyperplasia and angiogenesis of adjacent epidermis and inversely correlated with expression of the endogenous angiogenesis inhibitor, IFN-beta. *Int J Oncol.* 14(3):401-8.

8. Birnboin, H. C. and J. Doly (1979). A rapid alkaline extraction procedure for screening recombinant plasmid DNA. *Nucleic Acid Res.* 7: 1513

9. Blanch, V.J., Piskurich, J.F., and Kaetzel, C.S. (1999) Cutting edge: coordinate regulation of IFN regulatory factor-1 and polymeric Ig receptor by proinflammatory cytokines. *J. Immunol* 162: 1232-1235.

10. Bluyssen, H.A.R, Durbin, J.F.. and Levy, D.E. (1996) ISGFγp48, a specificity switch for interferon activated transcription factors. *Cyt. Growth. Fact. Rev.* 7: 11-17.

11. Bonner, J., Chalkley, R. G., Dahmus, M., Fambrough, D., Fugimura, F., Huang, R. C. C., Huberman, J., Jensen, R., Marushige, K., Ohlenbusch, H., Olivia, B. and Widholm, J. (1968) Isolation and characterization of chromosomal nuclear proteins. *Methods in Enzymol.* 12(B), 3-65.

12. Bovolenta, C., Driggers, P. H., Marks, M. S., Medin., J.A., Politis, A. D.,Vogel, S. N., Levy, D. E., Sakaguchi, K., Appella, E., Coligan, J. E. (1994) Molecular interactions between interferon consensus. 91(11):5046-50.

13. Bradford, M. M., (1976) A rapid and sensitive method for the quantitation of microgram quantities of protein utilizing the principle of protein-dye binding. *Anal Biochem.* 72:248-54.

14. Brass, A., Kehrli, E., Eisenbies, C., Strorb,U., and Singh, H. (1996) Pip, a lymphoid restricted IRF, contains a regulatory domain that is important for autoinhibition and ternary complex formation with the Ets factor PU.1. *Genes Dev.* 10: 2335-2347.

15. Brass, A.L., Zhu, A.Q., and Singh, H. (1999) Assembly requirements of PU.1/Pip (IRF-4) activator complexes inhibiting function invivo using fused dimers *EMBO J.* 18: 977-991.

16. Burysek, L., Yeow, W.S., and Pitha, P.M. (1999) Unique properties of a second Human herpesvirus-8 encoded interferon regulatory factor (vIRF-2). *J Hum. Virol.* 2: 19-32.

17. Cha, Y., and Deisseroth, A. B. (1994) Human interferon regulatory factor-2 gene. *J. Biol. Chem.* 269: 5279-5287.

18. Chaturvedi, M. M. and Kanungo, M. S. (1985). Analysis of chromatin of the brain of young and old rats by micrococcal nuclease and DNase I. *Biochem. Int.* 6, 357-63.

19. Church, G. M. and Gilbert, W. (1984) Genomic Sequence. *Proc. Natl. Acad. Sci. USA.* 81: 1991-1995.

20. Crepieux, P., Coll, J., Stehelin, D. (1994) The Ets family of proteins: weak modulators of gene expre sion in quest for trancriptional parteners. *Crit Rev Oncogene*. 5: 615-638.

21. Daly, C., Reich, N.C.(1993) Double-stranded RNA activates novel factors that bind to the interferon stimulated response element *Mol.Cell. Biol.* 13: 3756-3764.

22. Darnell, J. E., Kerr, I. M., and Stark, G. R., (1994) Jak STAT pathways and transcriptional activation in response to IFNs and other extracellular signalling proteins. *Science* 264: 1415-1421.

23. DeMaeyer E., and DeMaeyer-Guignard, J. (1988) In: *Interferon and other regulatory cytokines*, Wiley, New York.

24. Der, S. D., Zhou, A., Williams, B.R., Silverman, R.H. (1998) Identification of genes differentially regulated by interferon alpha, beta, or gamma using oligonucleotide arrays. *Proc Natl Acad Sci U S A.* 95(26): 15623-8.

25. Driggers, P.H., Ennist, D.L., Gleason, S.L., Mak, W.H., Marks, M.S., Levi, B.Z., Flanagan, J.R., Appella, E., and Ozato, K. (1990) An interferon γ-regulated protein that binds the interferon-inducible enhancer element of major histocompatibility complex class I genes. *Proc. Natl. Acad. Sci. USA* 87. 3743-3747.

26. Duncan, G.S., Mittrucker, H.W., Kagi, D., Matsuyama, T. and Mak, T.W. (1996) The transcription factor interferon regulatory factor-1 is essential for natural killer cell function in vivo. *J.Exp.Med.* 184: 2043-2043.

27. Eisenbeis, C.F., Singh, H., and Storb, U. (1995) Pip, a novel IRF family member, is a lymphoid-specific, PU.1 dependent transcriprtional activator. *Genes Dev.* 9: 1377-1387.

28. Escalante, C.R., Yie, J., Thanos, D., and Aggarwal, A.K. (1998) Structure of IRF-1 with bound DNA reveals determinants of interferon regulation. *Nature* 391: 103-104.

29. Falvo, J.V., Thanos, D., and Maniatis, T. (1995) Reversal of intrinsic DNA bends in the IFNβ gene enhancer by transcription factors and the architectural protein HMG I (Y). *Cell* 83: 1101-1111

30. Fan, C. M., and Maniatis, T., (1989) Two different virus-inducible elements are required for human β–interferon gene regulation. *EMBO J.* 8: 101-110.

31. Fujita, T., Kimura, Y., Miyamoto, M., Barsoumian, E. L., and Taniguchi, T. (1989a) Induction of endogenous IFN-α and IFN-β genes by a regulatory transcription factor IRF-1. *Nature* 337: 270-272.

32. Fujita, T., Reis, L. F. L., Watanabe, N., Kimura, Y., and Taniguchi, T., (1989b) Induction of the transcription factor IRF-1 and interferon-β mRNAs by cytokines and activators of second-messenger pathways. *Proc. Natl. Acad. Sci. USA*. 86: 9936-9940.

33. Fujita, T., Shibuya, H., Hotta, H., Yamanishi, K., and Taniguchi, T. (1987) Interferon -β gene regulation: tandemly repeated sequences of a synthetic 6 bp oligomer function as a virus-inducible enhancer. *Cell.* 49: 357-367.

34. Geller, D.A., Nguyen, D., Shapiro, R.A., Nussler, A., Di Silvio, M., Freeswick, P., Wang, S.C., Tweardy, D.J., Simmons, R.L., and Billiar, T.R. (1993) Cytokine induction of interferon regulatory factor-1 in hepatocytes. *Surgery* 114: 235-242.

35. Génin, P., Braganca, J., Darracq, N., Doly, J., and Civas, A. (1995) A novel PRD I and TG binding activity involved in virus-induced transcription of IFN genes. *Nuc. Acid Res.* 23: 5055-5063.

36. Grieder, F.B., and Vogel, S.N. (1999) Effects of the oral administration of interferon-alpha on antibody production in mice with induced tolerance. *J Interferon Cytokine Res.* 19: 895-900.

37. Hanahan, D. (1985) In : *DNA cloning voluma 1*, Glover, D., ed., IRL Press Ltd., London, UK.

38. Harada, H., Fujita, T., Miyamoto, M., Kimura, Y., Maruyama, M., Furia, A., Miyata, T., and Taniguchi, T., (1989) Structurally similar but functionally distinct factors, IRF-1 and IRF-2, bind to the same regulatory elements of IFN and IFN-inducible genes. *Cell* 58: 729-739.

39. Harada, H., Matsumoto, M., Sato, M., Kashiwazaki, Y., Kimura, T., Kitagawa, M., Yokochi, T., Tan, R.S.P., Takasugi, T., Kadokawa, Y., Schindler, C., Schreiber, R.D., Noguchi, S., and Taniguchi, T. (1996) Regulation of IFN- αβ genes: evidence for a dual fraction of the transcription factor complex ISGF3 in the production and action of IFNαβ. *Genes to Cells* 1: 995-1005.

40. Harada, H., Takahashi, E., Itoh, S., Harada, K., Hori, T.A., and Taniguchi, T. (1994) Structure and regulation of the human interferon regulatory factor 1 (IRF-1) and IRF-2 genes: implications for a gene network in the interferon system. *Mol. Cell. Biol.* 14:1500-15009.

41. Harada, H., Willison, K. Sakakibara, J., Miyamoto, M., Fujita, T., and Taniguchi,T., (1990) Absence of the type I IFN system in EC cells: transcriptional activator (IRF-1) and repressor (IRF-2) genes are developmentally regulated *Cell* 63: 303-312.

42. Hewish, D. R. and Burgoyne, L. A. (1973). Chromatin sub-structure. The digestion of chromatin DNA at regularly spaced sites by a nuclear deoxyribonuclease. *Biochem. Biophys. Res. Commun.* 52, 504-10.

43. Hiscott, J., Pitha, P., Génin, P., Nguyen, H., Heylbroeck, C., Mamane, Y., Algarté, M., and Lin, R. (1999) Trigerring the interferon response: the role of IRF-3 transcription factor. *J. Interferon Cytokine Res.* 19: 1-13.

44. Hobart, M., Ramassar, V., Goes, N., Urmson, J., and Halloran, P.F. (1997) FN regulatory factor-1 plays a central role in regulation of the expression of class I and class II MHC genes in vivo. *J. Immunol.* 158: 4260-4269.

45. Hobart, M., Ramassar, V., Goes, N., Urmson,, J., and Halloran, P.F. (1996) The induction of class I and II major histocompatibility complex by allogenic stimulation is dependent on the transcription factor interferon regulatory factor 1 (IRF-1) : observations in IRF-1 knockout mice. *Transplantation* 62: 1895-1901.

46. Holmes, D. S., Quigley, M. (1981) A rapid boiling method for the preparation of bacterial plasmids. *Anal Biochem* 114(1):193-7

47. Holtschke, T., Löhler, J., Kanno, Y., Fehr, T., Giese, N., Rosenbauer, F., Lou, J., Knobeloch, K.P., Gabriele, L., Waring, J.F., Bachmann, M.F., Zingernagel, R.M., Morse III, H.C., Ozato, K., and Horak., I. (1996) Immunodeficiency and chronic myelogenous leukemia-like syndrome in mice with targeted mutation of ICSBP gene *Cell* 87: 307-317.

48. Iadecola, C., Salkowski, C.A., Zhang, F., Aber, T., Nagayama, M., Vogel, S.N., and Ross, M.E. (1999) The transcriptional factor interferon regulatory factor 1 is expressed after cerebral ischemia and contributes to ischemic brain injury. *J. Exp. Med.* 189: 719-727.

49. Ish- Horowicz, D. and Burke, J. F. (1981) Rapid and efficient cosmid cloning. *Nucleic Acids Res* 9: 2989

50. Itoh, S., Harada, H., Nakamura, Y., White, R., Taniguchi, T. (1991) Assignment of the human interferon regulatory factor-1 (IRF1) gene to chromosome 5q23-q31. *Genomics* 10: 1097-1099.

51. John, J., McKendry, R., Pellegrini, S., Flavell, D., Kerr, I.M., and Stark, G.R. (1991) Isolation and characterization of a new mutant human cell line unresponsive to alpha and beta interferons. *Mol. Cell. Biol.* 11: 4189-4195.

52. Juang, Y.T., Lowther, W., Kellum, M., Au, W.C., Lin, R., Hiscott, J., and Pitha, P.M. (1998) Primary activation of interferon A and interferon B gene transcription by interferon regulatory factor-3. *Proc Natl. Acad. Sci. USA* 95: 9837-9842.

53. Kakidani, H., and Ptashne, M. (1986) GAL4 activates gene expression in mammalian cells. *Cell* 52: 161-167.

54. Kamijo, R., Harada, H., Matsuyama, T., Bosland, M., Gerecitano, J., Shapiro, D., Le, J., Koh, S.I., Kimura, T., Green, S.J., et al (1994) Requirement for transcription factor IRF-1 in NO synthase induction in macrophages. *Science* 263: 1612-1615.

55. Kawakami, T., Matsumoto, M., Sato, M., Harada, H., Taniguchi, T., and Kitigawa, M. (1995) Possible involvement of the transcription factor ISGF3(in virus-induced expression of the IFN-gene. *FEBS Lett.* 358: 225-229.

56. Kim, T. K., Maniatis, T., (1998) The mechanism of transcriptional synergy of an in vitro assembled interferon-β enhancesome. *Mol. Cell* . 1: 119-129.

57. Kimura, T., Nakayama, K., Penninger, J., Kitagawa, M., Harada, H., Matsuyama, T., Tanaka, N., Kamijo, R., Vilcek, J., Mak, T.W., and Taniguchi, T. (1994) Involvement of the IRF-1 transcription factor in antiviral responses to interferons. *Science* 264: 1921-1924.

58. Kirchhoff, S., Schaper, F, and Hauser, H. (1993) Interferon regulatory factor 1 (IRF-1) mediates cell growth inhibition by transactivation of downstream target genes. *Nucleic Acids Res.* 21: 2881-2889

59. Kirchoff, S., Koromilas, A.E., Schaper, F., Grashoff, M., Sonenberg, N. and Hauser, H. (1995) IRF-1 induced cell growth inhibition and interferon induction requires the activity of the protein kinase PKR. *Oncogene* 11: 439-445.

60. Kondo, T., Minamino, N., Nagamura-Inoue, T., Matsumoto, M., Taniguchi, T., and Tanaka, N. (1997) Identification and characterization of nucleophosmin B23 numatrin which binds the anti-oncogenic transcription factor IRF-1 and manifests oncogenic activity. *Oncogene* 15: 1275-1281.

61. Kuhl, D., de la Fuente, J., Chaturvedi, M., Parimoo, S., Ryals, J., Meyer, F. and Weissmann, C., (1987) Reversible silencing of enhancer by sequence derived from the human IFN-α promoter. *Cell.* 50: 1057-1069.

62. Kumar, A., Yang, Y.,-L., Flati, V., Der, S., Kadereit, S., Deb, A., Haque, J., Reis, L., Weissmann, C., and Williams, B.R.G. (1997) Deficient cytokine signaling in mouse embryo fibroblasts with a targeted deletion in the PKR gene: role of IRF-1 and NF-κB. *EMBO J.* 16: 406-416.

63. Kunkel, L.M., Monaco, A.P., Middlesworth, W., Ochs, H.D., Latt, S.A.(1985) Specific cloning of DNA fragments absent from the DNA of a male patient with X chromosome deletion. *Proc. Natl. Acad. Sci. USA* 82: 4778-4782

64. Le Stunff, C., and Rotwein, P. (1998) Growth hormone stimulates interferon regulatory factor-1 gene expression in liver. *Endocrinology* 139: 859-866.

65. Lengyel, P., (1982) Biochemistry of interferons and their actions. *Ann. Rev. Biochem.* 51:251-82.

66. Levy, D.E. (1995) Interferon induction of gene expression through the JAK STAT pathway. *Sem. Virol.* 6: 181-190.

67. Li, M., Lee, H., Guop, J., Neipel, F., Fleckenstein, B., Ozato, K., and Jung, J.U. (1998) Kaposi's sarcoma-associated herpesvirus viral interferon regulatory factor. *J. Virol.* 72: 5433-5440.

68. Lin, R., Heylbroeck, C., Pitha, P.M., and Hiscott, J. (1998) Virus dependent phosphorylation of IRF-3 transcription factor regulated nuclear translocation, transactivation potential and proteasome mediated degradation. *Mol. Cell Biol.* 18: 2986-2996.

69. Lin, R., Hiscott, J., (1999) A role for casein kinase II phosphorylation in the regulation of IRF-1 transcriptional activity. *Mol. Cell. Biochem.* 191: 169-180.

70. Lin, R., Mamane, Y., and Hiscott, J. (1999) Structural and functional analysis of interferon regulatory factor 3: localizatiuon of transactivation and autoinhibitory domains. *Mol. Cell. Biol.* 19: 2463-2474.

71. MacDonald, N. J., Kuhl, D., Maguire, D., Naf, D., Gallant, P., Goswamy, A., Hug, H., Bucler, H., Chaturvedi, M., de la Fuente, J., Ruffner, H., Meyer, F. and Weissmann, C. (1990) Different pathways mediate virus inducibility of the human IFN-α1 and IFN-β genes. *Cell.* 60: 767-779.

72. Mamane, Y., Heylbroeck, C., Genin, P., Algarte, M., Servant, M. J., LePage, C., DeLuca, C., Kwon, H. Lin, R., Hiscott, J. (1999) Interferon regulatory factors: the next generation. *Gene* . 237(1):1-14.

73. Marie, I., Durbin, J.E., and Levy, D.E. (1998) Differential viral induction of distinct interferon α genes by positive feedback through interferon regulatory factor-7. *EMBO J.* 17: 6660-6669.

74. Maruyama,M., Fujita,T. and Taniguchi,T.(1989) Sequence of a cDNA coding for human IRF-1. *Nucleic Acids Res.* 17 (8):3292.

75. Matsuyama, T., Grossman, A., Mittrücker, H.W., Siderovski, D.P., Kiefer, F., Kawakami, T., Richardson, C.D., Taniguchi, T., and Mak., T. (1995) Molecular cloning of LSIRF, a lymphoid-specific member of the interferon regulatory factor family that binds the interferon-stimulated response element (ISRE). *Nucleic Acids Res.* 23 : 2127-2136.

76. Matsuyama, T., Kimura, T., Kitagawa, M., Watanabe, N., Kundig, T., Amakawa, R., Kishihara, K., Wakeham, A., Potter, J., Furlonger, C., Narendran, A., Suzuki, H., Ohashi, P., Paige, C., Taniguchi, T., and Mak., T (1993) Targeted disruption of IRF-1 or IRF-2 results in abnormal type I IFN induction and abberant lymphocyte development *Cell* 75: 83-97.

77. Matsuyama, T., Kimura, T., Kitagawa, M., Watanabe, N., Kundig, T., Amakawa, R., Kishihara, K., Wakeham, A., Potter, J., Furlonger, C., Narendran, A., Suzuki, H., Ohashi, P., Paige, C., Taniguchi, T., and Mak., T (1993) Targeted disruption of IRF-1 or IRF-2 results in abnormal type I IFN induction and abberant lymphocyte development *Cell* 75: 83-97.

78. McKinsey, T. A., Brockman, J. A., Scherer, D. C., Al-Murrani, S. W., Green, P. L. and Ballard, D. W. (1996) Inactivation of IκBβ by the Tax protein of human T-cell leukemia virus type I: a potential mechanism for constitutive induction of NF-κB. *Mol. Cell. Biol.* 16: 2083-2090.

79. Meraz, M.A., White, J.M., Sheehan, K.C., Bach, E.A., Rodig, S.J., Dighe, A.S., Kaplan, D.H., Riley, J.K., Greenlund, A.C., Campbell, D., Carver-Moore, K., DuBois, R.N., Clark, R., Aguet, M., and Schreiber, R.D. (1996) Targeted disruption of the Stat1 gene in mice reveals unexpected physiologic specificity in the JAK-STAT signaling pathway. *Cell* 84: 431-442.

80. Mittrücker, H.W., Grossman, A., Matsuyama, T.,Küdidg, T.M., Potter, J., Shahinian, A., Wakeham, A., Paterson, B., Ohashi, P.S., and Mak, T.W.

(1997) Requirement for the transcription factor LSIRF, IRF-4 for mature B and T lymphocyte function. *Science* 275: 540-543.

81. Miyamoto, M., Fujita, T., Kimura, Y.,Maruyama, M., Harada, H., Sudo, Y., Miyata, T., and Taniguchi, T. (1988) Regulated expression of a gene encoding a nuclear factor, IRF-1, that specifically binds to IFN-β gene regulatory elements. *Cell* 54: 903-913.

82. Müller, U., Steinhoff, U., Reis, L.F., Hemmi, S., Pavlovic, J., Zingernagel, R.M., and Aguet, M.(1994) Functional role of type I and type II interferons in antiviral defence. *Science* 264: 1918-1921.

83. Nagapalli, S., and Atchison, M.L. (1998) Transcription factor Pip can enhance DNA binding by E47, leading to transcriptional synergy involving multiple protein domains. *Mol. Cell Biol.* 18: 4639-4650.

84. Nelson, N., Marks, M.S., Driggers, P.H., and Ozata, K. (1993) Interferon consensus sequence binding protein, a member of the interferon regulatory factor family suppresses interferon- induced gene transcription. *Mol. Cell. Biol.* 13: 588-599.

85. Nguyen, H., Hiscott, J. and Pitha, P. M. (1997a) The growing family of interferon regulatory factors. *Cyt. Growth Fact. Rev.* 8: 293-312.

86. Nguyen, H., Lin, R., and Hiscott, J. (1997b) Activation of multiple growth regulatory genes following inducible expression of IRF-1 or IRF RelA fusion proteins. *Oncogene* 15: 1425-1435.

87. Nguyen, H., Mustafa, A., Hiscott, J., and Lin, R. (1995) Transcription factor IRF-2 exerts its oncogenic phenotype through the DNA binding/transcription repression domain. *Oncogene* 11: 537-544.

88. Nonkwelo, C., Ruf, I.K., and Sample, J. (1997) Interferon-independent and induced regulation of Epstein-Barr Virus EBNA-1 gene transcription in Burkitt lymphoma. *J. Virol.* 71: 6887-6897.

89. Ogasawara, K., Hida, S., Azimi, N., Tagaya, Y., Sato, T., Yokochi-Fukuda, T., Waldmann, T.A., Taniguchi.,T., and Taki, S. (1998) Requirements for IRF-1 in the microenvironment supporting development of natural killer cells. *Nature* 391:709-703.

90. Ortiz, M.A., Light, J., Maki, R.A., and Assa-Munti, N. (1999) Mutation analysis of the Pip interaction Domain reveals critical residues for protien-protien interaction. *Proc. Natl. Acad. Sci. USA* 96: 2740-2745.

91. Ozawa, H., Matsuyama, T., Mak, T. W., Aizawa, S., Tokino, T., Oren, M. and Taniguchi, T. (1996) Cooperation of the tumor suppressors IRF-1 and p53 in response to DNA damage. *Nature* . 382: 816-818.

92. Parekh, B. S., Maniatis, T., (1999) Virus infection leads to localization hyperacetylaion of histones H3 and H4 at the IFN-β promoter. *Mol. Cell.* 3: 125–129.

93. Paschen, W., Gissel, C., Althausen, S., and Doutheil, J. (1998) Changes in interferon regulatory factor -1 mRNA levels after transient ischemia in rat brain. *Neuroreport* 9: 3147-3151.

94. Penninger, J.M., and Mak, T.W. (1998) Thymocyte selection in Vav and IRF-1 gene deficient mice. *Immunol Rev.* 165: 149-166.

95. Penninger, J.M., Sirard, C., Mittrucker, H.W., Chidgey, A., Kozieradzki, I., Nghiem, M., Hakem, A., Kimura, T., Timms, E., Boyd, R., Taniguchi, T., Matsuyama, T., Mak, T.W. (1997) The interferon regulatory transcription factor IRF-1 controls positive and negative selection of $CD8^+$ thymocytes. *Immunity* 7: 243-254.

96. Pestka, S., Langer, J. A., Zoon, K. C., and Samuel, C. E., (1987) Interferon and their action. *Annu. Rev. Biochem.* 56: 727-777.

97. Pine, R., Canova, A. and Schindler, C., (1994) Tyrosine phosphorylated p91 binds to single element in the ISGF2 IRF-1 promoter to mediate induction by IFN α and IFN β and is likely to autoregulate the p91 gene. *EMBO J.* 13: 158-167.

98. Pine, R., Decker, T., Kessler, D.S., Levy, D.E., and Darnell Jr., J.E. (1990) Purification and cloning of interferon stimulated gene factor 2 (ISGF2): ISGF2 (IRF-1) can bind to the promoters of both beta-interferon- and interferon-stimulated genes but is not a primary transcriptional activator of either. *Mol. Cell. Biol.* 10: 2448-2457.

99. Pinna, L.A. (1990) Caesin kinase II: An 'Eminence grise' in cellular regulation? *Biochim. Biophys. Acta* 1054: 267-284.

100. Pleiman, C. M., Hertz, W. M. and Cambier, J. C., (1994) Activation of phosphotidylinositol-3' kinase by Src-family Kinase SH3 binding to the p85 subunit. *Science* 263: 1609-1612.

101. Prost, S., Bellamy, C.O., Cunningham,D.S., and Harrison, D.J. (1998) Altered DNA repair and cysregulation of p53 in IRF-1 null hepatocytes. *FASEB J.* 12: 181-188.

102. Reis, L.F.L., Harada, H., Wolchok, J.D., Taniguchi, T. and Vilcek, J. (1992) Critical role of a common transcription factor, IRF-1, in the regulation of IFN-and IFN-inducible genes. *EMBO J.* 11: 185-193.

103. Reis, L.S., Ruffner, H., Stark, G., Aguet, M., and Weissmann, C. (1994) Mice devoid of interferon regulatory factor 1 (IRF-1) show normal expression of type I interferon genes. *EMBO J.* 13: 4798-4806.

104. Ronco, I., Karpova, A., Vidal, M., and Howley, P. (1998) Human papillomavirus 16 E6 oncoprotein binds to interferon regulatory factor-3 and inhibits its transcriptional activity. *Genes Dev* 12: 2061-2072.

105. Ruffner, H., Reis, L. F. L., Naf, D., Weissmann, C. (1993) Induction of type I interferon genes and interferon inducible genes in embryonal stem cells deviod of interferon regulatory factor 1. *Proc. Natl. Acad. Sci. USA.* 90: 1150-11507.

106. Sakatsume, M. and Finbloom, D. S. (1996) Modulation of the expression of the IFN-γ receptor b-chain controls responsiveness to IFN-g in human peripheral blood T-cells. *J Immunol.* 156: 4160-4166.

107. Sambrook, Fritsch, Maniatis. (1989) In: *Molecular cloning, A laboratory mannual*, Cold Spring Harbor Press. New York.

108. Sato, M., Hata, N., Asagiri, M., Nakaya, T., Taniguchi, T., and Tanaka, N. (1998) Positive feedback regulation of type I IFN genes by the IFN inducible transcription factor IRF-7. *FEBS Lett.* 441: 106-110.

109. Schafer, S.L., Lin, R., Moore, P.A., Hiscott, J., and Pitha, P.M. (1998) Regulation of Type I interferon gene expression by interferon regulatory factor-3 *J. Biol. Chem.* 273: 2714-2720.

110. Schreiber, E., Matthias, P., Muller, M. M. and Schaffner, W. (1989) Rapid detection of octamer binding protein with 'mini-extract', prepared from a small number of cells. *Nucleic Acids Res.* 17(15): 6419.

111. Sen, G. C., and Ransohoff, R. M., (1993) Interferon-induced antiviral actions and their regulation. *Annu. Rev. Biochem.* 42: 57-102.

112. Senaldi, G., Shaklee, C.L., Guo, J., Martin, L., Boone, T.W., Mak, T., and Ulich, T.R. (1999) Protection against the mortality associated with disease models mediated by TNF and IFN-gamma in mice lacking IFN regulatory factor-1. *J. Immunol.* 163: 6820-6826.

113. Sharf, R., Meraro, D., Azriel, A., Thornton, A.M., Ozato, K., Petricoin, E.F., Larner, A.C., Shaper, F., Hauser, H., and Levi, B.Z. (1997) Phosphorylation events modulate the ability of interferon consensus sequence binding protein to interact with interferon regulatory factors and to bind DNA. *J. Biol. Chem.* 272: 9785-9792.

114. Sharf. R., Azriel, A., Lejbkowicz, F., Winograd, S. S., Ehrlick, R., and Levi, B. Z. (1995) Functional domain analysis of interferon consensus sequence binding protein (ICSBP) and its association with interferon regulatory factors. *J. Biol. Chem.* 270: 13063-13069.

115. Simon, A.K., Desrois, M., Schmitt-Verhulst, A.M. (1997) Interferon-regulatory factors during development of CD4 and CD8 thymocytes. *Immunology* 91: 340-345.

116. Sims, S. H., Cha, Y., Romine, M., F., Gao, P. Q., Gottlieb, K. and Deisseroth, A. B. (1993) A novel interferon-inducible domain: structural and functional analysis of the human interferon regulatory factor 1 gene promoter. *Mol. Cell. Biol.* 13: 690-702.

117. Sims, T.N., Goes, N.B., Ramassar, V., Urmson, J., and Halloram, P.F. (1997) In vivo class II transactivator expression in mice is induced by a non-interferon -gamma mechanism in response to local injury. *Transplantation* 64: 1657-1664.

118. Stark, G.R., Kerr, I. M., Williams, B. R. G., Silverman R. H., and Schreiber R. D., (1998) How cells respond to interferons. *Annu. Rev. Biochem.* 67: 227-264.

119. Takaoka, A., Mitani, Y., Suemori, H., Sato, M., Yokochi, T., Noguchi, S., Tanaka, N., and Taniguchi, T., (2000) Cross talk between interferon-γ and -α/β signaling components in Caveolar membrane domains. *Science* 288: 2357-2360.

120. Taki, S., Sato, T., Ogasawara, K., Fukuda, T., Sato, M., Hida, S., Suzuki, G., Mitsuyama, M., Furuta, T., Kojima, S., Taniguchi, T., and Asano, Y. (1997)

Multistage regulation of Th-1 type immune responses by the transcription factor IRF-1. *Immunity* 6: 1-20

121. Talpaz, M., Kantarjian, H., McCredie, K., Trujillo, J., Keating, M., and Gutterman, J.U., (1987) Therapy of chronic myelogenous leukemia. *Cancer.* 59(3 Suppl):664-667.

122. Tamura, T., Ishihara, M., Lamphier, M.S., Tanaka, N., Oishi, I., Aizawa, S., Matsuyama, T., Mak, T.W., Taki, S., and Taniguchi, T. (1995) An IRF-1 dependent pathway of DNA damage induced apoptosis in mitogen activted T lymphocytes. *Nature* 376: 596-599.

123. Tan, R.S., Taniguchi, T., and Harada, H.(1996) Identification of lysyl oxidase gene as target of the antioncogenic transcription factor, IRF-1, and its possible role in tumor suppression. *Cancer Res.* 56: 2417-2421.

124. Tanaka, N., Ishihara, M., and Taniguchi, T. (1994a) Suppresion of e-myc or fos-B induced cell transformation by the transcription factor IRF-1. *Cancer Lett.* 83: 191-196.

125. Tanaka, N., Ishihara, M., Kitagawa, M., Harada, H., Kimura, T., Matsuyama, T., Lamphier, M.S., Aizawa, S., Mak, T.W. and Taniguchi, T. (1994b) Cellular commitment to oncogene-induced transformation or apoptosis is dependent on the transcription factor IRF-1. *Cell* 77: 829-839.

126. Tanaka, N., Kawakami, T. and Taniguchi, T. (1993) Recognition DNA sequence of interferon Regulatory Factor 1 (IRF-1) and IRF-2, regulators of cell growth and the interferon system. *Mol. Cell. Biol.* 13: 4531-4538.

127. Taniguchi, T., Harada, H., and Lamphier, M., (1995) Regulation of the interferon system and cell growth by the IRF transcription factors. *J. Cancer Res. Clin. Oncol.* 121: 516-520.

128. Thanos, D., Maniatis, T.,(1995) Virus induction of human IFN β gene expression requires the assembly of an enhancesome. *Cell* 83: 1091-1100.

129. Thornton, A.M., Ogryzko, V.V., Dent, A., Sharf, R., Levi, B.Z., Kanno, Y., Staudt, L.M., Howard, B.H., and Ozato, K (1996) A dominanat negative mutant of an IFN regulatory factor family protein inhibits both type I and type II IFN IFN-stimulated gene expression and antiproliferative activity of IFNs. *J. Immunol* 157: 5145-51554.

130. Upreti, M. and Rath, P.C. (2000) Recombinant murine Interferon Regulatory Factor-1 (IRF-1) and its DNA binding activity with a DNA sequence prevalent

in the promoters of mammalian genes induced by virus and Interferon. (unpublished).

131. Vaughan, P.S., Aziz, F., van Wijnene, A.J., Wu, S., Harada, H., Taniguchi, T., Saprano, K.J., Stein, J.L., and Stein, G.S. (1995) Activation of a cell-cycle regulated histone gene by oncogene transcription factor IRF-2. *Nature* 377: 362-365.

132. Veals, S.A., Santa maria, T., and Levy, D.E. (1993) Two domains of ISF3γ that mediate protein-DNA and protein-protein interactions during transcription factor assembly contribute to DNA-binding specificity. *Mol. Cell. Biol.* 13: 196-206.

133. Veals, S.A., Schindler, C., Leonard, D., Fu, X.,-Y., Aebersold, R., Darnell, Jr. J.E., and Levy, D.E. (1992) Subunit of an alpha-interferon-responsive transcription factor is related to interferon regulatory factor and myb families of DNA-binding proteins. *Mol.Cell. Biol.* 12: 3315-3324.

134. Wang, I.-M., Blanco, J.C.G., Tsai, S.Y., Tsai, M.J. and Ozato, K.(1996) Interferon regulatory factors and TFIIB cooperatively regulate interferon-responsive promoter activity in vivo and in vitro. *Mol.Cell.Biol.* 16: 6313-6324

135. Watanabe, N., Sakakibara, J., Hovanessian, A. G., Taniguchi, T., and Fujita, T. (1991) Activation of IFN- element by IRF-1 requires a post-translational event in addition to IRF-1 synthesis. *Nucl.Acid Res.* 19: 4421-4428.

136. Wathelet, M.G., Lin, C.H., Pareakh, B.S., Ronco, I.V., Howley, P.M., and Maniatis, T. (1998) Virus infection induces the assembly of coordinately activated transcription factors on the IFN-β enhancer in vivo. *Mol. Cell* 1: 507-518.

137. Wathelet, M.G., Lin, C.H., Pareakh, B.S., Ronco, I.V., Howley, P.M., and Maniatis, T. (1998) Virus infection induces the assembly of coordinately activated transcription factors on the IFN-β enhancer invivo. *Mol. Cell* 1: 507-518.

138. Weaver, B.K., Kumar, K.P., and Reich, N.C., (1998) Interferon regulatory factor-3 and CREB binding protien/p300 are subunits of double stranded RNA activated transcription factor DRAF1. *Mol. Cell Biol.* 18: 1359-1368.

139. Webster, N., Jin, J. R., Green, S., Hollis, M., and Chambon, P. (1988) The yeast UAS_G is a transcriptional enhancer in human HeLa cells in the presence of the GAL4 trans-activator. *Cell* 52: 169-178.

140. Weinberg, R., A., (1989) Oncogenes, antioncogenes and the molecular basis of multistep carcinogenesis. *Cancer Res.* 49: 3713-3721.

141. Weissmann, C., and Weber, H., (1986) The interferon genes. *Prog Nucleic Acid Res Mol Biol* 33: 251-300.

142. White, L.C., Wright, K.L., Felix, N.J., Ruffner, H., Reis, L.F., Pine, R., and Tinge, J.P. (1996) Regulation of LMP2 and TAP1 genes by IRF-1 explains the paucity of CD8- T cells in IRF-$1^{-/-}$ mice. *Immunity* 5: 365-376.

143. White, L.C., Wright, K.L., Felix, N.J., Ruffner, H., Reis, L.F., Pine, R., and Tinge, J.P. (1996) Regulation of LMP2 and TAP1 genes by IRF-1 explains the paucity of CD8- T cells in IRF-$1^{-/-}$ mice. *Immunity* 5: 365-376.

144. Willman, C.L., Sever, C.E., Pallavicini, M.G., Harada, H., Tanaka, N., Slovak, M.L., Yamamoto, H., Harada, K., Mecker, T.C., List, A.F., and Taniguchi, T (1993) Deletion of IRF-1, mapping to chromosome 5q31.3 in human leukemia and prelukemic myelodysplasias. *Science* 259: 968-971.

145. Yamada, G., Ogawa, M., Akagi, K., and Taniguchi, T., (1994) Specific depletion of the B-cell population induced by aberrant expression of human interferon regulatory factor 1 gene in transgenic mice. *Proc. Natl. Acad. Sci. USA* 88: 532-536.

146. Yamagata, L., Nishida, J., Tanaka, T., Sakai, R., Mitani., K., Yoshida, M., Taniguchi, T., Yyazaki, Y., and Hirai, H. (1996) A novel interferon regulatory factor family transcription factor, ICSAT/Pip, LSIRF, that negatively regulated the activity of interferon regulated genes. *Mol. Cell. Biol.* 16: 1283-1294.

147. Yamamoto, H., Lamphier, M.S., Fujita, T., Taniguchi, T., and Harada, H. (1994) The oncogenic transcription factor IRF-2 possesses a transcriptional repression and a latent activation domain. *Oncogene* 9: 1423-1428.

148. Yang, Y.L., Reis, L.F.L., Pavlovic, J., Aguzzi, A., Schaefer, R., Kumar, A., Williams, B.R.G., Aguet, M. and Weissman, C. (199ɔ) Deficient signaling in mice devoid of double-stranded RNA-dependent protein kinase. *EMBO J.* 14: 6095-6106.

149. Yoneyama, M., Suhara, W., Fukuhara, Y., Fukuda, M., Nishida, E., and Fujita, T (1998) Direct tiggering of the type I interferon system by virus infection: activation of a transcription factor complex containing IRF-3 and CBP/p300. *EMBO J.* 17: 1087-1095.

150. Yoneyama, M., Suhara, W., Fukuhara, Y., Fukuda, M., Nishida, E., and Fujita, T (1998) Direct tiggering of the type I interferon system by virus

infection: activation of a transcription factor complex containing IRF-3 and CBP/p300. *EMBO J.* 17: 1087-1095.

151. Yoneyama, M., Suhara, W., Fukuhara, Y., Sato, M., Ozato, K., and Fujita, T. (1996) Autocrine amplification of type I interferon gene expression mediated by interferon stimulated gene factor 3 (ISGF3). *J.Biochem.* 120: 160-169.

152. Yu-Lee, L. Y., Hrachovy, J. A., Stevens, A. M., and Schwarz, L. A., (1990) Interferon- regulatory factor 1 is an immediate-early gene under transcriptional regulation by Prolactin in Nb2 T cells. *Mol. Cell. Biol.* 10(6): 3087-3094.

153. Zhang, L., and Pagano, J.S.(1997) IRF-7, a new interferon regulatory factor associated with Epstein Barr Virus latency. *Mol. Cell. Biol.* 17: 5748-5757.

154. Zimring, J.C., Goodbourn, S., and Offerman, M.K. (1998) Human herpes virus 8 encodes an interferon regulatory factor (IRF) homolog that represses IRF-1 mediated transcription. *J. Virol* 72: 701-707.